



THE UNIVERSITY  
*of* ADELAIDE

**Sedimentology, Provenance, and Salt-Sediment  
Interaction in the Ediacaran Pound Subgroup, Flinders  
Ranges, South Australia**

**John Waldon Counts  
B.Sc., M.Sc.**

A thesis submitted for the degree of

**Doctor of Philosophy**

Australian School of Petroleum

Faculty of Engineering, Computer, and Mathematical Sciences

The University of Adelaide

Adelaide, South Australia

**July 2016**

*Shiny, speckled, red and sandy,  
A bonney layer, quite a dandy  
Rippled, stippled, grooved and fluted  
On bedding plane for inspection suited.  
A layer of red and some uniformity  
And nicely opposite a fine unconformity.  
Poised to announce the most famous of all  
The layer of life, standing tall*

*-Terry Krieg*

*"Bonney Sandstone"*

## Contents

<b>Figures and Tables</b> .....	<b>i</b>
<b>Abstract</b> .....	<b>iv</b>
<b>Declaration</b> .....	<b>vi</b>
<b>Acknowledgements</b> .....	<b>vii</b>
<b>Chapter 1: Introduction</b> .....	<b>1</b>
1.1: Contextual Statement.....	2
<b>Chapter 2: Background and Review of Relevant Literature</b> .....	<b>8</b>
2.1: Present-day Geography and Recent History .....	9
2.2: Palaeogeographic Context of the Adelaide Rift Complex .....	11
2.2.1: Configuration and Breakup of Rodinia.....	12
2.3: Geology of the Centralian Superbasin .....	16
2.3.1: Overview .....	16
2.3.2: Basin Fill .....	18
2.4: Stratigraphy and Sedimentology of the Adelaide Rift Complex .....	20
2.4.1: Callanna Group.....	21
2.4.2: Burra Group .....	24
2.4.3: Umberatana Group and Cryogenian Glaciation.....	27
2.4.4: Wilpena Group.....	33
2.4.5: Hawker and Lake Frome Groups.....	42
2.5: Salt-Sediment Interaction in the Adelaide Rift Complex .....	43
2.5.1: Minibasin Formation and Stratal Architecture .....	44
2.5.2: Minibasins in the Adelaide Rift Complex .....	46
2.6: Hydrocarbon-Bearing Analogues for the Adelaide Rift Complex .....	48
2.6.1: Gulf of Mexico .....	50

2.6.2 Offshore Brazil .....	53
2.6.3: Paradox Basin .....	55
2.7: References.....	58

**Chapter 3: Sedimentological interpretation of an Ediacaran delta: Bonney**

<b>Sandstone, South Australia .....</b>	<b>76</b>
3.1: Abstract.....	77
3.2: Introduction .....	78
3.3: Background .....	80
3.3.1: Previous Research .....	80
3.3.2: Study Area .....	83
3.4: Methodology.....	83
3.5: Results and Interpretation .....	86
3.5.1: Lithostratigraphic Divisions .....	86
3.5.2: Facies Analysis and Interpretation.....	92
3.5.3: Process and architectural classification.....	96
3.5.4: Interpretation of stacking patterns and architectural elements .....	97
3.6: Discussion.....	101
3.6.1: Regional Implications and Significance .....	101
3.6.2: Approaches to Sedimentological Interpretation with Limited Datasets ...	108
3.7: Conclusions.....	110
3.8: Acknowledgements .....	111
3.9: References.....	112

**Chapter 4: Paleogeography of an Ediacaran Fluvial-Deltaic System: A Case Study Integrating Sedimentology and Provenance .....**

4.1: Abstract .....	119
---------------------	-----

4.2: Introduction .....	120
4.3: Background .....	122
4.4: Methodology .....	126
4.4.1: Field Methods .....	126
4.4.2: Zircon Analysis.....	127
4.5: Sedimentology .....	133
4.5.1: Stratigraphy.....	133
4.5.2: Observed Lithofacies .....	134
4.5.3: Lithofacies Associations .....	143
4.5.4: Parasequence Interpretation: Integrating Stacking Patterns and Lithofacies .....	145
4.6: Detrital Zircon Geochronology .....	147
4.6.1: Bunyeroo Gorge .....	147
4.6.2: Mainwater Creek.....	149
4.6.3: Castle Rock.....	149
4.6.4: Comparison with Related Formations.....	150
4.7: Discussion.....	150
4.7.1: Sediment provenance.....	150
4.7.2: Implications for Early Life.....	152
4.8: Conclusions.....	158
4.9: Acknowledgements .....	159
4.10: References.....	160

<b>Chapter 5: Lateral Variability along the Margin of an Ediacaran Salt-Withdrawal Minibasin.....</b>	<b>166</b>
5.1: Abstract.....	167
5.2: Introduction .....	168

5.3: Geologic Setting.....	170
5.3.1: The Adelaide Rift Complex .....	170
5.3.2: Background Sedimentation.....	172
5.3.3: Character and Distribution of Diapirs in the Adelaide Rift Complex .....	172
5.4: Methodology.....	174
5.5: Observed Facies .....	175
5.5.1: Facies descriptions .....	175
5.5.2: Facies distribution .....	181
5.5.3: Facies interpretations .....	182
5.6: Discussion.....	186
5.6.1: Environmental controls on facies variability.....	186
5.6.2: Diapiric influence on sedimentary character and depositional processes.....	187
5.6.3: Diapir-related controls on facies change .....	190
5.6.4: Comparison with diapir-sediment interaction elsewhere .....	193
5.7: Conclusions.....	195
5.8: References.....	197

<b>Chapter 6: Sedimentology, depositional environments and significance of an Ediacaran salt-withdrawal minibasin, Billy Springs Formation, Flinders Ranges, South Australia.....</b>	<b>203</b>
6.1: Abstract.....	204
6.2: Introduction .....	205
6.3: Geological Setting .....	208
6.4: Background .....	211
6.5: Field And Laboratory Methodology .....	217
6.6: Observed Lithofacies: Description, Distribution and Interpretation .....	220
6.6.1: Planar-laminated silty mudstone (Lithofacies Mpl) .....	222

6.6.2: Convolute-laminated silty mudstone (Lithofacies Mcl).....	229
6.6.3: Lithofacies association 1: Planar-laminated and convolute-laminated mudstones.....	232
6.6.4: Matrix-supported diamictite (Lithofacies Dms).....	237
6.6.5: Lithofacies association 2: Diamictites, outsized clasts and onvolute- laminated mudstones .....	241
6.6.6: Tabular-bedded sandstone (Lithofacies Stb).....	246
6.7: Discussion and Significance .....	251
6.7.1: A glacial source for extrabasinal clasts?.....	251
6.7.2: Umberatana Syncline as a salt-withdrawal minibasin.....	253
6.7.3: Relevance to the Ediacaran metazoan assemblage .....	257
6.8: Conclusions.....	259
6.9: Acknowledgements .....	260
6.10: References.....	261
<b>Chapter 7: Conclusions .....</b>	<b>275</b>
7.1: Summary and Implications.....	276
7.2 Future work .....	280
<b>Chapter 8: Appendices .....</b>	<b>282</b>
8.1: Files on CD .....	283
8.2: Supplementary Figures, Chapter 4 .....	284
8.3: Supplementary Figures, Chapter 5 .....	294

# Figures and Tables

## CHAPTER 2

Figure 1: Present-day satellite view of the Flinders Ranges and surrounds, with geographic regions labelled.....	10
Figure 2: Major proposed reconstructions of cratonic configurations within the Rodinian supercontinent .....	12
Figure 3: Global palaeogeography at approximately 750 Ma. ....	15
Figure 4: Present-day Australia, showing the position of the Tasman line and the locations of Proterozoic cratons and basins.....	16
Figure 5: Map showing location of Centralian Superbasin.....	18
Figure 6: Correlations across the Centralian Superbasin. Modified from Walter et al. (1995).....	19
Figure 7: Generalized basin-fill stratigraphy of the Adelaide Rift Complex.....	21
Figure 8: Large stromatolite in the Trezona Formation, a fine-grained unit in the upper interglacial interval. ....	29
Figure 9: Glacial tillite in the upper Elatina Formation, Brachina Creek.....	30
Figure 10: Tidal rhythmites in the Elatina Formation near Pichi Richi .....	31
Figure 11: The basal Ediacaran GSSP ("Golden Spike") in Brachina Creek.....	33
Figure 12: A large tepee structure in the Nuccaleena dolomite .....	34
Figure 13: The Acraman ejecta layer in the Bunyerroo Formation, Bunyerroo Gorge. ....	35
Figure 14: Google Earth view of the Fortress Hill canyon complex in the Wonoka Formation on Umberatana Station.....	39
Figure 15: Fine-grained shales and rapidly deposited sands with load structures in the Ediacara Member in Brachina Gorge.....	40
Figure 16: Dickinsonia, an Ediacaran organism, on display in Parachilna. ....	40
Figure 17: Vertical burrows in the Parachilna Formation, Parachilna Gorge .....	42
Figure 18: Minibasins seen in seismic section, Kwanza Basin, offshore East Africa. Courtesy TGS..	44
Figure 19: Various stacking patterns of halokinetic sequences .....	45
Figure 20: Seafloor topography in the Gulf of Mexico.....	50
Figure 21: Schematic salt geometries in the Gulf of Mexico.....	51
Figure 22: Subsurface structure map of top of evaporite sequence, Campos-Santos region, offshore Brazil.....	54
Figure 23: Deposition model of salt diapirs and minibasins in the Paradox Basin.....	56

## CHAPTER 3

Figure 1: Stratigraphy of the Adelaide rift complex basin fill, showing the position of the Bonney Sandstone in relation to other units .....	82
Figure 2: Detailed geological map of the study area and its position within Australia .....	85
Figure 3: Summary log and palaeocurrents.....	88
Figure 4: Stratigraphic column of the Bonney Sandstone in Bunyerroo Gorge .....	89
Table 1: Facies found in the Bunyerroo Gorge section of the Bonney Sandstone .....	92
Table 2: Facies associations found in the Bunyerroo Gorge section of the Bonney Sandstone.....	93
Table 3: Brief definitions of architectural categories. ....	95
Figure 5: Notation scheme for relative influence of wave, tidal and fluvial processes. ....	97
Table 4: Summary and classification of shallow marine depositional elements... ..	103
Figure 6: Cartoon showing schematic progradational parasequences sets during a highstand systems tract.....	105
Figure 7: Correlation with Gehling's (1982) Bonney Sandstone measured sections.....	106

## CHAPTER 4

Figure 1: (A) Location of Adelaide Rift Complex within Australia. Cratonic provinces in red, basins in yellow. (B) Geologic setting of area of interest, including major structural elements of the region. (C) Regional geologic map of the Northern Flinders.....	121
Figure 2: General stratigraphy and relative rock relationships of the basin fill in the Adelaide Rift Complex.....	123
Figure 3: Measured section MW .....	128
Figure 4: Measured section CR .....	129



Figure 5: Representative photographs of Lithofacies A and B.....	131
Figure 6: Representative photographs of Lithofacies C-F. ....	132
Table 1: Lithofacies and lithofacies associations described in this study. ....	135
Figure 7: Paleocurrents from the two measured sections of the Bonney Sandstone .....	137
Figure 8: Detrital zircon geochronology of the Bonney Sandstone, Rawnsley Quartzite, and Billy Springs Formation.....	148
Figure 9: Comparison of probability peaks in figure 8 with selected potential sources for zircons. ...	153
Figure 10: Regional reconstruction of structural and tectonic elements, sediment pathways, and salt-sediment relationships in the Bonney Sandstone. Schematic only; not to scale. ....	155
Figure 11: Correlation of parasequences and paleogeography over a series of time slices, showing depositional environments over the course of the formation .....	157

## CHAPTER 5

Figure 1: Location of Adelaide Rift Complex within Australia; Geologic context and location of study area.....	171
Table 1: Summary of typical lithologies of formations seen in this study, for comparison with diapir-influenced character seen in the Mt. Frome region.....	174
Figure 2: Local geology of the Mt Frome diapir region .....	176
Figure 3: Sections and palaeocurrents measured in this study. ....	177
Table 2: Summary of lithofacies seen in the minibasin. ....	178
Figure 4: Sedimentologic features seen in the Brachina and Wonoka Formations .....	179
Figure 5: Lithologic features of the Bonney Sandstone .....	180
Figure 6: Facies relationship diagram for the Mt. Frome minibasin margin.....	184
Figure 7: Schematic block diagram reconstructions of depositional environments and local palaeogeography in the Mt Frome area over a series of time slices .....	188
Figure 8: Comparison between observed diapir-margin geometry in the Mt. Frome area and experimental models of growth faulting and salt roller generation.....	193

## CHAPTER 6

Figure 1: Map of Australia showing major cratonic provinces, selected sedimentary basins, and Centralian Superbasin. ....	208
Figure 2: Locator map showing Adelaide Basin and field sites in relation to surrounding basins and cratonic provinces .....	210
Figure 3: Generalized lithostratigraphy of the Adelaide Rift Complex, Wilpena Group, and Pound Subgroup. ....	211
Table 1: Summary of salt-withdrawal minibasin studies in published literature, including only those where some component of sedimentology has been described.....	213
Table 2: Comprehensive list and summary of previous investigations of the Billy Springs Formation that discuss sedimentology or stratigraphy.....	215
Figure 4: Geologic map of the field area .....	216
Table 3: Brief description of stratigraphic units, measured section OSCS. ....	218
Table 4: Brief description of stratigraphic units, measured section OSCN .....	219
Figure 5: Stratigraphic sections measured in this study .....	221
Figure 6: Planar-laminated mudstone in thin-section.....	222
Figure 7: QEMSCAN images of planar-laminated lithofacies, Unit OSCS-G.....	223
Figure 8: Planar-laminated mudstone lithofacies .....	224
Figure 9: Rhythmite histogram and analysis.....	227
Figure 10: Convolute-laminated lithofacies in thin-section.....	229
Figure 11: X-Ray diffraction analysis of silty mudstones from planar- and convolute-laminated lithofacies .....	234
Figure 12: Convolute laminated silty mudstone lithofacies: outcrop photos .....	235
Figure 13: Diamictites, boulders, and exotic clasts found in the Billy Springs Formation .....	238
Figure 14: Wide range of exotic clasts seen in two 2"x3" thin sections from upper unit OSCS-A .....	240
Figure 15: QEMSCAN images showing detailed mineralogy of sample in unit OSCS-H, diamictite lithofacies .....	242
Figure 16: Interbedded sandstone-mudstone lithofacies .....	247
Figure 17: Sand-dominated lithofacies in thin section .....	248
Figure 18: Sequence stratigraphic interpretation of the relationship between the Wonoka Formation, Billy Springs Formation, and Wilpena Group .....	251
Figure 19: Diapirs of the northern Flinders Ranges, cross section, and Gulf of Mexico analogue ....	258

## Appendix

Figure 1: Photos of loading structures and and convolute lamination .....	284
Figure 2: Representative outcrops of the Pound Subgroup in the northern Flinders Ranges .....	284
Figure 3: Additional photographs of Lithofacies A1 .....	285
Figure 4: Additional photographs of Lithofacies A2 .....	286
Figure 5: Additional photographs of Lithofacies A3 .....	287
Figure 6: Additional photographs of Lithofacies B1 .....	288
Figure 7: Additional photographs of Lithofacies B2 .....	289
Figure 8: Additional photographs of Lithofacies C .....	290
Figure 9: Additional photographs of Lithofacies D .....	291
Figure 10: Additional photographs of Lithofacies F.....	292
Table 1: Summary of youngest individual concordant zircon ages in each sample.....	292
Table 2: Detailed interpretations of sedimentary environments for sediments found in sections CR and MW.....	293
Figure 11: Landscapes and outcrop expression in study area .....	293
Figure 12: Representative lithologies in the Rawnsley Quartzite and Wilkawillina Formations.....	295
Table 3: Timing of movement of selected diapirs throughout the Adelaide Rift Complex.....	296
Figure 13: Map of diapirs in the central and northern Flinders Ranges .....	296
Figure 14: Hypothetical movement and cross-section of Mt. Frome diapir.....	297
Figure 15: Typical extrusive salt dome in the Arabian Gulf.....	297

## Abstract

*Much of our understanding of the sedimentary character and stratigraphic architecture of subsurface sedimentary deposits is derived from field-based studies of similar depositional systems exposed in outcrop. In South Australia, excellent surface exposures in the Neoproterozoic-Cambrian Adelaide Rift Complex provide a unique opportunity to examine a series of clastic sediments deposited in an ancient fluvial-deltaic to deep marine setting. Through extensive field and laboratory work, this study documents the sedimentology, stratigraphy, provenance, facies distribution and salt-sediment interaction of the upper Bonney Sandstone and Billy Springs Formation. These sediments formed part of the margin of the Australian subcontinent during the Ediacaran, a key time in Earth history just prior to the development of multicellular life. Field investigations reveal that the Bonney Sandstone is primarily comprised of sands and shales, often in progradational parasequences that become progressively sand-dominated upward. The formation thickens significantly to the north through the preservation of additional sediments that contain abundant fluvial features, suggesting a northern depocentre in the basin. Zircon data indicate that sediments may be sourced from the distant Musgrave Province and enter the basin from a large deltaic system in the northwest. These results provide substantial new information as to the palaeogeography of South Australia during this time, and are the product of interpretation using multiple lines of evidence and the study of numerous localities.*

*Throughout the Adelaide Rift Complex, salt diapirs penetrated the basin fill and formed adjacent rim synclines (minibasins) due to withdrawal of underlying salt. Salt-tectonized, passive-margin settings are significant components of hydrocarbon*

*systems in some of the world's most productive regions, yet these features are rarely exposed in outcrop as they are here. In the far northern Flinders Ranges, the Umberatana Syncline is interpreted as a salt-withdrawal minibasin that formed in a deeper-water setting. The map-view exposure of the structure allows the depositional processes and products in the minibasin interior to be studied in a way not possible elsewhere; deepwater minibasins are very rarely exposed at the surface. Field and petrographic work reveals a mud-dominated minibasin fill containing mass-flow deposits of varying stages of maturity, ranging from clast-bearing convolute-laminated slumps to sandy turbidites. In a more proximal setting, numerous measured sections along the margin of the Mt Frome minibasin clearly show that sediment character is influenced by diapir activity and the shedding of diapir-derived clasts. Lateral facies variability is controlled by growth faulting and diapir topography, with increased abundance of diapiric material near faults and highs, as well as thinning, onlap, and rotation of sediment blocks. These results, as well as those from elsewhere in the basin, are highly applicable to the prediction of reservoir, source, and seal quality in similar geologic settings in the subsurface.*

## Declaration

I certify that this work contains no material which has been accepted for the award of any other degree or diploma in any university or other tertiary institution and, to the best of my knowledge and belief, contains no material previously published or written by another person, except where due reference has been made in the text. In addition, I certify that no part of this work will, in the future, be used in a submission for any other degree or diploma in any university or other tertiary institution without the prior approval of the University of Adelaide and where applicable, any partner institution responsible for the joint-award of this degree.

I give consent to this copy of my thesis when deposited in the University Library, being made available for loan and photocopying, subject to the provisions of the Copyright Act 1968. The author acknowledges that copyright of published works contained within this thesis resides with the copyright holder(s) of those works. I also give permission for the digital version of my thesis to be made available on the web, via the University's digital research repository, the Library catalogue and also through web search engines, unless permission has been granted by the University to restrict access for a period of time.

John Waldon Counts

Date

# Acknowledgements

I wish to thank the many people who have supported me personally and professionally throughout this project. First, I would like to thank my spouse Shelagh Jessop for coming with me to Australia and being understanding during the long process of writing this thesis. I would also like to thank my parents, grandparents, and family for their constant support, which has come in many different forms over the years. Third, I would like to thank my academic advisor, Kathryn Amos for many technical comments and helpful discussions, and for supporting my application to come to the University of Adelaide in the first place. Thanks are also due to Peter McCabe, and Bob Dalgarno, who provided much helpful advice over the course of this PhD.

Many other thanks are due to those who contributed to this thesis:

- Bruce Ainsworth, Jim Gehling, Ric Daniel and Vic Gostin for many technical discussions that impacted this work significantly
- My former advisor and excellent field partner Steve Hasiotis
- My fellow PhD candidates, research colleagues, and coauthors- Sara Moron, Tessa Lane, Jess Trainor, Frank Rarity, and Rachel Nanson
- Field assistants Claudia Valenti, Koyejo Oyinloye, and Limeng Liu
- Flinders Ranges landowners Barbara and Warren Fargher (Wirrealpa Station), Edie and Gina Nichol (Maynard's Well Station), and Jenny and Chris Mahoney (Umberatana Station)
- DEWNR for granting scientific research permits to Ikara-Flinders Ranges National Park and Vulkathunha –Gammon Ranges National Park

Funding for this thesis is provided in part by the American Association of Petroleum Geologists Nancy Setzer Murray Memorial Grant and a University of Adelaide International Postgraduate Research Scholarship. I acknowledge the traditional inhabitants of the land on which this research was conducted.

# **Chapter 1: Introduction**



## 1.1: Contextual Statement

This thesis examines a series of clastic sediments within the Adelaide Rift Complex, a Neoproterozoic-Cambrian basin in South Australia. It is intended to fill a knowledge gap in the understanding of the basin fill, as well as to provide a case study in sedimentary analysis applicable to the larger geoscience community. This study is the first instance in which the interval in question has been described and interpreted in detail, and many of the depositional settings discussed here are rarely found elsewhere in the world. The goal of this work is to develop a more complete picture of the formations in question from a sedimentologic perspective, including, but not limited to:

- Process-based sedimentology and depositional processes
- Regional Provenance
- Reconstruction of paleogeography and depositional environments
- Sequence stratigraphic interpretation and significance
- Lateral facies change at a variety of scales
- Scale and distribution of depositional elements
- Influence of salt movement on sedimentary character

These aspects of the basin are examined from a reservoir analogue point of view, with the goal that the findings here may be applied to similar deposits during petroleum exploration and development. The well-exposed sedimentary succession preserved in the Flinders Ranges provides an excellent natural laboratory in which to examine many of the components of a sedimentary system at a different scale of observation than typically seen in the subsurface.

This thesis is divided into an initial literature review and four independent papers that are each formatted for publication in international journals. All papers focus on the Bonney Sandstone or the time-equivalent Billy Springs Formation. As of the submission date, Paper 1 has been published in the Australian Journal of Earth Sciences, Paper 2 has been submitted to the Journal of Sedimentary Research, Paper 3 is planned for submission in the near future to *The Depositional Record*, and Paper 4 has been published in *Sedimentology*. These papers form Chapters 3-6.

*Chapter 2*, an in-depth literature review, aims to put the sediments described here in a larger context by reviewing many of the existing studies on the larger geologic setting and sedimentary fill of the basin. This allows this thesis to be seen within the framework of previous investigations into the Adelaide Rift Complex. Information is presented on the global continental relationships during the time interval discussed here, followed by a discussion on the Centralian Superbasin, a large intracratonic basin that was contemporaneous with the sediments that are the focus of this study. Although very little has previously been written on the Bonney Sandstone specifically, several of the other stratigraphic intervals units have received more attention and are discussed in Chapter 2. Continued study of the formation over the past several decades has resulted in an increasing emphasis on the salt tectonic-influenced aspects of sedimentation, and the interaction between diapirism, minibasin formation, and ongoing deposition. This topic is reviewed in the second part of the chapter, as it is critical to the understanding of salt-sediment interaction discussed in Chapters 5 and 6. Since another important aspect of this study is the applicability of these sediments to petroleum exploration, some relevant subsurface analogues are also discussed, focusing on those that have a component

of salt-sediment interaction.

*Chapter 3* (Paper 1) focuses on the type section of the Bonney Sandstone exposed in Bunyeroo Gorge. This section was reexamined and remeasured for the first time since its initial description over 30 years ago in order to provide a baseline for comparison for the data collected in subsequent studies. This paper uses a variety of methods of sedimentologic interpretation (e.g., facies models, WAVE classification scheme of Ainsworth et al., 2011- see Chapter 3) to determine the environments of deposition for this interval. In this study, the section was interpreted as being primarily composed of a series of coarsening-upward parasequences composed of fluvially dominated, wave-influenced deltaic mouth bars. This is in contrast to previous descriptions, which viewed the type section of the Bonney Sandstone as being dominated by fining-upward, tidally influenced marine sediments. In addition to the new formation-specific interpretations, the section also presents a case study in using a variety of methodologies to interpret sedimentary succession when only limited amounts of data are available. This is often the case in the Precambrian, where many of the trace and body fossils that assist with environmental interpretation are absent. For this paper, data collection in the field was assisted by the Reservoir Analogues Research Group (RARG) at the University of Adelaide, who also participated in numerous subsequent discussions on how to best interpret these sediments. The text and figures in this paper are reproduced exactly as published in the Australian Journal of Earth Sciences in 2016.

*Chapter 4* (Paper 2) examines the same formation in a remote and little-known area, over 100 kilometres to the north to the section discussed in Paper 1. This paper seeks to build on the initial interpretation developed in the first chapter by examining the formation at a more regional scale in order to reconstruct the large-

scale paleogeography of the formation. It consists of two major parts: 1) sedimentologic and stratigraphic interpretation across the northern part of the basin, combining the observations from two new, extended measured sections with those in the previous chapter, and 2) geochronology of detrital zircons in the formation, with the goal of determining the ultimate provenance of Bonney Sandstone and reconstructing the complete source-to-sink depositional system. Fieldwork consisted of several weeks in the northern Flinders Ranges, where over two kilometres of section were measured at a metre-scale level of detail. Detrital zircon analysis of over 2000 individual grains from five localities was personally conducted by the author at the University of Adelaide, beginning with sample collection and culminating in age determination from mass spectrometer results. This work reveals important new information about inter-basin connections in Australia during the late Ediacaran, and the sedimentologic evidence discussed here supports new interpretations of depositional environments in the Adelaide Rift Complex at this time. It also shows that the Bonney Sandstone is an excellent example of a Precambrian fluvial-deltaic system in which lateral palaeoenvironmental changes can be determined across a wide spatial area, a setting analogous to many productive hydrocarbon systems in the subsurface elsewhere. This chapter has been submitted as a manuscript that is currently in review with the *Journal of Sedimentary Research*.

*Chapter 5* (Paper 3) focuses on another important feature in the Bonney Sandstone—its interaction with one of the many salt diapirs that were actively penetrating through the formation during its deposition. Salt-sediment interaction is relatively uncommon in outcrop exposures worldwide, but is a fundamental part of some of the world's largest petroleum systems, including those in the Gulf of Mexico,

Africa, and Brazil. In the area around Mt. Frome on the eastern side of the basin, the Bonney Sandstone and other stratigraphically adjacent units were deposited in a salt-withdrawal minibasin that formed next to an exposed diapir. The sediments described in this chapter are a direct look into the lateral variability of lithofacies along the rim of this minibasin, and show that sedimentary character is tied to topographic expression of the diapir and extensional faulting along the minibasin rim. Unlike the sandy, fluvial-deltaic character that defines the formation throughout the rest of the basin, the sediments seen adjacent to the diapir are often dominated by pebble and cobble conglomerates, heavy mineral sands, and syndepositional faulting. This is one of few studies to be conducted that describe diapir-influenced sediments setting from a sedimentologists' perspective and is one of the first to systematically study lateral variability in an ancient minibasin. Fieldwork for this study was conducted over several weeks in August of 2015.

*Chapter 6* (Paper 4) looks at a different minibasin in the far north of the larger Adelaide Rift Complex, which was formed in a much deeper-water setting than the one at Mt. Frome. Instead of the Bonney Sandstone, it is filled by the time-equivalent, finer-grained Billy Springs Formation, and was deposited in a shelf or slope environment instead of the shallow marine or continental setting at Mt. Frome, Bunyeroo Gorge, and elsewhere. The minibasin fill is dominated by planar- and convolute-laminated muds, with occasional sandy turbidites and exotic diapir-derived boulders—similar facies to those described in core from minibasins in the Gulf of Mexico and elsewhere. This study describes and analyses these sediments in detail, and discounts a previous hypotheses that some of these sediments are derived from glacial processes. This is one of very few studies to examine an outcropping minibasin that formed in a shelf-slope setting, which is where productive minibasins

are most commonly found today. Thus, this study provides another important outcrop analogue that can be used to better predict properties of similar deposits in the subsurface. Fieldwork was conducted in 2013, followed by substantial laboratory analyses, including QEMSCAN-derived mineralogy, petrography, Fourier analysis, and X-Ray diffraction. Like Chapter 1, this chapter is reproduced in full from the published version, which will appear in the international journal *Sedimentology* in 2016.

Chapter 7 concludes this thesis by discussing the key points and significance of each of these studies, and suggesting possibilities for future research. Each of these studies forms a critical part of the larger 'big picture' of sedimentation in the basin during a specific time interval. The results presented here are useful in understanding the evolution of clastic fluvial-deltaic systems over time, the ways that facies are distributed in these systems across a basin, and the response of sediments to active salt uplift and erosion. When viewed together, they provide a thorough assessment of the basin-scale palaeogeography and range of depositional environments in the Adelaide Rift Complex during the late Ediacaran.

## **Chapter 2: Background and Review of Relevant Literature**

This chapter provides an overview of the geologic history of the Adelaide Rift Complex (also known as the “Adelaide Geosyncline” and “Adelaide Fold Belt”) in South Australia, as recognized in the published literature. It focuses primarily on the sedimentology, stratigraphy, and depositional environments of lithostratigraphic units or depositional sequences within the basin, as well as its connections to relevant surrounding provinces and other coeval basins within Australia. This information provides the background necessary to fully understand the spatial, temporal, and stratigraphic context in which the Bonney Sandstone lies, and demonstrates the need for the investigations presented in this thesis.

## **2.1: Present-day Geography and Recent History**

The Adelaide Rift Complex is coincident with the modern Flinders and Mt. Lofty Ranges. It extends over 600 kilometres across South Australia from the Willouran Ranges in the north, to Kangaroo Island in the south. Today, the Flinders Ranges are in continuity with the genetically related Mt. Lofty and Willouran Ranges to the south and northwest, respectively (Fig. 1). The modern topographic expression of the Flinders Ranges is the product of Sprigg’s Orogeny, an somewhat enigmatic, intraplate episode taking place over the last several million years related to the transfer of stress from the margins of the Australian plate (Dyksterhuis and Muller, 2008). Uplift continues today; the ancient fold belt provides a zone of weakness in which to accommodate ongoing compression. The region is thus one of the most seismically active zones in Australia (C  lerier et al., 2005).

In the Flinders Ranges, excellent exposures of Neoproterozoic basin fill sediments are afforded in part by the arid climate and lack of substantial vegetation cover (Fig. 1). The region receives around 250-350 mm rainfall on average per year,



and is classified as semi-arid (Preiss, 1987). This was not always the case; Pleistocene valley fill deposits preserved in some catchments show the occurrence of permanent or semi-permanent wetlands between 33 and 17 ka (Williams et al., 2011). Numerous creeks now flow through the area, which are usually dry but are periodically (although rarely) inundated by major floods. These creeks provide access to many of the area's bedrock exposures, including many of the sections measured here. Exposure is also



Figure 1: Present-day satellite view of the Flinders Ranges and surrounds, with geographic regions labelled.

promoted by extensive pastoral land use, primarily for livestock grazing. European settlement began in the mid-19<sup>th</sup> century, with the establishment of sheep and cattle stations and the granting of mining leases. Both of these activities continue until the present, although most of the copper mines in the region were largely uneconomic due to low yields and

unsustainable transport costs, and did not last past the early 20<sup>th</sup> century (Mincham, 1977). The only mine currently operating in the Flinders is the Leigh Creek Coal Mine, which produces low-grade Triassic coal and closed in 2016.

Today, tourism is an important part of the Flinders Ranges Economy. Much of the region is protected by Ikara-Flinders Ranges and Vulkathunha-Gammon Ranges National Parks, as well as the Arkaroola Wilderness Preserve. Geologic investigations in these areas have been ongoing since the mid- to late 19<sup>th</sup> century, beginning in earnest with the identification of Flinders Ranges strata as Precambrian in age by R.C. Tate at the University of Adelaide in the late 19<sup>th</sup> century. This initiated many decades of further research, led by Walter Howchin, Sir Douglas Mawson, Reg Sprigg, and many others. Official mapping of the Parachilna sheet was completed by Dalgarno and Johnson in 1966, and in the northern Flinders by Coats in 1973. More recently, a number of detailed sedimentary studies of individual units in the basin fill were completed in the late 1970s through early 1990s by PhD candidates from Flinders University, the University of Adelaide, and elsewhere. However, in the past 20 years, most research in the Flinders Ranges has focused instead on the structural, salt tectonic, and palaeontological (rather than sedimentary) aspects of the basin.

## **2.2: Palaeogeographic Context of the Adelaide Rift Complex**

Much of the Proterozoic sedimentation and basin formation throughout Australia is related to the breakup of the supercontinent Rodinia and the formation of an Australia-Antarctica subcontinent. There have been at least three supercontinents in Earth history: Nuna and Rodinia in the Proterozoic, and Pangaea in the Paleozoic -Mesozoic (Meert, 2012). Supercontinent formation throughout

earth history may be cyclic; it is hypothesized that the amalgamation of continents into a single landmass insulates the asthenosphere and causes a build-up of heat that leads to breakup shortly after formation (Gurnis, 1988). Compared to other intervals in Earth history, Proterozoic paleogeography is poorly understood. The exact nature and location of Rodinia and the former geographic position of modern-day continental cratons remains under debate.

### 2.2.1: Configuration and Breakup of Rodinia

Piper (2000, 2007, 2009) has criticized the entire idea of Rodinia's existence, favouring instead a different supercontinent, Paleopangaea, that was a generally coherent landmass from 2700-600 Ma. He interprets Rodinian continental reconstructions as unlikely based on the improbability of the proposed continental movements, among other reasons, as these reconstructions require the individual landmasses to be isolated and move independently until their assembly. The Paleopangaea hypothesis disagrees with the apparently unified polar wander paths until 600 Ma. Most researchers, however, agree that evidence points to

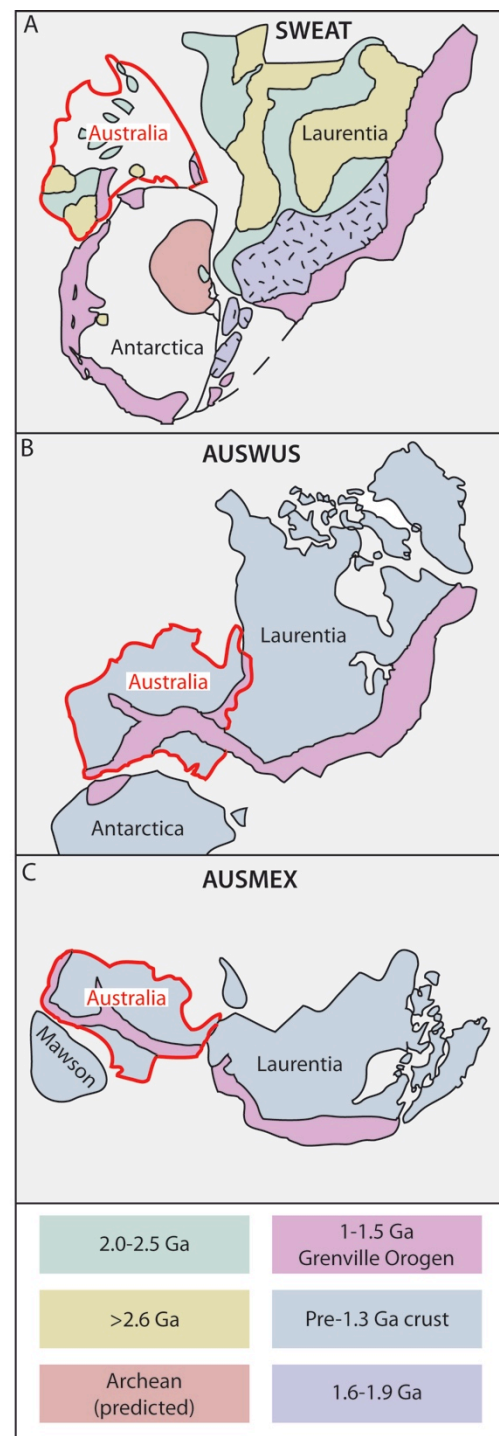


Figure 2: Major proposed reconstructions of cratonic configurations within the Rodinian supercontinent. Modified from Zhao et al., (2006)

Rodinia's existence. Several competing models for the configuration of the landmass have been proposed since the supercontinent was first named (McMenamin and McMenamin, 1990). Rodinia was most likely assembled from the fragments of Columbia around the beginning of the Neoproterozoic between 1050 and 900 Ma (Bogdanova et al. 2009). Assembly likely took place in numerous stages, with Laurentia, Siberia, and Amazonia being included prior to Baltica, India, and Australia. The breakup of Rodinia began shortly thereafter, between 825 and 700 Ma. It was during this phase that much of the sediment fill of the Centralian Superbasin and Adelaide Geosyncline were deposited, and the assembly of Gondwana began (Hoffman, 1999); amalgamation of Gondwanaland was complete by 530 Ma.

The configuration of continental cratons within Rodinia is the subject of much debate, and has implications for sediment provenance and palaeogeographic reconstruction in Australia. Each Rodinian palaeogeographic reconstruction is known by an acronym: SWEAT, AUSMEX, and AUSWUS (Zhao et al., 2006) (Fig.2), with some configurations having modifiers as both the ideas and configurations change through time. The AUSWUS (Australia-Western U.S.) hypothesis (described by Brookfield, 1993; Karlstrom et al., 1999, and others) places eastern Australia next to the western United States instead of near Canada. This hypothesis is based on the correlation of tectonic belts formed during the breakup of Rodinia, which may be shown to continue across North America into Australia (Fig. 2B). These correlations, however, have been questioned based on the reliability of paleomagnetic data used in both the SWEAT and AUSWUS reconstructions (Wingate et al., 2002). Wingate et al. (2002) formed another hypothesis, AUSMEX, (Australia-Mexico; Fig. 2C) which places Australia on the Laurentian margin in the relative position of present day

Mexico, although both continents were rotated relative to their current orientation. Some evidence for this hypothesis comes in the form of new Officer Basin well data that confirms a low latitude position for Australia between 810 and 750 Ma (Pisarevsky et al, 2007).

The SWEAT (Southwest US-East Antarctica) hypothesis (Fig. 2A) generally has the most support; it puts Australia and Antarctica in connection with the western margin of Laurentia. In this configuration, eastern Australia is in close juxtaposition to modern day Canada. Evidence also exists for a connection between the Shackleton Range of Antarctica and the rocks formed during the Grenville Orogeny in the southwestern United States around 1 Ga, giving the model its name and providing the primary evidence for this particular reconstruction. Li et al. (2008) undertook a large study of Rodinian continental reconstruction as part of a UNESCO-IGCP project to further investigate the supercontinent, concluding that the SWEAT hypothesis is most likely, but modifying it to place south China between Laurentia and Australia/Antarctica. They note the difficulty of reassembling Rodinia with the limited data available, and acknowledge that other hypotheses may also agree with available evidence. Giles et al. (2004) also modified the SWEAT configuration by rotating Australia relative to Laurentia.

Rifting and breakup of Rodinia began about 840 Ma and continued until around 750 Ma. According to Li et al. (2008) the cratons forming Australia and east Antarctica (and possibly south China) remained attached to one another and drifted away from the primary landmass (Fig. 3). The Adelaide Rift Complex was initiated during this time, as part of a tripartite aulacogen that ultimately resulted in an isolated Australia-East Antarctica subcontinent. This aulacogen formed part of what would ultimately become the continental margin; the eastern third of the current

continent of Australia would not accrete until the Phanerozoic. These original subcontinent boundaries are reflected in the distribution of Proterozoic rocks in Australia, which occur only to the west of the Tasman line (Fig. 4). Australia remained in low latitudes (<20 degrees) throughout the remainder of the Precambrian, including the time during which much of the basin fill (discussed here) was deposited. The paleogeographic position of Australia throughout the Neoproterozoic is determined in part by reliable paleomagnetic data from units in the Adelaide Rift Complex discussed below (Hoffman and Schrag, 2002; Hoffman and Li, 2009).

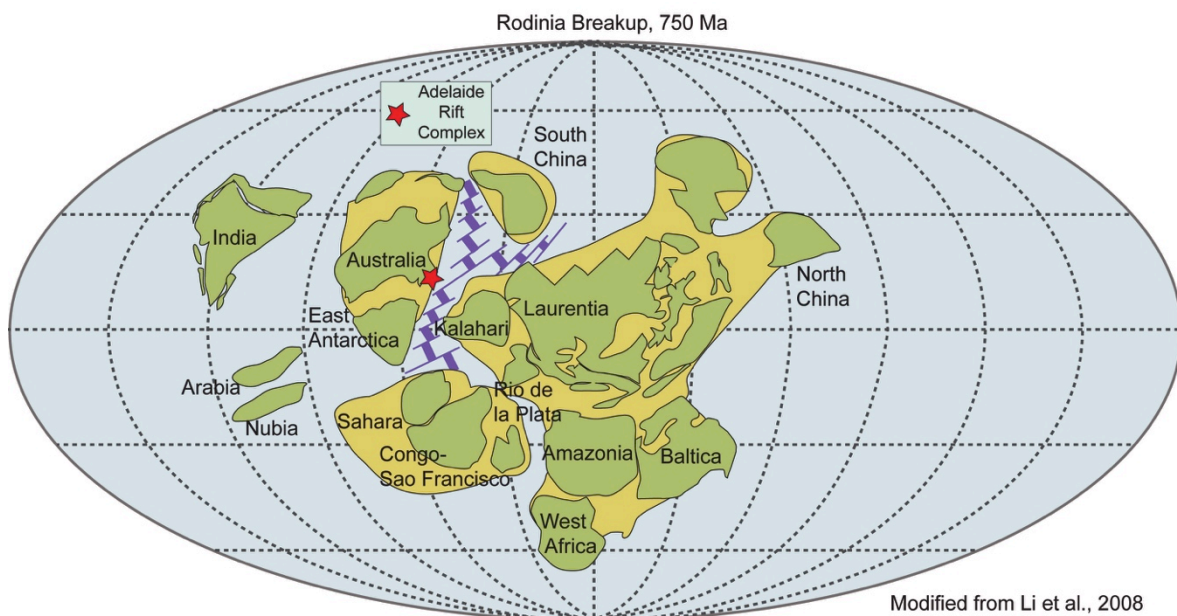


Figure 3: Global Palaeogeography at approximately 750 Ma.

The basin currently exists as a narrow, north-south trending trough bounded to the west by the relatively undeformed sediments of the Stuart Shelf, which lie unconformably atop the Paleoproterozoic and Early Mesoproterozoic volcanics, granites, and highly metamorphosed sediments of the Gawler Craton. To the east, the Adelaide Rift Complex is adjacent to the Curnamona Province, which is also

composed of older igneous and metamorphic continental crust (Preiss, 1987). The northern extent of the basin may have been limited by the Mulloorina Ridge, a gravity anomaly known only from the subsurface that likely represents Proterozoic basement (Von der Borch, 1980). The ultimate southern extent of the basin and surrounding provinces is unknown; potentially correlative sediments of Adelaidean age are found in Antarctica, but the exact relationships are unclear (Wysoczanski and Allibone, 2004). The basin was deformed through compression and shortening in the Cambrian Delamerian Orogeny, resulting in the upturned, folded and faulted sediments seen today.

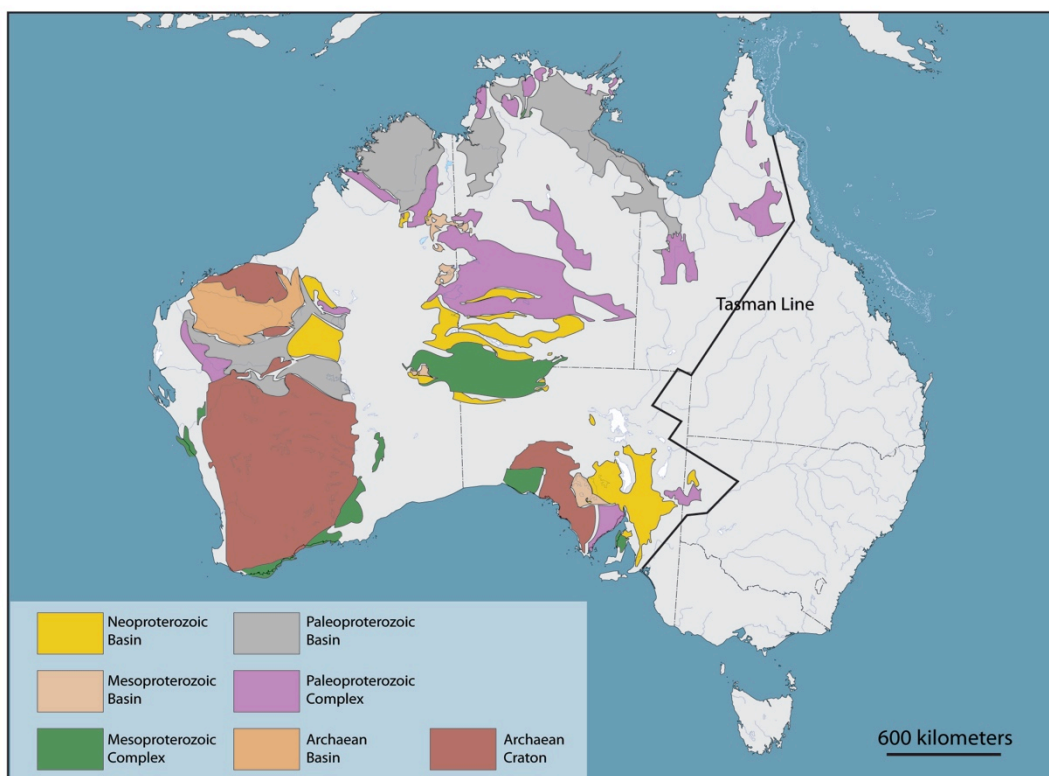


Figure 4: Present-day Australia, showing the position of the Tasman line and the locations of Proterozoic cratons and basins. From Parker (1993).

## 2.3: Geology of the Centralian Superbasin

### 2.3.1: Overview

The Adelaide Rift Complex shares many similarities with a larger intracratonic basin known as the Centralian Superbasin, which covered much of the Australian Subcontinent during the Neoproterozoic. The superbasin covered over 800,000 square miles, and comprised the present-day Officer, Amadeus, Ngalia, Savory, and Georgina Basins (Fig. 5). These were likely connected to the Adelaide Geosyncline to at least some degree, as the sedimentary sequences in each of these basins share many similarities. Formation began roughly 800 Ma, and deposition continued until the Peterman Ranges Orogeny fragmented the once-continuous basin around 540 Ma (Walter et al., 1995). Basin formation was related to the breakup of Rodinia, and termination of subsidence and breakup of the basin was related to the collision of India and Australia and the assembly of Gondwana (Devries et al. 2008). Lindsay et al. (1987) interpreted basin formation to have taken place during two periods of crustal extension, at 900 and 600 Ma. Grey and Calver (2007) attempted to correlate the Ediacaran period across Australia; while absolute ages were difficult to determine, correlations were possible using an integrated approach that combined biostratigraphy, sequence stratigraphy, Carbon isotopes, and the Acraman ejecta.

Evidence for the Centralian Superbasin today exists in the form of lithostratigraphic similarities between existing, smaller structural basins. Unlike continental margin basins where mechanisms of formation can be readily explained, intracratonic basin formation is usually more enigmatic. The large scale of the Centralian Superbasin cannot be explained by local tectonic processes, and has been hypothesized to have been formed due to crustal thinning associated with a large mantle plume (Zhao et al. 1994)



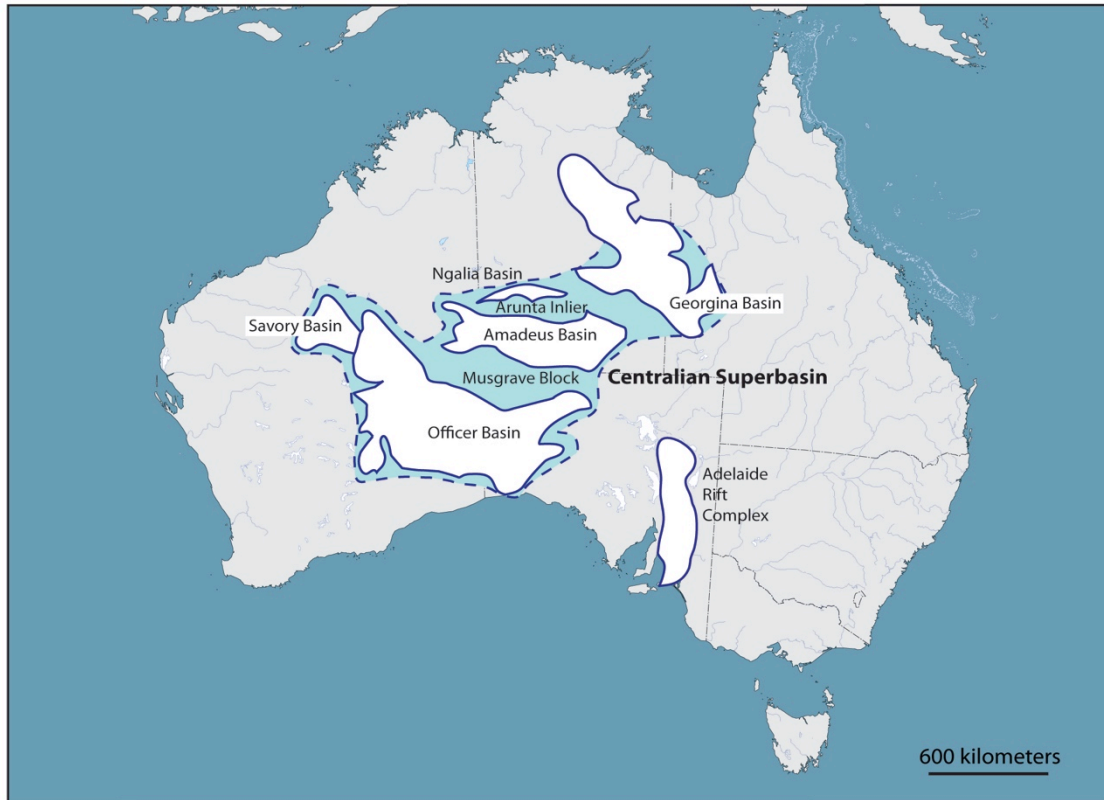


Figure 5: Map showing location of Centralian Superbasin, cratonic provinces, and constituent basins. Modified from Walter et al. (1995)

### 2.3.2: Basin Fill

Walter et al. (1995) divided the Centralian superbasin into four supersequences based on distinctive sedimentation patterns, and attempted to correlate strata across several basins (Fig. 6). Supersequence 1 contains a thick quartzitic sand that consistently lies at the base of the basin fill of each sub-basin; Preiss and Forbes (1981) believe these lowermost thick quartzites present in most central Australian basins were deposited prior to the Callanna Group in the Adelaide Geosyncline.

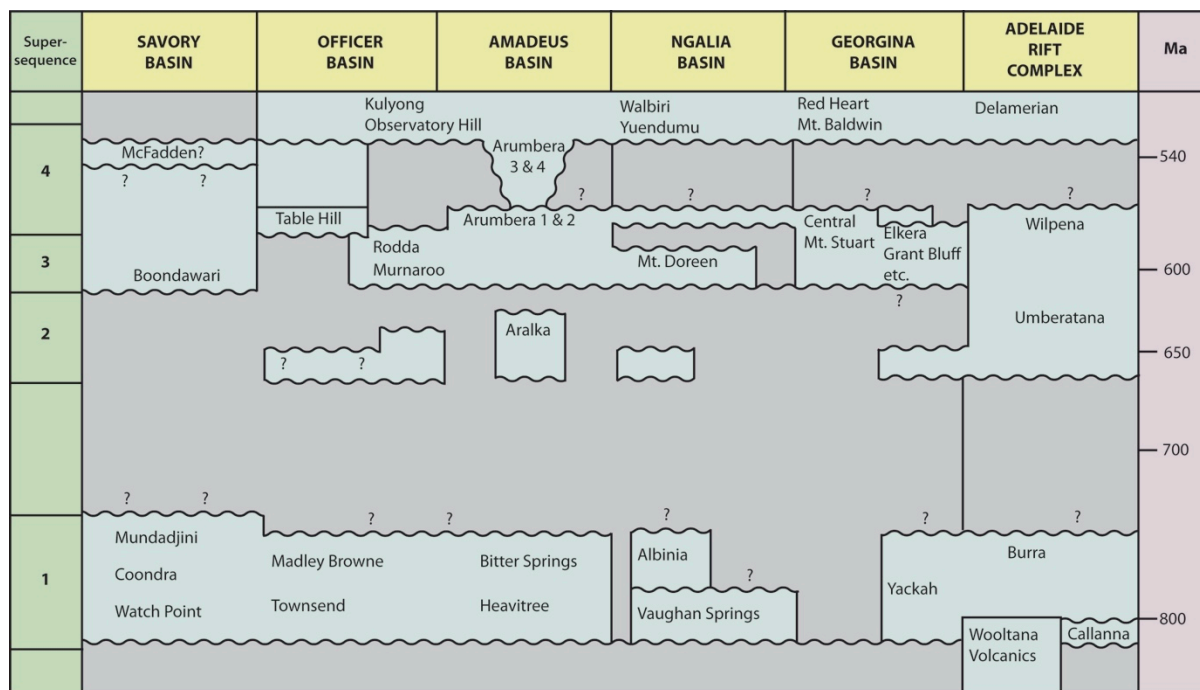


Figure 6: Correlations across the Centralian Superbasin. Modified from Walter et al. (1995)

Supersequence 2 is defined by the beginning of the Sturtian Glaciation, and is thus coincident with the Umberatana Group in the Flinders Ranges area. Lithologies in this supersequence are generally poorly sorted, glacially derived diamictites. Supersequence 3 likely correlates with the Marinoan/Elatina glaciation at the base, and continues into Wilpena Group equivalents. Glacial deposits are widespread, and are capped by a dolomitic unit in the Amadeus and Ngalia Basins. Preiss and Forbes (1981) believe that both the Sturtian and Marinoan glacial episodes can be correlated across central Australia, although in the Georgina Basin, no glacial deposits are present, suggesting that glaciation did not completely cover the current Australian continent. Supersequence 4 contains trace fossils and the Ediacaran biota, and is generally sand-dominated. Although sedimentation within individual sub-basins continued well into the Phanerozoic, they were no longer connected.

Most sediments filling the Centralian Superbasin during the Neoproterozoic were largely sourced from the 1000-1800 Ma Paleoproterozoic-Mesoproterozoic

Arunta Inlier (Collins and Shaw, 1995; Maidment et al. 2007) adjacent to the Amadeus and Officer Basins. Later, during the Peterman Orogeny, the Musgrave Block was uplifted and became the predominant source for the Amadeus Basin sediments in the Early and Middle Cambrian. In the late Cambrian and Early Ordovician, sediments became sourced from elsewhere in Gondwana that is consistent with Africa or Antarctica.

#### **2.4: Stratigraphy and Sedimentology of the Adelaide Rift Complex**

Initial deposition in the Adelaide Rift Complex is hypothesized to have begun around 840 Ma, based on isotopic work in the Wooltana Volcanics (Wingate et al., 1998), a thick sequence of basalts in the upper Arkaroola Subgroup. Rifting is related to the breakup of the supercontinent Rodinia, of which the western 2/3 of Australia was a part. The basin is believed to have gone through at least five separate rift cycles throughout its history, each of which is separated by a period of tectonic quiescence and sag-phase deposition. In each of these rift-sag cycles, reactivation of rifting coincides with the top of one of 16 sequence-sets defined by Preiss et al. (1993). In addition to these larger-scale rifting episodes, extension was likely ongoing throughout deposition of most of the fill, as syndepositional faulting is recognized throughout the basin.

The lithostratigraphic units that comprise the fill of the Adelaide Geosyncline are divided into three Supergroups, and numerous Groups, Subgroups, and Formations (Fig. 7). Stratigraphic units are discussed here in stratigraphic order from oldest to youngest, organized at a group level.

Chronostratigraphic units	Lithostratigraphic units, Flinders Ranges					Major events	Estimated Ages				
	Supergroup	Group	Subgroup	Selected Formations	Member						
?mid-Cambrian	Moralana	Lake Frome				Redbeds	~510 Ma				
Early Cambrian		Unnamed		Wirrealpa		marine limestone					
		Hawker		Billy Creek		redbeds, tuffs					
Marinoan	Heysen	Wilpena	Pound	Parachilna	Ediacara	archaeocyathan reefs	~510 Ma				
				Wilkawillina		worm-burrows					
				Rawnsley		thick sand sheet					
				Bonney		metazoan fossils					
				unnamed		Redbeds					
				Wonoka		submarine canyons					
		Sandison	ABC Range	bolide impact layer							
			Brachina	transgression-regression							
			Nuccaleena	transgression-regression							
		Sturtian	Umberatana	Yerelina	Elatina				Glaciation	?635 Ma or 580 Ma	
									Upalinna	Angepena	basin-margin redbeds
										Nepouie	Balcanoona
Yudnamutana	Tapley Hill						Tindelpina		transgression-regression	~650Ma	
	Wilyerpa								deglaciation, rifting	~660 Ma	
							Appila/Pualco				glaciation, rifting
Torrensian	Warrina	Burra	Belair			Sag basin, deltas	~790 Ma				
			Bungarider			Sag basin, deltas, deep-water dolomite					
			Mundallio			Skillogalee		paralic dolomite, magnesite			
			Emeroo			Kooringa		Burra Cu, felsic magma			
Willouran	Callanna	Curdimurka				major rifting, clastics, minor mafic volcanism	~800 Ma				
						Rook		major rifting, clastics, carbonates, evaporites			
						Wooltana		minor mafic and felsic volcanism			
						Wywyana		mafic volcanism	827±6 Ma		
		Arkaroola	Paralana			sag basin					

Figure 7: Generalized basin-fill stratigraphy of the Adelaide Rift Complex. Modified from Preiss (2010).

#### 2.4.1: Callanna Group

Perhaps the least studied interval in the Adelaide Rift Complex, the Callanna Group is poorly exposed in comparison to younger units in the basin. The Adelaide Geosyncline during this time was generally a fault-bounded rift basin, as opposed to

the passive continental margin it would become during most of its subsequent history (Preiss, 1987). Salt diapirs in the basin originated from evaporites in the Callanna Group, and created topographic relief at the surface that influenced deposition in several areas (Dalgarno and Johnson, 1968). The formation is therefore frequently tectonically deformed or exposed as allochthonous block within diapirs (Preiss, 2000). Detailed sedimentological studies are therefore rare; however, general lithologies have been worked out, and the stratigraphic sequence has been pieced together from numerous disparate outcrops.

The oldest *in situ* sedimentary unit that is exposed in situ in the basin fill is the ~1000 meter thick Paralana Quartzite in the Arkaroola Subgroup (part of the Callanna Group), which was unconformably deposited onto exposed basement (Thomson, 1966). It consists of a lower conglomeratic member containing cobble-sized grains of mixed lithology, and two upper sandstones that abruptly change from cross-bedded, poorly sorted sands at the base, to well sorted massive quartzites in the upper member. This sequence has been proposed to represent a deepening upward trend, beginning with the talus-slope deposition of the conglomerate and culminating in a shallow marine environment near the top of the formation—some areas near the top of the Paralana also contain columnar stromatolites (Preiss, 1987). Above the Paralana lies the Wywyana Formation, a metamorphosed carbonate unit composed of marble and amphibolite. It likely had a dolomitic precursor and is folded and intruded into the overlying unit, and thought by some (e.g., Coats and Blissett, 1971) to be the source of the diapirs in the region. Preiss (1987) considers the the Wywyana to be deposited in deeper water, away from wave influence, but also considers that it could have been lacustrine. Turner (1976) notes that most sedimentary structures in the Paralana and Wywyana have been

destroyed by metamorphism and tectonic deformation, at least in the Mt. Painter region of the Flinders Ranges.

The uppermost Arkaroola Subgroup contains a laterally consistent package of extrusive igneous rocks, known in the northern Flinders Ranges as the Wootana Volcanics. These are approximately correlative to several other igneous formations that are variably present across 250,000 km<sup>2</sup> in central Australia (Preiss 1987). These volcanics are predominantly basalts and are thus generally unsuitable for radiometric dating, and were deposited during a period of regional tensional stress that resulted in widespread igneous activity. Relative sea level was low during this interval, which ends at the base of the Curdimurka Subgroup at approximately 810 Ma (Preiss, 2000). The Curdimurka Subgroup is best exposed in the Willouran Ranges just north of the Flinders, and contains a number of cyclical lithologies that are found throughout the basin but cannot be confidently correlated with one another throughout the entire Adelaide Geosyncline. Repetitive deposition of siltstones, sandstones, and stromatolitic carbonates likely took place in multiple sub-basins that were semi-connected at different times (Mackay, 2011). The Curdimurka is known only in the northern part of the Adelaide Rift Complex; it is likely that other areas within the basin were topographic highs and areas of erosion (Preiss, 1987).

In the north, the lowermost unit of the Curdimurka is the Dome Sandstone, which contains a number of sand-rich lithologies that range from ~200~1500 meters thick. Channels, crossbedding, and local halite and dolomite suggest a fluvial or marginal marine environment. The felsic Rook Tuff lies atop the Dome and is one of the few units that can be dated with some degree of certainty (802 Ma) (Hill and Walter 2000), constraining the ages of other early formations in the basin fill. Together with the overlying Dunns Mine Limestone and Recovery Formations, this

interval represents a sustained period of marginal marine deposition. The Hogan Dolomite, with evaporite pseudomorphs, tepee structures, and polygonal cracks, and the siltstone-rich Cooranna and Boorloo Formations, record similar environments stratigraphically upward. The Curdimurka Subgroup therefore contains a number of transgressive-regressive cycles that reflect only minor changes in the basin environment. Lack of widespread continuity indicates that cyclicity is most likely tectonically controlled (Mackay, 2011).

#### *2.4.2: Burra Group*

The Burra Group, defined by Thomson et al. (1964) is more widespread than the Callanna, and is better exposed and better studied. It is present throughout the Adelaide Rift Complex, and generally can be correlated in some detail across the basin. In the Flinders Ranges, the Burra consists of two predominantly clastic subgroups at the base (the Emeroo and River Wakefield Subgroups), overlain by the dominantly carbonate subgroup Mundallio Subgroup. The Burra, like the Callanna Group, displays repeated depositional cycles of similar lithologies. Many sediment packages are interpreted as having been deposited in lacustrine or restricted environments.

The Emeroo subgroup is present in the North Flinders as the Humanity Seat Formation, Woodnamoka Phyllite, and Blue Mine Conglomerate. The Humanity Seat has been interpreted as a shallow-water and fluvially influenced environment, possibly in a braided river system with associated sheet-flooding and drainage into a shallow restricted body of water (O'Halloran, 1992). It is partially correlative with the Woodnamoka Phyllite to the west. The overlying Blue Mine Conglomerate contains mudcracks and ripple marks, and larger clasts of mixed lithology, and is thought to

have been deposited on a fluvially influenced shoreline (Coats and Blissett, 1971; Preiss, 1987). O'Halloran (1992) looked at these formations in a sedimentological and geochemical context, and placed the Blue Mine Conglomerate in braided stream and alluvial fan environments. He also noted evidence for tidal influence in the Emeroo Subgroup due to increasing connection with the larger ocean. To the south, the basal unit of the Emeroo Subgroup is the Rhynie Sandstone, a thick quartzite known for heavy mineral laminae that was deposited in a more landward, fluvially influenced setting than its' northern equivalents. The River Wakefield Subgroup intertongues with the Emeroo and was deposited after Rhynie time during an overall transgressive interval; facies suggest a depositional environment that is generally more marine-influenced than those below. These formations are dominantly silty or dolomitic, and represent at least two fining-upward sequences that are consistent throughout the basin.

In contrast to the underlying strata, the Mundallio Subgroup and most of the remaining upper basin fill have been relatively well-studied due to better exposures and less intense metamorphism in this part of the section. The Skillogalee Dolomite is the considered the primary unit and is the most widespread. In the Flinders Ranges, clastics dominate the lower Mundallio in a number of different formations, whereas the Skillogalee dominates the upper part of the sequence. Upphill (1979) interpreted the lower half of the subgroup to have been deposited in a variety of clastic-dominated environments, with minor dolomite-rich units deposited in a low-relief ramp-type setting that records numerous noncyclic facies changes. These sediments represent marginal marine and shallow marine environments. The Skillogalee includes recrystallized dolomites, Magnesite, and terrigenous clastics. These were thought by Upphill (1979) to have been deposited in shallow,



subaqueous mudflats with intermittent subaerial exposure and variable clastic supply. Nodular and intraclastic Magnesite beds are interpreted to be sedimentary in origin and were deposited in ephemeral, nearshore lakes.

More recently, Frank and Fielding (2003) re-examined Magnesite in the Skillogalee to better understand its' origin. As primary Magnesite is not extensively deposited as a sediment in the present-day, the precise origin of extensive deposits in the Neoproterozoic has been a longstanding controversy (the "Magnesite problem"), and is thought to be related to the differing geochemistry of the Precambrian oceans. Unlike Upphill (1979) and von der Borch and Lock (1979), Frank and Fielding support a marine rather than lacustrine origin for Skillogalee-type deposits, where Magnesite occurs without Calcium Sulfate minerals. Recent analyses support this idea (Kah et al., 2001; Hurtgen et al., 2002) suggesting that the Proterozoic oceans were carbonate-enriched and sulfate-poor, a chemistry that would promote Magnesite precipitation. Skillogalee equivalents ("ER4-ER7") in the Willouran Ranges described by Heithersay (1979) are interpreted as a generally shallowing upward cycle, from dark shales at the base, coarsening upward to sands, and finally to heterogeneous lithologies capped by cryptalgal and stromatolitic dolomites. This sequence is interpreted to represent the transition from a reducing, offshore environment below wave base, through an interval of progradation of deltaic and marginal marine strata, to nearshore and subtidal environments closer to the top. Primary Magnesite is absent in higher-energy environment of the Willouran Ranges, in keeping with the idea that its formation is related to restricted or lacustrine deposition in quieter water.

The Belair Subgroup is earliest Sturtian in age, but is lithologically more similar to the preceding Burra Group deposits, rather than those above. Composed

primarily of fine-grained clastics and immature sands, it is well-exposed in the southern Flinders Ranges, including much of the Clare Valley where it is economically important for mining and viticulture. The Mintaro Slate may represent the earliest glacial deposits in the basin, as it contains rare limestones that indicate the presence of sea ice, at least intermittently (Preiss et al., 2010). A significant unconformity exists at the top of the Burra Group separating these sediments from the Sturtian glacials above.

#### *2.4.3: Umberatana Group and Cryogenian Glaciation*

Lying unconformably above the Burra Group, and comprising the lower Heysen Supergroup, the Umberatana Group records the onset of significant glaciation in the basin. Sediments deposited during the Umberatana time (Sturtian and Marinoan ages) have been reliably constrained to low paleolatitudes by paleomagnetic data (Hoffman and Schrag, 2002, and references therein), while also containing sediments clearly derived from nearby glacial activity. Glacial sediments in the area were first recognized by Howchin (1900), and have since been the focus of much research in South Australia. These deposits were integral in formulating the original “Snowball Earth” hypothesis, i.e., the idea that Earth during this time was completely covered in glacial and sea ice during the Cryogenian period of the Neoproterozoic. Alternative views of the Snowball Earth hypothesis abound. Many of these call into question the reliability of paleomagnetic latitude data (e.g., Meert and van der Voo 1994; Meert and Torsvik, 2004), suggesting that Neoproterozoic glaciations were not as extensive as initially thought because continents were actually in higher latitudes. More recent studies have questioned whether ice cover was complete or only partial, based on sedimentary structures within glacial periods that require ice-free conditions (e.g., Williams et al., 2008; Le Heron et al. 2011a;

2011b). Eyles and Januszczak (2004) question instead whether many of the global 'glacial' deposits are indeed glacial at all-- they interpret many of the poorly sorted diamictites in numerous formations around the world to be mass-flow deposits that do not originate from a glacial source. They are specifically skeptical of several intervals in the Marinoan sequence previously interpreted as glacial, referring striated exotic clasts to tectonic and diapiric processes, while still acknowledging the presence of ice wedges in Elatina-correlative strata. Despite the controversy, the view that currently prevails is one of at least periodic glacial activity in low latitudes, but not the complete global ice cover that was initially proposed by Hoffman (1998). Two distinct glacial periods are found in the Umberatana Group, referred to as the Sturtian and the Marinoan.

#### *2.4.3.1: Sturtian Glacial Interval*

The lowermost units of the Umberatana Group are a laterally variable, correlative set of glacially deposited strata that are recognized as the beginning of the Sturtian Glaciation, the earlier of two distinct glacial periods in the Neoproterozoic. Preiss et al. (2011) recently reviewed many aspects of the geology of the Sturtian glaciation. They note that during Sturtian time, active rifting in the Adelaide Geosyncline led to the deposition of 3-5 kilometers of siltstones, sandstone, conglomerate, diamictite, and ironstone in the eastern and northern Flinders Ranges. Relationships between these lithofacies are complex; many interfinger and are laterally variable. In the southern Flinders, the Appila and Pualco Tillites and the Holowillena Ironstone are thick successions of diamictite and fine-grained hematite containing glacial dropstones. In the Northern Flinders, both the Merinjina Tillite and the Yudnamutana subgroup contain striated, basement-derived clasts, dropstones, and other evidence of glaciation (Link and Gostin, 1981). These

units record repeated glacial advancement and retreat, rather than a single episode. Lithologies during the Sturtian glacial episode were interpreted by Preiss et al. (2011) as glacial-marine outwash deposits, and core through the Sturtian sequence described by Eyles et al. (2007) also regard several Sturtian glacial sediments as being submarine in origin. They emphasize the contribution of glacial meltwater to the depositional processes in the Sturtian section, which has implications for the “snowball earth” hypothesis, wherein the ‘snowball’ is less ‘hard’ and did not completely shut down the hydrological cycle. Other authors (e.g., Le Heron et al. 2011a) agree that the abundance of sedimentary structures in the Sturtian sequence that require moving water are important evidence for a glacial event that was not completely global. Young and Gostin (1988, 1989, 1990, 1991) worked extensively on many of these sediments, and interpret them as glacially influenced subaqueous mass flow deposits.

#### 2.4.3.2: *Interglacial Formations*

Above these units, the overlying Tindelpina Shale Member of the Tapley Hill Formation contains no glacial debris and therefore marks the end of the Sturtian

glacial sequence. This formation, in the center of the Umberatana Group, consists of thousands of metres of black shale and marks a sustained period of deposition free from



Figure 8: Large stromatolite in the Trezona Formation, a fine-grained unit in the upper interglacial interval.

glacial influence. The Sturtian glacial interval here is capped by fine-grained, laminated limestones and peloidal dolomites of the Tindelpina Shale Member, unlike many other Neoproterozoic glacial episodes throughout the world, which terminate in a carbonate unit containing a suite of unique sedimentary features (Giddings and Wallace, 2009). Based on carbon isotopes, the formation has been interpreted as a stratified ocean related to an influx of glacial meltwater. Several other interglacial formations lie between the Tapley Hill and the onset of the subsequent Marinoan glaciation, recording a series of laminated silty shales and limestones (e.g., the Trezona Formation shown in Fig. 8) that were deposited in various marine environments. Sedimentation during this interval was also influenced by diapiric tectonics—the Enorama diapir was a topographic high (likely forming an island), which may have been scoured by glacial movement and provided a source for much of the increased sedimentation surrounding it (Lemon, 2000; Lemon and Gostin, 1990). The Yaltipena Formation, the stratigraphically highest interglacial in the Central Flinders, records a shallow marine carbonate environment that is part of the overall regression associated with the onset of the subsequent Elatina glaciation (Lemon and Gostin, 1990).

#### *2.4.3.3 Marinoan Glacial Interval*

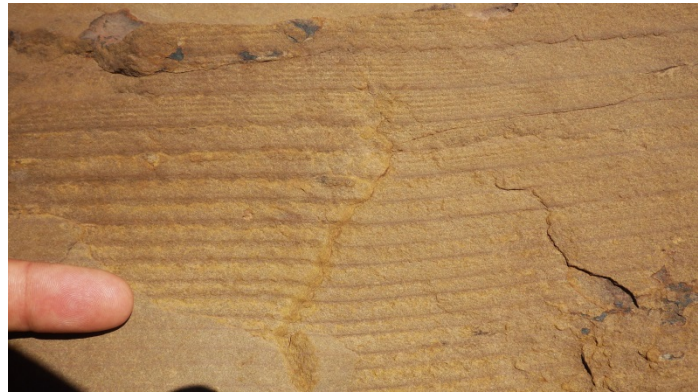
The Marinoan (Elatina) glacial interval comprises a single formation and its equivalent strata in the Flinders Ranges area, the



Figure 9: Glacial tillite in the upper Elatina Formation, Brachina Creek

Elatina Formation (Fig. 9). The formation is generally sandy in the lower half and heterogeneous in the upper half (Le Heron et al. 2011a), with the lower interval interpreted to be the product of fluvially deposited glacial outwash, and the upper portion representing a mix of environments, including outwash plains and tidal flats. The sequence records progressive deglaciation overall, with smaller-scale

fluctuations of glacial influence internally. Williams et al. (2008) and Williams et al. (2011) examined the sedimentology and depositional environments of the



*Figure 10: Tidal rhythmites in the Elatina Formation near Pichi Richi*

Elatina Formation throughout the basin. They found numerous

sedimentary facies, including terrestrial, ice-free permafrost zones on the adjacent Gawler Craton, fluvial-deltaic and shallow marine deposits in the central Flinders, and thick, glacially derived deeper-water sediments in the north Flinders. Like the Sturtian interval below, the presence of wave and tidal indicators, as well as laminated sediments with exotic dropstones, indicate that ice cover was intermittent during this period. Periglacial structures (e.g., sand wedges) in some facies indicate that climate during this time was strongly seasonal but generally arid. Williams et al. (2011) also found paleomagnetic data and found it to be reliable based on fold tests, and to record a mean paleolatitude of 6.5 degrees. Their observations confirm the presence of near-equatorial ice during this time, but also provide unequivocal evidence for open water movement during the Marinoan. The authors note the need for additional dating work, which could only be constrained to between 640 and 580 Ma.

The upper Elatina is strongly tidally influenced (Williams et al., 2008; Le Heron et al. 2011). Cyclic, mm- to cm-scale bundling of laminae (Fig. 10) within the formation has been the focus of several studies, and was initially thought to be the product of solar activity cycles (Williams and Sonnett, 1985; Sonnett and Williams, 1987). Later interpretations moved to a model requiring solar-tidal interaction (Zahnle and Walker, 1987; Sonnett et al., 1988), and finally to a purely tidal origin for the rhythmic sequence (Williams 1988; 1990; 1997) Although the tidal origin is currently generally accepted, some recent authors (e.g., Raub, 2010) have returned to the accepting the plausibility of the solar hypothesis.

Le Heron et al. (2011b) compared both the Sturtian and the later Marinoan intervals and found several differences in the glacial facies sequences and in the style of deglaciation, but noted that six distinct facies associations could be applied to both sequences. Diamictites (poorly sorted sediments) in both intervals are typified by a wide range of clast lithologies and are closely associated with cross-stratification, implying subaqueous deposition in conditions free of complete sea-ice cover. Other facies (hummocky cross-stratification beds, sheet sandstones deposited in outwash plains, and tidally influenced flaser bedding) also provide evidence that glacial periods were at least intermittent. However, the older Sturtian sequence is significantly thicker than the upper Elatina (maximum thicknesses of 4.5 kilometre vs. 1 kilometre), and is generally deposited in deeper, more marine conditions. Tillites in both the Sturtian and Marinoan sequences can be tentatively correlated to glaciogenic deposits in other basins in central and western Australia (Coats and Preiss 1980), implying that glaciation was widespread throughout Australia at the time (see discussion in chapter six).

#### 2.4.4: Wilpena Group



Figure 11: The basal Ediacaran GSSP ("Golden Spike") in Brachina Creek

The Elatina (and thus the Umberatana Group) is capped by the lowermost formation in the Wilpena Group: the laterally persistent, dolomitic Nuccaleena Formation. The base of the Nuccaleena is also the Global Stratotype Section and Point

(GSSP) that defines the base of the Ediacaran Period worldwide (Fig. 11) (Knoll et al., 2006). Nuccaleena-type "cap carbonates" often overlie glacial deposits in Neoproterozoic successions worldwide (Kennedy et al., 2001), leading to the hypothesis of a genetic link between the termination of glacial conditions and the deposition of these units. Cap carbonates often share a host of features that give clues to their formation; these include tepee structures, early cementation and brecciation, gas hydrate escape structures, and features indicating microbial binding (Kennedy et al., 2001). The formation of large tepee structures (Fig. 12) topped by small growth faults was interpreted by Gammon et al. (2005) to be the product of early subsurface diagenesis and expansive crystallization. Other authors, however, have alternate interpretations for these unusual structures. Allen and Hoffman (2005) believed them to be syndimentary giant wave ripples, and Kennedy (1996) suggested they are related to gas escape structures (cold seeps). More significant is the global persistence of these lithologies and the underlying mechanism behind their deposition. Rose and Maloof (2010) examined several proposed models for cap carbonate deposition after glaciation. Three mechanisms have been proposed:



1) a synchronous model wherein carbonates were deposited at the same time globally due to methane clathrate seeps,

2) a semi-diachronous model where meltwater from receding glaciers led to a stratified ocean and carbonate was precipitated by



Figure 12: A large tepee structure in the Nuccaleena dolomite.

microbes in a low-salinity ocean. Carbonate deposition would initially track receding glaciers but would then be isochronous once high-latitude glaciers had melted and meltwater was evenly distributed,

3) A diachronous model that relies on 'super-greenhouse' conditions during deglaciation, which led to acidic meteoric waters, rapid weathering, and subsequent alkaline oceans and cap carbonate deposition. In this scenario, carbonate deposition would be dependent on paleoelevation and would track rising sea level.

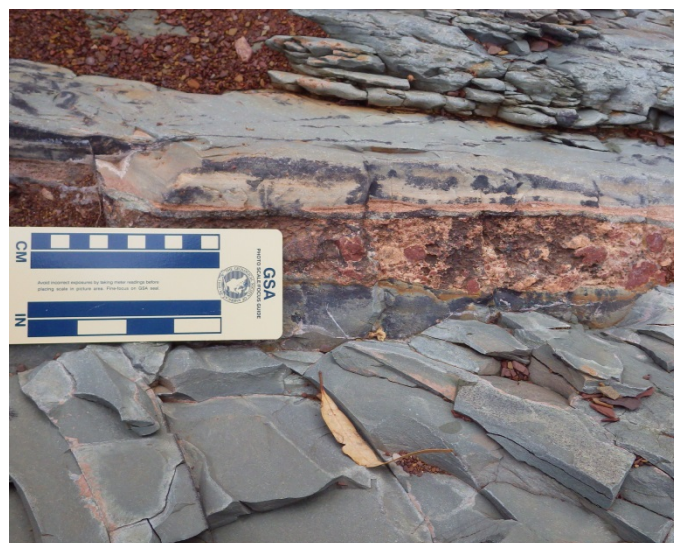
After a thorough review of sedimentology and isotope stratigraphy of the Nuccaleena in the Flinders Ranges, Rose and Maloof could not rule out any of the three models. Retallack (2011) proposes that the Nuccaleena is a terrestrial loess deposit, a view that has generally not taken hold.

Above the Nuccaleena, the Brachina Formation is a thick clastic unit that is widespread across the Adelaide Rift Complex, predominantly composed of shale and siltstone with sandstone interbeds in several stratigraphic members. The Brachina is generally regarded as a shallowing upward sequence, but specific interpretations of depositional environments have varied. Interpretations of the lower

members of the Brachina range from subtidal mudflat to deeper water turbidites, and the Moorilha and Bayley Range Siltstones in the middle and upper Brachina have been interpreted as tidal flats (Plummer, 1978). In parts of the Flinders, the upper Brachina intertongues with the overlying ABC Range Quartzite that may represent a series of prograding delta complexes (Preiss, 1987).

The ABC Range Quartzite was named by Mawson in 1939 after a series of prominent ridges in the Flinders Ranges where it is exposed. It is composed of relatively clean quartz sand and can be up to two kilometres thick due to synsedimentary faulting. If the prograding delta model is correct, the upper ABC Range may be time-equivalent to parts of the Brachina and record a shallow-marine to offshore transition. Von der Borch et al. (1988) interpret the top of the ABC Range Quartzite to be the top of a sequence that encompasses the lowermost Wilpena Group and the nearshore sediments of the ABC Range Sandstone deposited during regression.

The overlying Bunyeroo Formation is primarily made of alternating bands of red, green, and grey shales. The fine-grained, laminated lithologies suggest a deepwater environment, therefore represents a substantial



transgression following the ABC Range (Preiss, 1987; Von der Borch et al., 1988). The formation also contains a thin layer of coarser volcanic clasts believed to be deposited by the Acraman meteorite

impact event several hundred kilometres to the west (Fig. 13) (Gostin et al., 1986; Gostin and Zbik, 1999; Williams and Gostin, 2005). This ejecta blanket can be traced across South Australia and provides an unambiguous correlation horizon across hundreds of kilometres.

The Wonoka Formation has been the subject of much discussion in the literature, owing primarily to the occurrence of kilometre-deep canyons that begin within the mid-Wonoka and cut deeply into the Bunyeroo Formation. The Wonoka is well-exposed and widespread throughout the Flinders Ranges, and has also been studied with regard to its sedimentology, palaeontology, sequence stratigraphic context, and geochemistry. Urlwin (1992) used Strontium isotopes to give an age of 560-590 Ma for the Wonoka. Haines (1987) completed a thorough study of the Wonoka Formation for his thesis at the University of Adelaide, parts of which were later published as several research articles. He divided the Wonoka (outside the canyon fill) into eleven stratigraphic units based on the section at Bunyeroo Gorge. He interpreted the majority of the Wonoka to be an outer to middle shelf deposit, generally shallowing upward towards the Bonney Sandstone, with the uppermost units 8-11 marking a significant change to tidally influenced, shallow marine environments. In the revision of the Parachilna map sheet by Reid and Preiss (1999), these units were moved into the lower Bonney Sandstone and termed the Patsy Hill Member. Units 5-7 contain abundant, cyclic hummocky cross-stratification, and were the focus of a specific study (Haines, 1988). These unit designations provide the basis for much of the subsequent discussion of the Wonoka Formation. Haines (2000) also described body fossils of probable algal origin found in the upper part of the section. In the northern Flinders, evidence exists for numerous emergent diapirs that formed topographic highs or islands during late Wonoka time.

Dixon (1999) measured four detailed sections of Haines' units 1-5 within the Wonoka just north of Hawker, away from any canyon incision. Within unit 2, he described event beds and turbidites separated by siltstones. 'Event beds' in his study area were fine- to medium-grained sandstones with scoured bases and trough cross-bedding. These were overlain by turbidites with incomplete Bouma sequences of varying thickness; turbidite beds were also described as containing slumping and hummocky cross-stratification. This was interpreted to be a deepening-upward sequence. Facies in upper unit 2 and lower unit 3 suggest a subsequent shallowing upward sequence to a generally shallow marine environment encompassing the interval wherein canyons originate to the north. An erosional surface is noted in this interval, but no evidence for subaerial exposure was seen. Strongly Negative  $\delta^{13}\text{C}$  isotopes are interpreted as evidence for a stratified water body and possibly a restricted basin.

The origin of canyon structures in the Wonoka Formation (e.g., those in Fig. 14) has been the subject of much debate. Two questions generally frame the discussion: 1) Whether canyons were incised in a submarine or a subaerial environment, and 2) what mechanisms allow for such deep incision? These questions have been actively studied for several decades. Features that would eventually be recognized as canyons were first noted by Coats (1964) and were further described by Coats and Blissett (1971), among others. Detailed work on the canyons and their origin began in the 1980s with studies by Von der Borch et al. (1982; 1985). These initial studies tentatively favoured a submarine origin, with incision being the result of turbidity currents. Lack of classical turbidite deposits, however, led to the questioning of this hypothesis. Eickhoff et al. (1988) looked at both hypotheses and favoured a subaerial interpretation, based on sedimentary

facies within the canyon fill. A subaerial interpretation was also favoured by Christie–Blick et al. (1990), based on canyon fill as well as the sinuosity of the channels, which tend to meander in subaerial settings but are straighter in submarine canyons. Higgins (1997) supported a subaerial, fluvial-incision model for the Pamatta Pass canyon, based on isotope signature of the carbonate wall plaster and the inference of a pre-Delamerian deformation event. He also noted evidence for a multi-phase process of incision, with one event incising just after the Wearing Dolomite, and another during deposition of unit 3. Canyon fill is interpreted to be shallow marine due to rising sea level. More recently, Giddings et al. (2010) have returned to the original submarine hypothesis. They re-interpret canyon fill as lacking any definitive shallow-water indicators, and believe that wall-lining carbonates are deep marine rather than the terrestrial interpretation of previous workers. They also note the presence of phosphatized clasts and mass flow deposits, and note that canyons originate from deep-water facies within the Wonoka. The favoured hypothesis of canyon formation has thus ranged from a submarine model, to subaerial exposure, and back again to the submarine hypothesis. The debate is not yet settled; Retallack (2014) returns again to a subaerial interpretation, based on a variety of geochemical and sedimentological evidence.

Hypotheses for the mechanism of canyon formation in these studies have generally fallen into four categories: 1) kilometre-scale eustatic fall (this has generally been considered unlikely due to the scale of sea-level change required and lack of evidence for such a large fall elsewhere) 2) Regional uplift due to a large mantle plume (described in Williams and Gostin, 2000), 3) incision related to

Messinian-style drawdown of a restricted basin, or 4) submarine formation wherein no extreme hypotheses are needed, as recent studies have shown that canyon formation can happen in deepwater settings (e.g., Pratson and Coakley, 1996; Bertoni and Cartwright, 2005).

Jansyn (1990) noted a fault-bounded trough-like structure in the Wonoka near Wilpena Pound, believed to be coincident with the canyons to the north. In this trough, extensional faults occurred over zones of weakness, which were later further eroded by submarine currents. This may shed light on canyon formation, as deeper canyons may have been initiated in a similar manner. Jansyn



*Figure 14: Google Earth view of the Fortress Hill canyon complex in the Wonoka Formation on Umberatana Station.*

(1990) interprets units 2 and 3 to be deeper, shelf- slope deposits, units 4-9 to be prograding shelf sediments, and unit 10 in the Wonoka to represent a transgression.

The Wonoka Formation also contains a globally correlative  $\delta^{13}\text{C}$  excursion that is likely the most strongly negative  $\delta^{13}\text{C}$  value in Earth history. The  $\delta^{13}\text{C}$  value (i.e., the ratio of  $^{13}\text{C}$  to  $^{12}\text{C}$  compared to a standard) preserved in carbonate sediments can be used as a proxy to determine the ration of buried organic to inorganic carbon at a given point in time. As organisms preferentially uptake lighter  $\delta^{13}\text{C}$ , negative values typically occur when biomass is oxidized. The extremely negative values of the Wonoka/Shuram excursion (named for its simultaneous occurrence in Oman) suggested initially that this signal was diagenetic in origin.

Further analysis of evidence, however, suggests that it represents a primary marine signature (Fike et al., 2006), although this is not universally accepted and Grotzinger



Figure 15: Fine-grained shales and rapidly deposited sands with load structures in the Ediacara Member in Brachina Gorge

et al. (2011) suggest the possibility of an unprecedented global diagenetic event. Others (e.g., Derry, 2010; Swart and Kennedy, 2012) also do not rule out a diagenetic origin. The excursion also spans a significant time frame (around  $10^5$  y), indicating a continuous period of substantially altered ocean chemistry and

perturbation of the global carbon cycle (Le Guerroue, 2010). If the event is indeed

primary, it may be a product of the sustained oxidation of a large amount of lighter organic carbon. Such an event is not known from any other time in earth history, and ultimately, the nature and causes of this isotope excursion remain enigmatic. Elsewhere in the formation, Urlwin (1992) studied the  $\delta^{13}\text{C}$  isotope signature of the



Figure 16: Dickinsonia, an Ediacaran organism, on display in Parachilna. Field of view is approximately 5 cm.

Wonoka and found that it could be divided into two intervals: the lower Wonoka, which has a consistent negative signal of -8 to -7%, and the upper Wonoka, with a more positive -5 to -6% signature. He interpreted the upper signature to be

representative of shallow, partially restricted deposition in a lagoon, and the lower, more negative signal to be basinal in origin.

Above the Wonoka Formation, the Bonney Sandstone and the Rawnsley Quartzite constitute the Pound Subgroup. The Bonney Sandstone is generally lacking in detailed previous research, and the studies that do exist are discussed extensively in Chapters 3-6, so will not be summarized here. The Rawnsley Quartzite (Fig. 15) has received significantly more attention, although primarily studied from a sedimentological perspective by Gehling (1982; 2000) as it hosts a well-preserved soft-bodied Ediacaran metazoan assemblage (Fig. 16). These animals represent some of the first multicellular life-forms in earth history, and thus the depositional setting of the formation has significant implications for the evolution and development of complex life. The Rawnsley Quartzite is divided into three members, and the fossil assemblage is only found in the middle Ediacara Member. The lower Chace Member is predominantly composed of sands, sometimes with very coarse sand or granule stringers, and containing  $\wedge$ -shaped “petee” structures that have been interpreted as resulting from expansive crystallization on an evaporitic, intertidal tidal flat (Gehling, 1982). Elsewhere, the Chace Member contains evidence of channelization and fluvial influence (see chapter 4). The Ediacara Member contains a variety of lithofacies, including shelf, prodelta, delta front, delta top environments (Gehling, 2000), and has an erosive base that occasionally cuts down into the Bonney Sandstone. Fossils are found within and on the shoulders of incised valleys that are filled by shallow marine sediments. Jenkins et al. (1983) interpreted the Ediacara Member as having been deposited in shelf, tidally influenced lagoon, and barrier bar environments during a transgressive interval. Given the evolutionary implications for the stratigraphic context of the fossil



assemblage, surprisingly little research on the sedimentology and depositional environments of the formation has been done. Retallack's (2012) view of Ediacaran fauna as terrestrial lichens has been refuted by substantial sedimentologic and geochemical evidence from South Australia and elsewhere (Callow et al., 2013). The upper, unnamed member of the Rawnsley is several hundred metres thick, and returns to the intertidal sand flat environment similar to that in the Chace Member (Gehling, 1982).

#### 2.4.5: Hawker and Lake Frome Groups

The transition to the Phanerozoic is abrupt at the top of the Rawnsley Quartzite, where it is marked by the first occurrence of vertical burrowing (the ichnofossil *Treptichnus pedum*) in the lowermost Cambrian units, the Uratanna and Parachilna Formations (Fig. 17) (Droser and Gehling, 1999). These formations form part of the Hawker Group, an interval dominated by deposition on a broad carbonate ramp. Major carbonate units in the Hawker Group include the Wirrapowie and

Wilkawillina limestones and the Mernmerna Formation, which are all primarily composed of micritic limestone with archaeocyathid and *Renalcis* microbial buildups (James and Gravestock, 1990).

These formations are generally shelfal ('lagoonal' in the terminology of Youngs, 1977), but also include some higher-energy,

shallow water facies such as ooid shoals, especially in the northern and eastern



Figure 17: Vertical burrows in the Parachilna Formation, Parachilna Gorge

Flinders Ranges. Small platforms associated with structural features occur in the Wilkawillina Limestone in places (Clarke, 1990). Throughout the basin, shallower-water facies are seen south and east of the Wirrealpa Hill Hinge, a line that transects the basin diagonally and was likely a shelf break in the early Cambrian. These Cambrian units are considered to have been deposited across the region in the Arrowie Basin, which overlies and overlaps with the Adelaide Rift Complex but has a different depocentre. Higher in the Hawker Group, formations become more clastic, with Bunkers Sandstone and Oraparinna Shale still recording marine deposition. A series of volcanic arcs, in what is now the Murray Basin, developed off the coast during the early Cambrian, and their tuffs are preserved within these units (Preiss, 1987).

The uppermost deposits in the basin are likely Middle Cambrian based on biostratigraphy (Jago et al., 2006;), although their exact age is unknown (Jago et al., 2010). These formations are generally clastic, and are likely at least partially continental or terrestrial in origin (Moore, 1990; Jago et al., 2013). The Billy Creek Formation consists of intertidal and fluvial deposits (Moore, 1979), and the Balcoracana and Moodlatana Formations are paralic and cyclical, containing trilobites and their traces (Preiss, 1999). The Pantapinna Sandstone contains cross-stratification and turbidite sands, and has been interpreted as fluvial to shallow marine, with occasional open-marine influence (Jago and Gatehouse, 2014). In the Dawson Hill Member of the Grindstone Range Sandstone (the uppermost unit in the basin), sandstones are seen containing large cobble-sized clasts of unclear origin.

## **2.5: Salt-Sediment Interaction in the Adelaide Rift Complex**

Sedimentation in the basin is heavily influenced by several “rift and sag”

episodes that controlled the general rate of subsidence and accommodation. However, numerous sub-basins, or minibasins, also occur throughout the larger basin. These minibasins are generally 10-30 km wide and have a circular to elliptical shape, and are the product of withdrawal of the underlying Callanna Group evaporites as salt diapirs form piercements that penetrate through the upper basin fill (Dalgarno and Johnson, 1968). Similar features are present in salt-influenced settings throughout the world, and are often important components of petroleum reserves (e.g., those seen in Fig. 18). This chapter briefly discusses some key issues in the formation of these structures, and examines some potential analogues for minibasins found in the Flinders Ranges. Minibasins and their internal character are discussed in depth in chapters 5 and 6, both of which focus specifically on the internal character of specific minibasin sediments.

### *2.5.1: Minibasin Formation and Stratal Architecture*

Traditionally, salt-withdrawal mini-basins are thought to be the product of denser clastic sediment loading and sinking into an underlying less-dense, relatively thick layer of salt (Jackson and Talbot, 1986). However, Hudec et al. (2009) note

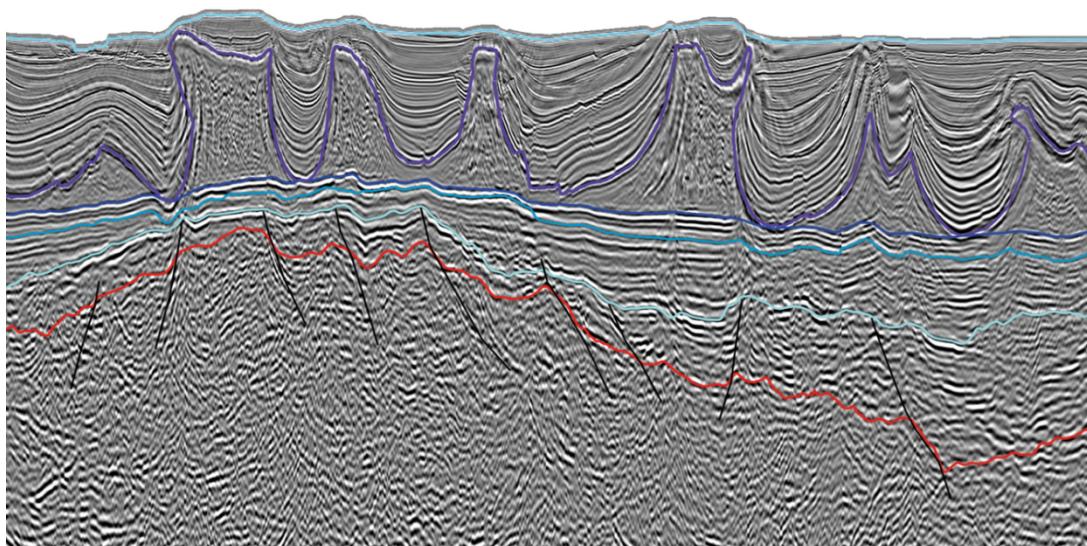


Figure 18: Minibasins seen in seismic section, Kwanza Basin, offshore East Africa. Courtesy TGS.

that mini-basin development often begins before sediments are compact enough to have a density greater than the salt that they displace. They propose a number of other mechanisms by which mini-basin formation could be initiated. These include 1) diapir shortening, where diapirs surrounding a mini-basin are inflated due to downslope salt movement, leaving the basin as a relative topographic low, 2) extensional diapir fall, where regional extension preferentially leads to subsidence and mini-basin formation atop existing diapirs, 3) decay of salt topography, where a salt bulge expressed on the seafloor decays by gravitational spreading once the salt flow stops, 4) differential sediment loading atop a diapir as sediments prograde seaward or are deposited around a localized depocentre, and 5) subsalt deformation, where either normal faulting or compression can initiate bathymetric lows that can evolve into mini-

basins. Goteti et al. (2012) further investigated mechanism (4) through computer modelling, and found it to be a valid mechanism of basin formation, but unlikely to be the one by which most minibasins form.

Collie and Giles (2011), Giles and Lawton (2002), and Giles and Rowan

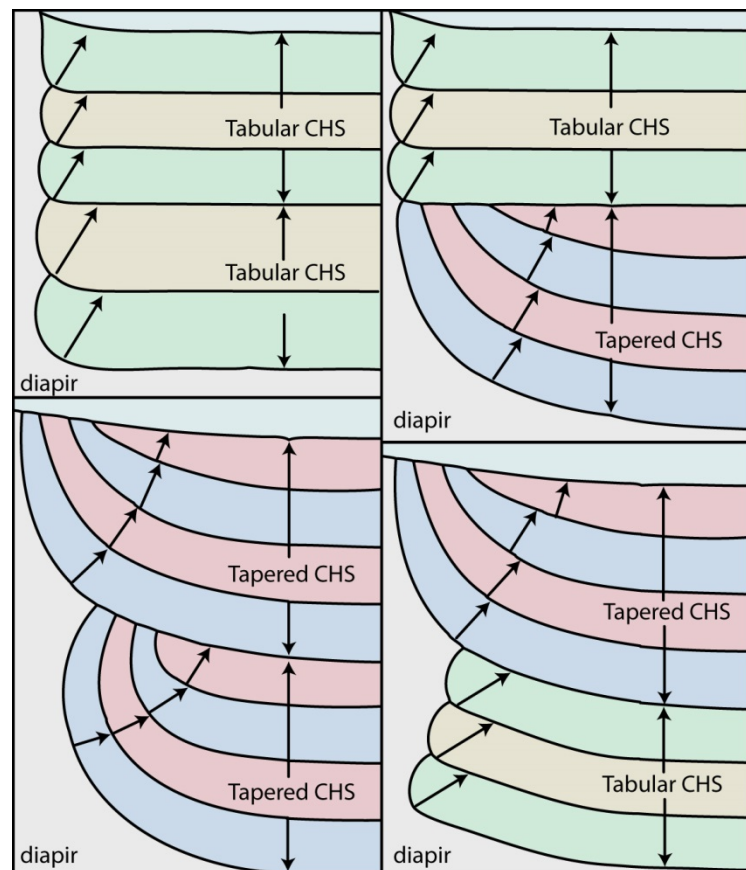


Figure 19: Various stacking patterns of halokinetic sequences. Modified from Giles and Rowan (2012).

(2011) examined the relationship between synsedimentary diapir activity and larger-scale stratigraphic patterns in adjacent sediments (Fig. 19). The influence of diapirs on stratigraphic architecture is dependent on several factors: 1) the rate of salt rise, 2) the rate of sediment accumulation, 3) the vertical velocity of the salt mass, 4) the rate of salt dissolution, and 5) the rate of subsidence. These processes create different stratal geometries of the surrounding sedimentary deposits, resulting in halokinetic sequences. Unlike depositional sequences that occur on a much larger-scale, halokinetic sequences are present only in the area immediately surrounding active diapirs. Sediments onlapping a diapiric high have two end member geometries, referred to as “wedge” and “hook”. Wedge geometries have a broad, <30 degree slope away from the diapir, with drape folding 300-1000 metres away from the diapir edge and gradational facies changes with increasing distance from the structure. Hook-type geometries dip away from the diapir much more rapidly, at 30-90 degree angles and with more abrupt facies changes. These geometries are dependent on the relative rates of sedimentation and diapir movement; hook-type geometries generally represent a relatively greater diapir rise to sedimentation rate ratio compared to wedge geometries. When stacked, hook and wedge sequence geometries can be classified into tabular and tapered composite halokinetic sequences (CHS), respectively (Giles and Rowan, 2012) (Fig. 17). Such geometries are important when considering the reservoir properties of minibasins.

### *2.5.2: Minibasins in the Adelaide Rift Complex*

Salt withdrawal minibasins are present throughout the Adelaide Rift Complex. Due to their size, shape, and known proximity to diapiric activity, many of the synclines in the central and northern Flinders most likely had some component of their subsidence related to salt withdrawal. In portions of the Flinders, this original

basin topography and architecture has been substantially overprinted by the Cambro-Ordovician Delamerian Orogeny. Many synclinal structures initially thought to have been structural or compressional in origin are likely to have initiated syndepositionally (Rowan and Vendeville, 2006). Diapirs were not recognized as such until 1960 (Webb, 1960), with most earlier authors hypothesizing that the dolomitic breccias found throughout the basin were the product of tectonics (see discussion in Mount, 1975).

A lack of high-quality seismic data prevents the exact nature of subsurface basin architecture from being fully deciphered, but Backe et al. (2010) were able to make some inferences from gravity and magnetic data. They note that the locations of salt diapirs are often controlled by deep basement extensional faults, as opposed to a flat basement with a decollement surface on top. Faults were inverted during the Delamerian Orogeny, with later Neoproterozoic and Cambrian strata formed anticlinal folds centered around diapirs and basement faults. This process of post-diapir and post-extensional compression and fault reversal is important to consider when searching for appropriate analogues. In addition, the involvement of deep basement faulting in determining diapir locations may make the morphology of Flinders-area minibasins somewhat different from some other salt-tectonized provinces around the world, although the later interaction between salt and sediments would still be analogous.

Several minibasins and diapirs in the Adelaide Rift Complex have been documented in some amount of detail. Dalgarno and Johnson (1968) summarized much of the existing knowledge, which has since been built upon through studies of individual minibasins and increasing knowledge of similar features elsewhere. In a University of Adelaide PhD thesis, Mount (1975) studied the Arkaba diapir in detail,

detailing the surrounding strata and the highly variable composition of large clasts found within the diapir body. Lemon (1985) conducted sandbox experiments to show that the Oratunga diapir shared many features with plastically behaving salt diapirs. Dyson (1996) showed how upward diapir growth can lead to the formation of large grabens, using the Oraparinna diapir as an example; Dyson (1999; 2004; 2004a; 2004b) also studied diapirs at Beltana, Wirrealpa, Pinda, and in the Willouran Ranges, providing excellent summaries of their modes of formation and associated sedimentary features. Collie and Giles (2011) looked at the Wirrealpa diapir and the surrounding Donkey Bore and Woodendinna synclines and found different halokinetic sequences and stratal geometries on either side of the diapir, suggesting unequal rates of subsidence or deposition in response to diapir rise. Lemon (2000) observed carbonate facies change in response to proximity of the Enorama diapir, demonstrating a significant influence of the diapir on the grain size and character of the surrounding Enorama Shale. More recently, Hearon et al. (2015) completed studies reconstructing halokinetic sequences surrounding diapirs in the Willouran Ranges to the northwest of the main basin axis. Despite these studies, many of the minibasins and diapirs in the basin have not been examined in any amount of detail, including those discussed in this thesis, and much work remains to be done.

## **2.6: Hydrocarbon-Bearing Analogues for the Adelaide Rift Complex**

Several factors are important to consider when interpreting reservoir analogues, including the size and shape of the basin, the depositional setting and nature of the sediment supply (e.g., subaerial vs. subaqueous, clastic vs. carbonate, sand vs. shale, etc.), relative rates of diapir rise and sediment subsidence, which influence the style and stacking pattern of halokinetic sequences surrounding the

diapir, and the post-depositional structural history of the basin. These issues directly influence the requirements that are necessary for a petroleum reservoir—the source, reservoir, and seal potential of the rocks.

Basins containing evaporite within their fill are found throughout the world, but are exposed only rarely. Many outcropping salt provinces share at least some similarities with the sediments in focus here; these are discussed in more detail in Chapter 6, which places certain minibasins in the Adelaide Rift Complex within a global context. Several salt-tectonized provinces that are actively producing hydrocarbons may also be considered analogues; some of these are well-known, and an examination of the diapirs and minibasins in these areas may shed light onto the important factors to consider when describing and interpreting salt-sediment interaction. This section discusses some aspects of salt tectonics in the Gulf of Mexico, offshore Brazil, and in the onshore Paradox Basin, which contain well-known, currently productive hydrocarbon reservoirs that are significantly influenced by salt withdrawal and diapirism. These areas have been extensively researched, with hundreds of published studies; it is therefore not possible to review the entire body of literature for each. Here, they are examined only briefly in order to provide a point of comparison for the Adelaide Rift Complex.



### 2.6.1: Gulf of Mexico

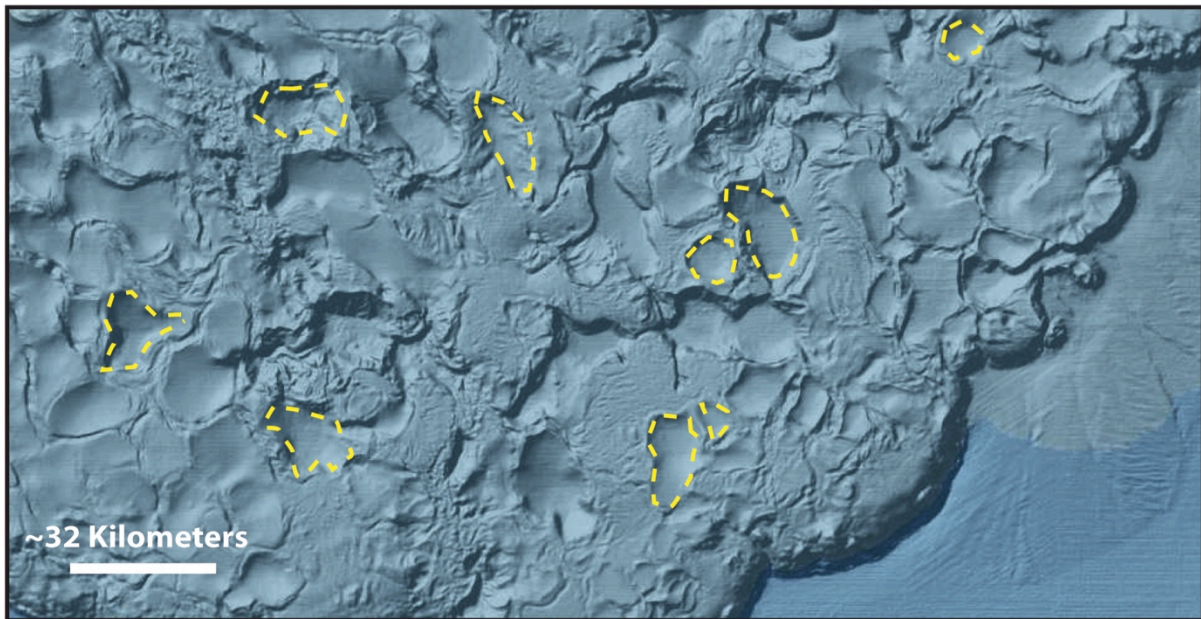


Figure 20: Seafloor topography in the Gulf of Mexico, showing salt-withdrawal minibasins in the Bucket-weld and Amalgamated salt-stock-canopy provinces of Pilcher et al. (2011). Some minibasins outlined to highlight boundaries ; others not outlined to better show topographic relief.

Salt tectonics and sedimentation in the Gulf of Mexico are complex and span a wide range of time, from the Mesozoic to the recent. In the Cenozoic, depositional environments varied greatly through time and across the basin (Galloway et al., 2000). The source of evaporite diapirs is the Jurassic Louann Salt, which is generally present between the Mississippi Canyon province and the outer Sigsbee Escarpment (Bryant et al., 1990). These boundaries form an offshore area of salt-related primary and secondary minibasins that are the focus of most of the petroleum exploration in the area (Fig. 20). Within this area, dozens of minibasins are present, each with a scale of tens of kilometres (Bouma and Bryant, 1995). Sedimentation and progradation of the shelf has taken place over tens of millions of years, from the Jurassic to the recent. Pilcher et al. (2011) recognize three provinces that are defined by the nature of salt structures. To the east, the disconnected salt-stock-canopy province contains relatively isolated diapirs separated by primary

basins formed on *in situ* salt. Importantly, secondary minibasins formed on the salt canopy are separated from source rocks and are thin and generally not productive. In this area, most production is centred around traps at the base of overhanging salt layers. In the amalgamated salt-stock-canopy province, salt supply was higher, and salt has detached and formed a canopy onto which secondary mini-basins have formed. Production in this province comes from both subsalt primary basins and secondary minibasins, which are often well-developed enough that the salt canopy is extruded and the base of the minibasin is welded to the underlying older sediment. Both of these provinces have seen considerable post-depositional compression. In the bucket-weld province, primary basins are more discontinuous, overlain by a thick salt canopy and welded to deep, young secondary minibasins. This province is likely the result of continued evolution of an amalgamated salt-stock-canopy province

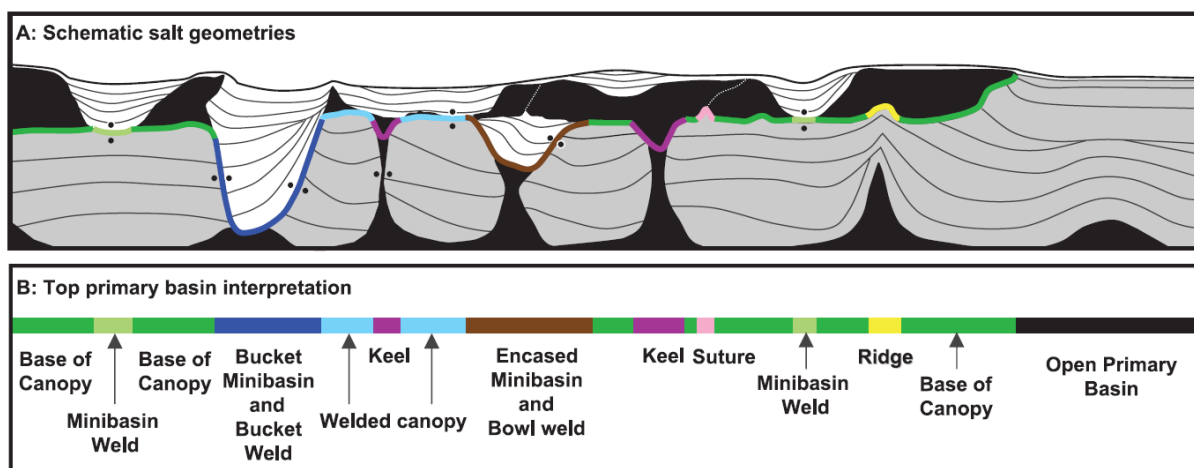


Figure 21: Schematic salt geometries in the Gulf of Mexico. From Pilcher et al., 2011.

precursor; few vertical feeders to the salt canopy remain.

The primary difference between these provinces is the overall supply of salt, with the disconnected salt-stock-canopy province having the least, and the bucket-weld province having the most. Although charge and trapping mechanisms are locally variable, several consistent play types are present in each of these provinces.

Minibasins form atop allochthonous salt layers as well as atop the primary bedded salt formation, forming a variety of welds and petroleum traps (Fig. 21). In the Adelaide Rift Complex, it is unknown whether an extensive, regional salt canopy was ever formed, although the isolated nature of individual diapirs does not suggest that this was the case. In this way the Flinders is most similar to the disconnected salt-stock-canopy province in the Gulf of Mexico. Although some Adelaide Rift Complex minibasins are completely surrounded by salt, it is not always clear whether the diapiric structure was still connected to the primary evaporite layer.

The character of minibasin fill in the Gulf of Mexico is known from core, wireline logs, and seismic data. Some minibasins contain thousands of metres of sediments, often with ponded sheet and channel sands that thicken into minibasin centre and erode underlying deposits, creating a series of unconformities. These sands are contained within background muds, and their distribution within and around minibasins is controlled by the length and gradient of the slope, the location of the sediment source, and the topography of the bounding salt ridges (Booth et al., 2003). In other minibasins, fill is composed of both mud- and sand-dominated turbidites, hemipelagic muds, and intrabasinal heterolithic mass transport complexes. Mass transport complexes (slumps) make up around 45% of the fill of the Fuji minibasin, for example, and are triggered by passive salt movement (Madof et al., 2009). Mallarino et al. (2006) also found that minibasin fill was composed of a series of dark- and light-grey muds, black clay, and well-sorted quartz sands, reflecting the balance between fine-grained background sedimentation and the deposition of sands during lowstand or regressive intervals. Piston core from some of these mass transport complexes show occasional larger clasts similar to those seen in some minibasins in the Adelaide Rift Complex (Olson and Damuth, 2009).

Rowan and Vendeville (2006) compared salt withdrawal basins in the Flinders with similar basins in the Gulf of Mexico. Based on experimental models, they examined the similarities in both areas, with the goal of determining if their deformation styles were the result of similar timing with regard to diapir formation and later compression. Using silicone “salt”, they created mature salt diapir structures through sediment loading adjacent to incipient diapirs, which were then subjected to compressive shortening. The results of these experiments matched both the Flinders Ranges and the Gulf of Mexico examples. The later compression was shown to be an important factor in the overall 3-D structure of the fold belt, and it explains both the remnant diapir morphology and shows the influence of diapirs on later patterns of folding. Diapirs were shown to occur at the terminations of strain-perpendicular folds that were cored by salt welds, and their spatial distribution formed a polygonal pattern that can be seen in both the Flinders and the Gulf of Mexico. In addition, the authors noted several other possible examples where similar structural deformation may have taken place—these include the Atlas Mountains in North Africa, the Zagros Mountains of Iran, the La Popa Basin in Mexico, and the Carpathian Mountains in Romania.

### *2.6.2 Offshore Brazil*

Like the Gulf of Mexico, the southeastern offshore continental margin of Brazil contains a thick section of Mesozoic salt that has penetrated and deformed the upper Cenozoic sediments. Three basins in offshore Brazil, the Espirito Santo, Campos, and Santos, are known or potential petroleum producers. The Campos and Santos basins (Fig. 22), like the Gulf of Mexico, can be divided into provinces based on salt-tectonic regime, with a proximal extensional province and a larger, more distal contractional domain (Demercian et al., 1993; Meisling et al., 2001).

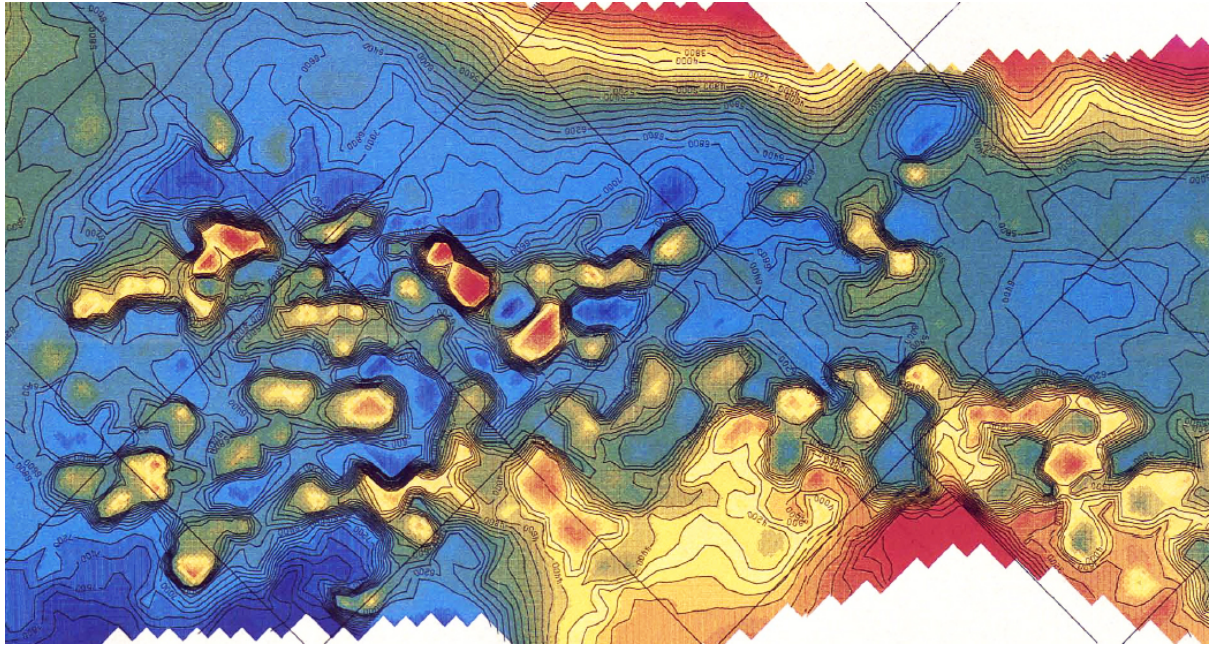


Figure 22: Subsurface structure map of top of evaporite sequence, Campos-Santos region, offshore Brazil. Highs in red/yellow are salt-related features; shoreline is toward top of picture. Modified from Demercian et al., (1993)

The Campos basin contains a significant proportion of Brazil's oil reserves, much of which is contained within salt-withdrawal mini-basins. Source rocks in the Campos Basin are pre-salt lacustrine carbonates (Meisling et al., 2001); many mini-basins are welded to the underlying section, forming an important pathway for hydrocarbon migration (Roberts et al., 2004). The Santos Basin is less-studied than the Campos, and is not yet known to contain as significant amount of a hydrocarbon accumulation. Only in the southern part of the Santos basin are true, well-developed minibasins present; these are formed on autochthonous salt that is separated by regularly spaced, high-amplitude diapirs and ridges (Modica and Brush, 2004). Minibasins in the Santos basin are 20 kilometres in diameter, and are filled with Cretaceous to recent hemipelagic mudstones (Jackson, 2012). Mass-transport complexes consisting of slide blocks and muddy debris flows are also found in the minibasin fill, where they detached from the topographically higher margin and were redeposited closer to the basin centre. In the Espirito Santo basin, minibasins are formed in Cretaceous-Cainozoic carbonates and sandstones. Salt structures show a

basinward transformation from salt rollers, to various types of diapir piercements, to allochthonous canopies. Like the Gulf of Mexico, these structural styles are dependent on the original depositional salt thickness, and more distal salt structures have been laterally compressed and extruded (Fiduk et al. 2004). Salt structures influence the locations of faults, which in turn influence the distribution of submarine canyons and reservoirs (Alves et al., 2009). Collapse features atop diapirs are common features in the Santos Basin (Guerra and Underhill, 2012).

Brazilian salt basins share many similarities to those seen here, although the Adelaide Rift Complex has not been interpreted to have the kind of basin-scale extension-compressional regimes that have been documented in Brazil and elsewhere. Most Brazilian minibasins are lacking in detailed sedimentologic and stratigraphic analysis; the depositional controls and internal architecture of these features in the area are not well-understood and could greatly benefit from insights gained from outcrop analogues.

### *2.6.3: Paradox Basin*

The Paradox Basin outcrops in the southwestern U.S., and differs from salt-tectonized provinces in Brazil and the Gulf of Mexico in that minibasin formation occurred in a continental environment (Fig. 23). It is therefore a better analogue for certain parts of the Bonney Sandstone, which may also be continental, and more is known about its sedimentology and stratigraphic architecture due to well-exposed outcrops. Oil and gas are produced from subsurface structures in a number of formations from the Devonian to the Cretaceous, including those that interact with diapirs (Stevenson and Wray, 2009). Thus, accurate facies models for salt-sediment interaction are essential for the prediction of the locations of hydrocarbon reserves in

this type of environment.

The Paradox Basin formed during Pennsylvanian extension atop a pre-existing Precambrian fracture system. Restriction of the basin resulted in very thick evaporite deposits, which mobilized shortly thereafter to affect subsequent sedimentation. Most basin deposits consist of fluvial sediments, aeolian dunes, playa lakes, and paleosols (Bromley, 1991), in isolated depocentres which shifted and evolved over time. In the Pennsylvanian, Permian, and Jurassic, the rise of salt ridges influenced the course of rivers in a fluvially dominated terrestrial environment, although primary drainage axes may differ between individual minibasins. Rivers

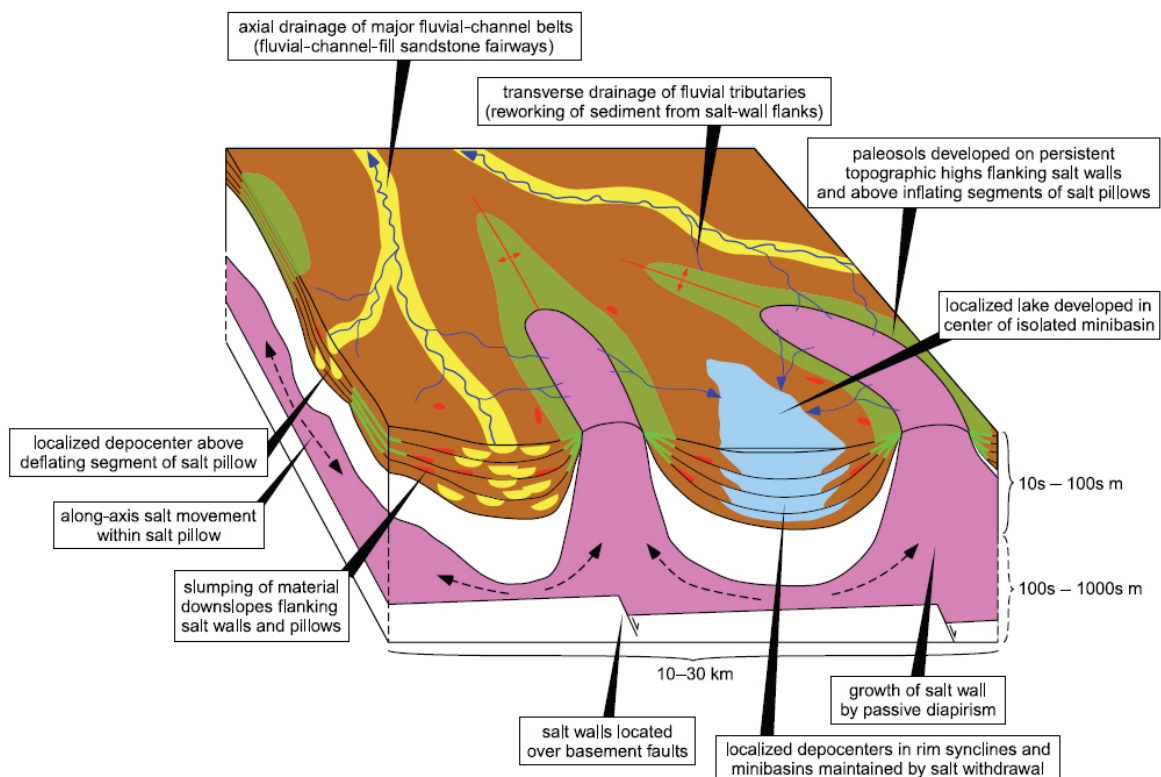


Figure 23: Deposition model of salt diapirs and minibasins in the Paradox Basin. From Matthews et al., 2007

either ran axially down elongate minibasin valleys, paralleling salt ridges, or transversely from salt-cored topographic highs (Matthews et al., 2007; Banham and

Mountney, 2013). Sediments thin and onlap onto diapir margins, and passive salt rise is a major control of facies distribution in the basin. Paleosols form on minibasin margins, with minibasin centres being either mud- or sand dominated, depending on the relative rates of subsidence and sedimentation. Gravels are more prone to occur as parts of fluvial deposits within minibasins, although the provenance of clasts and whether they are derived from diapirs has not been determined. Banham and Mountney (2013) showed that fluvially dominated minibasins followed a predictable evolution over time as minibasins are filled and flow is diverted from depocentres; a process that affects the development of reservoir facies. Many of these features may be compared favourably to those seen in and around the Mt. Frome minibasin, discussed in Chapter 5.



## 2.7: References

- AINSWORTH, R. B., VAKARELOV, B. K., AND NANSON, R. A., 2011, Dynamic spatial and temporal prediction of changes in depositional processes on clastic shorelines: Toward improved subsurface uncertainty reduction and management. *AAPG Bulletin*, **95**, 267-297.
- ALLEN, P.A., AND HOFFMAN, P.F., 2005, Extreme winds and waves in the aftermath of a Neoproterozoic glaciation. *Nature*, **433**, 123-127.
- ALVES, T. M., CARTWRIGHT, J., AND DAVIES, R. J., 2009, Faulting of salt-withdrawal basins during early halokinesis: effects on the Paleogene Rio Doce Canyon system (Espírito Santo Basin, Brazil). *AAPG Bulletin*, **93**, 617-652.
- BACKÉ, G., BAINES, G., GILES, D., PREISS, W., AND ALESCI, A., 2010, Basin geometry and salt diapirs in the Flinders Ranges, South Australia: Insights gained from geologically-constrained modelling of potential field data. *Marine and Petroleum Geology*, **27**, 650-665.
- BANHAM, S. G., AND MOUNTNEY, N. P., 2013, Evolution of fluvial systems in salt-walled mini-basins: a review and new insights. *Sedimentary Geology*, **296**, 142-166.
- BERTONI, C., AND CARTWRIGHT, J., 2005, 3D seismic analysis of slope-confined canyons from the Plio–Pleistocene of the Ebro Continental Margin (Western Mediterranean). *Basin Research*, **17**, 43-62.
- BOGDANOVA, S.V., PISAREVSKY, S.A., AND LI, Z.X., 2009, Assembly and Breakup of Rodinia (Some results of IGCP project 440). *Stratigraphy and Geological Correlation*, **17**, 259-274.
- BOOTH, J. R., DEAN, M. C., DUVERNAY, A. E., AND STYZEN, M. J., 2003, Paleobathymetric controls on the stratigraphic architecture and reservoir development of confined fans in the Auger Basin: central Gulf of Mexico slope. *Marine and Petroleum Geology*, **20**, 563-586.
- BOUMA, A. H., AND BRYANT, W. R., 1994, Physiographic features on the northern Gulf of Mexico continental slope. *Geo-Marine Letters*, **14**, 252-263.

- BROMLEY, M. H., 1991, Architectural features of the Kayenta Formation (Lower Jurassic), Colorado Plateau, USA: relationship to salt tectonics in the Paradox Basin. *Sedimentary Geology*, **73**, 77-99.
- BROOKFIELD, M.E., 1993. Neoproterozoic Laurentia-Australia fit. *Geology*, **21**, 683–686.
- BRYANT, W. R., BRYANT, J. R., FEELEY, M. H., AND SIMMONS, G. R., 1990, Physiographic and bathymetric characteristics of the continental slope, northwest Gulf of Mexico. *Geo-Marine Letters*, **10**, 182-199.
- CALLOW, R. H., BRASIER, M. D., AND MCILROY, D., 2013, Discussion: “Were the Ediacaran siliciclastics of South Australia coastal or deep marine?” by Retallack et al., *Sedimentology*, 59, 1208–1236. *Sedimentology*, **60**, 624-627.
- CÉLÉRIER, J., SANDIFORD, M., HANSEN, D. L., AND QUIGLEY, M., 2005, Modes of active intraplate deformation, Flinders Ranges, Australia. *Tectonics*, **24**, 1-17.
- CHRISTIE-BLICK, N., VON DER BORCH, C.C., AND DIBONA, P.A., 1990, Working hypothesis for the origin of the Wonoka Canyons (Neoproterozoic), South Australia. *American Journal of Science*, **290**, 295-332.
- CLARKE, J. D. A., 1990, An Early Cambrian carbonate platform near Wilkawillina Gorge, South Australia', *Australian Journal of Earth Sciences*, **37**, 471-483.
- CLIFTON, H.E., 1969, Beach lamination: nature and origin. *Marine Geology*, **7**, 553-559.
- COATS, R.P., 1964, Large scale Precambrian slump structures, Flinders Ranges. *Quarterly Geological Notes, Geological Survey of South Australia*, **11**, 1-2.
- COATS R. P., 1973, Copley map sheet. Geological Survey of South Australia Geological Atlas 1:250 000 Series, sheet H54-9.
- COATS, R. P., AND BLISSETT, A. H., 1971, Regional and economic geology of the Mt. Painter Province. *Bulletin of the Geological Survey of South Australia*, **43**, 426 p.
- COATS, R. P., AND W. V. PREISS, 1980, Stratigraphic and geochronological

- reinterpretation of late Proterozoic glaciogenic sequences in the Kimberley region, Western Australia. *Precambrian Research*, **13**, 181-208.
- COLLIE, A.J., AND GILES, K., 2011, Comparison of Lower Cambrian Carbonate Facies and Halokinetic Sequences in Minibasins Developed on Opposite Sides of Wirrealpa Diapir, Central Flinders Ranges, South Australia. *AAPG Search and Discovery Article* 50442.
- COLLINS, W. J., AND SHAW, R. D., 1995, Geochronological constraints on orogenic events in the Arunta Inlier: a review. *Precambrian Research*, **71**, 315-346.
- DALGARNO, C. R., AND JOHNSON, J. E., 1966, Parachilna: Geological Atlas Series Sheet H 54-13, scale 1:250,000. Geological Survey of South Australia, Adelaide.
- DALGARNO, C. R., AND JOHNSON, J. E., 1968, Diapiric structures and late Precambrian-early Cambrian sedimentation in Flinders Ranges, South Australia. In: Braunstein, J., and O'Brien, G.D. (eds.) *AAPG Memoir*, **8**, 301-314.
- DEMERCIAN, S., SZATMARI, P., AND COBBOLD, P. R., 1993, Style and pattern of salt diapirs due to thin-skinned gravitational gliding, Campos and Santos basins, offshore Brazil. *Tectonophysics*, **228**, 393-433.
- DERRY, L. A., 2010, A burial diagenesis origin for the Ediacaran Shuram–Wonoka carbon isotope anomaly. *Earth and Planetary Science Letters*, **294**, 152-162.
- DEVRIES, S. T., PRYER, L. L., AND FRY, N., 2008, Evolution of Neoproterozoic and Proterozoic basins of Australia. *Precambrian Research*, **166**, 39-53.
- DIXON, J., 1999, Forcing factors influencing deposition of the Wonoka Formation, Flinders Ranges, South Australia, and triggers for canyon development. University of Adelaide BSc Honors Thesis, unpublished.
- DROSER, M. L., GEHLING, J. G., AND JENSEN, S., 1999, When the worm turned: Concordance of Early Cambrian ichnofabric and trace-fossil record in siliciclastic rocks of South Australia. *Geology*, **27**, 625-628.
- DYKSTERHUIS, S., AND MÜLLER, R. D., 2008, Cause and evolution of intraplate

- orogeny in Australia. *Geology*, **36**, 495-498.
- DYSON, I.A., 1996, A new model for diapirism in the Adelaide Geosyncline. *MESA Journal*, **3**, 41-48.
- DYSON, I. A., 1999, The Beltana Diapir: a salt withdrawal mini-basin in the northern Flinders Ranges: *Mines and Energy of South Australia Journal*, **15**, 40-46.
- DYSON, I. A., 2004, Geology of the eastern Willouran Ranges—evidence for earliest onset of salt tectonics in the Adelaide Geosyncline. *MESA Journal*, **35**, 48-56.
- DYSON, I.A., 2004a, Christmas Tree Diapirs and Development of Hydrocarbon Reservoirs: A Model from the Adelaide Geosyncline, South Australia. *In: Salt-sediment interactions and hydrocarbon prospectivity: Concepts, Applications, and Case Studies for the 21st Century* (Eds P.J. Post, D.L. Olson, K.T. Lyons, S.L. Palmes, P.F. Harrison and N.C. Rosen) 24th GCSSEPM Bob F. Perkins Research Conference, 133-165.
- DYSON, I. A., 2004b, Geology of the eastern Willouran Ranges—evidence for earliest onset of salt tectonics in the Adelaide Geosyncline. *MESA journal*, **35**, 48-56.
- DYSON, I. A. 2003, A new model for the Wonoka canyons in the Adelaide Geosyncline: *MESA Journal*, **31**, 49-58.
- EICKHOFF, K.H., VON DER BORCH, C.C., AND GRADY, A.E., 1988, Proterozoic canyons of the Flinders Ranges (South Australia): submarine canyons or drowned river valleys?. *Sedimentary Geology*, **58**, 217-235.
- EYLES, N., AND JANUSCZAK, N., 2004, 'Zipper-rift': a tectonic model for Neoproterozoic glaciations during the breakup of Rodinia after 750 Ma. *Earth-Science Reviews*, **65**, 1-73.
- EYLES, C.H., EYLES, N., AND GREY, K., 2007, Palaeoclimate implications from deep drilling of Neoproterozoic strata in the Officer Basin and Adelaide Rift Complex of Australia; a marine record of wet-based glaciers. *Palaeogeography, Palaeoclimatology, Palaeoecology*, **248**, 291-312.
- FIDUK, J.C., BRUSH, E.R., ANDERSON, L.E., GIBBS, P.B., AND ROWAN, M.G., 2004, Salt

deformation, magmatism, and hydrocarbon prospectivity in the Espirito Santo Basin, offshore Brazil. *In: Salt-Sediment Interactions and Hydrocarbon Prospectivity: Concepts, Applications, and Case Studies for the 21st Century: Houston, Gulf Coast Section Society of Economic Paleontologists and Mineralogists, 24th Annual Research Conference, 370-392.*

Fike, D. A., Grotzinger, J. P., Pratt, L. M., and Summons, R. E., 2006, Oxidation of the Ediacaran ocean. *Nature*, **444**, 744-747.

FRANK, T.D., AND FIELDING, C.R., 2003, Marine Origin for Precambrian, carbonate-hosted magnesite? *Geology*, **31**, 1101-1104.

GALLOWAY, W. E., GANEY-CURRY, P. E., LI, X., AND BUFFLER, R. T., 2000, Cenozoic depositional history of the Gulf of Mexico basin. *AAPG Bulletin*, **84**, 1743-1774.

GAMMON, P.R., MCKIRDY, D.M., AND SMITH, H.D., 2005, The timing and environment of tepee formation in a Marinoan cap carbonate. *Sedimentary Geology*, **177**, 195-208.

GEHLING, J.G., 1982, Sedimentology and Stratigraphy of the Late Precambrian Pound Subgroup, Central Flinders Ranges, S.A. University of Adelaide MSc thesis.

GEHLING, J. G., 2000, Environmental interpretation and a sequence stratigraphic framework for the terminal Proterozoic Ediacara Member within the Rawnsley Quartzite, South Australia. *Precambrian Research*, **100**, 65-95.

GIDDINGS, J. A., AND WALLACE, M.W., 2009, Sedimentology and C-isotope geochemistry of the 'Sturtian' cap carbonate, South Australia. *Sedimentary Geology*, **216**, 1-14.

GIDDINGS, J.A., WALLACE, M.W., HAINES, P.W., AND MORNANE, K., 2010, Submarine origin for the Neoproterozoic Wonoka canyons, south Australia. *Sedimentary Geology*, **223**, 35-50.

GILES, K.A., AND LAWTON, T.F., 2002, Halokinetic sequence stratigraphy adjacent to the El Papalote diapir, northeastern Mexico. *AAPG Bulletin*, **86**, 823-840.

GILES, K. A., AND ROWAN, M. G., 2012, Concepts in halokinetic-sequence

deformation and stratigraphy. *Geological Society, London, Special Publications*, **363**, 7-31.

GILES, K. A., LAWTON, T. F., AND ROWAN, M. G., 2004, Summary of halokinetic sequence characteristics from outcrop studies of La Popa salt basin, northeastern Mexico. *In: Salt-Sediment Interactions and Hydrocarbon Prospectivity: Concepts, Applications, and Case Studies for the 21st Century: 24th Annual Gulf Coast Section. SEPM. Bob F. Perkins Research Conference Program and Abstracts*, 16 p.

GOSTIN, V. A., AND ZBIK, M., 1999, Petrology and microstructure of distal impact ejecta from the Flinders Ranges, Australia. *Meteoritics and Planetary Science*, **34**, 587-592.

GOSTIN, V.A., HAINES, P.W., JENKINS, R.J.F., COMPSTON, W., AND WILLIAMS, I.S., 1986, Impact Ejecta within Late Precambrian Shales, Adelaide Geosyncline, South Australia. *Science*, **233**, 198-200.

GOTETI, R., INGS, S.J., AND BEAUMONT, C., 2012, Development of salt minibasins initiated by sedimentary topographic relief. *Earth and Planetary Science Letters*, **339**, 103-116.

GREY, K., AND CALVER, C.R., 2007, Correlating the Ediacaran of Australia. *Geological Society, London, Special Publications*, **286**, 115-135.

GROTZINGER, J. P., FIKE, D. A., AND FISCHER, W. W., 2011, Enigmatic origin of the largest-known carbon isotope excursion in Earth's history. *Nature Geoscience*, **4**, 285-292.

GUERRA, M. C., AND UNDERHILL, J. R., 2012, Role of halokinesis in controlling structural styles and sediment dispersal in the Santos Basin, offshore Brazil. *Geological Society, London, Special Publications*, **363**, 175-206.

GURNIS, M., 1988, Large-scale mantle convection and the aggregation and dispersal of supercontinents. *Nature*, **332**, 695-699.

HAINES, P.W., 1987, Carbonate shelf and basin sedimentation, late Proterozoic Wonoka Formation, South Australia . University of Adelaide Unpublished PhD

Dissertation.

- HAINES, P. W., 2000, Problematic fossils in the late Neoproterozoic Wonoka Formation, South Australia. *Precambrian Research*, **100**, 97-108.
- HAINES, P.W., 1988, Storm-dominated mixed carbonate/siliciclastic shelf sequence displaying cycles of hummocky cross-stratification, late Proterozoic Wonoka Formation, South Australia. *Sedimentary Geology*, **58**, 237-254.
- HEARON IV, T. E., ROWAN, M. G., GILES, K. A., KERNEN, R. A., GANNAWAY, C. E., LAWTON, T. F., AND FIDUK, J. C., 2013, Allochthonous salt initiation and advance in the Flinders and eastern Willouran Ranges, South Australia: using outcrops to test subsurface-based models from the northern Gulf of Mexico. *AAPG Bulletin*, **99**, 293-331.
- HEITHERSAY, P.S., 1979, Sedimentology of the Burra group in the East Rooks area, Northeastern Willouran Ranges, South Australia. University of Adelaide BSc Honors Thesis, unpublished.
- HIGGINS, J., 1997, Pamatta Pass Canyon Complex: Neoproterozoic Wonoka Formation, Flinders Ranges, South Australia. University of Adelaide BSc Honors Thesis, unpublished.
- HILL, A.C., AND WALTER, M.R., 2000, Mid-Neoproterozoic (~830-750 Ma) isotope stratigraphy of Australia and global correlation. *Precambrian Research*, **100**, 181-211.
- HOFFMAN, P. F., AND SCHRAG, D. P., 2002, The snowball Earth hypothesis: testing the limits of global change. *Terra Nova*, **14**, 129-155.
- HOFFMAN, P. F., 1999, The break-up of Rodinia, birth of Gondwana, true polar wander and the snowball Earth. *Journal of African Earth Sciences*, **28**, 17-33.
- HOFFMAN, P. F., AND LI, Z. X., 2009, A palaeogeographic context for Neoproterozoic glaciation. *Palaeogeography, Palaeoclimatology, Palaeoecology*, **277**, 158-172.
- HOWCHIN, W., 1900, Preliminary Report on glacial beds of Cambrian age in South Australia. *Royal Society of South Australia Transactions*, **25**, 10.

- HUDEEC, M.R., JACKSON, M.P., AND SCHULTZ-ELA, D.D., 2009, The paradox of minibasin subsidence into salt: Clues to the evolution of crustal basins. *Geological Society of America Bulletin*, **121**, 201-221.
- HURTGEN, M.T., ARTHUR, M.A., SUITS, N.S., AND KAUFMAN, A.J., 2002, The sulfur isotopic composition of Neoproterozoic seawater sulfate: Implications for a snowball Earth?. *Earth and Planetary Science Letters*, **203**, 413–429.
- JACKSON, C. A. L., 2012, The initiation of submarine slope failure and the emplacement of mass transport complexes in salt-related minibasins: A three-dimensional seismic-reflection case study from the Santos Basin, offshore Brazil. *Geological Society of America Bulletin*, **124**, 746-761.
- JACKSON, M.T., AND TALBOT, C.J., 1986, External shapes, strain rates, and dynamics of salt structures. *Geological Society of America Bulletin*, **97**, 305-323
- JAGO, J. B., AND GATEHOUSE, C. G., 2014, A small trace fossil assemblage from the middle Cambrian Pantapinna Sandstone, Flinders Ranges, South Australia and its paleoenvironmental significance. *Australian Journal of Earth Sciences*, **61**, 837-841.
- JAGO, J. B., ZANG, W. L., SUN, X., BROCK, G. A., PATERSON, J. R., AND SKOVSTED, C. B., 2006, A review of the Cambrian biostratigraphy of South Australia. *Palaeoworld*, **15**, 406-423.
- JAGO, J. B., GATEHOUSE, C. G., POWELL, C. M., CASEY, T., AND ALEXANDER, E. M., 2010, The Dawson Hill Member of the Grindstone Range Sandstone in the Flinders Ranges, South Australia. *Transactions of the Royal Society of South Australia*, **134**, 115-124.
- JAGO, J. B., GATEHOUSE, C. G., AND CASEY, T., 2013, Response to GJ Retallack's 'Discussion' of Jago et al.(2013). *Australian Journal of Earth Sciences*, **60**, 543-545.
- JAMES, N. P., AND GRAVESTOCK, D. I., 1990, Lower Cambrian shelf and shelf margin buildups, Flinders Ranges, South Australia. *Sedimentology*, **37**, 455-480.



- JANSYN, J., 1990, Strato-tectonic evolution of a large subsidence structure associated with the late Proterozoic Wonoka Formation at Wilpena Pound, central Flinders Ranges, South Australia. University of Adelaide unpublished BSc Honors Thesis.
- JENKINS, R. J. F., FORD, C. H., AND GEHLING, J. G., 1983, The Ediacara member of the Rawnsley quartzite: The context of the Ediacara assemblage (late Precambrian, Flinders Ranges). *Journal of the Geological Society of Australia*, **30**, 101-119.
- KAH, L. C., LYONS, T. W., AND CHESLEY, J. T., 2001, Geochemistry of a 1.2 Ga carbonate-evaporite succession, northern Baffin and Bylot Islands: implications for Mesoproterozoic marine evolution. *Precambrian Research*, **111**, 203-234.
- KARLSTROM, K.E., HARLAN, S.S., WILLIAMS, M.L., MCLELLAND, J. AND GEISSMAN, J.W., 1999, Refining Rodinia: geologic evidence for the Australia–Western U.S. connection in the Proterozoic. *GSA Today*, **9**, 1–7.
- KENNEDY, M. J., 1996, Stratigraphy, sedimentology, and isotopic geochemistry of Australian Neoproterozoic postglacial cap dolostones: deglaciation,  $\delta^{13}\text{C}$  excursions, and carbonate precipitation. *Journal of Sedimentary Research*, **66**, 1050-1064.
- KENNEDY, M. J., CHRISTIE-BLICK, N., AND SOHL, L. E., 2001, Are Proterozoic cap carbonates and isotopic excursions a record of gas hydrate destabilization following Earth's coldest intervals?. *Geology*, **29**, 443-446.
- KNOLL, A., WALTER, M., NARBONNE, G., AND CHRISTIE-BLICK, N., 2006, The Ediacaran Period: a new addition to the geologic time scale. *Lethaia*, **39**, 13-30.
- LE GUERROUÉ, E., 2010, Duration and synchronicity of the largest negative carbon isotope excursion on Earth: the Shuram/Wonoka anomaly. *Comptes Rendus Geoscience*, **342**, 204-214.
- LE HERON, D.P., COX, G., TRUNDLEY, A., AND COLLINS, A.S., 2011(a), Two Cryogenian glacial successions compared: Aspects of the Sturt and Elatina sediment records of South Australia. *Precambrian Research*, **186**, 147-168.

- LE HERON, D.P., COX, G., TRUNDLEY, A., AND COLLINS, A.S., 2011(b), Sea ice-free conditions during the Sturtian glaciation (early Cryogenian), South Australia. *Geology*, **39**, 31-34.
- LEMON, N.M., 1985, Physical modelling of sedimentation adjacent to diapirs and comparison with late Precambrian Oratunga breccia body in central Flinders Ranges, South Australia. *AAPG Bulletin*, **69**, 1327-1338.
- LEMON, N.M., 2000, A Neoproterozoic fringing stromatolite reef complex, Flinders Ranges, South Australia. *Precambrian Research*, **100**, 109-120.
- LEMON, N.M., AND GOSTIN, V.A., 1990, Glacigenic sediments of the late Proterozoic Elatina Formation and equivalents, Adelaide Geosyncline of South Australia. In: Jago, J.B., and Moore, P.S., (eds.) The Evolution of a Late Precambrian-Early Paleozoic rift complex: the Adelaide Geosyncline. *Geological Society of South Australia, Special Publication* **16**, 149-163.
- Li, Z.X., Bogdanova, S.V., Collins, A.S., Davidson, A., De Waele, B., Ernst, R.E., Fitzsimmons, I.C.W., Fuck, R.A., Gladkochub, D.P., Jacobs, J., Karlstrom, K.E., Lu, S., Natapov, L.M., Pease, V., Pisarevsky, S.A., Thrane, K., and Vernikovsky, V., 2008, Assembly, configuration, and break-up history of Rodinia: a synthesis. *Precambrian Research*, **160**, 179-210.
- LINDSAY, J.F., AND LEVIN, J.H., 1996, Evolution of a Neoproterozoic to Palaeozoic intracratonic setting, Officer Basin, South Australia. *Basin Research*, **8**, 403-424.
- LINK, P. K, AND GOSTIN, V.A., 1981, Facies and paleogeography of Sturtian glacial strata (late Precambrian), South Australia. *American Journal of Science*, **281**, 353-374.
- MACKAY, W. G., 2011, Structure and sedimentology of the Curdimurka Subgroup, northern Adelaide Fold Belt, South Australia. Unpublished PhD thesis, University of Tasmania.
- MADOF, A. S., CHRISTIE-BLICK, N., AND ANDERS, M. H., 2009, Stratigraphic controls on a salt-withdrawal intraslope minibasin, north-central Green Canyon, Gulf of Mexico: Implications for misinterpreting sea level change. *AAPG Bulletin*, **93**,

535-561.

- MAIDMENT, D.W., WILLIAMS, I.S., AND HAND, M., 2007, Testing long-term patterns of basin sedimentation by detrital zircon geochronology, Centralian Superbasin, Australia. *Basin Research*, **19**, 335-360.
- MALLARINO, G., BEAUBOUEF, R. T., DROXLER, A. W., ABREU, V., AND LABEYRIE, L., 2006, Sea level influence on the nature and timing of a minibasin sedimentary fill (northwestern slope of the Gulf of Mexico). *AAPG Bulletin*, **90**, 1089-1119.
- MATTHEWS, W. J., HAMPSON, G. J., TRUDGILL, B. D., AND UNDERHILL, J. R., 2007, Controls on fluviolacustrine reservoir distribution and architecture in passive salt-diapir provinces: Insights from outcrop analogs. *AAPG Bulletin*, **91**, 1367-1403.
- Mawson, D., 1939, The Late Proterozoic Sediments of South Australia. Report of the Australian and New Zealand Association for the Advancement of Science, **24**, 79-88.
- MacMenamin, M.A., and MacMenamin, D.L.S., 1990, The emergence of animals: the Cambrian breakthrough. Columbia University Press, New York.
- MEERT, J.G., 2012, What's in a name? The Columbia (Paleopangaea/Nuna) supercontinent. Unpublished manuscript.
- MEERT, J. G., AND TORSVIK, T. H., 2004, Paleomagnetic Constraints on Neoproterozoic 'Snowball Earth' Continental Reconstructions. In: Jenkins, G.S., McMenamin, M., McKay, C.P., and Sohl, L. The Extreme Proterozoic: Geology, Geochemistry, and Climate. American Geophysical Union, p. 5-11.
- MEERT, J.G., AND VAN DER VOO, R., 1994, The Neoproterozoic (1000-540 Ma) glacial intervals: No more snowball earth? *Earth and Planetary Science Letters*, **123**, 1-13.
- MEISLING, K. E., COBBOLD, P. R., AND MOUNT, V. S., 2001, Segmentation of an obliquely rifted margin, Campos and Santos basins, southeastern Brazil. *AAPG Bulletin*, **85**, 1903-1924.
- MINCHAM, H., 1977, The Story of the Flinders Ranges. Rigby, Adelaide, 305 p.

- MODICA, C.J., AND BRUSH, E.R., 2004, Postrift sequence stratigraphy, paleogeography, and fill history of the deep-water Santos Basin, offshore southeast Brazil. *AAPG Bulletin*, **88**, 923-945.
- MOORE, P. S., 1979, Deltaic Sedimentation--Cambrian of South Australia. *Journal of Sedimentary Research*, **49**, 1229-1244.
- MOORE, P. S., 1990, Origin of redbeds and variegated sediments, Cambrian, Adelaide Geosyncline, South Australia. *Geological Society of Australia Special Publication*, **16**, 334-350.
- MOUNT, T. J., 1975, Diapirs and diapirism in the Adelaide 'Geosyncline' South Australia. University of Adelaide unpublished PhD thesis.
- O'HALLORAN, G., 1992, Sedimentology and Nd isotopic geochemistry of some early Adelaidean rocks from the northern Flinders Ranges, S.A. University of Adelaide BSc Honors Thesis, unpublished.
- OLSON, H. C., AND DAMUTH, J. E., 2010, Character, Distribution and Timing of Latest Quaternary Mass-Transport Deposits in Texas—Louisiana Intraslope Basins Based on High-Resolution (3.5 kHz) Seismic Facies and Piston Cores. In: *Submarine Mass Movements and Their Consequences*, Springer, Netherlands, 607-617.
- Parker, A.J., 1993, Chapter 2: Geological Framework. in: Drexel, J.F., Preiss, W.V. and Parker, A.J. (Eds), *The Geology of South Australia. Vol. 1, The Precambrian. South Australia Geological Survey Bulletin*, **54**, 171-203.
- PILCHER, R.S., KILSDONK, B., AND TRUDE, J., 2011, Primary basins and their boundaries in the deep-water northern Gulf of Mexico: Origin, trap types, and petroleum system implications. *AAPG Bulletin*, **95**, 219-240.
- PIPER, J.D., 2000, The Neoproterozoic Supercontinent: Rodinia or Palaeopangaea?. *Earth and Planetary Science Letters*, **176**, 131-146.
- PIPER, J.D., 2007, The Neoproterozoic supercontinent Palaeopangaea. *Gondwana Research*, **12**, 202-227.
- PIPER, J.D., 2009, Comment on "Assembly, configuration, and break-up history of

- Rodinia: A synthesis” by Li et al.[*Precambrian Res.*, 160 (2008) 179–210].  
*Precambrian Research*, **174**, 200-207.
- PISAREVSKY, S.A., WINGATE, M.T.D., STEVENS, M.K., AND HAINES, P.W., 2007,  
Palaeomagnetic results from the Lancer 1 stratigraphic drillhole, Officer Basin,  
Western Australia, and implications for Rodinia reconstructions. *Australian  
Journal of Earth Sciences*, **54**, 561-572.
- PLUMMER, P. S., 1978, Stratigraphy of the lower Wilpena Group (late Precambrian),  
Flinders Ranges, South Australia. *Transactions of the Royal Society of South  
Australia*, **102**, 25-38.
- PRATSON, L.F., AND COAKLEY, B.J., 1996, A model for the headward erosion of  
submarine canyons induced by downslope-eroding sediment flows. *Geological  
Society of America Bulletin*, **108**, 225-234.
- PREISS, W.V., BELPERIO, A.P., COWLEY, W.M. AND RANKIN, L.R., 1993,  
Neoproterozoic. Chapter 6 in: Drexel, J.F., Preiss, W.V. and Parker, A.J. (Eds),  
The Geology of South Australia. Vol. 1, The Precambrian. *South Australia  
Geological Survey Bulletin*, **54**, 171-203.
- PREISS, W.V., AND FORBES, B.G., 1981, Stratigraphy, correlation and sedimentary  
history of Adelaidean (Late Proterozoic) basins in Australia. *Precambrian  
Research*, **15**, 255-304.
- PREISS, W. V., GOSTIN, V.A., MCKIRDY, D.M., ASHLEY, P.M., WILLIAMS, G.E., AND  
SCHMIDT, P.W., 2011, The glacial succession of Sturtian age in South Australia:  
the Yudnamutana Subgroup. *Geological Society, London, Memoirs*, **36**, 701-  
712.
- PREISS, W. V., KORSCH, R. J., BLEWETT, R. S., FOMIN, T., COWLEY, W. M., NEUMANN,  
N. L., AND MEIXNER, A. J., 2010, Geological interpretation of deep seismic  
reflection line 09GA-CG1: the Curnamona Province–Gawler Craton Link Line,  
South Australia. *Geoscience Australia, Record*, **10**, 66-76.
- PREISS, W.V. (Compiler), 1987, The Adelaide Geosyncline—late Proterozoic  
stratigraphy, sedimentation, paleontology and tectonics. *Bulletin of the  
Geological Survey of South Australia* **53**, 438 p.

- PREISS, W.V., 1999, PARACHILNA, South Australia, sheet SH54-13 (second edition). South Australia. Geological Survey. 1:250 000 Series – Explanatory Notes.
- PREISS, W.V., 2000, The Adelaide Geosyncline of South Australia and its significance in Neoproterozoic continental reconstruction. *Precambrian Research* **100**, 21-63.
- RAUB, T.D., 2010, Stratigraphic context revitalizes solar interpretation for the Neoproterozoic deglacial Elatina rhythmites. *Geological Society of America Abstracts with Programs*, **42**, 402.
- REID, P., AND PREISS, W.V., 1999, Parachilna Sheet SH54-13. 1:250 000 scale Geological Map and Explanatory Notes, Primary Industries and Resources South Australia. Second edition. 52p.
- RESTALLACK, G.J., 2011, Neoproterozoic loess and limits to snowball Earth. *Journal of the Geological Society, London*, **168**, 289-307.
- RESTALLACK, G. J., MARCONATO, A., OSTERHOUT, J. T., WATTS, K. E., AND BINDEMAN, I. N., 2014, Revised Wonoka isotopic anomaly in South Australia and Late Ediacaran mass extinction. *Journal of the Geological Society*, **171**, 709-722.
- RESTALLACK, G. J., 2012, Were Ediacaran siliciclastics of South Australia coastal or deep marine?. *Sedimentology*, **59**, 1208-1236.
- ROBERTS, M.J., METZGAR, C.R., LIU, J., LIM, S.J., 2004, Regional assessment of salt weld timing, Campos Basin, Brazil. In Salt-Sediment Interactions and Hydrocarbon Prospectivity: Concepts, Applications, and Case Studies for the 21st Century. 24th Annual Gulf Coast Section SEPM Foundation, Bob F. Perkins Research Conference.
- ROSE, C.V., AND MALOOF, A.C., 2010, Testing models for post-glacial 'cap dolostone' deposition: Nuccaleena Formation, South Australia. *Earth and Planetary Science Letters*, **296**, 165-180.
- ROWAN, M.G., AND VENDEVILLE, B.C., 2006, Foldbelts with early salt withdrawal and diapirism: Physical model and examples from the northern Gulf of Mexico and

- the Flinders Ranges, Australia. *Marine and Petroleum Geology*, **23**, 871-891.
- SONNETT, C.P., FINNEY, S.A., AND WILLIAMS, C.R., 1988, The lunar orbit in the late Precambrian and the Elatina sandstone laminae. *Nature*, **335**, 806-808.
- SONNETT, C.P., AND WILLIAMS, G.E., 1987, Frequency modulation and stochastic variability of the Elatina varve record: a proxy for solar cyclicity? *Solar Physics*, **110**, 397-410.
- STEVENSON, G. M., AND WRAY, L. L., 2009, History of petroleum exploration of Paleozoic targets in the Paradox Basin. in Houston et al., The Paradox Basin Revisited – New Developments in Petroleum Systems and Basin Analysis: *RMAG Special Publication*, 1-23.
- SWART, P. K., AND M. J. KENNEDY. 2012, Does the global stratigraphic reproducibility of  $\delta^{13}\text{C}$  in Neoproterozoic carbonates require a marine origin? A Pliocene–Pleistocene comparison. *Geology*, **40**, 87-90.
- THOMSON, B.P., COATS, R.P., MIRAMS, R.C., FORBES, B.G., DALGARNO, C.R., AND JOHNSON, J.E., 1964, Precambrian rock groups in the Adelaide Geosyncline: a new subdivision. *Quarterly Geological Notes, Geological Survey of South Australia*, **9**, 1-19.
- THOMSON, B. P., 1966, The lower boundary of the Adelaide system and older basement relationships in south Australia. *Journal of the Geological Society of Australia*, **13**, 203-228.
- TURNER, G. R., 1976, Stratigraphy, structural geology and metamorphism of the Callanna beds and base of the Burra Group in the Arkaroola Village area, South Australia. Unpublished University of Adelaide BSc Honors Thesis.
- UPPHILL, R. K., 1980, Sedimentology of the Late Precambrian Mundallio Subgroup: A clastic-carbonate (Dolomite, Magnesite) sequence in the Mt. Lofty and Flinders Ranges, South Australia. Unpublished University of Adelaide PhD Dissertation.
- URLWIN, B., 1992, Carbon isotope stratigraphy of the late Proterozoic Wonoka formation of the Adelaide fold belt : diagenetic assessment and interpretation of

isotopic signature and correlations with previously measured isotopic curves. Unpublished University of Adelaide BSc Honors Thesis.

- VON DER BORCH, C.C., AND LOCK, D., 1979, Geological Significance of Coorong Dolomites. *Sedimentology*, **26**, 813-824.
- VON DER BORCH, C. C., GRADY, A. E., ALDAM, R., MILLER, D., NEUMANN, R., ROVIRA, A., AND EICKHOFF, K., 1985, A large-scale meandering submarine canyon: outcrop example from the late Proterozoic Adelaide Geosyncline, South Australia. *Sedimentology*, **32**, 507-518.
- VON DER BORCH, C. C., SMIT, R., AND GRADY, A.E., 1982, Late Proterozoic submarine canyons of Adelaide Geosyncline, South Australia, *AAPG Bulletin*, **66**, 332-347.
- VON DER BORCH, C.C., CHRISTIE-BLICK, N., AND GRADY, A. E., 1988, Depositional sequence analysis applied to Late Proterozoic Wilpena Group, Adelaide Geosyncline, South Australia. *Australian Journal of Earth Sciences*, **35**, 59-72.
- VON DER BORCH, C. C., 1980, Evolution of late proterozoic to early paleozoic Adelaide foldbelt, Australia: Comparisons with postpermian rifts and passive margins. *Tectonophysics*, **70**, 115-134.
- WALTER, M.R., VEEVERS, J.J., CALVER, C.R., AND GREY, K., 1995, Neoproterozoic stratigraphy of the Centralian Superbasin, Australia. *Precambrian Research*, **73**, 173-195.
- WEBB, B.P., 1960, Diapiric structures in the Flinders Ranges. *Australian Journal of Science*, **22**, 390-391.
- WILLIAMS, G.E., 1988, Cyclicity in the late Precambrian Elatina Formation, South Australia: solar or tidal signature? *Climatic Change*, **13**, 117-128.
- Williams, G.E., 1990, Tidal rhythmites: key to the history of the Earth's rotation and lunar orbit. *Journal of Physics of the Earth*, **38**, 475-491.
- WILLIAMS, G.E., 1997, Precambrian length of day and the validity of tidal rhythmite paleotidal values. *Geophysical Research Letters*, **24**, 421-424.



- WILLIAMS, G.E., AND GOSTIN, V.A., 2000, Mantle plume uplift in the sedimentary record: origin of kilometre-deep canyons within late Neoproterozoic successions, South Australia. *Journal of the Geological Society*, **157**, 759-768.
- WILLIAMS, G.E., AND GOSTIN, V.A., 2005, Acraman-Bunyerroo impact event (Ediacaran), South Australia, and environmental consequences: twenty-five years on. *Australian Journal of Earth Sciences*, **52**, 607-620.
- WILLIAMS, G.E., AND SONNETT, C.P., 1985, Solar signature in sedimentary cycles from the late Precambrian Elatina Formation, Australia. *Nature*, **318**, 523-527.
- WILLIAMS, G.E., GOSTIN, V.A., MCKIRDY, D.M., AND PREISS, W.V., 2008, The Elatina glaciation, late Cryogenian (Marinoan Epoch), South Australia: Sedimentary facies and palaeoenvironments. *Precambrian Research*, **163**, 307-331.
- WILLIAMS, G. E., GOSTIN, V. A., MCKIRDY, D. M., PREISS, W. V., AND SCHMIDT, P. W., 2011, The Elatina glaciation (late Cryogenian), South Australia. *Geological Society, London, Memoirs*, **36**, 713-721.
- WINGATE, M. T., CAMPBELL, I. H., COMPSTON, W., AND GIBSON, G. M., 1998, Ion microprobe U–Pb ages for Neoproterozoic basaltic magmatism in south-central Australia and implications for the breakup of Rodinia. *Precambrian Research*, **87**, 135-159.
- WINGATE, M.T., PISAREVSKY, S.A., AND EVANS, D.A., 2002, Rodinia connections between Australia and Laurentia: no SWEAT, no AUSWUS?. *Terra Nova*, **14**, 121-128.
- WYSOCZANSKI, R. J., AND ALLIBONE, A. H., 2004, Age, correlation, and provenance of the Neoproterozoic Skelton Group, Antarctica: Grenville age detritus on the margin of East Antarctica. *The Journal of Geology*, **112**, 401-416.
- YOUNG, G. M., AND GOSTIN, V.A., 1988, Stratigraphy and sedimentology of Sturtian glaciogenic deposits in the western part of the North Flinders Basin, South Australia. *Precambrian Research*, **39**, 151-170.
- YOUNG, G.M., AND GOSTIN, V.A., 1989, An exceptionally thick upper Proterozoic (Sturtian) glacial succession in the Mount Painter area, South Australia.

*Geological Society of America Bulletin*, **101**, 834-845.

YOUNG, G.M., AND GOSTIN, V.A., 1990, Sturtian glacial deposition in the vicinity of the Yankaninna Anticline, north Flinders Basin, South Australia. *Australian Journal of Earth Sciences*, **37**, 447-458.

YOUNG, G.M., AND GOSTIN, V.A., 1991, Late Proterozoic (Sturtian) succession of the North Flinders Basin, South Australia: an example of temperate glaciation in an active rift setting. In Anderson, J.B., and Ashley, G.M., *Glacial Marine Sedimentation: Paleoclimatic Significance. GSA Special Publication* **261**, 207-222.

YOUNGS, B.C., 1977, The sedimentology of the Cambrian Wirrealpa and Aroona Creek Limestones: *Geological Survey of South Australia Bulletin* **47**, 73 p.

ZAHNLE, K.J. AND WALKER, J.C.G., 1987, Climatic oscillations during the Precambrian Era. *Climatic Change*, **10**, 269-284.

ZHAO, J.X., McCULLOCH, M.T., AND KORSCH, R.J., 1994, Characterisation of a plume-related ~ 800 Ma magmatic event and its implications for basin formation in central-southern Australia. *Earth and Planetary Science Letters*, **121**, 349-367.

ZHAO, G., SUN, M., WILDE, S.A., LI, S., AND ZHANG, J., 2006, Some key issues in reconstructions of Proterozoic supercontinents. *Journal of Asian Earth Sciences*, **28**, 3-19.

# Statement of Authorship

Title of Paper	Sedimentological interpretation of an Ediacaran delta: Bonney Sandstone, South Australia
Publication Status	<input checked="" type="checkbox"/> Published <input type="checkbox"/> Accepted for Publication <input type="checkbox"/> Submitted for Publication <input type="checkbox"/> Unpublished and Unsubmitted work written in manuscript style
Publication Details	Counts, John; Rarity, F., Ainsworth, B., Amos, K., Lane, Tessa; Moron, S., Trainor, J., Valenti, C., and Nanson, R. (2016), Sedimentological interpretation of an Ediacaran delta: Bonney Sandstone, South Australia. Australian Journal of Earth Sciences, in press

## Principal Author

Name of Principal Author (Candidate)	John W. Counts		
Contribution to the Paper	All manuscript text; all figure drafting; fieldwork; final descriptions and interpretations		
Overall percentage (%)	85%		
Certification:	This paper reports on original research I conducted during the period of my Higher Degree by Research candidature and is not subject to any obligations or contractual agreements with a third party that would constrain its inclusion in this thesis. I am the primary author of this paper.		
Signature	<table border="1" style="float: right;"> <tr> <td>Date</td> <td>18/4/2016</td> </tr> </table>	Date	18/4/2016
Date	18/4/2016		

## Co-Author Contributions

By signing the Statement of Authorship, each author certifies that:

- i. the candidate's stated contribution to the publication is accurate (as detailed above);
- ii. permission is granted for the candidate to include the publication in the thesis; and
- iii. the sum of all co-author contributions is equal to 100% less the candidate's stated contribution.

Name of Co-Author	Frank Rarity		
Contribution to the Paper	Fieldwork; Post-fieldwork discussions; assistance with WAVE classification system; assistance with interpretation		
Signature	<table border="1" style="float: right;"> <tr> <td>Date</td> <td>16/06/2016</td> </tr> </table>	Date	16/06/2016
Date	16/06/2016		

Name of Co-Author	Bruce Ainsworth		
Contribution to the Paper	Fieldwork; post-fieldwork discussions; review and assistance with environmental interpretations		
Signature	<table border="1" style="float: right;"> <tr> <td>Date</td> <td>15/6/16</td> </tr> </table>	Date	15/6/16
Date	15/6/16		

Name of Co-Author	Kathryn Amos
Contribution to the Paper	Fieldwork; Post-fieldwork discussions
Signature	Date 19/05/16

Name of Co-Author	Tessa Lane
Contribution to the Paper	Fieldwork, including photography; Post-fieldwork discussions
Signature	Date 26/05/16

Name of Co-Author	Sara Morón
Contribution to the Paper	Fieldwork; Section thickness calculations; Post-fieldwork discussions
Signature	Date 19/05/16

Name of Co-Author	Jessica Trainor
Contribution to the Paper	Fieldwork; Post-fieldwork discussions
Signature	Date 19/05/16

Name of Co-Author	Claudia Valenti
Contribution to the Paper	Fieldwork
Signature	Date 1/7/2016

Name of Co-Author	Rachel Nanson
Contribution to the Paper	Post-fieldwork discussions
Signature	Date 19/5/16

**Chapter 3: Sedimentological interpretation of an  
Ediacaran delta: Bonney Sandstone, South  
Australia**

J. W. Counts, F. Rarity, R. B. Ainsworth, K. J. Amos, T. Lane, S. Morón, J.  
Trainor, C. Valenti and R. Nanson

*As published in the Australian Journal of Earth Sciences, 2016*

### 3.1: Abstract

*The type section of the late Ediacaran (ca 565 Ma) Bonney Sandstone in South Australia provides an opportunity to interpret a succession of Precambrian clastic sediments using physical sedimentary structures, lithologies and stacking patterns. Facies models, sequence stratigraphic analysis, and process-based architectural classification of depositional elements were used to interpret depositional environments for a series of disconformity-bounded intervals. This study is the first detailed published work on the Bonney Sandstone, and provides additional context for other Wilpena Group sediments, including the overlying Rawnsley Quartzite and its early metazoan fossils. Results show that the »300 m-thick section studied here shows a progressive change from shallow marine to fluvially dominated sediments, having been deposited in storm-dominated shelf and lower shoreface environments, lower in the section, and consisting primarily of stacked channel sands, in a proximal deltaic environment near the top. Based on the degree of influence of wave, tidal or fluvial depositional processes, shallow marine sediments can be classified into beach, mouth bar, delta lobe and channel depositional elements, which can be used to assist in predicting sandbody geometries when only limited information is available. Sediments are contained within a hierarchical series of regressive, coarsening-upward sequences, which are in turn part of a larger basin-scale sequence that likely reflects normal regression and filling of accommodation throughout a highstand systems tract. Paleogeographic reconstructions suggest the area was part of a fluvially dominated clastic shoreline; this is consistent with previous reconstructions that indicate the area was on the western edge of the basin adjacent to the landward Gawler Craton. This research fills in a knowledge gap in the depositional history of a prominent unit in the Adelaide*

*Rift Complex and is a case study in the interpretation of ancient deposits that are limited in extent or lacking diagnostic features.*

### **3.2: Introduction**

Over the past several decades, a variety of methods have been proposed to assist in determining the paleoenvironmental and paleogeographic settings of ancient sediments. In this paper, we provide a case study in interpreting a succession of Precambrian strata using a combination of methodologies, focusing on the classification and interpretation scheme described by Ainsworth, Vakarelov, and Nanson (2011) and Vakarelov and Ainsworth (2013), but also incorporating elements from Galloway (1975), Posamentier and Walker (2006), Reading (2009), and Walker (1984a). Unlike Phanerozoic depositional systems, Precambrian clastic sediments deposited before the evolution of complex life usually require interpretations to be based purely on physical processes, without the overprint of biogenic structures or the presence of diagnostic body fossils. The purpose of this study is to describe and interpret the type section of the Ediacaran Bonney Sandstone in Bunyeroo Gorge, South Australia, with the goals of: (1) applying modern interpretation techniques to gain a better understanding of the depositional environments in the formation, in order to better reconstruct the area's paleogeography at the time of deposition; (2) examining how these environments change over time in order to reconstruct the relative sea-level history and sequence stratigraphic setting of the region; and (3) assessing the effectiveness of a using combined interpretation methods when faced with a limited set of data.

With Precambrian rocks making up only 1.5% of surface rocks globally, similar systems are relatively rare worldwide when compared with their Phanerozoic

counterparts (Blatt and Jones, 1975). Although the physical and chemical factors that affect sedimentation are still largely applicable to the Precambrian, the specific environmental conditions prevalent at the time were different from those today. The lack of multicellular life, differing atmospheric composition, and an increased rate of weathering and sedimentation affected the makeup and distribution of sedimentary environments (Bose et al., 2012). In addition, Precambrian deposits are biased overall towards craton interiors owing to the extensive tectonic modification of continental margins over time (Donaldson, Eriksson, and Altermann, 2009). Thus, the strata discussed here provide a unique opportunity to study an ancient succession of shallow-marine sediments on the margin of the Precambrian subcontinent that included Australia, which resulted from the Neoproterozoic fragmentation of the supercontinent Rodinia (Li et al., 2008).

In this study, we use aspects of several different, but mutually complementary methods in conjunction with one another to obtain a holistic view of a succession of clastic sediments. This approach to interpretation is warranted here because the data set consists solely of physical, inorganic sedimentary structures, lithologies and stratigraphic trends, with no trace or body fossils to assist in narrowing down the environmental setting. Interpretation of the section is also hampered by the paucity of detailed previous work on the formation and lack of detailed regional context for the section described here. A single outcrop section, however, can still result in significant new information, as interpreted depositional processes can reveal much about the larger depositional environments, paleogeography and geobody morphology of a region.



### **3.3: Background**

#### *3.3.1: Previous Research*

This study is the first detailed published work on the upper Bonney Sandstone, a clastic-dominated unit that was deposited on the AustraliaEast Antarctica subcontinent in the Ediacaran Period (Preiss, 1999). The subcontinent was formerly part of Rodinia, a supercontinent that existed as a stable landmass from around 1 Ga until around 850 Ma (Bogdanova, Pisarevsky, and Li, 2009). By the time of deposition of the sediments discussed here, this subcontinent was independent and would have existed at low latitudes, just north of the paleoequator (Li et al., 2008). Deposition of the Bonney Sandstone took place in the Adelaide Rift Complex, a Neoproterozoic to Cambrian basin on the margin of this subcontinent that began as a rift around 800 Ma. Beginning around 690 Ma, sag-phase deposition and continued Rodinian breakup led to the basin having an open oceanic connection to the east-southeast (present-day orientation; Preiss, 1990, 2000), and by the Ediacaran it had evolved into a passive margin (Preiss, 2000). The Adelaide Rift Complex is coeval with parts of the Amadeus, Georgina, Ngalia, Officer and Savory basins, which formed the much larger (2 million km<sup>2</sup>) Centralian Superbasin across much of central Australia. Although generally not considered within the bounds of the larger Superbasin (Walter et al., 1995), the Adelaide Rift Complex shows many lithological similarities, and thus may have been a part of the Centralian depositional system. The modern-day Flinders Ranges expose several thousand metres of both clastic and carbonate basin-fill sediments, which were deposited in a variety of shelf, shallow-marine, and continental environments over the course of ca 300 Ma. Sedimentation began around 800 Ma and culminated in the Middle Cambrian (Jago, Gatehouse, Powell, Casey, and Alexander, 2010), although the absolute dates of

many basin sediments are not clear and are interpolated from the few chronological markers that exist (Preiss, 2000). For a comprehensive summary of basin stratigraphy, see Preiss (1987).

Many sediments were affected by syndepositional diapir movement, where basal evaporites from the lowermost Callanna Group penetrated stratigraphically higher formations and in places pierced the surface (Dalgarno and Johnson, 1968; Kernén et al., 2012; Hearon, Rowan, Lawton, Hannah, and Giles, 2015; Counts and Amos, 2016). After the majority of sedimentation ceased in the Cambrian, the Delamerian Orogeny (514–190 Ma; Foden, Elburg, Dougherty-Page, and Burt, 2006) intensely deformed basin sediments, resulting in folded and faulted strata now widely exposed in cross-section. These sediments are bounded to the west by the Gawler Craton and onlapping sediments of the Stuart Shelf, and to the east by the smaller Curnamona Cratonic Nucleus (Drexel et al., 1993). Both of these adjacent continental provinces would have been at least periodically subaerially exposed throughout much of basin history, with the basin fill being dominantly marine (Drexel et al., 1993; Preiss, 1987).

The Bonney Sandstone is a part of the Wilpena Group (Figure 1), whose base is at the Global Boundary Stratotype Section and Point that defines the worldwide beginning of the Ediacaran period (Knoll, Walter, Narbonne, and Christie-Blick, 2006). It is the lowermost unit of the Pound Subgroup, immediately preceding the Rawnsley Quartzite, which hosts the well-known Ediacaran metazoan fossil assemblage. Youngest concordant zircon dates by Ireland, Flottmann, Fanning, Gibson, and Preiss (1998) constrain Bonney deposition to no older than around 556 (+/-24 Ma) Ma. The formation is part of a large-scale shallowing-upward sequence (sequence Marinoan 4; Preiss, 2000) that encompasses sediments from the

Bunyeroo Formation to the Rawnsley Quartzite, and terminates at the Ediacaran Cambrian boundary. Below the Bonney Sandstone, the underlying Bunyeroo and Wonoka formations are composed primarily of clastic and carbonate mudstones, respectively, and the overlying Rawnsley Quartzite, including the Ediacara and Chace members, was deposited in a variety of shallow marine and intertidal environments (Gehling, 2000). In the revision of the Parachilna map sheet, Reid and Preiss (1999) revised the Bonney Sandstone to include sediments that had previously been in the Wonoka Formation, known as the Patsy Hill Member. These carbonates are not included in this study; here, we focus on the clastic sands and silty mudstones that make up the upper portion of the formation, as well as the lower portion of the Rawnsley Quartzite (the Chace Member).

Previous research on the formation either has been very general or has not been published in peer-reviewed literature. Forbes (1971) initially defined the type

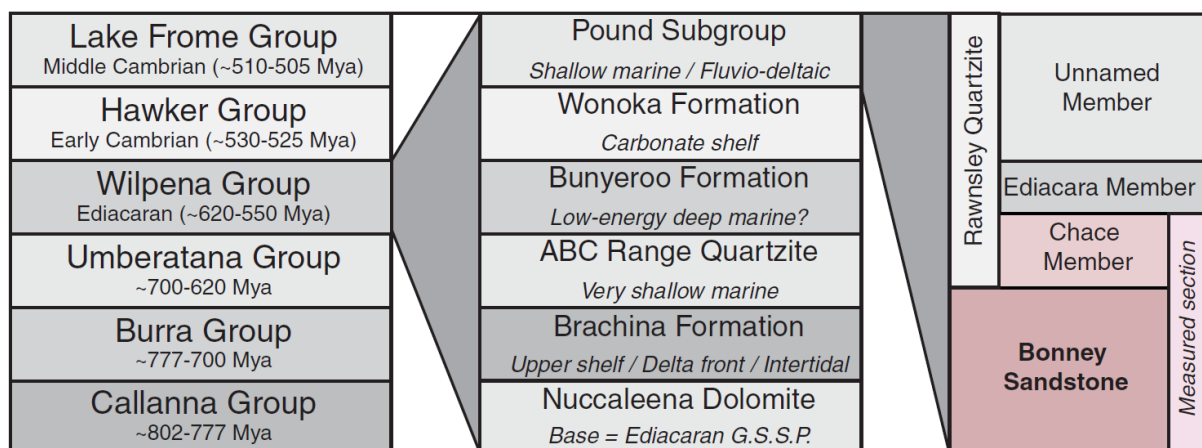


Figure 1: Stratigraphy of the Adelaide rift complex basin fill, showing the position of the Bonney Sandstone in relation to other units. A comprehensive description of all stratigraphic units can be found in Preiss (1987).

locality in Bunyeroo Gorge, but only provided brief lithological descriptions. The only detailed study to date is that of Gehling (1982), which included the Bonney Sandstone in an unpublished thesis primarily devoted to the context and palaeontology of the Ediacaran faunal assemblage. Gehling (1982) measured the

section we describe here, as well as many other Bonney Sandstone outcrops in the area; the two studies are compared below. He interprets the Bonney Sandstone as comprising seven individual facies, generally interpreted as having been deposited in tidally influenced, marginal-marine environments, usually in fining-upward sequences in delta lobes prograding basinward from the northwest. Most environments are interpreted as having been intertidal or subtidal, with a thin interval of alluvial deposition near the top of the formation.

### *3.3.2: Study Area*

The Bonney Sandstone section measured is exposed in Bunyeroo Gorge, South Australia (Figure 2; approximately  $-31.413341^{\circ}\text{S}$ ,  $138.544719^{\circ}\text{E}$ ). At the field site the formation is striking approximately  $035^{\circ}$  and is tilted significantly, dipping  $\sim 65^{\circ}\text{E}$ . Here, Bunyeroo Creek cuts through the upper Wilpena Group at approximately  $90^{\circ}$  to strike, creating a cross-sectional view of the formation. Sediments comprising the Bonney Sandstone are exposed in the sub-vertical walls of the creek bed, permitting observations on a relatively continuous exposure of the formation.

### **3.4: Methodology**

Stratigraphic units were measured with the use of a laser range-finder, tape measure and handheld GPS. Features measured included grain size, average bed thickness, lithological and stratigraphic trends (e.g. small-scale fining-upward sequences), key surfaces, sedimentary structures and paleocurrent directions. Units were divided into facies based on the recurrence of lithological characteristics, generally a combination of both grain size and sedimentary structures (Table 1). This separation was based on the interpreted depositional process responsible for each

one. Facies that repeatedly occurred stratigraphically adjacent to one another were grouped into facies associations, which represent multiple depositional processes occurring within a continuous time frame (Table 2). Genetically related intervals within the formation were identified based on facies stacking patterns, fining or coarsening-upward profiles in outcrop, and transgressive or erosive surfaces bounding such intervals. Once these features were identified, environments of deposition and specific depositional elements for each interval were interpreted primarily using methods described in Ainsworth et al. (2011), Vakarelov and Ainsworth (2013) and Walker (1984a).

Today, interpretation commonly utilises a facies models concept, well summarised by Walker (1979, 1984a), and Walker and James (1992). In this approach, sedimentary characteristics are used to define facies and facies associations, which are then assigned to a particular environment in the model, based on similarity to deposits observed in modern settings and inferences as to how such models would have been different in past conditions. Environments (e.g. delta front) contain a number of sub-environments (e.g., distributary mouth bars, channels, levees), each with a particular set of processes operating that allow deposits to be distinguished from one another. Facies models commonly take the form of idealised sequences of facies, block diagrams showing 3-D sediment relationships, or map-view schematics of sub-environments (Walker, 1984a). Galloway (1975) represented deltaic systems by a wave-tidal-fluvial ternary diagram, with each end-member of the spectrum representing a unique delta geomorphology associated with the process. This ternary diagram was expanded upon by Ainsworth et al. (2011) to incorporate all coastal environments and mixed-process systems, allowing intervals showing multiple processes to be classified as, for instance,

'wave-dominated, fluviially influenced, and tidally affected' (*Wft*). Vakarelov and Ainsworth (2013) also placed an emphasis on the interpretation of stacking patterns at intra- and inter-parasequence scale, the nature of bounding surfaces as either transgressive or regressive, and a standardised classification of sedimentary units into a hierarchy of idealised depositional elements. All of these approaches are components of the interpretation discussed here.

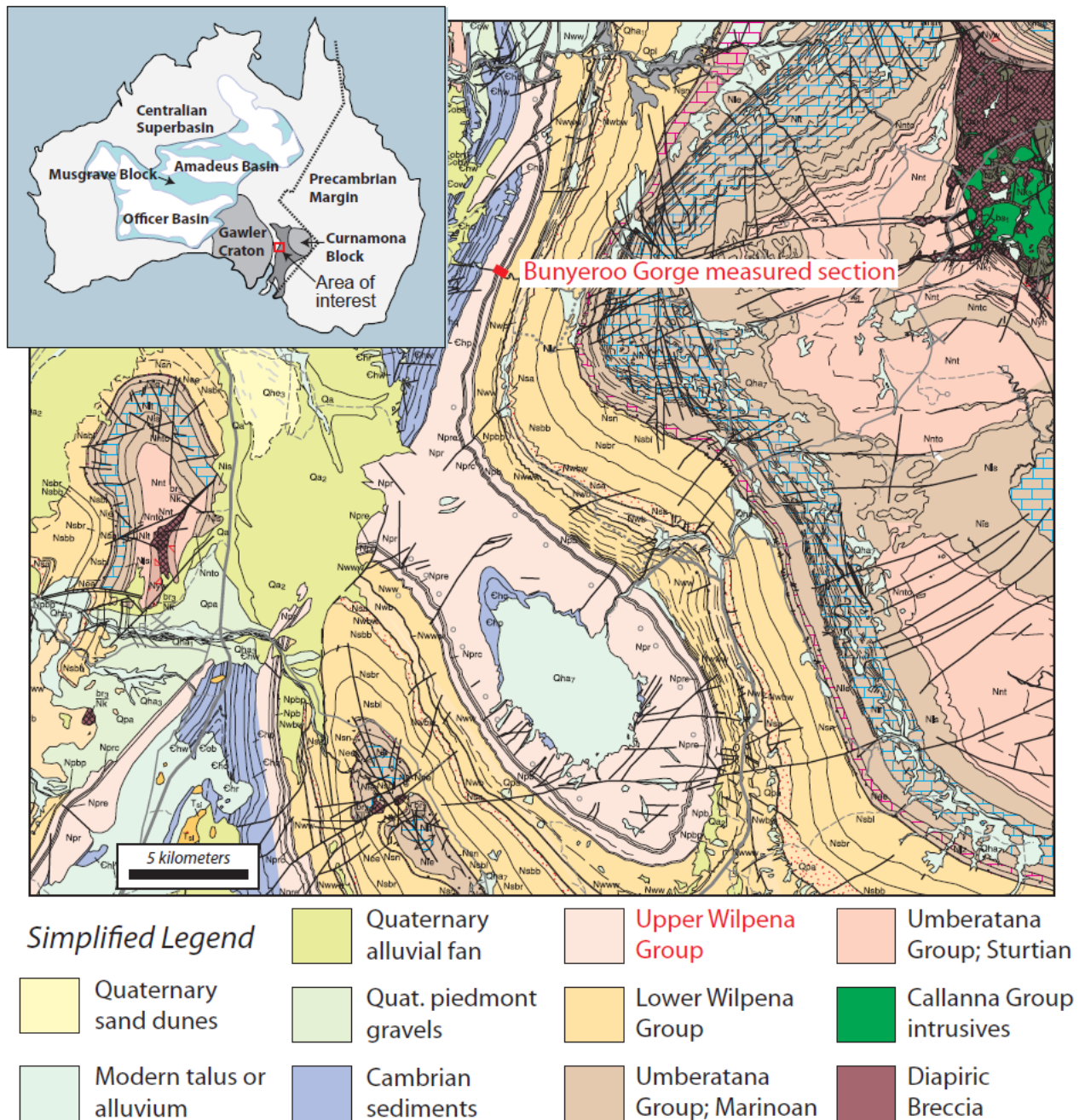


Figure 2: Detailed geological map of the study area and its position within Australia. Taken from Reid et al. (1999)

### **3.5: Results and Interpretation**

#### *3.5.1: Lithostratigraphic Divisions*

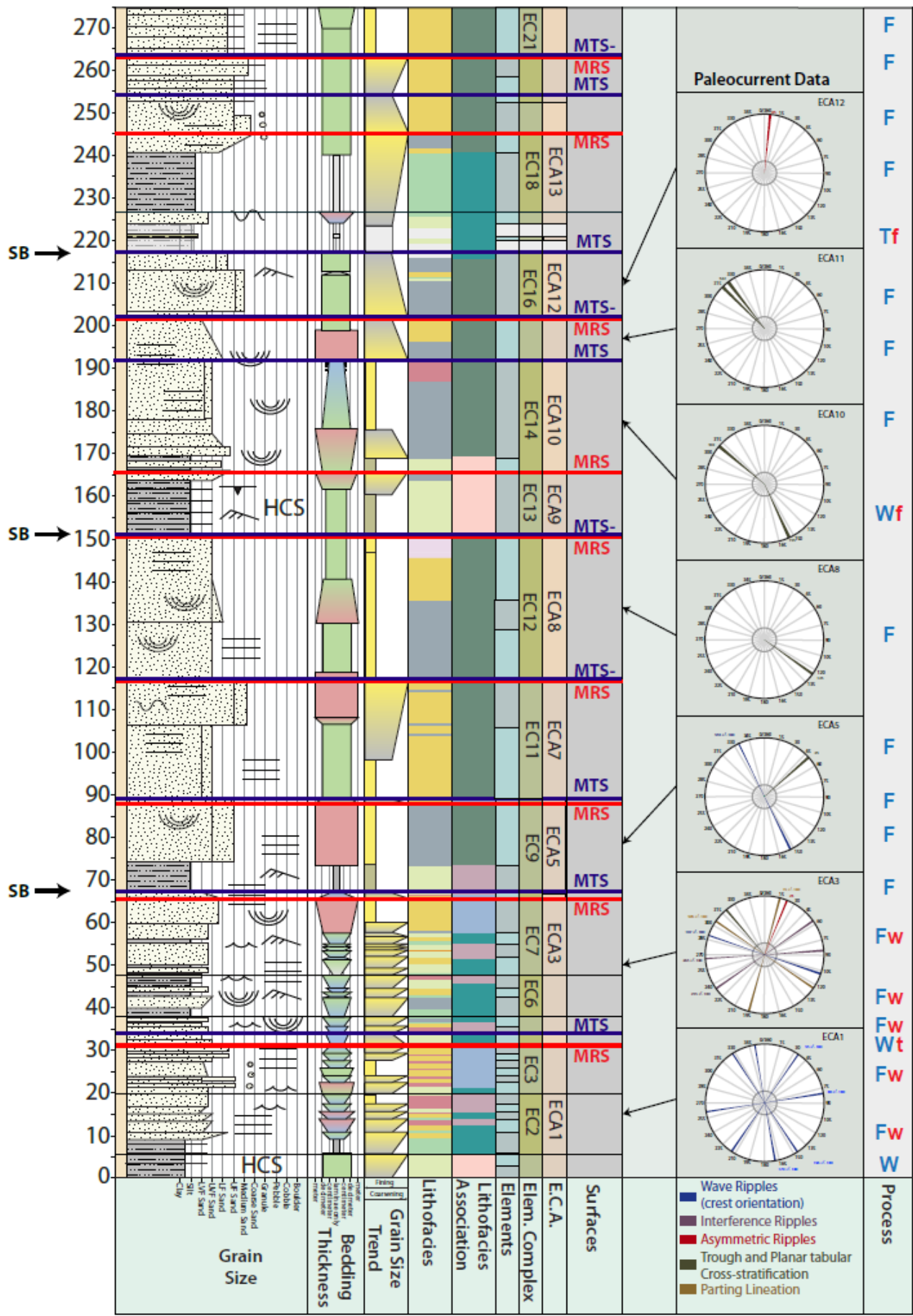
Bonney Sandstone sediments exposed in Bunyeroo Gorge are composed of a variety of clastic lithologies, with grainsizes ranging from silty mudstones to granules. Sandstones are dominant; the mean grainsize of sandstones increases overall up-section, from dominantly very fine- to fine-grained or very fine-grained near the base, to medium-grained near the top. Sandstones in most intervals, however, are rarely coarser than fine-grained, and range from cleaner quartz arenites to muddy, feldspathic sandstones, with occasional granule stringers present. At the scale of outcrop observations, sandstone beds were most commonly tabular and continuous. The outcrop is only incipiently weathered at creek level; sandstone beds commonly weather in relief, forming small ridges perpendicular to the creek bed, with finer-grained intervals forming reentrants. The few instances where channel forms or scours were observed were noted on the log. The section is approximately 270 m thick, including the Chace Member (Figures 3, 4), and the Bonney Sandstone can be divided into three general lithological divisions: (1) a lower division, about 75 m thick, consisting of interbedded fissile silty mudstones and very fine-grained sandstones, in decimetre-scale beds contained within coarsening-upward packages; (2) a middle unit composed almost entirely of amalgamated sandstones, also about 75 m thick, which can be described as a single, vertically interconnected sandstone containing few or none of the mudstones seen in the lower Bonney Sandstone; and (3) an upper heterogeneous interval, ~85 m thick with lower quality exposure, consisting of muddy siltstones interbedded with sandstones on a metre scale. These divisions are independent of genetic or sequence stratigraphic boundaries, but are useful for correlation. A similar tripartite division

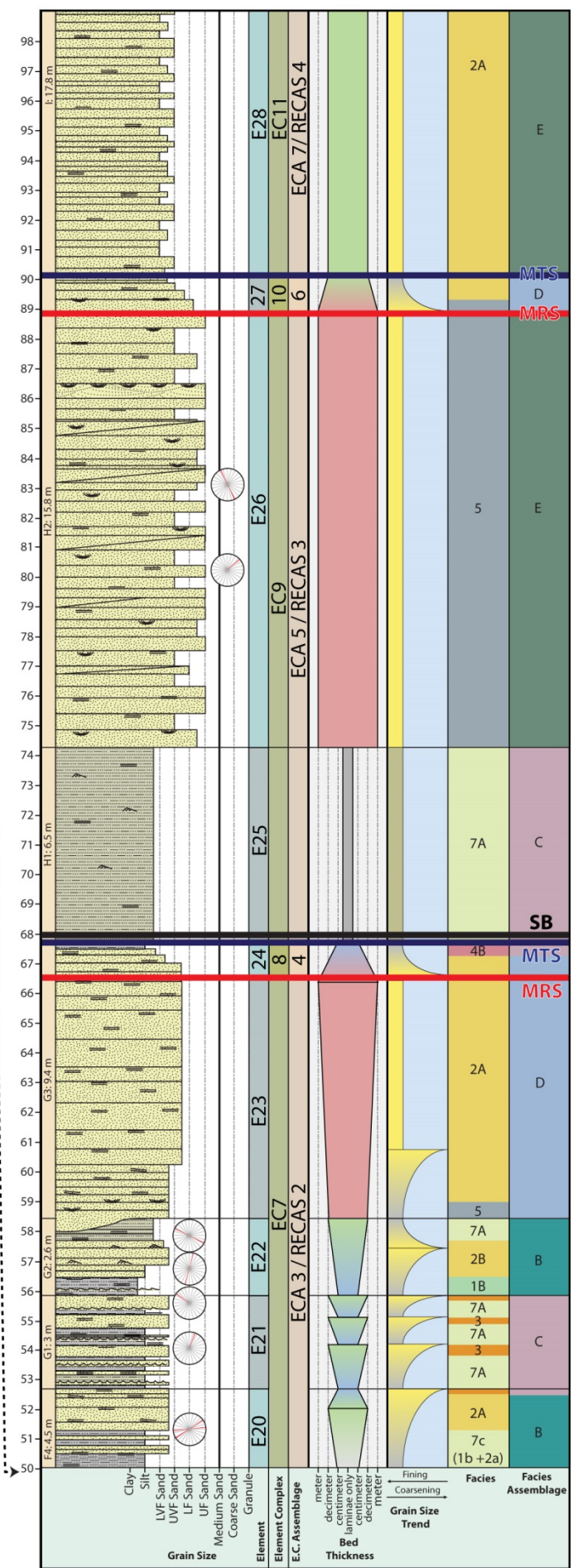
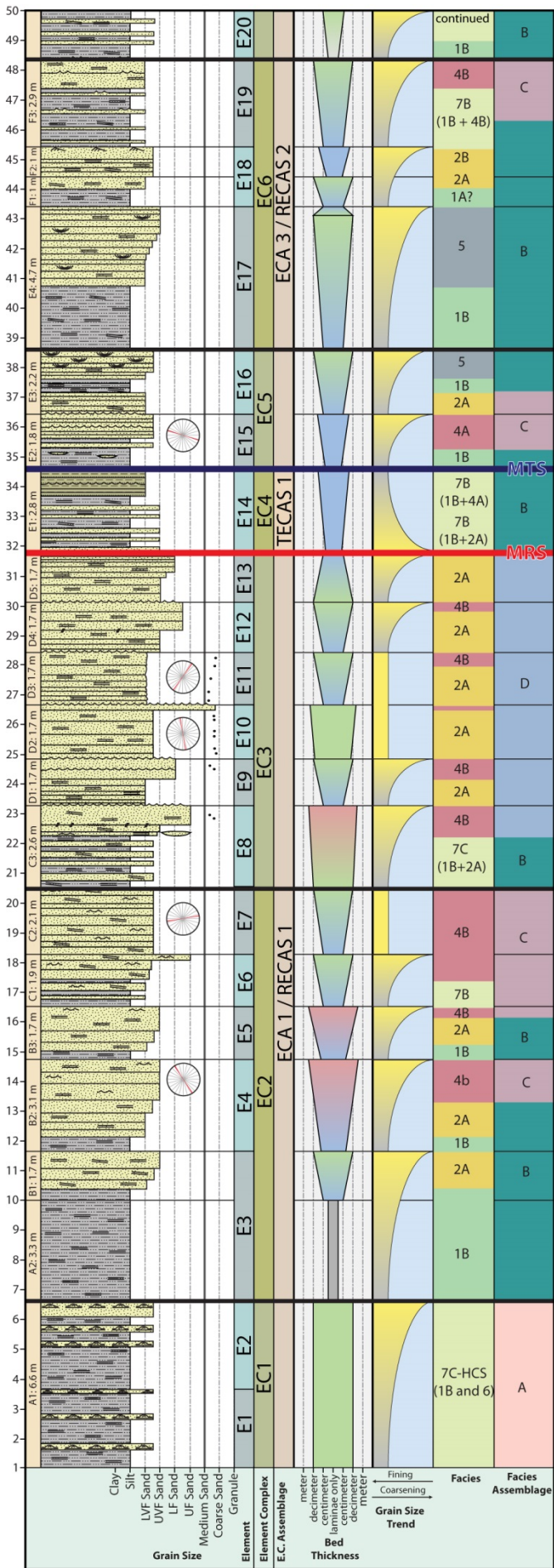
was observed by Gehling (1982). Gehling (1982) also notes that the overlying Chace Member of the Rawnsley Quartzite is separated from the Bonney Sandstone by a non-erosive unconformable contact, which he identifies as a type 2 sequence boundary based on the change in sedimentary character from muddy, reddish sandstones to cleaner light coloured sands. The upper sandy unit described here (at 239 m and above) is recognised as a lithological boundary and interpreted to be the Chace Member on the basis of Gehling's (1982) regional work; however, our specific interpretations as to the depositional environment and nature of the contact differ.

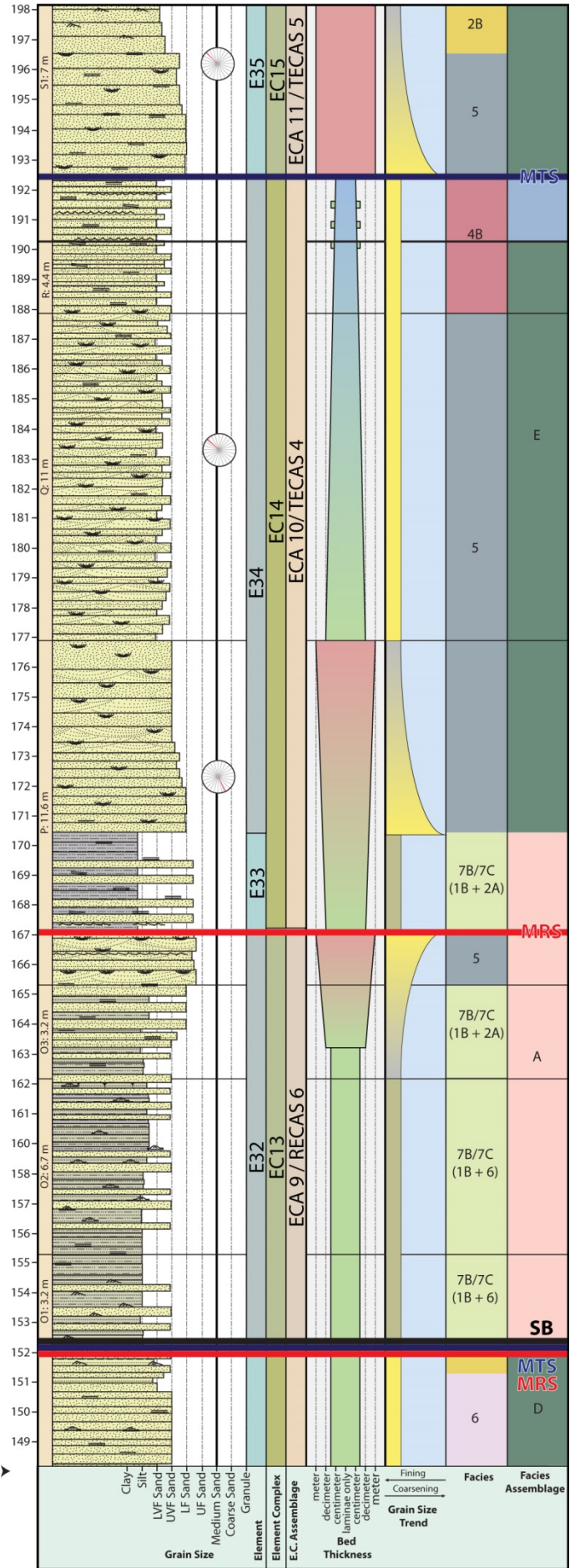
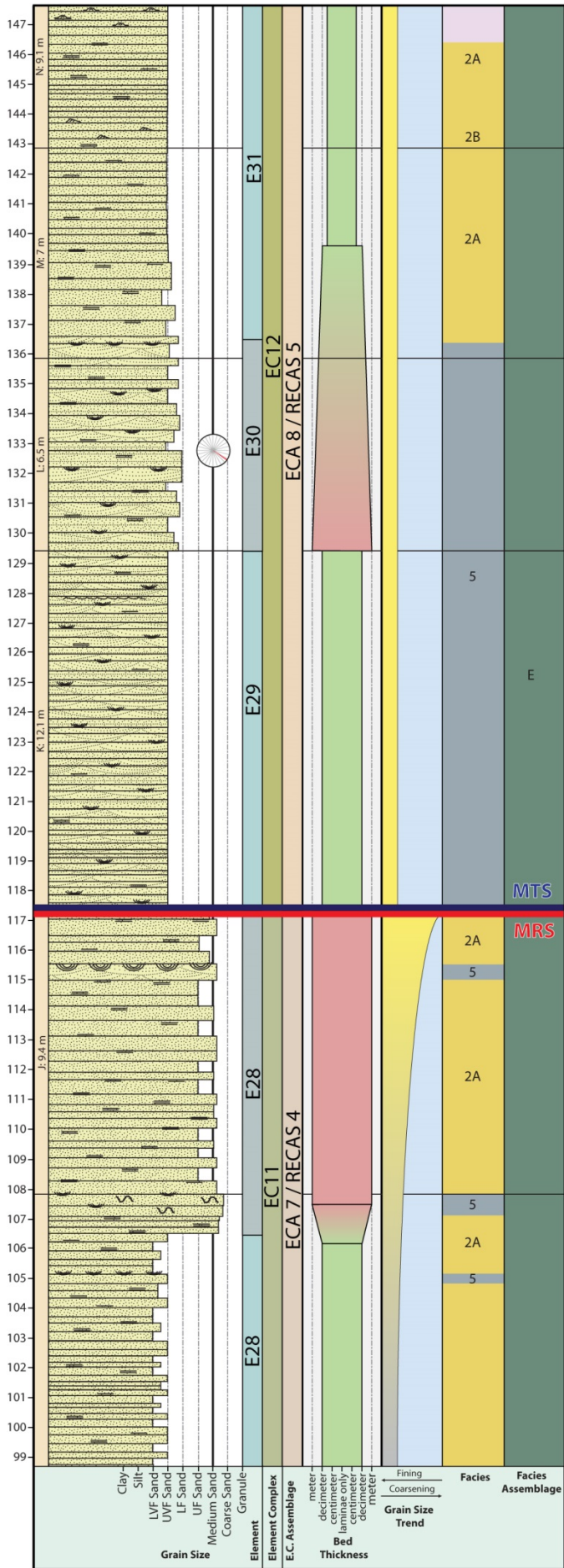
*Figure 3 (page 88): Summary log and palaeocurrents. For detailed information, see complete log in Figure 4 and interpretations in Tables 1, 2 and 4. SB, sequence boundary; EC, element complex; ECA, element complex assemblage; MTS, maximum transgressive surface; MRS, maximum flooding surface; HCS, hummocky cross stratification.*

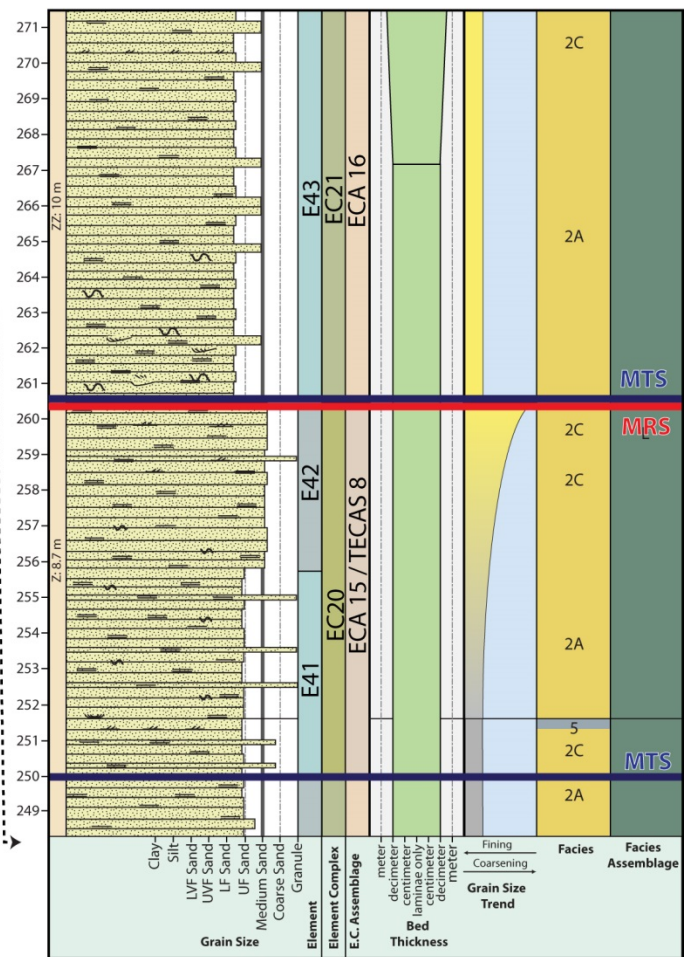
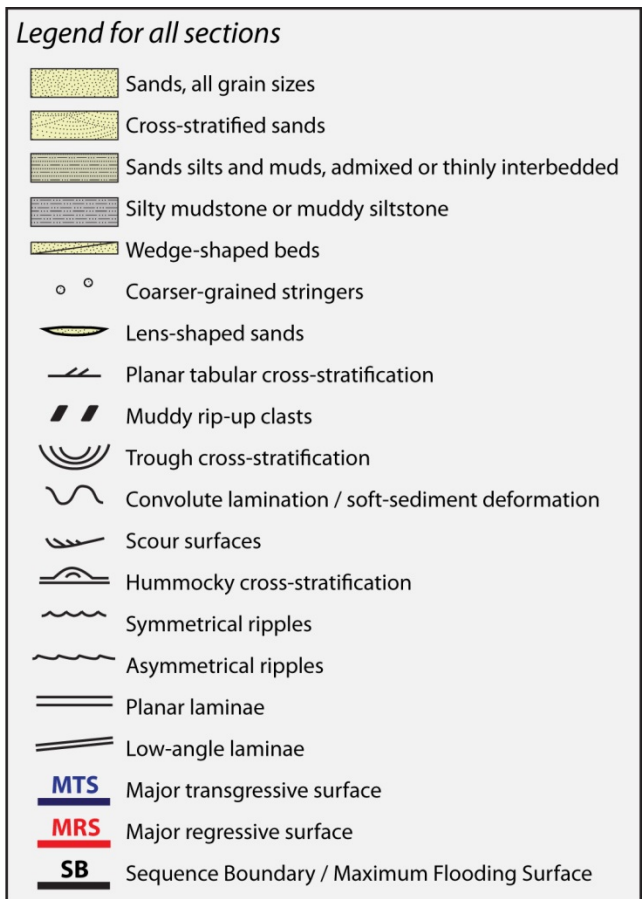
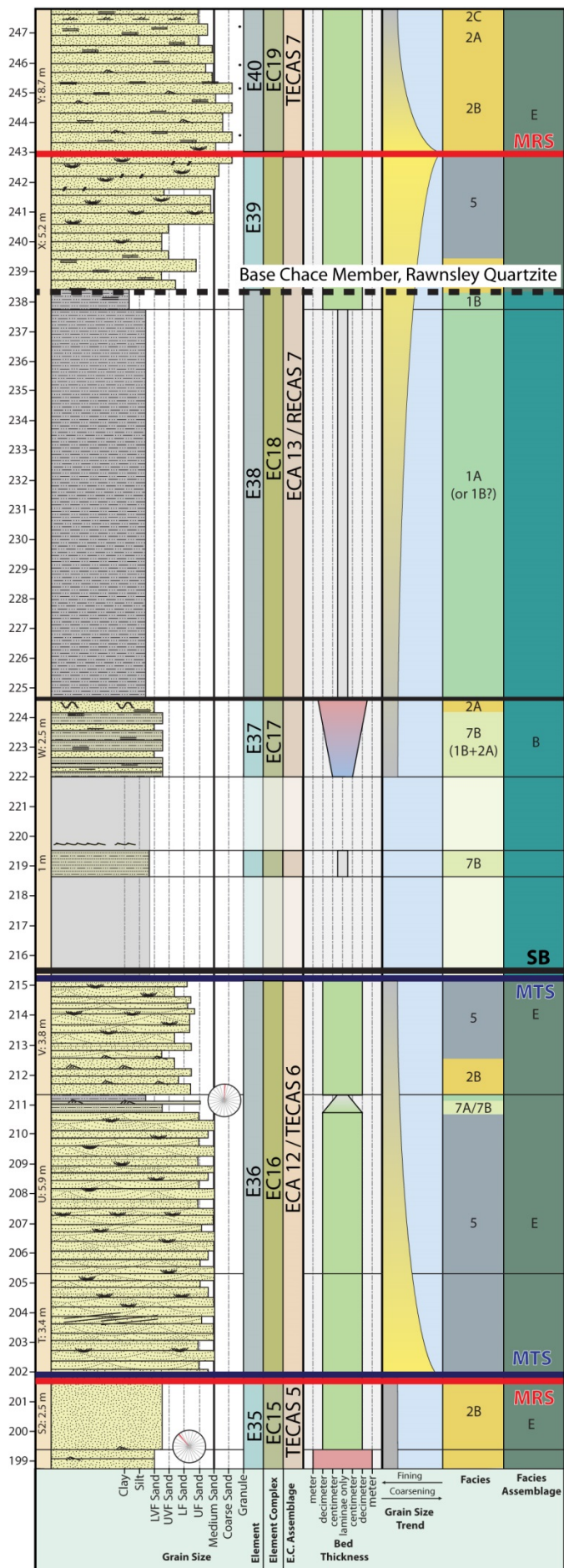
*Figure 4 (pages 89-91): Stratigraphic column of the Bonney Sandstone in Bunyeroo Gorge, showing lithologies, parasequences and parasequence boundaries, grainsize and thickness trends across beds, facies and facies associations.*











### 3.5.2: Facies Analysis and Interpretation

Within this lithostratigraphic framework, sediments can be divided into seven distinct facies, summarised in Table 1. Facies are composed of mudstones, interbedded heterolithic sandstones and silty mudstones, and sandstones containing a variety of sedimentary structures. Facies are distributed unevenly throughout the section, with the thickness of coarsening-upward intervals being much smaller (24 m) in the lower 75 m, and increasing to tens of metres in the middle and upper units, with some exceptions.



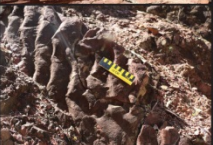
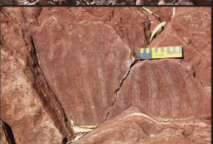



#	Facies	Sub-facies/ Description	Representative Photo	Depositional Process
1	Massive/ Planar Siltstones and Mudstones	1a: Massive 1b: Planar-laminated		Gravitational settling; low-energy deposition
2	Planar and Low-angle Laminated Sandstone	2a: Low-angle to planar laminated 2b: with asymmetric ripples 2c: with cross-stratification		Dominated by upper flow regime (high-energy), with some lower flow regime bed-forms (unidirectional)
3	Sandstone with Interference Ripples	May also occur with with low-angle and planar lamination		Flow in more than one direction; two sets of unidirectional currents operating within a short time frame; lower flow regime
4	Sandstone with Symmetrical Ripples	4a: Symmetrical ripples only 4b: with low-angle and planar lamination		Oscillatory flow caused by wave action
5	Cross- stratified Sandstone	Trough or tabular cross- stratification, sometimes with planar laminae, without additional sedimentary structures		Down-current migration of dunes due to unidirectional flow
6	Hummocky Cross- stratified Sandstone	Visible HCS, without other sed. structures		Combination of oscillatory and unidirectional flow
7	Heterolithic Strata (mud/sand)	7a: Interlaminated (mm) 7b: Interbedded (cm-scale) 7c: Interbedded (dm-scale) May also have asymmetric ripples.		Alternating low/high energy over a range of time scales.

Table 1: Facies found in the Bunyeroo Gorge section of the Bonney Sandstone. Colour of facies column corresponds to that seen in Figures 3 and 4.

Based on the fine-grained nature of Facies 1, these sediments are most likely the product of gravitational settling (Ashley, 1990). Occasional thin sandstone laminae may be the result of episodic deposition in an overall low-energy environment (cf. Colquhoun, 1995; Swift, Hudelson, Brenner, and Thompson, 1987). Planar-laminated sandstones in Facies 2 are likely the product of upper flow regime and unidirectional flow (Cheel, 1990), and also contain rare asymmetric ripples (Facies 2b) or cross-stratification (Facies 2c), indicating that flow became turbulent and dropped into the lower flow regime. Sandstones with asymmetric interference ripples (Facies 3) indicate two directions of flow affecting the same bedform, whereas symmetrically rippled sandstones (Facies 4), indicate oscillatory flow conditions that suggests the presence of waves (Reading, 2009). Linear wave ripple crests are not strongly orientated in a particular direction, ranging from northsouth to eastwest. In Facies 5, tabular, cross-stratified sandstones denote relatively high-energy conditions, and uncommon scours indicate erosive events or channelisation.

<b><i>Facies Association</i></b>	<b><i>Constituent Facies</i></b>				<b><i>Interpretation</i></b>
A	7B/7C		5		Storm-dominated lower shoreface
B	1B	2A	7B	5	Lower shoreface
C	4B	7A/7B		3	Distal upper shoreface
D	2A/ 2B	4B	5	6	Proximal upper shoreface
E	2A/2B/2C		5		Channel fill / Proximal delta fan

*Table 2: Facies associations found in the Bunyeroo Gorge section of the Bonney Sandstone. Colour of facies association row corresponds to facies column in Figure 3; facies colour corresponds to that seen in Figures 3 and 4.*

Paleocurrent readings on these troughs are most commonly northwestsoutheast, but are more likely to only show an apparent direction and are thus less reliable than direct measurements from bedding-plane views. Hummocky crossstratified

sandstones in Facies 6 are the product of both unidirectional and oscillatory flow affecting the same sediment surface (Dumas and Arnott, 2006). Heterolithic strata in Facies 7 indicate rapidly changing depositional conditions over a relatively short time-scale. This facies is subdivided based on the scale of interbedding, which is a product of the time frame and sedimentation rate in which these alternating lithologies were deposited.

Recurring combinations of facies can be grouped into six facies associations (Table 2). although facies are interpreted to the level of a specific, direct process, the presence of multiple facies occurring together can be a better indicator of the overall environment and larger-scale mechanisms responsible for deposition. Each facies association is interpreted to represent a general depositional environment, with each being a unique combination of individual facies. Based on the presence of thin, hummocky cross-stratified sandstones interbedded with silty mudstones, Facies Association A is interpreted as a storm-dominated lower shoreface. Silty mudstones are likely the result of normal, background sedimentation, and hummocky cross-stratified sandstones are likely event deposits affected by storm waves but below the reach of fair weather waves. This is similar to other storm-dominated shelves described by Walker (1984b) and Basilici, de Luca, and Poire (2012). Facies Association B is similar in that it only occurs in the lower part of the section and also contains thick packages of silty mudstones, but it does not contain the abundant Hummocky cross-stratification (HCS), found in Facies Association A, would indicate substantial storm influence. Mudstones in Facies Association B are commonly overlain by sands containing trough cross-stratification, asymmetric ripples and planar to low-angle laminae. It is thus also interpreted as lower shoreface, below normal wave base, although potentially closer to the shoreline given its proximity to

sands. Upper shoreface environments are represented in Facies Associations C and D, with C being somewhat deeper and more distal owing to higher mud/shale content. Facies Association D consists primarily of thick amalgamated sandstones with little mudstone content, commonly in tabular beds with wave ripples indicating a more proximal area of deposition. These sediments are similar to shoreface sands described by Feldman, Fabijanic, Faulkner, and Rudolph (2014) and Lambiase and Tulot (2013), and may have been deposited in a foreshore environment near the tops of shallowing-upward intervals where low-angle and planar-laminated sands become the dominant sedimentary structures. In Facies Association E, sandstones

Element (E)	An architectural unit that represents the smallest unique, identifiable geomorphological feature and its subsurface equivalent, from which larger-scale architectural units are built.
Element Complex (EC)	An architectural unit that represents a grouping of genetically related elements and element sets that were deposited under similar process conditions in the same part of a depositional system. Element complex boundaries can occur along strike and along dip direction and are marked by the presence of distinct stratigraphic surfaces or abrupt facies boundaries.
Element Complex Assemblage (ECA)	An architectural unit that is formed by a group of genetically related element complexes (or element complex sets if such are defined) that can cumulatively be considered to have been formed under similar process conditions. Element complex assemblages are conceptually similar to depositional systems.

*Table 3: Brief definitions of architectural categories. Taken from Vakarelov and Ainsworth (2013).*



are almost entirely composed of high-energy unidirectional flow indicators such as dune-scale cross-stratification. However, neither sediments rarely have evidence of fluvial processes like channel scours, lateral accretion surfaces or a fluvial-style stratigraphic architecture. Thus, these sediments are interpreted as in the marine environment but with some degree of fluvial influence, i.e. a proximal deltaic environment such as a delta front or delta fan, with some degree of channelisation inferred, but not directly seen in the study area.

Within the formation, the abundance of mudstones decreases upward, as reflected in the described facies and affecting their interpretation (Figures 3, 4). Some upper and middle Bonney sediments (e.g., intervals 75-150 m and 165-217 m) are lacking in basal mudstones, and the sandstone unit thickness is highest in the middle part of the section. Environments of deposition based on facies associations are interpreted as generally becoming progressively shallower upward, being dominated by more distal marine environments at the base, shallow marine sediments in the middle, and fluvial-deltaic sediments at the top.

### *3.5.3: Process and architectural classification*

Vertical trends in grain size and facies stacking patterns allowed the identification of a series of intervals that are separated by interpreted transgressive and regressive surfaces (shown in Figures 3, 4). These intervals can be identified at a variety of hierarchical levels and have been classified into a series of categories: elements, element complexes (ECs) and element complex assemblages (ECAs)—that are fully defined in Vakarelov and Ainsworth (2013) and reproduced in Table 3. Categories are also hierarchical; elements, for example, can be grouped together to form an element complex, and element complexes can be further grouped into

ECAs. All categories may display stratigraphic trends that may allow them to be considered parasequences, as the term does not contain a scale in its definition.

Applying this scheme to our data sets, element-scale intervals usually comprise a series of metre-scale coarsening-upward sediments with silty mudstones at their bases and amalgamated sandstones at their tops, or simply comprise amalgamated sandstones. In element complexes and ECAs, elements are usually stacked atop one another, with the overall sand content of these smaller units increasing upward and forming coarsening-upward profiles at scale of tens of metres. Surfaces bounding the intervals are commonly sharp, and marked by a change from sandstones to mudstones or sandstones to finer-grained sandstones upward. Once identified, shallow marine sediments within ECs were classified as to the primary, secondary or tertiary process operating in the interval—either wave, tidal, or fluvial—denoted by a Wft acronym with initials representing the respective amount of influence (Figure 5; Ainsworth et al., 2011). Each interval was thus assigned a stacking pattern (transgressive or regressive) and ranking of process order (e.g. Fw), which was then used to determine the possible range of architectural units (e.g., mouth bar, delta lobe, etc.) using those categories defined by Vakarelov and Ainsworth (2013). From these, the most likely EC was selected.

## Depositional Process

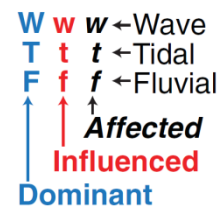


Figure 5: Notation scheme for relative influence of wave, tidal and fluvial processes.

### 3.5.4: Interpretation of stacking patterns and architectural elements

The distributions of facies and facies associations within each coarsening-upward or fining-upward interval are shown on the stratigraphic columns. Intervals

were classified as either transgressive or regressive based on the sequence of interpreted depositional energies and environments as determined from the constituent facies and facies associations. Most intervals are interpreted as regressive owing to their overall coarsening-upward and shallowing-upward profile. These are commonly bounded by composite surfaces that represent both maximum flooding and maximum regression. Alternatively, regressive ECAs may be separated by very thin transgressive, fining-upward intervals (transgressive element complex assemblages, or TECAs), interpreted to represent the remnants of thicker transgressive deposits that have mostly been eroded during the overlying regressive interval. Thick amalgamated sands overlie many TECAs and are interpreted as channels or proximal deltaic deposits; these may be infilling incised valleys cut during transgression. Valleys are primarily filled by these sands during subsequent regressive intervals, as most of the underlying transgressive deposits are eroded as fluvial sands prograde basinward. Higher in the section (above »165 m), subtle fining-upward trends in amalgamated sands may represent gradual or minor transgressions but do not return the system to fully marine conditions. Base-level changes reflected in TECAs and regressive ECAs (RECAEs) are contained within four major regressive intervals, separated by three maximum flooding surfaces at 68, 152 and 215 m from the base of the formation. These intervals comprise multiple ECAs and are interpreted as sequences, and their bounding surfaces as sequence boundaries. In the single section measured here, the contact between the Bonney Sandstone and Chace Member (at 238 m) cannot clearly be identified as a sequence boundary and is interpreted as a continuation of the regressive sequence beginning at the base of ECA 13. The Chace Member has a slight increase in grainsize compared with the units below, reflecting the continued shallowing-upward

trend throughout the formation, but otherwise was not observed to have substantial differences from many of the underlying sands. Throughout the section, regressive ECs and regressive ECAs are interpreted to represent progradational, regressive shoreline pulses, with rapid relative sea-level transgressions between them. Deposition of individual elements is likely not a product of regional base level change, but instead may represent lateral, localised changes in the locus of deposition resulting from lobe-switching or avulsion.

Sediments have varying degrees of wave, tidal and fluvial influence, although definitively tidally influenced sediments are rare, and most intervals can be classified as regressive and fluvially dominated. This results in a narrow range of morphological possibilities for the shallow marine deposits making up each interval. Lower Bonney shallow marine sandstones in ECAs 13, for instance, predominantly comprise sedimentary structures generated by unidirectional, upper flow regime currents. Symmetrical wave ripples are also present, but are considered to be a secondary process, and are orientated in a variety of directions, suggesting complex shoreline geometry, changing shoreline orientation or a variety of non-parallel sand bodies affected by shoaling waves. These features, combined with the stacked small-scale, coarsening-upward elements, suggest that these intervals are composed of a series of fluvial mouth bars, deposited in a marine environment with at least moderate wave influence. Individual mouth bars are represented by the sandy tops of each element, with the shaly bases marking a return to quieter, lower shoreface conditions. Sandstones in ECAS 48 all consist of fluvially dominated processes, with little or no evidence that indicates substantial influence from other processes. These intervals consist almost entirely of planar, low-angle and trough cross-stratified amalgamated sands. Although these sedimentary structures can be

found in a range of depositional settings, the conspicuous lack of features characteristic of other processes indicates that these sands are likely the infill of channels in a proximal fluvio-deltaic setting. The lack of coastal plain fines, potential overbank deposits, lateral accretion surfaces and other characteristics of a fully continental setting indicate that these sands, while strongly fluvial in origin, were still deposited in the marine realm where channels are no longer tightly confined. ECA 9 marks a return to more distal deposition, and the heterolithic beds with HCS show the additional influence of tidal and wave processes. In the upper Bonney Sandstone, the increasingly coarse grainsizes, granule stringers, and cross-stratified sandstones of ECAs 1016 suggest that these sediments continue a formation-scale coarsening-upward trend and may be even more proximal than those below. The northwest-southeast directionality of paleocurrents in ECAs 810 indicate channels orientated in those directions, with bidirectionality possibly resulting from tidal influence. Bidirectional paleocurrents are not seen in the same bed and measurements may be biased owing to the orientation of outcrop exposures, so a tidally influenced channel is not the preferred interpretation. Unlike other intervals, ECA 13 is fine-grained and poorly exposed, and may represent another significant flooding event. On a formation scale, the Bonney Sandstone is thus interpreted here as transitioning from wave-dominated, lower shoreface environment at its base, to a series of distal, marine, delta mouth bars in the lower portion, to proximal fluvio-deltaic channel sands near the top (Table 4). ECs and ECA categories in the Bonney Sandstone are detailed in Table 4, along with a schematic graphic of each element complex, after Vakarelov and Ainsworth (2013). Note that these elements apply only to shallow marine portions of each sequence, and some ECAs only contain a single element complex. Table 4 shows the evidence used to determine

the range of processes, the constituent facies and the variety of options considered for each element complex interval.

### **3.6: Discussion**

#### *3.6.1: Regional Implications and Significance*

The presence of a fluvial-deltaic system in the Bonney Sandstone provides further context regarding basin evolution and paleogeography in the Adelaide Rift Complex. The Bonney Sandstone and Chace Member of the Rawnsley Quartzite are the only units in the Wilpena Group to show evidence of fluvial processes (Preiss, 1987), likely marking a maximum regressive interval within the group. However, definitive evidence of subaerial exposure (e.g., mudcracks) was not seen, although fine-grained sediments are generally not present at the tops of regressive intervals. An alternative explanation for fine-grained mudstones higher the section is that they result from overbank, coastal-plain deposition or marginal marine, low-energy processes; however, no characteristics exist in these intervals that are definitively diagnostic. Although a red colour persists throughout the Bonney Sandstone and has been recently used as supporting evidence of extensive subaerial exposure (Retallack, Marconato, Osterhout, Watts, and Bindeman, 2014), red shales are not necessarily indicative of terrestrial environments (Tarhan, Droser, and Gehling, 2015). No other indications of paleosol formation were seen in the section measured here, despite it being less than 10 km from the Brachina Gorge section described by Retallack et al. (2014) as containing multiple paleosol horizons. Many of the lines of evidence for a subaerial interpretation of other Wilpena Group sediments have also been called into question (e.g., Callow, Brasier, and McIlroy, 2013), and we consider the Bonney Sandstone in the study area to have been fully deposited in the marine

realm. The presence of tidally influenced facies, although not definitive, suggests that the basin was linked to the larger ocean and not completely restricted.






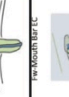

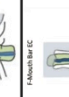

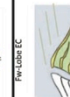
On a large scale, the formation-level shallowing-upward trend seen in the Bonney Sandstone is likely the result of continued progradation and progressive infilling of accommodation in the basin, resulting in increased exposure of upper formation sediments to shoreface and continental processes. Shallowing-upward systems composed of multiple, increasingly proximal parasequences are characteristic of highstand systems tracts (Van Wagoner et al., 1988), as sediments prograde into the basin and fill up available accommodation; this is interpreted to be the case here (Figure 6). As neither parasequences nor systems tracts are defined by their scale, this formation could also be interpreted as consisting of multiple highstand systems tracts, stacked atop one another, with sequence boundaries in between. Sequence boundaries are defined by their regional nature, and thus a full sequence stratigraphic interpretation is beyond the scope of this study. The tentative regional correlation in Figure 7, however, suggests that these surfaces may indeed be regionally extensive. Gehling (2000) interprets the top of the Bonney Sandstone as a type 2 sequence boundary, but does not recognise internal sequences within the Bonney Sandstone based on his regional mapping.

Element Complex Assemblage	Element Complex	Features indicating depositional process			Grain size and bed thickness trends	Constituent Facies	Constituent Facies Associations	Most Likely Depositional Processes	Possible Architectural Classifications	
		Wave	Tidal	Fluvial						
ECA 16 / ?	EC21	Planar- to low-angle lamination, planar tabular cross-stratification	Planar- to low-angle lamination, planar tabular cross-stratification	Planar- to low-angle lamination, planar tabular cross-stratification, small scours	Trends not apparent	2	E	F		
ECA 15 / TECAS 8	EC20	Planar- to low-angle lamination, planar tabular cross-stratification	Planar- to low-angle lamination, planar tabular cross-stratification	Planar- to low-angle lamination, planar tabular cross-stratification	Sandy, faintly coarsening-upward profile	5 2	E	F		
ECA 14 / TECAS 7	EC19	Planar- to low-angle lamination, trough cross-stratification	Planar- to low-angle lamination, trough cross-stratification, planar tabular cross-stratification	Trough cross-stratification, Planar- to low-angle lam., Asymmetric ripples, planar tabular cross-strat.	Sandy fining-upward profile	2	E	F		
ECA 13 / RECAS 7	EC18	Planar- to low-angle lamination, trough cross-stratification	Heterolithic beds	Asymmetric ripples	Sands at top, coarsening-upward from thick muds	1 2 5	E F	F		
ECA 12 / TECAS 6	EC17	Planar- to low-angle lamination, trough cross-stratification	Planar- to low-angle lamination, trough cross-stratification	Planar- to low-angle lamination, trough cross-stratification, Asymmetric ripples	Trends not apparent	2 7	F	Tf Ft		
ECA 11 / TECAS 5	EC16	Planar- to low-angle lamination, trough cross-stratification	Planar- to low-angle lamination, trough cross-stratification	Planar- to low-angle lamination, trough cross-stratification, Asymmetric ripples	Sandy fining-upward profile	1 2 5 7	E F	F		
ECA 10 / TECAS 4	EC15	Planar- to low-angle lamination, trough cross-stratification	Planar- to low-angle lamination, trough cross-stratification	Planar- to low-angle lamination, trough cross-stratification, Asymmetric ripples	Sandy fining-upward profile	2 5	D E	F		
ECA 9 / RECAS 6	EC14	HCS, Planar- to low-angle lamination, trough cross-stratification	Heterolithic beds	Asymmetric ripples, trough cross-stratification	Single large-scale coarsening-upward interval	4 5 7	A D	F Fw		
ECA 8 / RECAS 5	EC13	Planar- to low-angle lamination, trough cross-stratification, HCS	Planar- to low-angle lamination, trough cross-stratification	Planar- to low-angle lamination, trough cross-stratification	Trends not apparent	2 5 6	D	F Fw		
ECA 7 / RECAS 4	EC12	Planar- to low-angle lamination, trough cross-stratification	Planar- to low-angle lamination, trough cross-stratification	Planar- to low-angle lamination, trough cross-stratification	Single sandy, large-scale coarsening-upward interval	2 5	D	F		
ECA 6 / TECAS 4	EC11	Planar- to low-angle lamination, trough cross-stratification	Planar- to low-angle lamination, trough cross-stratification	Planar- to low-angle lamination, trough cross-stratification	Sandy fining-upward profile	2 5	D	F		
ECA 5 / RECAS 3	EC10	Planar- to low-angle lamination, trough cross-stratification	Planar- to low-angle lamination, trough cross-stratification	Trough cross-stratification, Planar- to low-angle lamination, wedge-shaped, discontinuous beds	Single large-scale coarsening-upward interval	7 5	C E	F		
ECA 4 / TECAS 3	EC8	Planar- to low-angle lamination	Planar- to low-angle lamination	Planar- to low-angle lamination	Fining-upward profile	2 4	C D	F		
ECA 3 / RECAS 2	EC7	Symmetrical Ripples, interference ripples, Planar- to low-angle lamination	Interference ripples planar- to low-angle lamination, heterolithic beds	Scour/erosive surfaces asymmetric ripples	Series of coarsening- and thickening-upward intervals, with increasing sand content upward	1 2 3 5 7	B C D	Fw		
ECA 2 / RECAS 1	EC6	Symmetrical Ripples, Planar- to low-angle lamination, Trough cross-stratification	Planar- to low-angle lamination, trough cross-stratification, heterolithic bedding	Planar- to low-angle lamination, trough cross-stratification	Series of coarsening- and thickening-upward intervals	1 2 4 5 7	B C	Fw Wf		



	EC5	Symmetrical Ripples, Planar- to low-angle lamination, Trough cross-stratification	Planar- to low-angle lamination, Trough cross-stratification	Planar- to low-angle lamination, Trough cross-stratification	Two coarsening-upward intervals	1 2 4 5	B C	<b>Fw</b> <b>Wf</b>	    
ECA 2 / ECAS 1	EC4	Planar- to low-angle lamination	Planar- to low-angle lamination, Heterolithic beds	Planar- to low-angle lamination, Trough cross-stratification	Fining-upward profile	7	B	<b>Wf</b> <b>TW</b>	    
	EC3	Symmetrical Ripples, Planar- to low-angle lamination	Planar- to low-angle lamination	Planar- to low-angle lamination	Series of coarsening and thickening-upward intervals, usually sand-dominated			<b>Fw</b> <b>Wf</b>	    
	EC2	Symmetrical Ripples, Planar- to low-angle lamination	Planar- to low-angle lamination	Planar- to low-angle lamination	Series of coarsening and thickening-upward intervals, with increasing sand content upward	1 2 4 7	B C	<b>Fw</b> <b>Wf</b>	    
ECA 1 / ECAS 1	EC1	HCS	Heterolithic beds		Increasing sand upward	7	A	<b>W</b>	

See detailed stratigraphic column in Figure 3		Primary depositional process	Secondary depositional process	Tertiary depositional process	See detailed stratigraphic column in Figure 3	See Table 1	See Table 2	See Vakarelov and Ainsworth (2013)	
---	--	------------------------------	--------------------------------	-------------------------------	---	-------------	-------------	------------------------------------	---

Element Complex	Definition	Element Complex	Definition
	<b>W Beach</b> - Shore-parallel linear unit with very little or no influence from rivers and tides. Includes foreshore as well as both lower and upper shoreface facies		<b>Wf Lobe</b> - Delta lobe forming laterally to Mouth Bar Element Complex due to along-shore migration of sediment from wave action; always next to MB
	<b>Wf Beach</b> - Shore-parallel linear unit; linear coastline where foreshore is extended by tides and intertidal bars are formed.		<b>TW Mouth Bar</b> - Central portion of delta lobe, reworked by wave action to be more elongate along shore than Fluvially dominated MBs
	<b>TW Beach</b> - Shore-parallel linear unit; linear coastline supplied by small rivers but without any shoreline protrusion; fluvial sediments reworked by waves		<b>F Mouth Bar</b> - Central portion of delta lobe along ansemi-protected coast with little or no tidal influence, elongated along shore, moderately heterogeneic
	<b>TW Barrier</b> - Barrier EC forming in areas with higher tidal range; increased heterogeneity due to tidal channels and associated washover facies		<b>TW Mouth Bar</b> - Fan-like deposits containing numerous individual mouth bars, or elongate sandy systems that are separated by indistributary units
	<b>TW Tidal Flat</b> - EC that forms landward of a barrier and shoreward of the mainland, consisting of sediment that fills lagoon after the onset of regression		<b>TW Tidal Flat</b> - Delta lobe, lateral to Mouth Bar, supplied by fluvial sediment with some degree of wave reworking. Represents a single pulse of shoreline progradation.


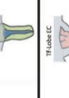
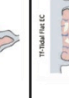
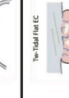
Element Complex	Definition
	<b>TW Tidal Flat</b> - Broad area periodically inundated by tides, usually containing both muds and sands, less fluvial influence than <b>Tf</b>
	<b>TW Tidal Flat</b> - Broad area periodically inundated by tides, usually containing both muds and sands, may be cut by tidal channels
	<b>TW Tidal Flat</b> - Broad area periodically inundated by tides, usually containing both muds and sands, less fluvial influence than <b>Tf</b>
	<b>TW Tidal Flat</b> - Broad area periodically inundated by tides, usually containing both muds and sands, less fluvial influence than <b>Tf</b>

Table 4 (Preceding pages): Summary and classification of shallow marine depositional elements. Graphical representations of ECs from Vaklerov and Ainsworth (2013). Stratigraphic locations of ECs and ECAs are shown on the measured sections in Figures 3 and 4.

## Sequence Stratigraphic Interpretation

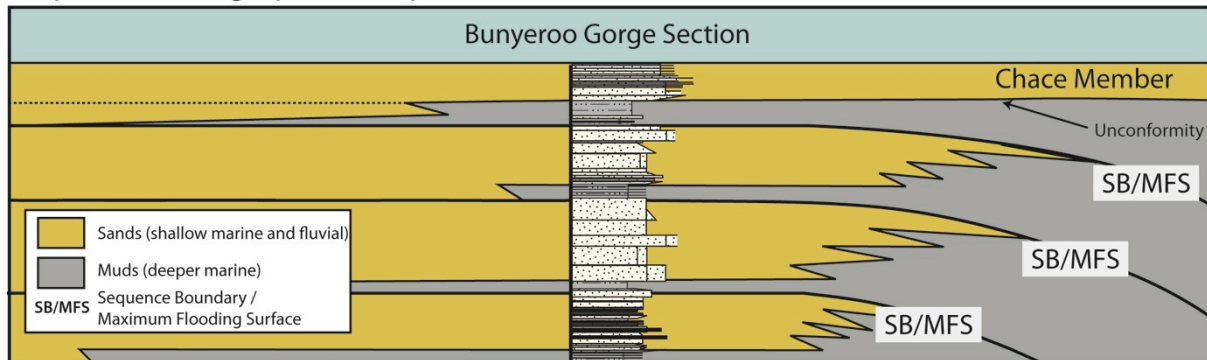


Figure 6: Cartoon showing schematic progradational parasequences sets during a highstand systems tract. This model fits with the observations seen here in the Bonney Sandstone. Modified from Van Wagoner et al. (1988).

Flooding events and generation of new accommodation space at all scales may be due to a number of possible mechanisms but are most likely related to either eustatic sea-level change or changes in regional tectonic subsidence. As the sediments were likely adjacent to a continental craton on the margin of a former rift basin with a very thick fill, it is likely that subsidence was substantial and rapid in the area. In addition, Wilpena Group sediments in the basin show no evidence for rapid (1 Ma-scale or less) global sea-level and climate fluctuations, as in, for example, the early Permian (Miller, McCahon, and West, 1996). However, without extensive sequence stratigraphic correlation, a definitive cause of relative sea-level fluctuations cannot be established. It is also possible that parasequences are the result of an autocyclic process that is not related to sea-level change. In a fluvial-deltaic shallow marine system, parasequences can be generated by lobe-switching and lateral shifting of facies near river mouths (Swift, Phillips, and Thorne, 1992). This is interpreted as being the most likely case with the smaller elements and ECs.

Correlations by the authors using five of Gehling's (1982; appendix) measured sections of the Bonney Sandstone are useful in demonstrating along-strike consistency of internal lithostratigraphic divisions across approximately 70 km, providing a way of estimating the size of depositional units present (Figure 7). While

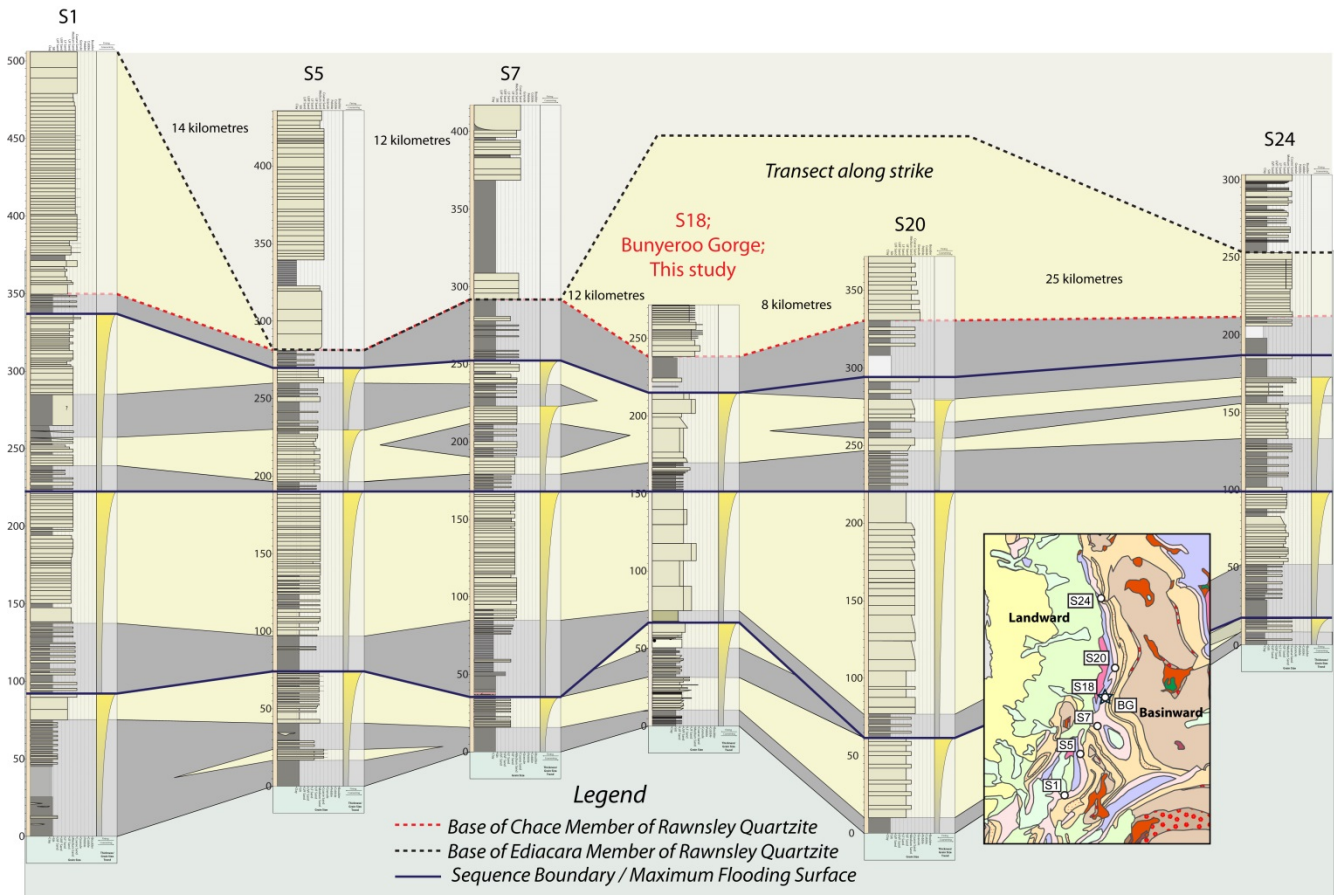


Figure 7: Correlation with Gehling's (1982) Bonney Sandstone measured sections. Locations shown in inset map.

individual beds cannot be correlated across these sections, general divisions and maximum flooding surfaces can be. Based on regional paleogeography, it is likely that the northsouth transect defined by these points is roughly parallel to the paleoshoreline. The paleocurrent data in Gehling (1982) show a range of currents in cross-stratification in all directions except west, a result similar to the collated paleocurrents seen here. Both this study and that of Gehling (1982) recognise the overall shallowing-upward nature of the formation, and a comparison of the same measured section between the two studies over 30 years apart shows that most

observations are in agreement, although some interpretations differ. Notably, most intervals were interpreted by Gehling (1982) as being fining-upward, rather than coarsening as described here. Additionally, lower Bonney sediments were interpreted by Gehling (1982) as having a substantial degree of tidal influence; instead, the section is interpreted here as being dominated by fluvial processes with only a small contribution from waves and tides. The 'petee' structures described in the Chace Member were not observed in the section measured here. Since these features are thought to be related to evaporite crystallisation and expansion within sands, they are critical to Gehling's (1982, 2000) intertidal interpretation for this unit. In our observations, this unit's lithologies consist only of cross-stratified and planar-laminated, granule-bearing sands, and as such it is interpreted to be similar to the high-energy deltaic channel-fills seen elsewhere in the mid- to upper Bonney Sandstone.

Zircon data from Ireland et al. (1998) indicate a Grenville-age source of these sandstones, possibly from the Musgrave province to the north, indicating that fluvial input from the Gawler Craton was likely minor. Thus, the deltaic system seen here most likely originated in another part of the basin, rather than coming directly from the landmass directly west of the study area. As the possible origin of sands is far to the north, a northern origin for the locus of the delta is favoured, and would be consistent with more north-south paleocurrents for unidirectional flow indicators seen here. These sediments may have entered from the northern part of the semi-restricted basin and been transported southward along the western basin margin. The widespread occurrence of very similar facies in distal Bonney Sandstone equivalents (e.g., Punkerri Sandstone, Arumbera Sandstone; Grey and Calver, 2007) suggests a widespread interval of shallow marine conditions across Australia,

which can now be better compared with the continental margin where the section here was deposited.

### *3.6.2: Approaches to Sedimentological Interpretation with Limited Datasets*

This study demonstrates the benefit of a multi-faceted approach to interpretation in sedimentary successions that are lacking in certain diagnostic criteria or context, limited in exposure, or on which few previous studies have been conducted. Ideally, interpretation would incorporate many lines of evidence: geochemistry, ichnology, stratigraphic context, regional correlations, paleontology, etc. In the section described here, the lack of these sources of information necessitates that individual facies be the building block for further analyses. When interpreted correctly, the distinction between two facies is a meaningful separation that reflects a fundamental difference in the depositional conditions over time and/or space. In some cases, a single facies alone can substantially restrict the range of possible depositional environments; facies may show a process directly responsible for sediment emplacement that is unique to certain environments (oscillatory flow, for example, which is limited only to environments occurring within wave base). In other instances, information about the variety of these processes operating (in the form of facies associations) is needed to understand a particular depositional setting. Stratigraphic occurrence of two or more facies together, however, does not inherently create a meaningful facies association. Adjacent juxtaposition of facies may cross sequence or parasequence boundaries, and environments may rapidly shift between one facies and another. Thus, when assigning facies associations, some degree of interpretation is required that takes into account the processes expected to co-occur in a given environment. Once assigned, facies associations can be applied to standard facies models to allow for the interpretation of large-scale

environments (delta front, shoreface, etc.).

Facies models provide an archetype from which interpretation can be based on, which can take on a range of forms. However, sedimentary successions in the 'real world' rarely conform perfectly to idealised spatial or stratigraphic models of facies occurrence, creating uncertainty in interpretation. The system of architectural classification defined by Vakalerov and Ainsworth (2013) provides a way to deal with this uncertainty. By providing a fixed set of depositional elements at a hierarchy of levels for each process (W-T-F)-stacking pattern (transgressive/ regressive) combination, unlikely interpretations are eliminated as possibilities. The scale of parasequences seen here requires interpretation at the level of the element complex, an architectural unit representing a group of smaller elements deposited under similar process conditions in the same part of a depositional system. Thus, uncertainty in interpretation in the Bunyeroo Gorge section is expressed as a narrow range of possible ECs, which are based on extensive observations in a variety of modern and ancient sediments. This process-based classification applies only to shallow marine deposits as it is built to assist in the interpretation of petroleum reservoir geometries in the subsurface. It does not contain architectural elements for sedimentary deposits in deepwater or shelfal systems, nor for those in continental or fluvial environments. As such, in real-world sedimentary successions, a mixed approach to interpretation is required, incorporating both an architectural classification and assumptions using facies models. In addition to inherently promoting uncertainty owing to deviation from a rarely occurring ideal, facies models alone do not fully describe all aspects of a sedimentary succession. Properties at both larger and smaller scales exist that assist in putting together a complete picture of the interval in question. Lower shoreface environments, for example, may

encompass both mudstones and amalgamated sandstones at the top, and contain sedimentological trends within and across the lower shoreface facies association. The process-based analysis of parasequences applied here (Vaklerov and Ainsworth, 2013) also provides a way to add additional information to an interpretation based on facies associations. The 25 defined ECs provide more precise information on the morphology of geobodies within a given environment than the more general facies associations; e.g., subclasses of the shoreface environment include beach, lobe, mouthbar, etc. This is important in the prediction of stratigraphic and spatial architecture of these units, which are potential reservoir analogues. This method also allows for transparency at all stages of the interpretation process (shown in Table 4), permitting the reader to better understand the available evidence and the ways that conclusions were drawn.

### **3.7: Conclusions**

The Bonney Sandstone section in Bunyerroo Gorge provides an opportunity to demonstrate that reasonable, reproducible interpretations can be made in a sedimentary succession that consists solely of lithologies and physical sedimentary structures. The formation in the study area is part of a progradational, fluvially dominated deltaic system with minor influence from wave and tidal processes, and increasing proximality over time. Identified depositional elements include proximal fluvial-deltaic channels, fluvial mouth bars, tidally and fluvially influenced delta lobes, and wave-dominated shorefaces, as determined using both facies models and process-based architectural classification. Sediments are primarily contained within regressive intervals on a scale of tens of metres, bound by composite maximum transgressive regressive surfaces, although in some cases, these surfaces are

separated and a transgressive interval is preserved. Four major shallowing-up sequences are found in the formation, separated by three maximum flooding surfaces. The results shown here provide new information regarding the paleogeographic and sea-level history of South Australia, and also provide context for the early metazoan fossil assemblage in the overlying Ediacara member, which immediately postdates the sediments described here.

### **3.8: Acknowledgements**

This research is supported by a University of Adelaide International Postgraduate Research Scholarship and the AAPG Nancy Setzer Murray Memorial Grant. This paper forms TRAX manuscript number 347. Access to field localities was granted by DEWNR scientific research permit Q26318-1. We acknowledge the traditional inhabitants of the land on which this research was conducted.



### 3.9: References

- AINSWORTH, R.B., VAKARELOV, B.K., AND NANSON, R.A., 2011, Dynamic spatial and temporal prediction of changes in depositional processes on clastic shorelines: Toward improved subsurface uncertainty reduction and management: *AAPG Bulletin*, v. **95**, p. 267-297.
- ASHLEY, G.M., 1990, Classification of large-scale subaqueous bedforms: A new look at an old problem SEPM bedforms and bedding structures: *Journal of Sedimentary Research*, v. **60**, p. 160-172.
- BASILICI, G., DE LUCA, P.H.V., AND POIRE, D.G., 2012, Hummocky cross-stratification-like structures and combined-flow ripples in the Punta Negra Formation (Lower-Middle Devonian, Argentine Precordillera): A turbiditic deep-water or storm-dominated prodelta inner-shelf system?: *Sedimentary Geology*, v. **267**, p. 73-92.
- BLATT, H., AND JONES, R.L., 1975, Proportions of exposed igneous, metamorphic, and sedimentary rocks: *Geological Society of America Bulletin*, v. **86**, p. 1085-1088.
- BOGDANOVA, S.V., PISAREVSKY, S.A., AND LI, Z.X., 2009, Assembly and breakup of Rodinia (some results of IGCP Project 440): *Stratigraphy and Geological Correlation*, v. **17**, p. 259-274.
- Bose, P.K., Eriksson, P.G., Sarkar, S., Wright, D.T., Samanta, P., Mukhopadhyay, S., Mandal, S.B., and Altermann, W., 2012, Sedimentation patterns during the Precambrian: A unique record?: *Marine and Petroleum Geology*, v. **33**, p. 34-68.
- CALLOW, R.H., BRASIER, M.D., AND MCILROY, D., 2013, Discussion: 'Were the Ediacaran siliciclastics of South Australia coastal or deep marine?' by Retallack et al., *Sedimentology*, 59, 1208-1236: *Sedimentology*, v. **60**, p. 624-627.
- CHEEL, R. J., 1990, Horizontal lamination and the sequence of bed phases and stratification under upper-flow-regime conditions: *Sedimentology*, v. **37**, p. 517-529.

- COLQUHOUN, G. P. 1995). Siliciclastic sedimentation on a storm-and tide-influenced shelf and shoreline: The Early Devonian Roxburgh Formation, NE Lachlan Fold Belt, southeastern Australia. *Sedimentary Geology*, 97, 69-98.
- COUNTS, J.W., AND AMOS, K.J., 2016, Sedimentology, depositional environments and significance of an Ediacaran salt-withdrawal minibasin, Billy Springs Formation, Flinders Ranges, South Australia. *Sedimentology*. doi: 10.1111/sed.12250
- DALGARNO, C.R., AND JOHNSON, J.E., 1968, Diapiric structures and late Precambrian early Cambrian sedimentation in Flinders Ranges, South Australia. *in*: J. Braunstein and G. D. O'Brien, eds., *Diapirism and Diapirs*, Tulsa, OK: *AAPG Memoir* 8, p. 301-314.
- DONALDSON, J.A., ERIKSSON, P.G., AND ALTERMANN, W., 2009, Actualistic versus non-actualistic conditions in the Precambrian sedimentary record: Reappraisal of an enduring discussion. *in*: W. Altermann and P. L. Corcoran (Eds.), *Precambrian sedimentary environments: A modern approach to ancient depositional systems*. Tulsa, OK: *International Association of Sedimentologists Special Publication* 33, 313 p.
- DREXEL, J.F., PREISS, W.V., AND PARKER, A.J., eds., 1993, *The geology of South Australia: The Precambrian*. Adelaide, SA: Mines and Energy South Australia, Geological Survey of South Australia, v. 54, 242 p.
- DUMAS, S., AND ARNOTT, R.W.C., 2006, Origin of hummocky and swaley cross-stratification—the controlling influence of unidirectional current strength and aggradation rate: *Geology*, v. 34, p. 1073-1076.
- FELDMAN, H.R., FABIJANIC, J.M., FAULKNER, B.L., AND RUDOLPH, K.W., 2014, Lithofacies, parasequence stacking, and depositional architecture of wave-to tide-dominated shorelines in the Frontier Formation, Western Wyoming, USA: *Journal of Sedimentary Research*, v. 84, p. 694-717.
- FODEN, J., ELBURG, M.A., DOUGHERTY-PAGE, J., AND BURTT, A., 2006, The timing and duration of the Delamerian Orogeny: Correlation with the Ross Orogen and implications for Gondwana assembly: *The Journal of Geology*, v. 114, p. 189-

210.

- FORBES, B.G., 1971, Stratigraphic subdivision of the Pound Subgroup (Late Precambrian South Australia). *Transactions of the Royal Society of South Australia*, v. **95**, p. 219-225.
- GALLOWAY, W.E., 1975, Process framework for describing the morphological and stratigraphic evolution of deltaic depositional systems. *in*: M. L. Broussard, ed., *Deltas* (2nd ed., pp. 87-98). Houston Geological Society, Houston, Texas.
- GEHLING, J.G., 1982, Sedimentology and stratigraphy of the late Precambrian Pound Subgroup, Central Flinders Ranges, S.A: University of Adelaide MSc thesis, Adelaide SA, Australia.
- GEHLING, J.G., 2000, Environmental interpretation and a sequence stratigraphic framework for the terminal Proterozoic Ediacara Member within the Rawnsley Quartzite, South Australia: *Precambrian Research*, v. **100**, p. 65-95.
- GREY, K., AND CALVER, C.R., 2007, Correlating the Ediacaran of Australia. Geological Society London Special Publications, v. **286**, p. 115-135.
- HEARON, T.E., ROWAN, M.G., LAWTON, T.F., HANNAH, P.T., AND GILES, K.A., 2015, Geology and tectonics of Neoproterozoic salt diapirs and salt sheets in the eastern Willouran Ranges, South Australia: *Basin Research*, v. **27**, p. 183-207.
- IRELAND, T.R., FLOTTMANN, T., FANNING, C.M., GIBSON, G.M., AND PREISS, W.V., 1998, Development of the early Paleozoic Pacific margin of Gondwana from detrital-zircon ages across the Delamerian orogeny: *Geology*, v. **26**, p. 243-246.
- JAGO, J.B., GATEHOUSE, C.G., POWELL, C.M., CASEY, T., AND ALEXANDER, E.M., 2010, The Dawson Hill member of the Grindstone Range Sandstone in the Flinders Ranges, South Australia: *Transactions of the Royal Society of South Australia*, v. **134**, p. 115-124.
- KERNEN, R.A., GILES, K.A., ROWAN, M.G., LAWTON, T.F., AND HEARON, T.E., 2012, Depositional and halokinetic-sequence stratigraphy of the Neoproterozoic Wonoka Formation adjacent to Patawarta allochthonous salt sheet, Central

- Flinders Ranges, South Australia: Geological Society, London, Special Publications, v. **363**, p. 81-105.
- KNOLL, A., WALTER, M., NARBONNE, G., AND CHRISTIE-BLICK, N., 2006, The Ediacaran Period: A new addition to the geologic time-scale: *Lethaia*, v. **39**, p. 13-30.
- LAMBIASE, J.J., AND TULOT, S., 2013, Low energy, low latitude wave-dominated shallow marine depositional systems: Examples from northern Borneo: *Marine Geophysical Research*, v. **34**, p. 367-377.
- Li, Z.X., Bogdanova, S.V., Collins, A.S., Davidson, A., De Waele, B., Ernst, R.E., Fitzsimons, I.C.W., Fuck, R.A., Gladkochub, D.P., Jacobs, J. and Karlstrom, K.E., 2008, Assembly, configuration, and break-up history of Rodinia: A synthesis: *Precambrian Research*, v. **160**, p. 179-210.
- MILLER, K.B., MCCAHERN, T.J., AND WEST, R.R., 1996, Lower Permian (Wolfcampian) paleosol-bearing cycles of the US Midcontinent: Evidence of climatic cyclicity: *Journal of Sedimentary Research*, v. **66**, p. 71-84.
- POSAMENTIER, H., AND WALKER R.G., eds., 2006, Facies models revisited: SEPM Special Publication, v. **85**, Tulsa, Oklahoma, USA, 527 p.
- PREISS, W.V., 1987, The Adelaide Geosyncline—late Proterozoic stratigraphy, sedimentation, paleontology and tectonics: *Bulletin of the Geologic Survey of South Australia*, v. **53**, 438 p.
- PREISS, W.V., 1990, A stratigraphic and tectonic overview of the Adelaide Geosyncline, South Australia, in: J. B. Jago and P. S. Moore (Eds.), The evolution of a late Precambrian-early Palaeozoic rift complex: The Adelaide Geosyncline, Geological Society of Australia Special Publication, v. **16**, Sydney, NSW, 133 p.
- PREISS, W.V., 1999, Parachilna sheet SH54-13. 1: 250 000 scale geological map and explanatory notes (2nd ed., p 52). Adelaide, SA: Primary Industries and Resources South Australia.
- PREISS, W.V., 2000, The Adelaide Geosyncline of South Australia and its significance in Neoproterozoic continental reconstruction: *Precambrian*

*Research*, v. **100**, p. 21-63.

READING, H.G., ed., 2009, *Sedimentary environments: Processes, facies and stratigraphy*. Oxford, UK, Blackwell Publishing, 688 p.

REID, P., AND PREISS, W.V., 1999, Parachilna map sheet. South Australian Geological Survey Geological Atlas 1:250,000. 54-13.

RESTALLACK, G.J., MARCONATO, A., OSTERHOUT, J.T., WATTS, K.E., AND BINDEMAN, I.N., 2014, Revised Wonoka isotopic anomaly in South Australia and Late Ediacaran mass extinction: *Journal of the Geological Society*, v. **171**, p. 709-722.

SWIFT, D.J., HUDELSON, P.M., BRENNER, R.L., AND THOMPSON, P., 1987, Shelf construction in a foreland basin: Storm beds, shelf sandbodies, and shelf-slope depositional sequences in the Upper Cretaceous Mesaverde Group, Book Cliffs, Utah: *Sedimentology*, v. **34**, p. 423-457.

SWIFT, D.J.P., PHILLIPS, S. AND THORNE, J.A., 1992, Sedimentation on continental margins, V. Parasequences. *in*: D.J.P. Swift, G.F. Oertel, R.W. Tillman and J.A. Thorne, eds., *Shelf sand and sandstones bodies: Geometry, facies and sequence stratigraphy: Special Publication of the International Association of Sedimentologists*, v. **14**, p. 153-187, Blackwell Publishing Ltd., Oxford, UK.

TARHAN, L.G., DROSER, M.L., AND GEHLING, J.G., 2015, Depositional and preservational environments of the Ediacara member, Rawnsley Quartzite (South Australia): Assessment of paleoenvironmental proxies and the timing of 'ferruginization': *Palaeogeography, Palaeoclimatology, Palaeoecology*, v. **434**, p. 4-13.

VAKARELOV, B.K., AND AINSWORTH, R.B., 2013, A hierarchical approach to architectural classification in marginal-marine systems: Bridging the gap between sedimentology and sequence stratigraphy: *AAPG Bulletin*, v. **97**, p. 1121-1161.

VAN WAGONER, J. C., POSAMENTIER, H. W., MITCHUM, R. M., VAIL, P. R., SARG, J. F., LOUITIT, T. S., AND HARDENBOL, J., 1988, An overview of the fundamentals of sequence stratigraphy and key definitions. SEPM Special Publication, v. **42**, p.

39-45.

WALKER, R.G., 1979, Facies and facies models. General introduction. *in*: R. G. Walker, ed., Facies models. Toronto, CA: Geological Association of Canada, Geoscience Canada Reprint Series 1.

WALKER, R.G., 1984a, General introduction: Facies, facies sequences, and facies models. *in*: R. G. Walker (Ed.), Facies Models (2nd ed.). Toronto, CA: Geological Association of Canada, Geoscience Canada Reprint Series 1.

WALKER, R.G., 1984b, Shelf and shallow marine sands. *in*: R. G. Walker, ed., Facies models (2nd ed.). Toronto, CA: Geological Association of Canada, Geoscience Canada Reprint Series 1.

WALKER R.G., AND JAMES N.P., eds., 1992, Facies models—response to sea level change. St. John's, Newfoundland: Geological Association of Canada. 409 p.

# Statement of Authorship

Title of Paper	Paleogeography, sedimentology, and provenance of an Ediacaran fluvial-deltaic system, South Australia
Publication Status	<input type="checkbox"/> Published <input type="checkbox"/> Accepted for Publication <input checked="" type="checkbox"/> Submitted for Publication <input type="checkbox"/> Unpublished and Unsubmitted work written in manuscript style
Publication Details	Counts, J. W. and Amos, K. J. (2016), Paleogeography, sedimentology, and provenance of an Ediacaran fluvial-deltaic system, South Australia (unpublished manuscript)

## Principal Author

Name of Principal Author (Candidate)	John W. Counts		
Contribution to the Paper	All aspects except supervisor review		
Overall percentage (%)	95%		
Certification:	This paper reports on original research I conducted during the period of my Higher Degree by Research candidature and is not subject to any obligations or contractual agreements with a third party that would constrain its inclusion in this thesis. I am the primary author of this paper.		
Signature		Date	18/4/2016

## Co-Author Contributions

By signing the Statement of Authorship, each author certifies that:

- i. the candidate's stated contribution to the publication is accurate (as detailed above);
- ii. permission is granted for the candidate to include the publication in the thesis; and
- iii. the sum of all co-author contributions is equal to 100% less the candidate's stated contribution.

Name of Co-Author	Kathryn J. Amos,		
Contribution to the Paper	Review and commentary		
Signature		Date	6/7/2016

Please cut and paste additional co-author panels here as required.

**Chapter 4: Paleogeography of an Ediacaran  
Fluvial-Deltaic System: A Case Study Integrating  
Sedimentology and Provenance**

J. W. Counts and K. J. Amos

*Submitted to the Journal of Sedimentary Research, 2016*

*Additional figures (not in original submission) are included in Appendix 8.2*



Counts, J.W. & Amos, K.J. (2016). Paleogeography of an Ediacaran Fluvial-Deltaic System: A Case Study Integrating Sedimentology and Provenance. *Journal of Sedimentary Research, Submitted for Publication.*

NOTE:

This publication is included on pages 119 - 165 in the print copy of the thesis held in the University of Adelaide Library.

# Statement of Authorship

Title of Paper	Lateral variability along the margin of an Ediacaran salt-withdrawal minibasin, Adelaide Rift Complex, South Australia
Publication Status	<input type="checkbox"/> Published <input type="checkbox"/> Accepted for Publication <input type="checkbox"/> Submitted for Publication <input checked="" type="checkbox"/> Unpublished and Unsubmitted work written in manuscript style
Publication Details	Counts, J. W., Amos, K., Dalgarno, C.W., and Hasiotis, S.T., in preparation, Lateral facies variation along the margin of a Neoproterozoic salt-withdrawal minibasin, Adelaide Rift Complex, South Australia (working title), manuscript completed 2016.

## Principal Author

Name of Principal Author (Candidate)	John W. Counts		
Contribution to the Paper	All manuscript text; all figure drafting; fieldwork; final descriptions and interpretations		
Overall percentage (%)	90%		
Certification:	This paper reports on original research I conducted during the period of my Higher Degree by Research candidature and is not subject to any obligations or contractual agreements with a third party that would constrain its inclusion in this thesis. I am the primary author of this paper.		
Signature	<table border="1"> <tr> <td>Date</td> <td>18/4/2016</td> </tr> </table>	Date	18/4/2016
Date	18/4/2016		

## Co-Author Contributions

By signing the Statement of Authorship, each author certifies that:

- i. the candidate's stated contribution to the publication is accurate (as detailed above);
- ii. permission is granted for the candidate to include the publication in the thesis; and
- iii. the sum of all co-author contributions is equal to 100% less the candidate's stated contribution.

Name of Co-Author	Kathryn Amos		
Contribution to the Paper	Manuscript review and discussion		
Signature	<table border="1"> <tr> <td>Date</td> <td>06/07/2016</td> </tr> </table>	Date	06/07/2016
Date	06/07/2016		

Name of Co-Author	C. R. Dalgarno		
Contribution to the Paper	Pre- and post-fieldwork discussions; initial identification of field area and its significance; review of manuscript		
Signature	<table border="1"> <tr> <td>Date</td> <td>22/4/16</td> </tr> </table>	Date	22/4/16
Date	22/4/16		

Name of Co-Author	Steve Hasiotis
Contribution to the Paper	Fieldwork and in--field discussions and interpretations
Signature	

Date	20-May-2016
------	-------------

# **Chapter 5: Lateral Variability along the Margin of an Ediacaran Salt-Withdrawal Minibasin**

J. W. Counts, C. R. Dalgarno, K. J. Amos, and S. T. Hasiotis

*Manuscript completed 2016*

*Additional figures (not in planned submission) are included in Appendix 8.3*

## 5.1: Abstract

*Depositional processes adjacent to exposed evaporite diapirs have only rarely been studied, yet are key to understanding the nature of sediments that are part of economically important hydrocarbon systems around the world. In the Adelaide Rift Complex of South Australia, well-exposed diapirs and their associated rim synclines (minibasins) allow the character and distribution of these sediments to be studied in detail. This study examines sediments deposited in a Neoproterozoic and Cambrian minibasin that was in close proximity to an exposed diapir body. Numerous sections were measured along the minibasin margin, allowing the sedimentation processes, facies, and lateral variability of sediments to be determined. Deposition took place in a variety of environments, ranging from shallow marine carbonates to subaerially exposed floodplains. Minibasin sedimentation adjacent to the diapir is characterized by an abundance of gravity flow deposits including turbidites and debrites, heavy mineral-laminated sands, and allochthonous coarser-grained clasts within otherwise sandy and shaly lithologies. Coarser deposits consist of exotic lithologies brought to the surface by the diapir from deeper in the basin and redeposited into the minibasin depocentre. Sedimentary facies most affected by the diapir are unevenly distributed, and are concentrated in areas where depositional thinning and growth faulting are most common. Depositional elements seen in the Mt. Frome minibasin are also recognized elsewhere throughout the Adelaide Rift Complex, and share similarities with other areas around the world where salt intersects the surface and affects background sedimentation. This study is one of few to examine sedimentary character in detail in an outcropping minibasin, and is one of the first to describe lateral variability of sediments along an outcropping minibasin margin. The sediments discussed here provide a unique analogue for*

*subsurface and seafloor deposits elsewhere where salt-sediment interaction cannot be studied in detail.*

## **5.2: Introduction**

Salt-tectonic deformation affects over 120 basins around the world, including some of the world's largest petroleum-producing fields, yet most of these provinces occur only in the subsurface or on deepwater continental margins (Hudec and Jackson, 2007). Among those visible at the surface, many are inaccessible due to lack of well-exposed surficial geology, remote outcrop locations, or geopolitics, and many outcrop studies focus primarily on structural aspects of diapir emplacement and the reconstruction of halokinetic sequences (e.g., Backe et al., 2010; Giles and Lawton, 2002; Hearon et al., 2015). Salt-influenced depositional settings are therefore lacking in the type of detailed sedimentological analysis that can only be done on outcrops where both diapirs and their surrounding sediments are well-exposed. The purpose of this study is to describe and interpret salt-sediment interaction and lateral facies change along the margin of an Ediacaran salt-withdrawal minibasin from South Australia, with the goal of using these findings as analogues for more inaccessible deposits elsewhere. This is accomplished through detailed geological mapping and the measurement of eight stratigraphic sections from the diapir contact into the minibasin interior.

Subsidence of sedimentary strata due to the mobilization of underlying evaporites often results in the formation of small basins at a scale of tens of kilometres. These minibasins (rim synclines) are often important elements of hydrocarbon systems, forming topographic lows and depocentres on the seafloor or land surface (Bryant et al., 1990; Booth et al., 2003). In the study area described

here, minibasin sediments are exposed at the surface in oblique plan view, permitting continuous observations near the western contact between the diapir body and the minibasin. Exposed strata show multiple indications of interaction between sediments and the diapir body, resulting in erosive surfaces and unique lithofacies not present in the minibasin formations outside of the halotectonic influence of the diapir. As such, the results shown here provide a unique record of the direct effects of synsedimentary halokinesis and diapir exposure on sedimentary and stratigraphic character. These findings should prove useful for the interpretation of analogous hydrocarbon systems elsewhere. This paper is one of the few published outcrop studies to document spatial changes in minibasin lithofacies at this scale of observation anywhere in the world.

Even in productive, well-studied areas in the subsurface, a complete understanding of salt-sediment interaction is hampered by the inability to collect the type of sedimentological data needed to fully characterize minibasin depositional processes. The various methods of obtaining subsurface data each have advantages and limitations, especially in the often complexly deformed, deepwater settings where many hydrocarbon systems occur. Seismic data, for instance, provides a large scale view of stratigraphic architecture, but is unable to resolve detailed features that may affect reservoir properties, especially at minibasin margins where strata may be significantly upturned. Core may provide a high-resolution, one-dimensional view of sediments, but the expense of obtaining multiple cores over a small area prevents it from being a tool to make the kind of meso-scale observations and analyses that are possible in outcrops. Thus, gaps in subsurface data sets may be filled by information from outcrop analogues, as a supplement to more limited direct observations.

Recent outcrop studies have begun to look at salt-withdrawal minibasins from a sedimentological perspective (e.g., Matthews et al., 2007; Kernen et al., 2012; Banham and Mountney, 2013a, 2013b, 2014; Ribes et al., 2015; Counts and Amos, 2016), showing that the findings from this type of study can be applied elsewhere and significantly add to our understanding of the environments, processes, and architectural elements of minibasin fill. However, given that such studies remain relatively rare, an opportunity exists for much more work to be done on the sedimentological aspects of salt tectonics. Ultimately, minibasins may benefit from a facies models approach, in much the same way that shallow marine and deltaic systems have. This study is another step toward that greater level of understanding.

The minibasin described here is one of many in the Adelaide Rift Complex, a Neoproterozoic aulacogen containing a thick sedimentary fill that has been significantly affected by co-occurring diapir movement and sedimentation (Dalgarno and Johnson, 1968; Dyson, 1996; Rowan and Vendeville, 2006). Excellent exposures permit minibasin sediments to be studied in an oblique view, revealing both lateral and stratigraphic changes in lithofacies around the minibasin margins. The goals of this study are to: (1) document minibasin sediments and how they differ in the Mt. Frome minibasin from the background sedimentation elsewhere in the region; (2) Interpret the depositional environments and geomorphologic elements present in minibasin, and (3) determine the ways that salt movement and proximity to an exposed diapir body affect depositional processes in the study area.

### **5.3: Geologic Setting**

#### *5.3.1: The Adelaide Rift Complex*



The minibasin sediments discussed here lie in the Adelaide Rift Complex, a north-south trending basin now partially exposed in the Flinders Ranges of South Australia (Fig. 1). Beginning as a tripartite aulacogen, basin sedimentation began during the breakup of Rodinia



Figure 1: Location of Adelaide Rift Complex within Australia; Geologic context and location of study area. Red square in inset marks location of larger map.

around 800 Ma (Preiss, 1987, Bogdanova et al., 2009). Infilling took place until the Middle Cambrian, as the basin gradually evolved from a restricted rift into a passive margin (Preiss, 1987; 2000). A compressional episode, the Delamerian Orogeny, deformed basin sediments in the mid-Cambrian and shortened the basin in an east-west direction by as much as 10-20% (Paul et al., 1999). By Ediacaran time, the Adelaide Rift Complex formed part of the edge of an Australia-East Antarctica subcontinent, which was likely in low latitudes just north of the equator (Li et al, 2008). The southern end of the basin is inferred to be an oceanic connection, and the northern extent may have also consisted of a deeper-water depocentre (Preiss, 1987, Counts and Amos, 2016).

### *5.3.2: Background Sedimentation*

In order to assess the effects of syndepositional diapirism, the typical 'background' lithologies and depositional environments in the stratigraphic interval of interest outside the minibasin must first be understood. These are summarized in Table 1, and belong to the Wonoka Formation, Bonney Sandstone, Rawnsley Quartzite, and Hawker Group. Elsewhere in the basin, these formations are usually separated by unconformities, and span approximately 40 million years of deposition (Preiss, 2000). The base of the Wilpena Group (Mawson, 1941), marks the Global Stratotype Section and Point (GSSP) for base of the Ediacaran Period at ~632-5 Ma (Knoll et al., 2006). The Wilpena Group, which is the focus of this study, was deposited during the Ediacaran Period, and is comprised of two large-scale shallowing-upward sequences. In the Lower Cambrian, much of the basin was blanketed by a fine-grained carbonate ramp (Hawker Group), deepening to the north with a variety of microbial, sponge, and archaeocyathid reef buildups (Dalgarno, 1964; James and Gravestock, 1990).

### *5.3.3: Character and Distribution of Diapirs in the Adelaide Rift Complex*

Evaporites in the basin fill are likely the product of restriction during the initial period of rifting, although they are never seen in place as bedded salt. Salt mobilization was initiated early, and continued at least until the late Early Cambrian (Dalgarno and Johnson, 1968; Dyson, 2004; Reilly, 2001). Throughout much of its history, basin topography may have resembled modern-day salt-tectonized provinces similar to those seen in the Gulf of Mexico and elsewhere. Indeed, much of the current structural complexity in the basin likely predates the Delamerian Orogeny and is likely the product of syndepositional salt tectonism (Rowan and

Vendeville, 2006). The Delamerian compressional event exaggerated existing synforms and antiforms, reactivated and reversed growth faults, and tilted strata such that diapirs and their adjacent minibasins can now be viewed in map, cross-sectional, and oblique views. When exposed, diapirs are most often found as kilometre-scale irregular-shaped bodies that are isolated from one another by tens of kilometres. Specific locations where diapir mobilization occurs are likely controlled by pre-existing basement faults (Backe et al., 2010).

A lack of subsurface data prevents complete characterization of the distribution and 3D morphology of salt bodies. In many diapirs visible in cross-section, salt can be seen to break out and flow laterally along bedding planes (Dyson, 2004). The effects of salt withdrawal are evident in strata throughout the basin, with minibasins of various scales occurring adjacent to most exposed diapirs. Minibasins are often asymmetric, indicating differential subsidence across their axes, and are occasionally bounded by bucket welds where salt has moved upward and been evacuated from the minibasin margin. Asymmetry in stratal thickness is also seen on either side of diapirs themselves, a result of the changing locus of minibasin subsidence over time.

Present-day diapir bodies exposed at the surface do not contain any remaining evaporite minerals; current exposures often consist of a mixed-lithology breccia with a microcrystalline dolomitic matrix (Preiss, 1987). The current diapir expression is often interpreted as a caprock, formed when the evaporite matrix of the diapir is dissolved or replaced by carbonate (Dyson, 2004). The high density of clasts seen is the result of the concentration of undissolvable sediments as they are left behind during weathering of more soluble material (Cooper, 1991). Clasts within this matrix are highly angular, ranging in size from pebbles to large blocks several

hundreds of meters in size, and are composed of a wide variety of lithologies, interpreted as originating from underlying strata or basement, entrained within the plastically flowing diapir as it moves upward through the country rock (Dalgarno and Johnson, 1968).

Formation	Summary Description	Interpretation	Primary Reference
Wilkawillina Limestone	230 m thick, three members, generally massive, grey, clean lime mudstone and wackestone, with abundant archaeocyath- <i>Renalcis</i> bioherms and shelly fossils	Carbonate ramp blanketing the majority of the basin. Occasional structurally controlled bioherms with associated lagoons and subaerial exposure surfaces.	Clarke 1986
Rawnsley Quartzite	400 m thick, three members; the lowermost Chace Member consists of clean, algal-laminated quartzites, separated from above units by a deep incision surface. The Ediacara Member is characterized by cross-stratified channelized sands and thinly bedded siltstones, among other facies. It hosts the well known "Ediacaran fauna", and is overlain by a thick, unnamed unit of clean sandstones similar to that seen at the base.	Intertidal sand flat and sabkha in the Chace Member, with a relative sea level fall in the Ediacara Member incising valleys and depositing shallow marine clastics as incised valley fill, including prodeltaic silts, mass-flow fluidized channels, and storm-dominated delta front sands. The upper member is primarily composed of thick wave- and tide-influenced shallow marine delta sands.	Gehling 1982; Gehling 2000
Bonney Sandstone	~300 m thick in the type section; two members: the lower Patsy Hill Member and an upper unnamed member. The Patsy Hill Member was traditionally included in the Wonoka Formation and was revised to the Bonney Sandstone in 1999. The Patsy Hill Member consists of limestone-sandstone parasequences with algal and stromatolitic features in carbonates and red, micaceous sandstones. Upper member consists of several coarsening upward parasequences of reddish siltstones and sandstones.	Patsy Hill Member- shallow marine to lagoonal stormy carbonate ramp, shallowing up to ooid shoals and hardgrounds, with clastics being subtidal or intertidal. In the 'traditional' Bonney, fluvial-deltaic sands prograding onto a fine-grained shelf, forming a highstand systems tract with sands originating from the Musgrave Province to the north via the Willouran Trough.	Haines, 1990; Counts and Amos, in review; Counts et al., 2016
Wonoka Formation	700 m thick; basal Wearing Dolomite Member contains shale and dolomicrite. Divided originally into 12 units containing calcareous siltstones, silty limestones, red and green siltstones and mudstones. Major unconformity at top of formation marked by kilometre deep canyons that incise into the Bunyerroo Formation.	Storm-dominated carbonate ramp/shelf, capped by lagoonal and intertidal carbonates, deepening substantially to the north with interspersed diapiric islands along the hinge line.	Haines 1990
Brachina Formation	1250 m thick, three members; Red-brown and olive green siltstones and shale, sometimes cyclically interbedded with cross-stratified sandstones, gradational upper contact with ABC Range Sandstone	Generally very low energy, subtidal clastic shelf conditions, progressively shallowing-upward to progradational deltaic sands from the Gawler Craton	Leeson 1970; Plummer, 1978; Preiss, 1993

Table 1: Summary of typical lithologies of formations seen in this study, for comparison with diapir-influenced character seen in the Mt. Frome region.

## 5.4: Methodology

The focus of this study is an asymmetric minibasin on the eastern flank of Mount Frome. The Mt. Frome minibasin and diapir (Fig. 2A-2B) were identified from regional geologic maps (Reid and Preiss, 1999) and reconnaissance field trips. The study area is part of the Mt. Frome Ridge adjacent to Lake Frome on the eastern edge of the Flinders Ranges. The arid climate in the region permits excellent

exposures due to lack of vegetation and soil cover (see Appendix 8.3, Fig. 1); however, exposure is not completely continuous as the region is intermittently covered by thin calcarosols (McKenzie et al., 2004), Pleistocene terraces and Quaternary alluvium.

Eight transects were surveyed, spanning five kilometres along the diapir-sediment contact (Fig. 2C, 3). Lithostratigraphic contacts and faults were mapped along the transect in more detail than the original geologic map, and field observations were later combined with high-resolution aerial photos to produce the map in Figure 2C. At certain points along the transect, stream cuts or eroded hilltops exposed relatively continuous sections of underlying bedrock, permitting measurement of stratigraphic sections. Unit thicknesses were determined using tape measure and GPS (generally  $\pm 2-4$  metres accuracy). Paleocurrent readings were taken where sedimentary structures were clear enough to permit unambiguous data, in the form of ripples, cross-stratification, or channel forms. Two directions were recorded for symmetrical ripples and other bi-directional features.

## **5.5: Observed Facies**

### *5.5.1: Facies descriptions*

Near the minibasin rim, the diapir itself is characterized by a fine-grained dolomitic matrix with numerous large (granule- to boulder-sized) angular clasts of varying lithologies (Figs. 4A and 4B). Observed rock types include basalts and fine-grained mafic volcanics, occasional schistose metamorphics, and consolidated, bedded, often fine-grained sedimentary rocks. Eight facies were observed within the minibasin fill, distinguished by a particular combination of lithologies and sedimentary structures (Table 2; Figs. 4 and 5). Facies were grouped into four facies

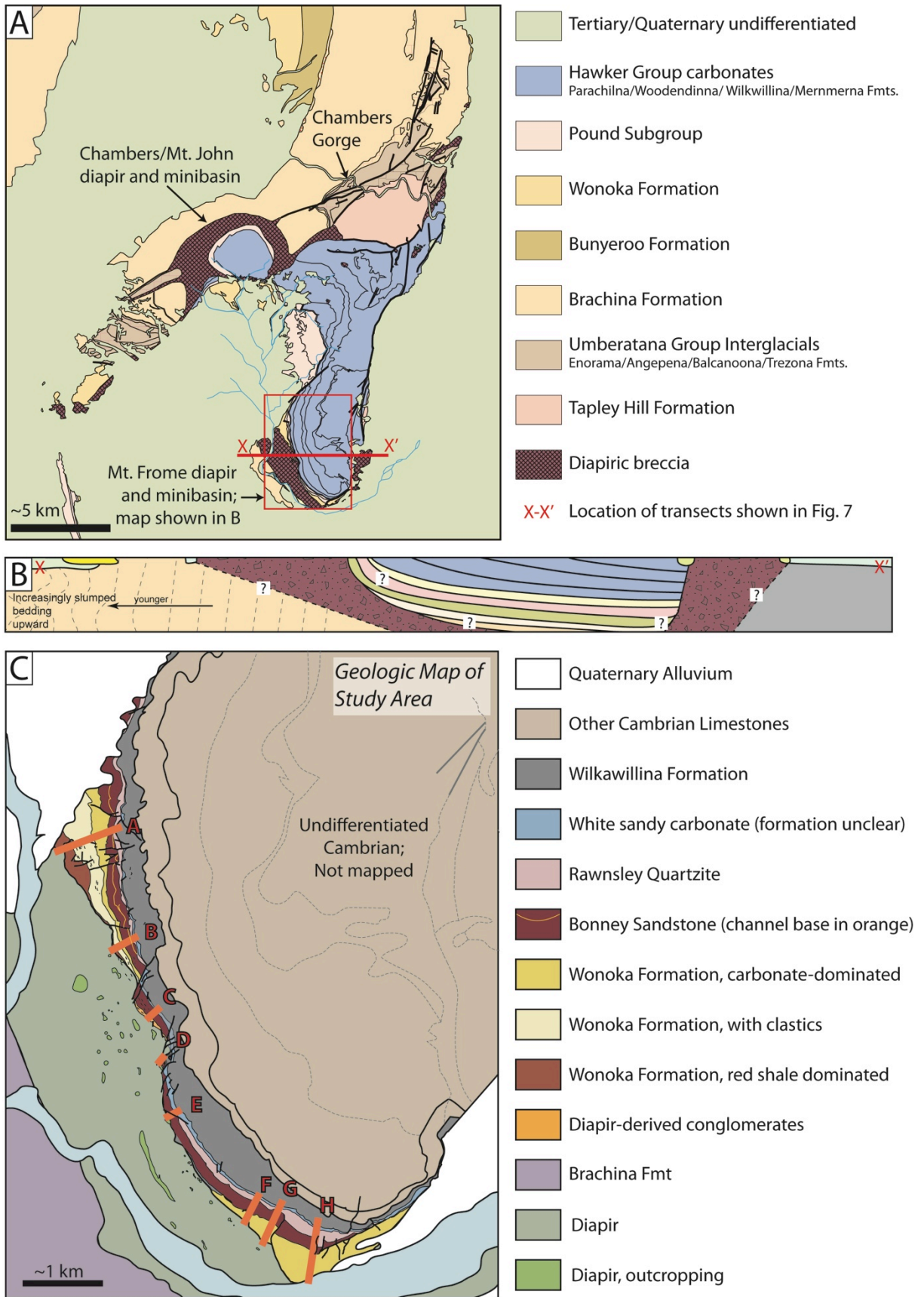


Figure 2: (A) Local geology of the Mt Frome diapir region. Measured sections shown in Figure 3 form a transect along the minibasin margin from point A to A'. (B) Schematic cross-section across the minibasin from A to A'. Subsurface geometries are specula

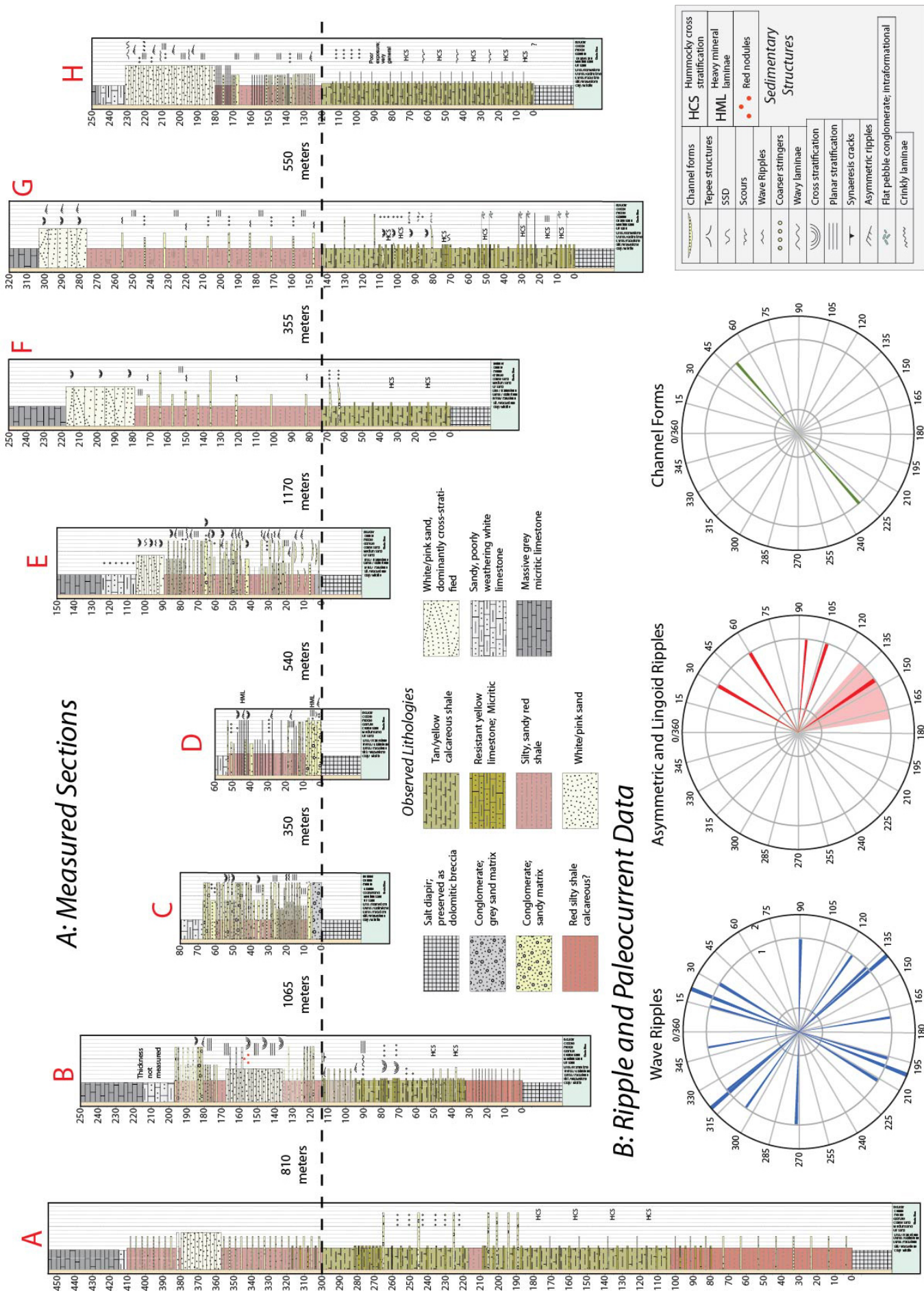


Figure 3: (A) Sections measured in this study. All sections at same scale; datum is base of Bonney Sandstone. Locations shown on Figure 5; waypoints noted are available in supplementary data. (B) Combined paleocurrent data from all sections. For wave (symmetrical) ripples, crest orientations are shown.

Age	Unit	F.A.	Facies Name	Description	Figure
Cambrian	Hawker Group	4	H	Massive, grey, well-indurated micritic limestone, in beds 2-3 metres thick. No larger grains or internal structure visible, aside from occasional irregular laminae.	
			G	Weathered, poorly outcropping white sandy limestone; transitional zone with overlying carbonates	
	Bonney Sandstone	2	F	Cross-stratified and planar- to irregularly laminated clean, mud-free quartz sandstone, in decimeter- to half metre-scale beds. Individual beds may be indistinct. Tepee ('petee' structures of Gehling, 1982) are seen occasionally, as well as small mud rip-up clasts on some bedding plane surfaces.	
			E	Interbedded red shale, fine-grained sandstone, and pebble conglomerates. Conglomerates occur as decimetre-scale discrete beds, sometimes directly lying atop rippled surfaces with little apparent scouring or erosion. Sands and conglomerates may be parts of sandier intervals that fine upward. Sands in close association with conglomerates often contain high concentrations of heavy minerals, especially nearest to the diapir contact. Mudstones containing isolated clasts are also common. Max. clast size rarely exceeds small cobbles, except for immediately adjacent to the diapir where boulders occur.	7E-7I
Ediacaran	Bonney Sandstone	1	D	Interbedded brick-red shales and fine-grained sandstones. Sands range from very common, centimetre-scale beds, to thicker decimetre and half-metre thick beds with planar- and ripple-lamination and cross-stratification. Sands often topped by asymmetrical or symmetrical ripples that are commonly draped by a thin mud layer. Many ripples have cm-scale wavelengths and sub-cm-scale amplitudes, and are sometimes flat-topped.	7A-7D
			C	Interbedded calcareous shale, limestone, and clastic pebble conglomerates. Conglomerates occur as discontinuous beds of metres across, often lens-shaped or with clear channel forms and scoured bases. Clasts range from sand- to cobble-sized, dominated by pebbles, and the clast density is highly variable, ranging from dense gravel concentrations to individual grains interspersed in a sandy limestone matrix.	6E, 6F
			B	Interbedded yellow calcareous shale and resistant limestone, very similar to Facies A. Colour difference in the shales is the primary feature that distinguishes Facies A and B, although cleaner, resistant limestones are more abundant in Facies A	
	Wonoka Formation		A	Red calcareous shale and resistant limestones interbedded at varying, irregular frequency. Shales are planar-laminated and lacking in sedimentary structures. Limestone beds are 10-80 cm thick and massive, or containing hummocky cross-stratification planar and asymmetric ripple lamination, and discrete beds of intraformational flat pebble conglomerates. Limestones contain no visible grains and are composed of micrite with some degree of recrystallization.	6C, 6D

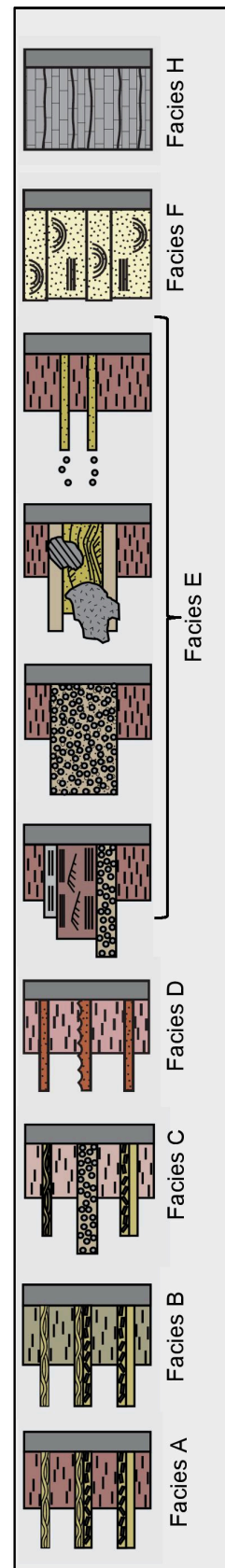
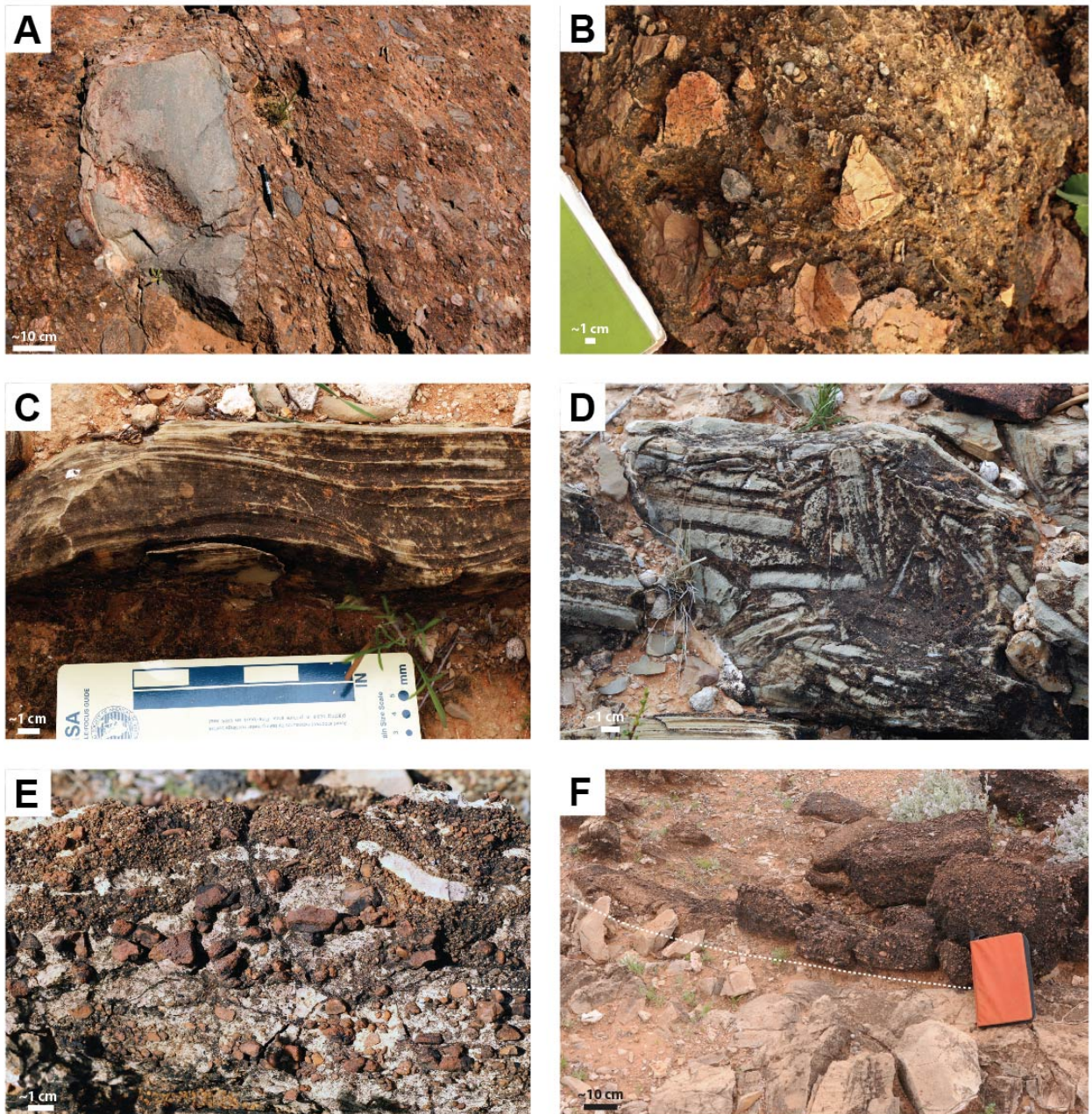


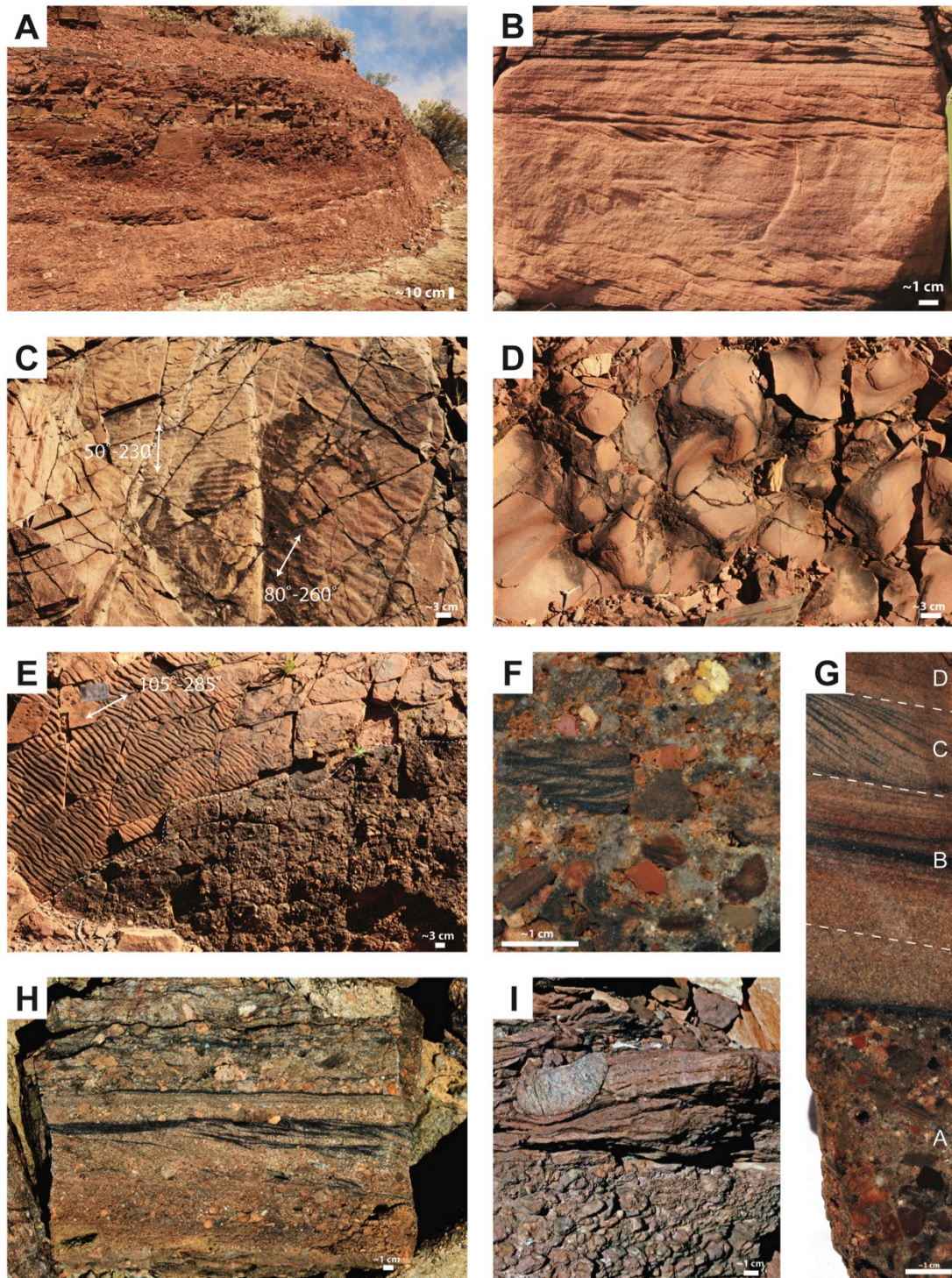
Table 2: Summary of lithofacies seen in the minibasin, and schematic representation of each lithofacies in cross-section. While bed thickness is variable, each drawing is intended to represent 1-2 vertical metres of section. Colours are generally representative of sediment colour, and lithologic patterns correspond to those in Figure 4. Facies G not shown due to poor exposure. See Appendix 8.3, Figure 2 for photos of Lithofacies F and H.



these are sharp. Palaeocurrents measured for this study were most frequently taken in Facies D and E, shown in Figure 3; these show a clear eastward-dominated (or east-west, in the case of oscillatory-flow ripples) flow direction.



*Figure 4: Sedimentologic features seen in the diapir and Wonoka Formation. (A, B) Typical diapir character in the study area, showing both dolomitic matrix and angular clasts. (C) Hummocky cross-stratification often present in the lower Wonoka Formation, limestone matrix. (D) Flat-pebble carbonate conglomerate in Wonoka limestones. Clasts are similar composition to surrounding matrix. (E) Lithology of conglomerate bands in upper Wonoka Formation, often containing a mixture of rounded clastic pebbles and flat carbonate pebbles/cobbles. (F) Conglomerate-filled channel of clastic pebbles in upper Wonoka, near section G. Base of channel marked by white line is in sharp contact with underlying limestones.*



**Figure 5: Lithologic features of the Bonney Sandstone.** (A) Characteristic Bonney Sandstone lithofacies, dominated by red shale and interbedded with centimetre- to decimetre scale fine-grained sandstones, and in places, pebble conglomerates. (B) Fine-grained sand bed, showing asymmetrical ripples and planar laminae. (C) Two sets of symmetrical ripples on adjacent bedding planes with palaeocurrents of 50°-230° and 80°-260°, Section D. (D) Interference ripples atop sand bed affected by two or more current directions; Section E. (E) Symmetrical ripples in Section E; Paleocurrent 105°-285°. Directly overlying rippled bed is a sandy pebble conglomerate marked by white dashed line. (F) Typical conglomeratic facies (G) Relatively complete Bouma sequence in Bonney sand/conglomerate bed, polished, slabbed hand sample. Bouma divisions annotated. (H) Conglomeratic facies with abundant heavy mineral laminae. I) Mixed conglomerate and muddy sandstone bed

### 5.5.2: *Facies distribution*

Facies are generally stacked atop one another and rarely repeated stratigraphically upward. Laterally, facies are unevenly distributed across the study area (Figs. 3 and 6). Facies A occurs only at the base of the Wonoka Formation in the northern part of the study area near sections A and B. Facies B and C are present in both the northern and southern portions of the minibasin, but they thin onto a central diapir high and are not present toward the centre of the transect. The red sands and shales of Facies D also occur in the northern and southern sections; however the inverse is generally true of the pebble/cobble-dominated sediments of Facies E, which is present predominantly in the central portion of the transect where the Precambrian strata are thinnest. In the Mt. Frome area, Facies E often takes the form of lens-shaped beds filled with conglomerates and sands. Conglomerates in these beds may be capped by fining-upward sands, but more commonly are unsorted and in sharp contact with over- and underlying sandy shales. These discontinuous beds range in scale from metres to tens of metres laterally, and are generally less than 1 metre thick.

Facies F occurs in the Bonney Sandstone as a discrete, sharp-based unit, tens of metres thick, that incises into the typical sand-shale Bonney lithologies in the northern part of the study area. The unit is traceable in aerial photos across hundreds of kilometres, and can be seen to truncate beds lower in the section. Clean, white sandstones of Facies F also occur in the unit overlying the Bonney Sandstone, the Rawnsley Quartzite, in sections E-H, although there it is more dominated by irregularly laminated sands. The transition zone to carbonates (Facies G) is persistent across the minibasin. It is here interpreted to be Cambrian in age, as no carbonates are present in the upper Ediacaran section elsewhere. Hawker Group

carbonates (Facies H) blanket the minibasin at the top of the sections measured, and are lithologically consistent throughout.

### 5.5.3: *Facies interpretations*

Facies A and B, fine-grained carbonates, are interpreted to be relatively similar in their environments of deposition, likely on a carbonate ramp or shelf. The common presence of hummocky cross-stratification intermittently interspersed between thicker intervals of lower-energy sedimentation suggests that the area was periodically affected by storms which caused reworking of cleaner (less clastic shale content), shallower-water carbonates into the deeper parts of the basin. The lack of wave ripples in these facies indicates they were still below normal wave base, but above storm wave base. The red coloration in Facies A has previously been interpreted as the product of increased oxygenation of the water, related to ‘deep shelf currents below a stagnant middle shelf zone’ (Haines, 1990). This may also likely be the case here, as the formation has often been interpreted as shallowing-upward, and Facies A is found below the more reduced lime mudstones of Facies B. Flat pebble conglomerates in these facies are all composed of carbonate, and thus are thought to originate nearby and be the product of redeposition after being ripped up by storm currents.

Facies C marks the earliest stratigraphic occurrence of clastic grains, in the form of pebble beds. These are often in association with cleaner, hummocky cross-stratified limestones, which suggests that they too may be event beds. Clasts are similar, though more rounded, to those seen in the diapir matrix itself. Channel forms and discontinuous, massive accumulations of pebbles in random orientations or with a faint horizontal fabric indicate that these deposits are localized debris flows. They

likely originate on or near the exposed topographic high of the Mt. Frome diapir, where clasts transported to the surface in the diapir matrix erode downslope in loosely defined channels and fans. Clasts are all within a relatively narrow size range, indicating that clasts were hydrodynamically sorted and decreasing in grain size away from the diapir. Given the surrounding shelfal context of the formation and the limestone matrix of the formation, gravel beds and channels were likely deposited underwater. The diapir itself, however, may have been subaerially exposed and formed an island, or may have eroded subaqueously; definitive evidence of either of these is not preserved.

In Facies D and E, environments were significantly different-- the switch to clastic deposition indicates a widespread change in sediment availability. Based on sedimentary features seen in the study area, sediments in Facies D and E may have been deposited in a marginal marine or continental setting. Ripple marks are common throughout both of these facies. Straight, symmetrical ripples with sub-centimeter-scale wavelengths and millimetre-scale amplitudes are evidence that water depth was very shallow (Immenhauser, 2009), and current was at times oscillatory but very weak. Sand beds are often capped by flat-topped ripples, which form when wave ripples are modified during subaerial exposure (Reineck and Singh, 1973). Differing crest orientations in closely adjacent beds and thin mud drapes atop many ripple sets may also suggest some degree of tidal influence. Shrinkage cracks are not seen, although ripples at a similar scale with flat-topped geometries have been interpreted in the past as indicative of tidal-flat deposition (Ericksson and Simpson, 2012). Thin sands may have been deposited as small channels, overbank splays, or washover fans on an alluvial plain or tidally influenced sand flat, an interpretation which is consistent with the degree of fluvial influence and general

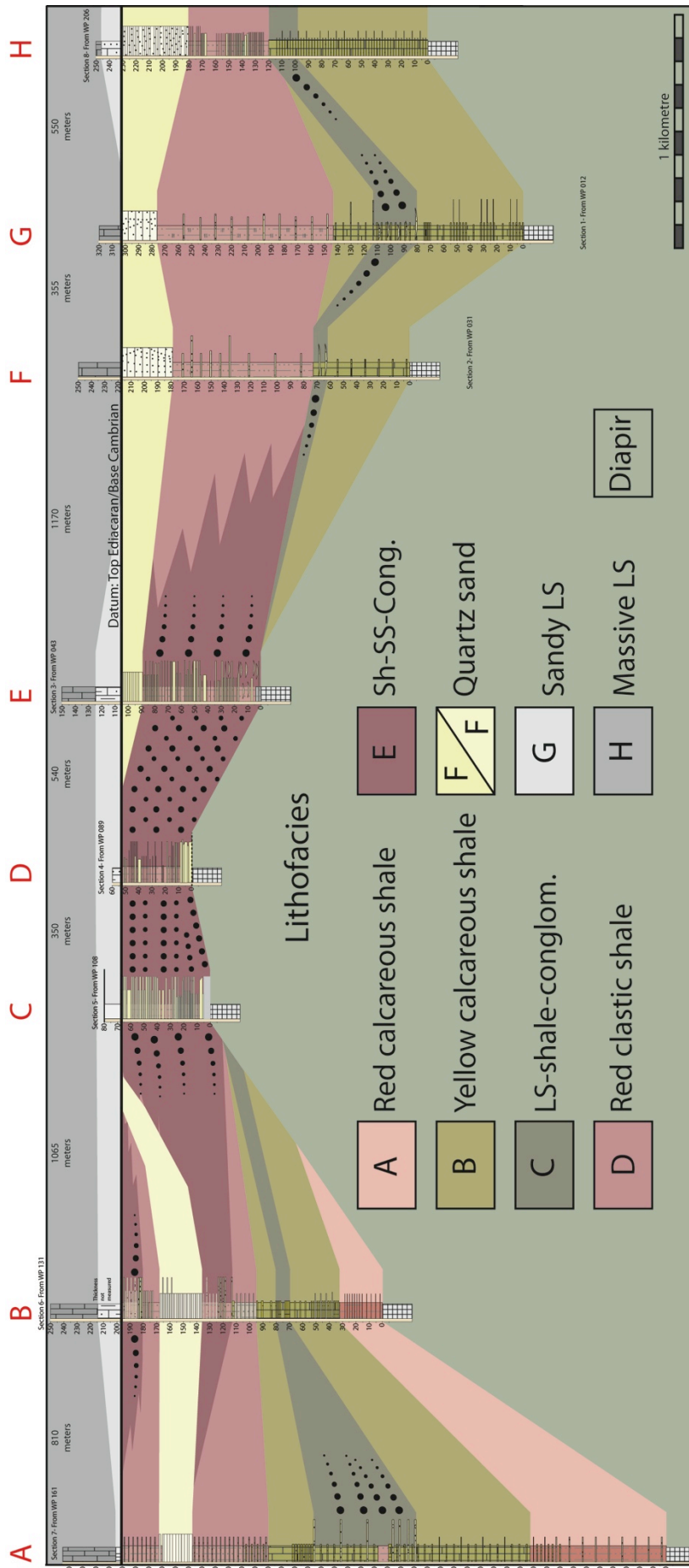


Figure 6: Facies relationship diagram for the Mt. Frome minibasin margin. Labelled sections correspond to those in Figure 3. Diagram is schematic and does not show the complexities of facies change between sections.

marginal marine conditions seen in the formation throughout the larger basin. Many sandy beds also show evidence of waning flow and decreasing depositional energy over the course of bed deposition, as seen in decreasing grain sizes, increasing amounts of mud, and ripple sets with progressively smaller wavelengths and amplitudes. These types of small, fining-upward beds can form in both marine and continental environments.

The feature that distinguishes Facies E, the presence of pebble-dominated conglomerates, is interpreted to be the result of reworking from an exposed diapir caprock; intervals without this lithology indicate times where reworking was not occurring. Pebble clasts in this facies are of the same mixed composition as those in Facies C below, and are thus likely to be from the same diapir source. Pebble beds sometimes cover rippled surfaces without cutting into them (e.g., Fig. 5E), indicating a firm substrate of muds or muddy sands and little erosive capability during pebble conglomerate deposition. If the area was indeed subaerially exposed at the time, the exposed diapir may have resulted in salt glaciers that were weathered and eroded, where the evaporite matrix dissolved and the remaining clastic pebbles transported into the minibasin and reworked into the sands and shales seen in Facies D (Bruthans et al., 2009). Many of the pebble conglomerates in Facies F do show erosive bases, and are likely to be channel deposits that result from small streams on the alluvial plain or tidal flat surface.

The quartzitic sands of Facies F may represent marine sediments deposited during a transgressive event. In the northern part of the section where this facies fills a large channel form, it may represent the fill of an incised valley, as the white, cross-stratified sands do not show features associated with fluvial processes. Beds are tabular, and sands are mature, lacking in mud and fining-upward sequences;

channel forms and lateral accretion surfaces were not seen. Where this facies occurs higher in the section (the upper portions of Sections E-H; Fig. 6), it is characterized by irregular laminae which may be the result of algal binding and may represent an intertidal environment. In this interval, sediments closely match previous descriptions of the Chace Member of the Rawnsley Quartzite. "Petee" structures have also been cited as an intertidal indicator in these sediments, believed to be formed by expansive crystallization of evaporites within sands (Gehling, 1982; 2000).

Facies G represents a transition between the clastics in the Precambrian and the subsequent Cambrian carbonates. This facies likely forms as sands are gradually diluted by carbonate muds as sea levels rose and blanketed the basin by thick marine limestones. It is genetically more similar to the limestones above than the sands below, likely representing the same shelf conditions as the Wilkawillina Formation, but with a slightly higher clastic content that prevents crystallization and forming of resistant ledges. The massive limestones of Facies H show no diapiric influence in the study area, and are thus interpreted to have been deposited in a similar environment to that seen in the rest of the basin, a broad carbonate ramp of moderate depth with little depositional energy. Although archaeocyathid reefs are known from elsewhere in the formation, they were not seen on the minibasin margin in the study area.

## **5.6: Discussion**

### *5.6.1: Environmental controls on facies variability*

The distribution, character, and sequence of facies can be used to create qualitative depositional models for the time frames during which each formation was



deposited. These models take the form of a series of block diagrams that schematically reconstruct the Mt. Frome minibasin and diapir through time (Fig. 7). The earliest of these, representing the time of deposition of the Wonoka Formation (Facies A-C), shows the minibasin inundated by seawater, with a diapiric high that was possibly emergent during deposition. Subaqueous deposition is confirmed by the predominance of carbonates, while diapir extrusion or exposure is indicated by the channelized, discontinuous gravel beds in Facies C that are sourced from the diapir. These beds are more common in the periodically exposed, fluvial- and tidally influenced Bonney Sandstone, and the model for that interval therefore contains a number of gravel fans originating from the diapir high, as well as channels and splay deposits on the floodplain or washover flat. The basin at this time may have been occasionally inundated, as subsidence was rapid and the minibasin is not far from coeval marine deposits to the north and west. The large incised valley in the north of the minibasin likely contained a braided river system, as this was the case for many Pre-Devonian fluvial systems (Davies and Gibling, 2010). In Facies F, G, and H, little evidence of diapir activity is seen, aside from significant thinning and rare reworked pebbles. The diapir may have been a topographic high during this time, but was likely not actively eroding. The same is likely true for the Early Cambrian; no coarse material was seen here. For these reasons, both the Rawnsley and Cambrian reconstructions only show the diapir as a more gentle topographic high without exposure of the caprock or diapir body.

#### *5.6.2: Diapiric influence on sedimentary character and depositional processes*

Sediments in the Mt. Frome minibasin contain many features that are not seen away from diapiric influence. These features can be reasonably explained by the minibasin's proximity to an evaporite diapir body that was exposed at the

## Environmental Controls on Facies Change

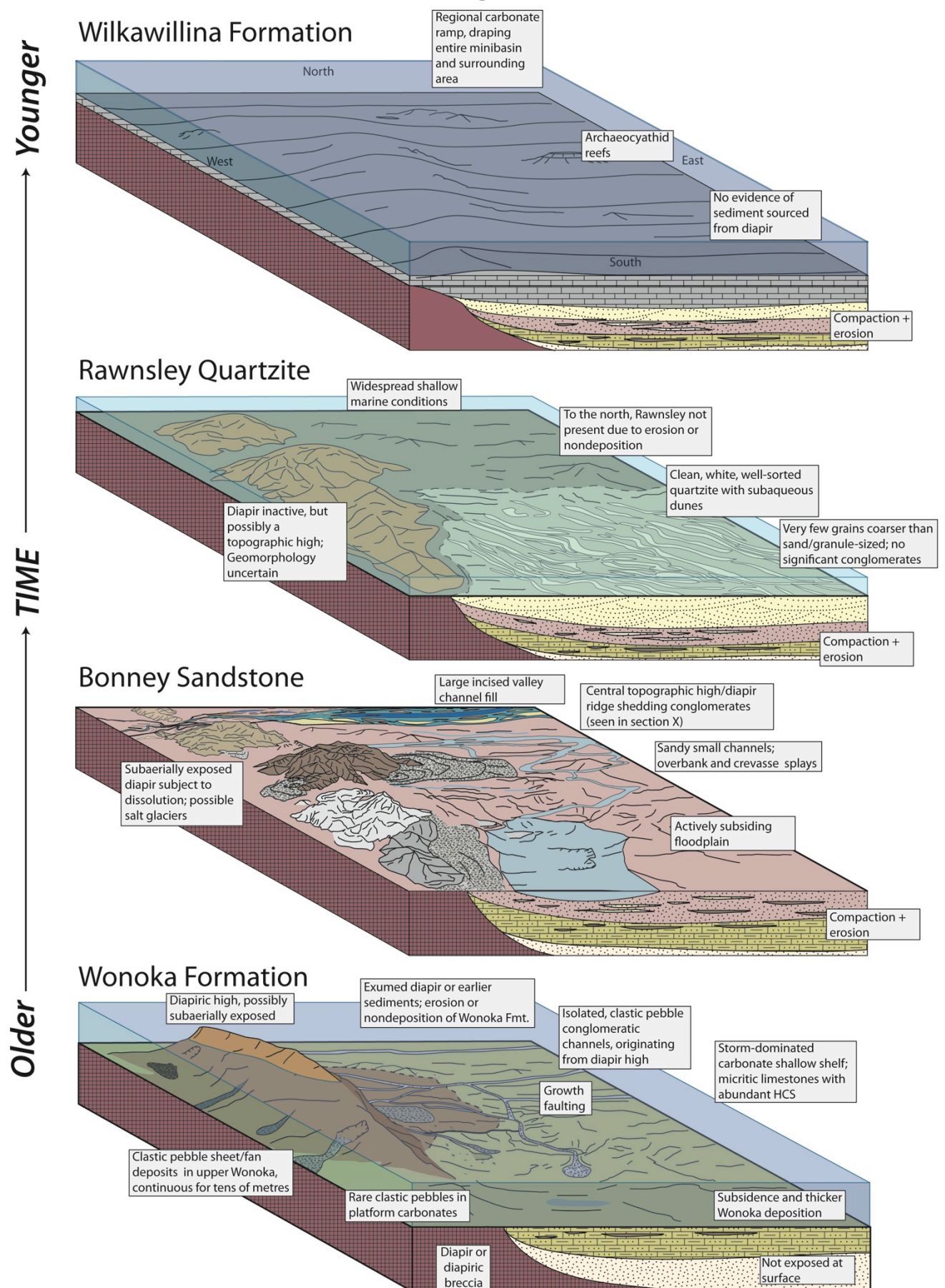


Figure 7: Schematic block diagram reconstructions of depositional environments and local palaeogeography in the Mt Frome area over a series of time slices corresponding to each formation. Blocks are vertically exaggerated and not to scale. View of block diagrams is from obliquely south to north, covering the area seen in Figure 5C. See labels and text for description of various elements.

sediment surface during the time of deposition, either subaerially or on the seafloor. Abundant heavy mineral laminae, pebble and cobble conglomerates of extrabasinal clasts, and changes in overall stratigraphic architecture are characteristic of sediments adjacent to the exposed diapir. Clasts within gravity flow deposits were clearly lithified at the time of deposition, as evidenced by their roundness relative to those within the preserved diapir (Fig. 5F). Many clasts are also metamorphic or volcanic, suggesting they have been brought up from deep within the basin, as these lithologies are known only from the basement or the earliest deposits in the basin fill.

In addition, sediments within the minibasin can be characterized as having a substantial increase in the abundance of gravity-driven mass flow deposits when compared to the same formations elsewhere, resulting in a larger variety of architectural elements than 'background' sedimentation (e.g., discontinuous conglomerate-filled beds). The greater depositional energy of these processes (relative to background sedimentation) and the closer proximity to a source of large clasts results in changes in lithology as well as geomorphology. The discontinuous geometries and internal character of conglomeratic beds are consistent with deposition in debris flows and channels, which originated from the diapir high and flowed basinward into the minibasin depocentre. These deposits are most common nearest to the minibasin margin, and where minibasin sediments thin onto the central diapiric high.

Similar sedimentologic features have been recorded near other diapirs elsewhere, both in the Adelaide Rift Complex (Dalgarno and Johnson, 1968, Appendix 8.3, Table 1 and Fig. 3) and in other salt-tectonized basins where salt has intersected the surface (Giles and Lawton, 2002). Elsewhere in the basin, deposits near the Patawarta and Pinda diapirs contain similar conglomeratic facies to those

seen here (Kernen et al., 2012), and are only ~50 km from the study area. In the minibasins adjacent to these diapirs, evidence suggests salt breccias were allowed to flow laterally into the surrounding sediments (Dyson 2004, Hearon et al., 2015). Sediments in the Umberatana minibasin are also considered time-equivalent to the Bonney Sandstone (Counts and Amos, 2016), and contains large diapir-derived clasts and immature gravity flow deposits. These observations, combined with those reported here, confirm that a recurring pattern of characteristic lithofacies exist in these minibasin environments, and that such lithofacies can be used to characterize diapir-sediment interaction on a general level. Taken individually, such features are not diagnostic of these settings, but may be used as supporting evidence when direct relationships are not clear. Such features are also likely seen in other salt-tectonic provinces in other locations as well. These include:

- anomalously shallow water facies in otherwise deeper basins;
- clastic-carbonate mixtures;
- growth faulting both laterally and downdip from diapir margin;
- angular unconformities associated with tilting;
- debris flows and turbidites resulting from diapir topography;
- paleocurrents that do not fit with larger basin paleogeography;
- condensed sedimentation on diapir margin;
- isolated exotic blocks and pebbles in otherwise fine-grained strata.

### *5.6.3: Diapir-related controls on facies change*

Stratigraphic units and the facies within them are variable in thickness and character along the minibasin margin, resulting in lateral heterogeneity of the minibasin fill. Lateral changes in facies are likely a result of the influence of structural features including faults, differential subsidence, and rugosity of the diapir-sediment

contact. Most notably, overall formation thicknesses below the Cambrian are considerably lower near the middle of the transect between sections B and E. This area is coincident with a facies change, where conglomerates of Facies E become substantially more abundant (Fig. 6). Sections seen on the north and south ends of the transect contain facies more in line with 'normal' background sediments that are lacking in conglomerates or channel forms, and that preserve additional units and facies not seen in the transect centre.

This central portion of the minibasin margin contains a number of other features that shed light on the increase in conglomerates. In the study area, two primary fault complexes are seen that offset sediment by tens of metres, laterally juxtaposing Facies D and E against the diapir body (Fig. 8A). These faults, near Sections C and D, down-drop both the diapir and the basin fill sediments to the south or southwest. In some places, fault zones are composed of a series of indistinct fault planes and breccias that are highly ferruginized (Fig. 8B). The changes in sediment thickness across these faults indicates that they were likely concurrent with deposition, but the sharp nature of some contacts indicate that faulting likely continued during early, pre-lithification burial. Sediment blocks between faults were also normally faulted and rotated, as strike directions change in the downthrown fault block near section D (Fig. 8A). It is likely that these faults continue into the diapir body, but the lack of bedding planes within the diapir prevents measurement of throw. Fault slip and rotation of downthrown blocks may be caused by continual uneven subsidence of the onlapping minibasin sediments onto the diapir, or alternatively, the fault surface may act as a periodically reactivated shear plane and growth fault. In either scenario, the diapir high between sections C and D may be considered a growth ridge or "salt roller" caused by the

accommodation of sediment at the toe of the northern growth fault. Similar geometries are seen in sandbox experiments done by Brun and Mauduit (2008; 2009) who modelled syndepositional fault growth atop a viscous medium that represents an underlying salt layer (Fig. 8C, 8D). This growth fault and ridge geometry explains the geometry of the diapir margin, and such features are common components of models that describe the breakout and advance of allochthonous salt (e.g., Hudec and Jackson, 2006).

The correlation between the occurrence of conglomeratic Facies E and growth faulting strongly indicates that some aspects of facies distribution along the diapir margin are controlled by structural features. Fault scarps along topographic highs expose newly-eroded diapiric material and provide a source of coarser sediment, which is then reworked through erosion and mass-flow processes. Clasts from the diapir are rounded and redeposited into the discontinuous channels and lenses seen in the Facies C and E. On the topographic high near the centre of the transect, background sedimentation rates are lower, and conglomerates thus form a higher proportion of the overall formation thickness (Fig. 6). Topographic highs, syndepositional faults, and diapir proximity are all associated with an increase in diapir-derived conglomeratic lithologies, and affect facies stacking patterns along the minibasin rim across a kilometre-scale area. Facies distribution also likely changes basinward, as the largest clast sizes are found closest to the diapir contact, and usually become smaller with increasing stratigraphic and spatial distance from the diapir. A hypothetical model of minibasin formation is shown in Appendix 8.3, Fig. 4.

Facies distribution here is therefore an interplay between the available accommodation, depositional environment, sediment sources, diapir exposure, and sedimentation rates. In the Mt. Frome minibasin, these factors effectively control the

spatial distribution and stacking patterns of facies, including the net-to-gross ratio of conglomerates to sandy shales.

#### 5.6.4: Comparison with diapir-sediment interaction elsewhere

In some present-day basins, active diapirs can be seen to break out onto a subaerially or subaqueously exposed surface, providing a modern analogue for what was likely occurring in the Mt. Frome area in the Precambrian. Emergent salt is seen today, for example, in and around the Arabian Gulf, where diapirs are

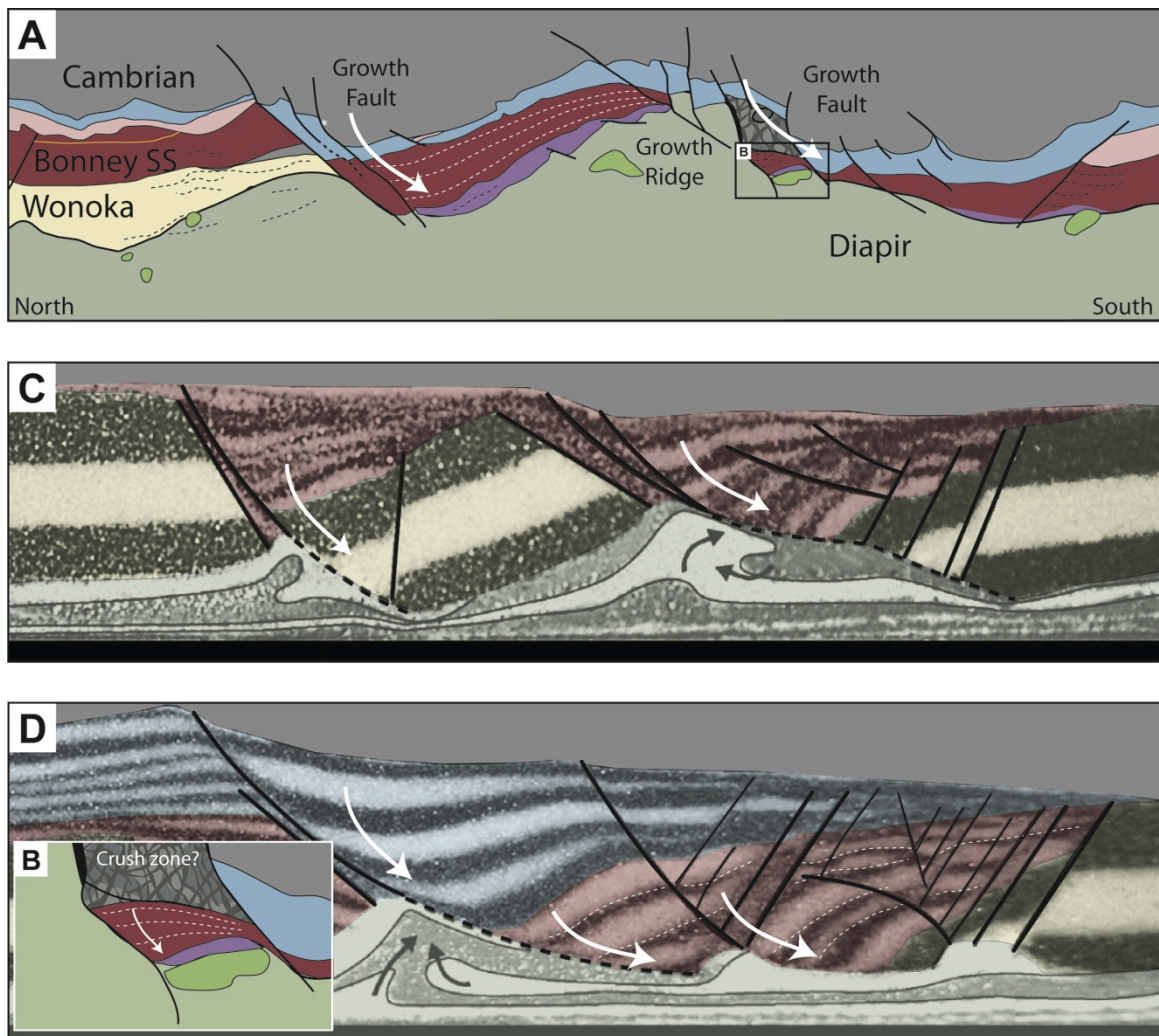


Figure 8: (A-D) Comparison between observed diapir-margin geometry in the Mt. Frome area and experimental models of growth faulting and salt roller generation. (A) Enlargement of the central portion of the geologic map in Figure 7, rotated to the horizontal. (B) Early-stage sandbox model of salt roller generation, showing rotated sediments and stratal thinning. Salt diapir simulated by silicone putty. (C) Advanced rollover model, compared to inset in (D) where Bonney Sandstone block has been strongly rotated and thins onto a diapir high. (B) and (C) modified from Brun and Mauduit (2009).

sourced from Ediacaran-Cambrian evaporites. On shore, these diapirs form salt glaciers that flow laterally at the surface (*namakiars*), where they behave in much the same way as water ice glaciers (Talbot and Pohjola, 2009). Diapirs also occur offshore in that region, with circular salt bodies forming isolated, offshore islands on a shallow marine carbonate ramp with fringing coral reefs (Edgell, 1996; Alsharhan and Kendall, 2003; Peters et al., 2003; Thomas et al., 2015). Like the ancient diapirs seen in this study, the modern Arabian diapirs also contain abundant brecciated clasts brought to the surface from deeper in the basin, composed of widely varying lithologies and a wide range of sizes, up to kilometre-scale (see Appendix 8.3, Fig. 5). Diapiric islands show onlap and thinning of Miocene and younger sediments, and are capped by a Holocene submarine deposit composed of “unsorted, angular, matrix-supported clasts” (Bruthans et al., 2009). Subaerially exposed salt in the arid Zagros Mountains in nearby Iran has also been shown to transport clasts and non-evaporitic sediments out onto the surface, leaving behind an insoluble residue of clay, gravel, and larger debris (Bruthans et al., 2009). Insoluble clasts are and reworked by fluvial processes, leading to deposits that may be similar to those seen in the Bonney Sandstone described here. Such reworking is likely occurring in the marine diapirs as well, redepositing allochthonous exotic clasts into carbonate sands and muds (Alsharhan and Kendall, 2003) similar to that seen in the Wonoka Formation. These instances provide some insight into the nature of similar deposits in the Flinders Ranges, and are useful in reconstructing the paleogeography of the region as depicted in Figure 7. However, many aspects of these types of deposits remain unknown from an actualistic perspective, and an opportunity exists for more work to be done that is focused on a better understanding of ancient analogues.



Extrusive salt similar to that seen in the Adelaide Rift Complex diapirs is seen in deeper water settings as well, breaking out laterally along bedding planes (Wu et al., 1990) and forming open-toed salt sheets that intersect the seafloor (Hudec and Jackson, 2006). Subaqueous salt glaciers have been described in both ancient and modern sediments, e.g., Triassic Tunisia (Masrouhi and Koyi, 2012), and more recently in the Gulf of Mexico (Hudec and Jackson, 2006), where salt breaks out from a thin sedimentary cover or forms subaqueous topographic highs where the salt body is covered by a thin veneer of overlying sediment. In the Gulf of Mexico, cap rocks of undissolved material remain where salt has at one time intersected the seafloor surface and been dissolved by seawater, with the thickness dependent on the volume of salt dissolved (Talbot, 1993). These features are in line with those described in the Adelaide Rift complex by Dyson (2004) and others. The specific depositional processes and characteristics operating near open-toed allochthonous salt on the seafloor have not been fully described in modern settings, where sedimentation is likely a complex interplay between salt dissolution, reworking and redeposition of allochthonous clasts, background sedimentation, and salt movement. Due to the difficulty of accessing such deposits on the seafloor, outcropping sediments in similar ancient settings provide the only insight into these processes. Mt Frome and other Flinders Ranges diapirs may therefore be the best opportunity to examine sedimentary processes and products in a setting very similar to that occurring today on salt-tectonized continental margins around the world.

## **5.7: Conclusions**

Sediments in the Mt. Frome minibasin were deposited in a variety of shallow-marine and continental environments that were influenced by proximity to an

extrusive diapir body. The exposure, erosion, and dissolution of evaporites containing a high density of allochthonous clasts created a unique depositional setting, resulting in processes and products dissimilar to the background sedimentation elsewhere in the basin. Dominant diapir-related features in minibasin sediments include abundant pebble conglomerates (an anomalously large grain size for the interval), channelization and gravity flow deposits, depositional thinning and onlap, and rotational growth faulting. Conglomerates are sourced from fault scarps that expose fresh diapir matrix, as evidenced by facies relationships and compositional similarity. This study is one of the first to systematically describe the lateral variability of sediments along the rim of a salt-withdrawal minibasin, and is one of few to study the detailed interaction of salt and sediment in an ancient setting from a sedimentological perspective. Other diapirs in the region and modern diapirs elsewhere in the world both show similar facies in surrounding sediments; when combined with the observations reported here, this consistency shows that these settings contain a recurring set of features that can be useful in predicting the sedimentary character of these deposits. Such features may be used as sedimentological criteria for syndepositional salt movement and exposure when direct evidence is not present or more ambiguous, and may assist in creating predictive models of reservoir distribution in salt-influenced basins. This study further demonstrates that areas affected by salt tectonics should be considered unique sedimentary environments, as the processes operating and their resulting impact on sediments have no exact analogues elsewhere in the geologic record.

## 5.8: References

- ALSHARHAN, A.S., AND KENDALL, C.S.C., 2003, Holocene coastal carbonates and evaporites of the southern Arabian Gulf and their ancient analogues. *Earth-Science Reviews*, v. **61**, p. 191-243.
- BACKÉ, G., BAINES, G., GILES, D., PREISS, W., AND ALESCI, A., 2010, Basin geometry and salt diapirs in the Flinders Ranges, South Australia: insights gained from geologically-constrained modelling of potential field data. *Marine and Petroleum Geology*, v. **27**, p. 650-665.
- BANHAM, S.G., AND MOUNTNEY, N.P., 2013a, Evolution of fluvial systems in salt-walled mini-basins: a review and new insights. *Sedimentary Geology*, v. **296**, p. 142-166.
- BANHAM, S.G., AND MOUNTNEY, N.P., 2013b, Controls on fluvial sedimentary architecture and sediment-fill state in salt-walled mini-basins: Triassic Moenkopi Formation, Salt Anticline Region, SE Utah, USA. *Basin Research*, v. **25**, p. 709-737.
- BANHAM, S.G., AND MOUNTNEY, N.P., 2014, Climatic versus halokinetic control on sedimentation in a dryland fluvial succession. *Sedimentology*, v. **61**, p. 570-608.
- BOGDANOVA, S.V., PISAREVSKY, S.A., AND LI, Z.X., 2009, Assembly and breakup of Rodinia (some results of IGCP Project 440). *Stratigraphy and Geological Correlation*, v. **17**, p. 259-274.
- BOOTH, J.R., DEAN, M.C., DUVERNAY, A.E., AND STYZEN, M.J., 2003, Paleobathymetric controls on the stratigraphic architecture and reservoir development of confined fans in the Auger Basin: central Gulf of Mexico slope. *Marine and Petroleum Geology*, v. **20**, 563-586.
- BRUN, J.P., AND MAUDUIT, T.P.O., 2008, Rollovers in salt tectonics: the inadequacy of the listric fault model. *Tectonophysics*, v. **457**, p. 1-11.
- BRUN, J.P., AND MAUDUIT, T.P.O., 2009, Salt rollers: structure and kinematics from analogue modelling. *Marine and Petroleum Geology*, v. **26**, p. 249-258.

- BRUTHANS, J., FILIPPI, M., ASADI, N., ZARE, M., ŠLECHTA, S., AND CHURÁČKOVÁ, Z., 2009, Surficial deposits on salt diapirs (Zagros Mountains and Persian Gulf Platform, Iran): characterization, evolution, erosion and the influence on landscape morphology. *Geomorphology*, v. **107**, p. 195-209.
- BRYANT, W.R., BRYANT, J.R., FEELEY, M.H., AND SIMMONS, G.R., 1990, Physiographic and bathymetric characteristics of the continental slope, northwest Gulf of Mexico. *Geo-Marine Letters*, v. **10**, p. 182-199.
- CLARKE J.D.A., 1988, Geology of the Hawker Group (Early Cambrian), Wilkawillina Gorge, South Australia. Flinders University of South Australia, PhD thesis
- COOPER, A.M., 1991, Late Proterozoic hydrocarbon potential and its associated with diapirism in Blinman #2, central Flinders Ranges, South Australia. University of Adelaide Honours thesis, unpublished.
- COUNTS, J.W. AND AMOS, K.J., in review, Paleogeography of an Ediacaran Fluvial-Deltaic System: A Case Study Integrating Sedimentology and Provenance.
- COUNTS, J.W., RARITY, F., AMOS, K., AINSWORTH, R.B., LANE, T., MORÓN, S., TRAINOR, J., AND VALENTI, C., 2016, Sedimentologic interpretation of an Ediacaran delta: Bonney Sandstone, South Australia, *Australian Journal of Earth Sciences*.
- DALGARNO, C.R., 1964, Lower Cambrian stratigraphy of the Flinders Ranges. *Transactions of the Royal Society of South Australia*, v. **88**, p. 129-144.
- DALGARNO, C.R., AND JOHNSON, J.E., 1968, Diapiric structures and late Precambrian-early Cambrian sedimentation in Flinders Ranges, South Australia. In: Braunstein, J., and O'Brien, G.D. (eds.) *AAPG Memoir* v. **8**, p. 301-314.
- DAVIES, N.S., AND GIBLING, M.R., 2010, Cambrian to Devonian evolution of alluvial systems: the sedimentological impact of the earliest land plants: *Earth-Science Reviews*, v. **98**, p. 171-200.
- DYSON, I.A., 1996, A new model for diapirism in the Adelaide Geosyncline. *MESA Journal*, v. **3**, p. 41-48.

- DYSON, I.A., 2004, Christmas Tree Diapirs and Development of Hydrocarbon Reservoirs: A Model from the Adelaide Geosyncline, South Australia. In: Salt-sediment interactions and hydrocarbon prospectivity: Concepts, Applications, and Case Studies for the 21st Century (Eds P.J. Post, D.L. Olson, K.T. Lyons, S.L. Palmes, P.F. Harrison and N.C. Rosen) 24th GCSSEPM Bob F. Perkins Research Conference, p. 133-165.
- EDGEHILL, H.S., 1996, Salt tectonism in the Persian Gulf basin. *Geological Society, London, Special Publications*, v. **100**, p. 129-151.
- ERICKSSON, K.A., AND SIMPSON E., 2012, "Precambrian tidal facies." In: Principles of Tidal Sedimentology, p. 397-419. Springer Netherlands,.
- GEHLING, J.G., 1982. Sedimentology and Stratigraphy of the Late Precambrian Pound Subgroup, Central Flinders Ranges, S.A. University of Adelaide MSc thesis.
- GEHLING, J.G. (2000). Environmental interpretation and a sequence stratigraphic framework for the terminal Proterozoic Ediacara Member within the Rawnsley Quartzite, South Australia. *Precambrian Research*, v. **100**, p. 65-95.
- GILES, K.A., AND LAWTON, T.F. (2002). Halokinetic sequence stratigraphy adjacent to the El Papalote diapir, northeastern Mexico. *AAPG Bulletin*, v. **86**, p. 823-840.
- HAINES, P.W., 1990. A late Proterozoic storm-dominated carbonate shelf sequence: the Wonoka Formation in the central and southern Flinders Ranges, South Australia. In: *Geological Society of Australia, Special Publication* v. **16**, p. 177–198.
- HEARON, T.E., ROWAN, M.G., LAWTON, T.F., HANNAH, P.T., AND GILES, K.A., 2015,. Geology and tectonics of Neoproterozoic salt diapirs and salt sheets in the eastern Willouran Ranges, South Australia. *Basin Research*, v. **27**, p. 183-207.
- HUDEK, M.R., AND JACKSON, M.P., 2006, Advance of allochthonous salt sheets in passive margins and orogens. *AAPG Bulletin*, v. **90**, p. 1535-1564.
- HUDEK, M.R., AND JACKSON, M.P., 2007 Terra infirma: understanding salt tectonics.

- Earth-Science Reviews*, v. **82**, p. 1-28.
- IMMENHAUSER, A., 2009, Estimating palaeo-water depth from the physical rock record. *Earth-Science Reviews*, v. **96**, p. 107-139.
- JAMES, N.P., AND GRAVESTOCK, D.I., 1990, Lower Cambrian shelf and shelf margin buildups, Flinders Ranges, South Australia. *Sedimentology*, v. **37**, p. 455-480.
- KERNEN, R.A., GILES, K.A., ROWAN, M.G., LAWTON, T.F., AND HEARON, T.E., 2012, Depositional and halokinetic-sequence stratigraphy of the Neoproterozoic Wonoka Formation adjacent to Patawarta allochthonous salt sheet, Central Flinders Ranges, South Australia. *Geological Society, London, Special Publications*, v. **363**, p. 81-105.
- KNOLL, A., WALTER, M., NARBONNE, G., AND CHRISTIE-BLICK, N., 2006, The Ediacaran Period: a new addition to the geologic time scale. *Lethaia*, v. **39**, p. 13-30.
- LEESON, B., 1970. Geology of the Beltana 1:63 360 map area. *South Australia. Geological Survey Report of Investigations*, v. **35**.
- Li, Z.X., Bogdanova, S.V., Collins, A.S., Davidson, A., De Waele, B., Ernst, R.E., Fitzsimons, I.C.W., Fuck, R.A., Gladkochub, D.P., Jacobs, J., Karlstrom, K.E., Lu, S., Natapov, L.M., Pease, V., Pisarevsky, S.A., Thrane, K., and Vernikovsky, V., 2008, Assembly, configuration, and break-up history of Rodinia: a synthesis. *Precambrian Research*, v. **160**, p. 179-210.
- MASROUHI, A., AND KOYI, H.A. (2012). Submarine 'salt glacier' of Northern Tunisia, a case of Triassic salt mobility in North African Cretaceous passive margin. *Geological Society, London, Special Publications*, v. **363**, p. 579-593.
- MATTHEWS, W.J., HAMPSON, G.J., TRUDGILL, B.D., AND UNDERHILL, J.R., 2007, Controls on fluviolacustrine reservoir distribution and architecture in passive salt-diapir provinces: Insights from outcrop analogs. *AAPG Bulletin*, v. **91**, p. 1367-1403.
- MAWSON, S.D., 1941, The Wilpena Pound formation and underlying Proterozoic sediments. *Transactions of the Royal Society of South Australia*, v. **65**, p. 295-300.

- MCKENZIE, N., JACQUIER, D., ISBELL, R. AND BROWN, K., 2004, Australian Soils and Landscapes. An Illustrated Compendium. (CSIRO Publishing, Melbourne).  
URL: [www.publish.csiro.au/pid/3821.htm](http://www.publish.csiro.au/pid/3821.htm)
- PAUL, E., FLÖTTMANN, T., AND SANDIFORD, M., 1999, Structural geometry and controls on basement-involved deformation in the northern Flinders Ranges, Adelaide Fold Belt, South Australia. *Australian Journal of Earth Sciences*, v. **46**, p. 343-354.
- PETERS, J.M., J. FILBRANDT, J. GROTZINGER, M. NEWALL, M. SHUSTER, AND AL-SIYABI, H., 2003, Surface-piercing Salt Domes of interior north Oman, and their significance of the Ara Carbonate “Stinger” hydrocarbon play, *Geoarabia*, v. **8**, p. 231–270.
- PLUMMER, P.S., 1978, The upper Brachina subgroup: a late Precambrian intertidal deltaic and sandflat sequence in the Flinders Ranges, South Australia. University of Adelaide PhD Thesis.
- PREISS, W.V., 1987, The Adelaide Geosyncline—late Proterozoic stratigraphy, sedimentation, paleontology and tectonics. *Bulletin of the Geological Survey of South Australia*, v. **53**, 438 p.
- PREISS, W.V., 2000, The Adelaide Geosyncline of South Australia and it's significance in Neoproterozoic continental reconstruction. *Precambrian Research*, v. **100**, p. 21-63.
- REID, P., AND PREISS., W.V., 1999, Parachilna map sheet. *South Australian Geological Survey Geological Atlas 1.250,000*, 54-13.
- REILLY, M.R.W., 2001, Deepwater Reservoir Analogue-Bunkers Sandstone, Donkey Bore Syncline, Flinders Ranges Australia. University of Adelaide National Centre for Petroleum Geology and Geophysics Honours Thesis.
- REINECK, H.E., AND SINGH, I.B., 1973, Depositional sedimentary environments: with reference to terrigenous clastics. Springer-Verlag Berlin-Heidelberg-New York. 550 p.
- RIBES, C., KERGARAVAT, C., BONNEL, C., CRUMEYROLLE, P., CALLOT, J.P., POISSON,

- A., TEMIZ, H., AND RINGENBACH, J.C., 2015, Fluvial sedimentation in a salt-controlled mini-basin: stratal patterns and facies assemblages, Sivas Basin, Turkey. *Sedimentology*, v. **62**, p. 1513-1545.
- ROWAN, M.G., AND VENDEVILLE, B.C., 2006, Foldbelts with early salt withdrawal and diapirism: physical model and examples from the northern Gulf of Mexico and the Flinders Ranges, Australia. *Marine and Petroleum Geology*, v. **23**, p. 871-891.
- TALBOT, C.J., 1993, Spreading of salt structures in the Gulf of Mexico. *Tectonophysics*, v. **228**, p. 151-166.
- TALBOT, C.J., AND POHJOLA, V., 2009, Subaerial salt extrusions in Iran as analogues of ice sheets, streams and glaciers. *Earth-Science Reviews*, v. **97**, p. 155-183.
- THOMAS, R.J., ELLISON, R.A., GOODENOUGH, K.M., ROBERTS, N.M., AND ALLEN, P.A., 2015 Salt domes of the UAE and Oman: Probing eastern Arabia. *Precambrian Research*, v. **256**, p. 1-16.
- WU, S., BALLY, A.W., AND CRAMEZ, C., 1990, Allochthonous salt, structure and stratigraphy of the north-eastern Gulf of Mexico. Part II: Structure. *Marine and Petroleum Geology*, v. **7**, p. 334-370.



# Statement of Authorship

Title of Paper	Sedimentology, depositional environments and significance of an Ediacaran salt-withdrawal minibasin, Billy Springs Formation, Flinders Ranges, South Australia
Publication Status	<input checked="" type="checkbox"/> Published <input type="checkbox"/> Accepted for Publication <input type="checkbox"/> Submitted for Publication <input type="checkbox"/> Unpublished and Unsubmitted work written in manuscript style
Publication Details	Counts, J. W. and Amos, K. J. (2016), Sedimentology, depositional environments and significance of an Ediacaran salt-withdrawal minibasin, Billy Springs Formation, Flinders Ranges, South Australia. Sedimentology. doi: 10.1111/sed.12250

## Principal Author

Name of Principal Author (Candidate)	John W. Counts			
Contribution to the Paper	All aspects except supervisor review			
Overall percentage (%)	95%			
Certification:	This paper reports on original research I conducted during the period of my Higher Degree by Research candidature and is not subject to any obligations or contractual agreements with a third party that would constrain its inclusion in this thesis. I am the primary author of this paper.			
Signature		<table border="1"> <tr> <td>Date</td> <td>18/4/2016</td> </tr> </table>	Date	18/4/2016
Date	18/4/2016			

## Co-Author Contributions

By signing the Statement of Authorship, each author certifies that:

- i. the candidate's stated contribution to the publication is accurate (as detailed above);
- ii. permission is granted for the candidate to include the publication in the thesis; and
- iii. the sum of all co-author contributions is equal to 100% less the candidate's stated contribution.

Name of Co-Author	Kathryn J. Amos,			
Contribution to the Paper	Review and commentary			
Signature		<table border="1"> <tr> <td>Date</td> <td>19/05/2016</td> </tr> </table>	Date	19/05/2016
Date	19/05/2016			

Please cut and paste additional co-author panels here as required.

**Chapter 6: Sedimentology, depositional  
environments and significance of an Ediacaran salt-  
withdrawal minibasin, Billy Springs Formation,  
Flinders Ranges, South Australia**

J. W. Counts and K. J. Amos

*As published in Sedimentology, 2016*

## 6.1: Abstract

The late Ediacaran Billy Springs Formation is a little-studied, mudstone-dominated unit deposited in the Adelaide Rift Complex of South Australia. Sediments are exposed in an approximately 11 km by 15 km synclinal structure interpreted as a salt-withdrawal minibasin. The stratigraphic succession is characterized by convolute-laminated slump deposits, rhythmically laminated silty mudstones, rare diamictites and fining-upward turbidite lithofacies. Lithofacies are the product of deposition in a deepwater slope or shelf setting, representing one of the few such examples preserved within the larger basin. Although exact correlations with other formations are unclear, the Billy Springs Formation probably represents the distal portion of a highstand systems tract, and is overlain by coarser sediments of the upper Pound Subgroup. Diamictite intervals are interpreted to be the product of mass flow processes originating from nearby emergent diapirs, in contrast to previous studies that suggest a glacial origin for extrabasinal clasts. Within the spectrum of outcropping minibasins around the world, the sediments described here are unique in their dominantly fine-grained nature and overall lithological homogeneity. Exposures such as these provide an opportunity to better understand the sedimentological processes that operate in these environments, and provide an analogue for similar settings in the subsurface that act as hydrocarbon reservoir-trap systems.

## 6.2: Introduction

Although salt-withdrawal minibasins form a significant portion of the world's hydrocarbon-bearing strata, outcrop exposures of these types of environments are relatively limited in number (Table 1); hence, they are understudied with regard to detailed mesoscale sedimentation processes and products that make up minibasin fill. The purpose of this paper is to describe and interpret the Billy Springs Formation, a succession of predominantly clastic sediments deposited in a depocentre interpreted as a salt-withdrawal minibasin on the late Ediacaran (Neoproterozoic) passive margin of southern Australia. These sediments are well-exposed in the northern Flinders Ranges, allowing detailed outcrop observations that can be used to better understand similar deposits in the subsurface around the world.

Salt-withdrawal minibasins are found throughout the world in a wide range of depositional settings. In the marine realm, they often create circular or elliptical topographic lows on the sea floor (Bouma and Bryant, 1994; Brown et al., 2004; Mallarino et al., 2006), and many contribute to petroleum trapping mechanisms at depth (Pilcher et al., 2011). Intraslope minibasin deposits are often dominated by gravity-driven flow (especially turbidites; e.g. Lamb et al., 2006) and can trap coarser-grained sediments originating from slope canyons and delta fans (Winker, 1996; Prather, 2000). Previous detailed studies of minibasin sedimentation in ancient deposits come primarily from core data (e.g. Mannie et al., 2014) as well as limited outcrops around the world, including elsewhere in the Flinders Ranges of Australia (see Table 1 and references therein). Table 1 presents a summary of published outcrop studies of salt-withdrawal minibasins that include at least some description of the sedimentology of the basin fill deposits. The formation, infilling

history and stratigraphic architecture of these types of basins have also been studied in detail in the Gulf of Mexico and other offshore settings in recent years through subsurface data (e.g. Prather, 2000; Madof et al., 2009; Pilcher et al., 2011, and many others). The present study seeks to examine the type of sedimentary fill and history of sedimentation of a Neoproterozoic minibasin from a process and lithofacies perspective, on a different scale than typically seen in either seismic, core or wireline data.

In the Flinders Ranges, numerous individual salt diapirs (preserved as dolomitic breccias) and several kilometres of basin fill are well-exposed at the surface (Preiss, 1987; Dyson, 1996). Folding and uplift in the Late Cambrian allows for both cross-sectional and plan view examination of diapirs and adjacent strata. The Umberatana Syncline, previously interpreted as a salt-withdrawal minibasin (Dyson, 2005; Rowan and Vendeville, 2006), exposes sediments of the Billy Springs Formation, a mudstone-dominated lithostratigraphic unit that has been hypothesized to represent the deepwater or downslope equivalent of shallow marine coarser sediments to the south (Von der Borch and Grady, 1982). Previous studies of this unit have been limited in scope; this article presents the first detailed description and interpretation of the sedimentary lithofacies, depositional environments and significance of the Billy Springs Formation. The primary aim of this paper is to provide a case study in minibasin sedimentation, thereby demonstrating an unambiguous record of the depositional processes and products involved in the infilling of a Precambrian minibasin. Specific research goals of this study are as follows:

- Documentation of the succession of sediments in the minibasin, and

determination of the processes responsible for their emplacement and whether depositional characteristics are a result of minibasin formation itself, or of external forces. This is accomplished through field classification of sediments into lithofacies, laboratory analysis to better understand lithological properties, interpretation of lithofacies based on established sedimentological principles and the recognition of the larger geological context in which the minibasin lies.

- Incorporation of the Billy Springs Formation into a larger palaeogeographic and sequence stratigraphic context, which can be used to better understand the history of the region and of Precambrian Australia as a whole. Outlining the evidence for the Umberatana Syncline as a salt-withdrawal minibasin.
- Using both the observations herein and existing research, to determine how this minibasin compares to others described in the geological record, and to those that are parts of productive hydrocarbon systems. What are the features seen here that are also frequently noted in minibasins elsewhere? Can this minibasin be accurately used as an analogue to predict the properties of some subsurface deposits?

Answers to these questions require a basic understanding of the Billy Springs Formation, which is necessary for any further insight into its larger significance.

Although salt-withdrawal minibasins have been well-studied in the subsurface, they have generally not been regarded as unique depositional environments in a sedimentological sense, with a few recent exceptions (e.g. Banham and Mountney, 2013a,b, 2014; Ribes et al., 2015; Venus et al., 2015). Although much is dependent on surroundings, detailed studies of minibasins in a diverse array of settings can be collated to reveal common depositional processes and stratigraphic trends, allowing

generalizations to be made that can ultimately result in predictive models for minibasin sedimentology. In combination with geophysical and core data, outcrops are key to a full understanding of the overall stratigraphic architecture of these deposits. All new outcrop studies, therefore, provide new information on the distribution and lateral variability of lithofacies in these deposits.

### 6.3: Geological Setting

During much of the Neoproterozoic, the Adelaide Rift Complex was a rift basin occupying part of Rodinia, a large supercontinent that existed until approximately 750 Ma (Li et al., 2008; Bogdanova et al., 2009). Most reconstructions based on palaeomagnetic data place Australia in low latitudes, between the palaeoequator and 30° north (Li et al., 2008). By the late Ediacaran, Rodinia had already broken apart, and Australia was part of a smaller subcontinent (Johnson, 2013). This subcontinent consists of a number of smaller Neoproterozoic basins and

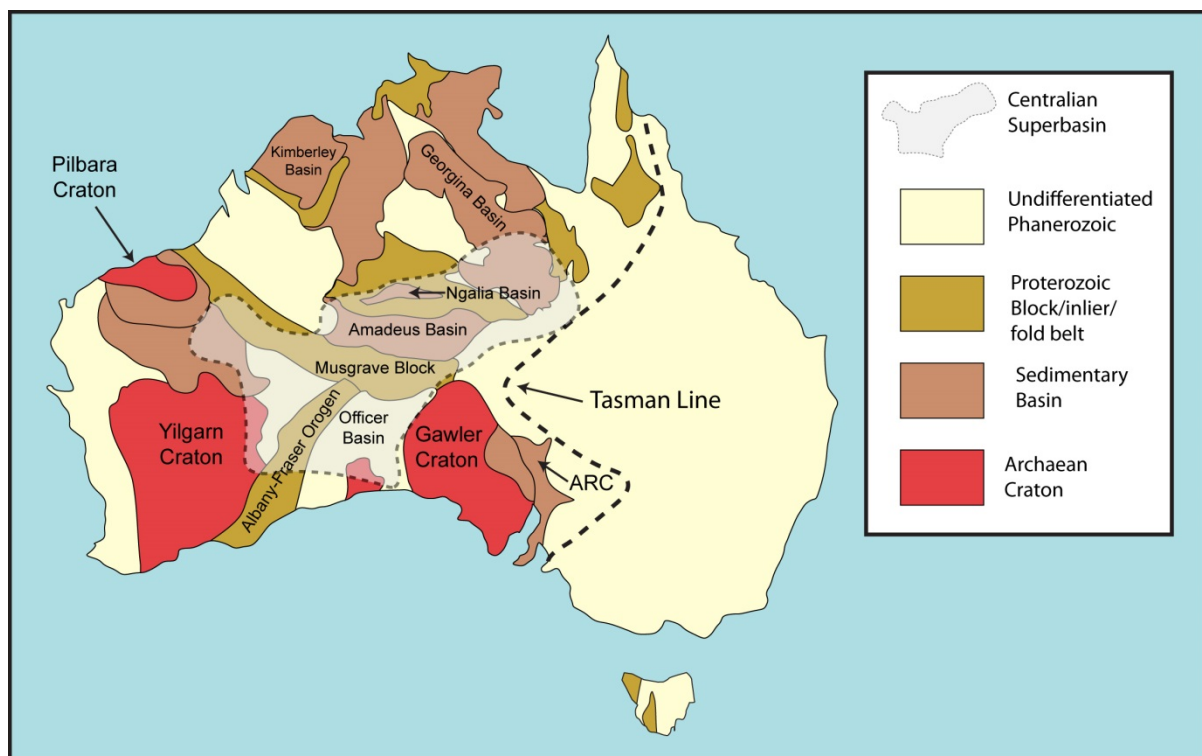


Figure 1: Map of Australia showing major cratonic provinces, selected sedimentary basins, and Centralian Superbasin.

cratonic provinces, and includes modern-day Australia to the west of the Tasman Line (Fig. 1).

Throughout basin history, the Adelaide Rift Complex was adjacent to the Gawler Craton to the west and the smaller Curnamona Craton to the east (present-day orientation; Fig. 2). Both of these provinces are composed primarily of prerift Proterozoic igneous rocks, which were relatively stable during basin formation and fill, and were periodically subaerially exposed (Drexel et al., 1993). To the south and east, the margin was probably connected to the larger ocean, although the degree of restriction and connectivity varied with sea-level and local tectonics over time (Preiss, 1987). Basal units in the basin fill are characterized by volcanics and evaporites, and were probably deposited in an incipient rift system. By the Ediacaran, it is generally accepted that the rift had evolved into a passive continental margin (eastward-facing in the present day), with the large Curnamona Craton possibly forming a large island offshore (Preiss, 1990), because Australia east of the Tasman Line had not yet amalgamated onto the older western portion of the subcontinent (Johnson, 2013). The northern extent of the rift complex may have been limited by the Muloorina Ridge, a basement gravity high that may have been exposed prior to the latest Ediacaran, although this remains speculative (Preiss, 1990). During the later Ediacaran, sediments thicken dramatically to the north, with the Pound Subgroup reaching 2500 m in the Gammon Ranges area (Gehling, 1982), compared to 813 m thick in the type section in Bunyerroo Gorge (Forbes, 1971).



The basin fill is complex, with numerous (>100) formal lithostratigraphic units deposited roughly from the early Cryogenian (ca 830 Ma; Preiss, 2000) to the Middle Cambrian (Drexel et al., 1993; Fig. 3). Infilling took place in multiple phases, beginning with the early rift sediments of the Callanna Group and culminating with the uplift and folding of the basin fill during the Cambrian–Ordovician Delamerian Orogeny

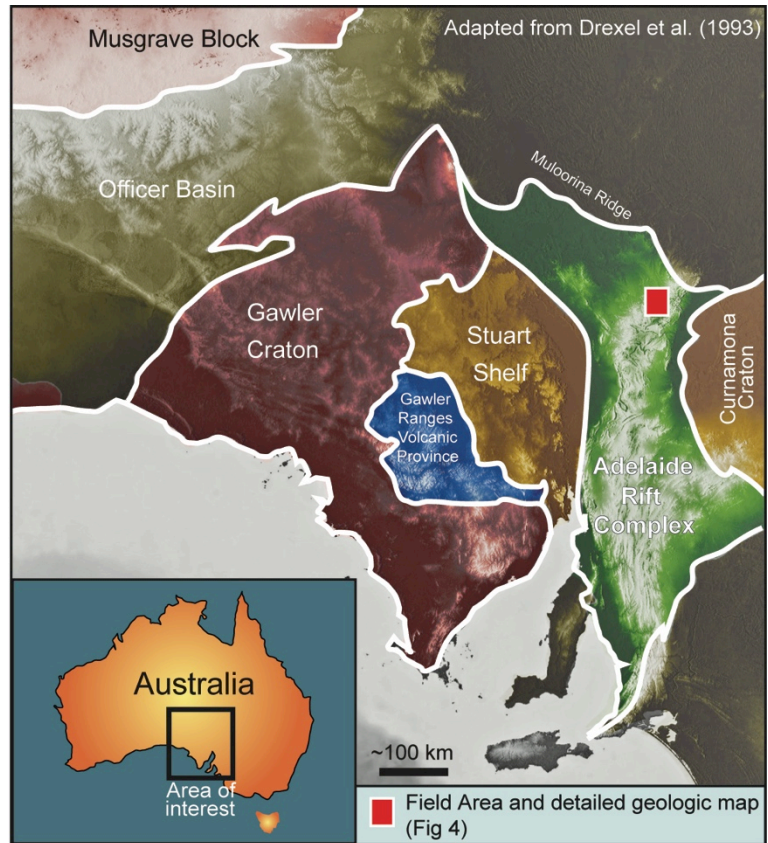


Figure 2: Locator map showing Adelaide Basin and field sites in relation to surrounding basins and cratonic provinces. The Officer Basin is of a similar age to the Adelaide Basin, and the Warburton Basin is Cambro-Ordovician in age.

(Preiss, 1987). In addition to larger-scale rifting episodes, syndepositional extensional faulting is recognized throughout the basin. Salt diapirs originating from Callanna Group evaporites were also active during deposition of later basin fill, with indications of syndepositional diapir activity as early as the Sturtian glacial episode (represented by the Burra Group; see Fig. 3) and continuing through to the cessation of deposition in the Early Cambrian (Dalgarno and Johnson, 1968). Diapir mobilization was probably caused by loading of the thick accumulation of sediments in the narrow, rapidly subsiding rift-sag basin, although Davison et al. (1996) note

that little or no overburden is required to initiate salt movement; however, this depends on the nature of the evaporite matrix and whether it is mixed with carbonate or clastic lithologies. Exposures of the Callanna Group in situ are found only in the distant outliers and margins of the basin; the unit is known primarily from allochthonous blocks, sometimes hundreds of metres in diameter, found within diapiric breccia (Preiss, 1987). No salt remains at the surface, with diapir matrix

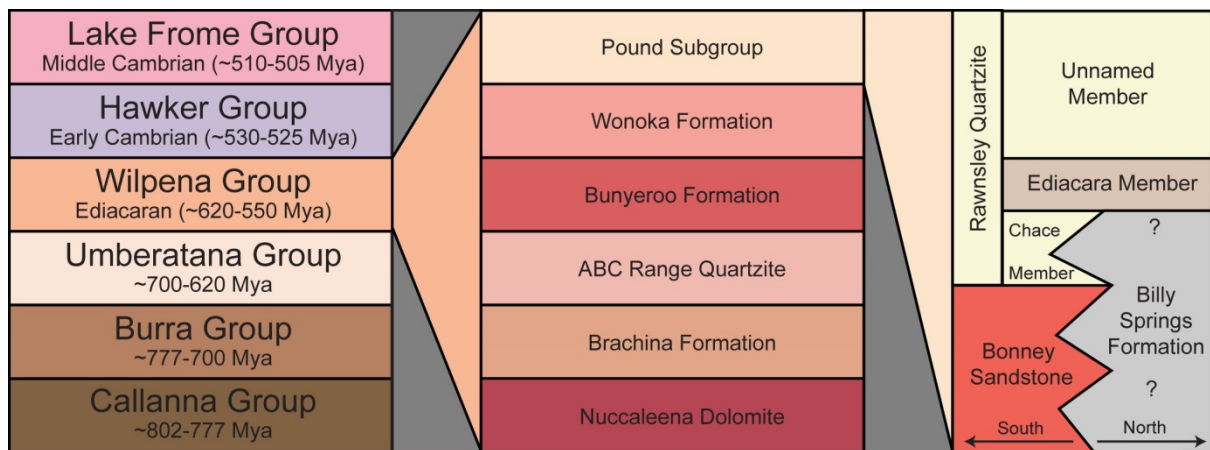


Figure 13: Generalized lithostratigraphy of the Adelaide Rift Complex, Wilpena Group, and Pound Subgroup.

having been replaced by a fine-grained dolomite, although pseudomorphs of halite crystals are common and the evaporite origin of these bodies is well-established (Dalgarno and Johnson, 1968). The Billy Springs Formation forms the one of the latest Precambrian (Ediacaran) units in the Adelaide Rift Complex and, like many of the sediments in the basin, its distribution and internal character are likely to be influenced by the continued mobilization of underlying salt.

#### 6.4: Background

The Billy Springs Formation is exposed only in two areas in the northern Flinders Ranges, the Umberatana and Mount Freeling Synclines, which lie north-west and north of Arkaroola Village, respectively (Fig. 4). Few in-depth geological studies have previously been conducted on these exposures. Previous

sedimentological interpretations of this interval generally favour a marine lower shelf or slope depositional environment for the Billy Springs deposits (e.g. Von der Borch and Grady, 1982; Jenkins, 2011). DiBona et al. (1990) note that the shelf-slope transition in the underlying Wonoka Formation lies only *ca* 15 km south of the Umberatana Syncline, which also contains kilometre-scale incised canyons near the study area. Exact stratigraphic correlations with other units in the basin have varied with different authors, although it is generally agreed upon that Billy Springs Formation sediments tie to either the upper Wonoka Formation, the lower Bonney Sandstone, or both (Coats and Blissett, 1971; Reid, 1992; Pell et al., 1993; Von der Borch and Grady, 1982; Table 2). In addition, various authors have differently interpreted the presence of large clasts within mudstones and siltstones of the Billy Springs Formation as the product of either glacial processes (Jenkins, 2011) or mass flow deposits (Von der Borch et al., 1982). Previous investigations have recognized the basic depositional framework of the Billy Springs Formation, but have mostly been brief or reconnaissance studies in speciality journals, have focused on exposures elsewhere or have not been published in peer-reviewed literature. Detailed sedimentology, petrography and provenance, as well as the larger significance of the formation, remain poorly understood. This study seeks to incorporate observations from these previous studies with this work in order to create a more comprehensive model for the evolution of minibasin fill over time.

Location	Age/Formation	Environment of Deposition	Brief Description of Minibasin Sediments	Reference
<b>Precaspian Basin, Kazakhstan</b>	Permian-Triassic reservoirs, with topographic influence at present	Fluvio-lacustrine, Terrestrial	Modern minibasin sedimentology used as analog for underlying minibasin reservoirs. Facies include braided fluvial channels and associated floodplain/overbank deposits; paleosols, lacustrine sediments, evaporites from reprecipitated salt originating from salt walls	Barde et al. 2002
<b>Ural Mtns, Russia</b>	Permian-Triassic	Fluvio-lacustrine; Terrestrial	Analogous to sediments described by Barde et al. in Kazakhstan; channel fill, lacustrine delta/sheet flood deposits, calcretes	Newell et al. 2012
<b>Sivas Basin, Turkey</b>	Oligocene-Miocene	Fluvial, Lacustrine, Sabkha, Shallow Marine	Clastics and carbonates formed in a generally continental setting in multiple minibasins, which are surrounded by salt walls. Sediments show lateral thickness variability, unconformities, and grain-size changes.	Callot et al 2014; Ringenbach et al 2013
<b>Paradox Basin, Utah, USA</b>	Pennsylvanian-Triassic; Honaker Trail, Cutler, and Chinle Fmts.	Fluvial-lacustrine; Terrestrial	Channel sandstones, mudstones and conglomerates, lacustrine muds, paleosols, and eolian deposits (in Chinle fmt), with numerous sedimentologic features varying due to salt-related topographic changes	Matthews et al. 2007; Banham and Mounthney 2013
<b>Sverdrup Basin, Nunavut, Canada</b>	Multiple Paleozoic-Cenozoic Formations	Various, inc. Fluvial-Deltaic	Limited sedimentology reported, though basin fill ranges from Carboniferous-Eocene and likely represents a wide range of environments. In the L. Cret. Isachsen fmt., channel sands and basal debris flows of mixed lithology clasts onlap allocthonous diapirs.	Jackson and Harrison 2006
<b>Northwest Yemen</b>	Miocene	Alluvial-Lacustrine-Beach-Shallow Marine-Reef, in an arid climate	Not described as a 'minibasin', but actively rising diapir influencing sedimentation processes and unit thicknesses. Debris flows, conglomerates, flanking reefs, growth faults and unconformities common.	Davison et al 1996
<b>Flinders Ranges, South Australia</b>	Cryogenian; Enorama Shale	Shallow marine-reefs and carbonate mounds	Exposed diapiric island colonized by stromatolites and calcimicrobes, later drowned by SL rise and deposition of the deepwater Enorama Shale.	Lemon 2000
<b>Finders Ranges, South Australia</b>	Lower Cambrian; Hawker Group Carbonates	Platform Carbonates-Shoreface- Reef-Midslope	A range of lithologies including carbonate turbidites, debris flows, bioherms, sabkha, and tidal flats. Clastics include shoreface sands. Sediments show significant lateral facies change adjacent to diapir	Collie and Giles 2011
<b>Flinders Ranges, South Australia</b>	Cryogenian-Ediacaran; Burra and Umberatana, Groups	Storm-influenced shallow marine and shoreface, subaerially exposed dolomitic flat	Dominantly siliciclastics comprising large-scale T-R sequences; some carbonates; olistostromes and other units thinning/fining away from margin of Oladdie diapir	Dyson and Rowan 2004

<b>Flinders Ranges, South Australia</b>	Ediacaran (Marinoan); Oratunga Diapir, Umberatana Group	Generally Shallow Marine	Limestones, dolomites, shales and sandstones that thin against the diapir margin; some fluvio-glacial sands/diamictites; several unconformities	Lemon 1985
<b>Amadeus Basin , Northern Territory, Australia</b>	Neoproterozoic-Early Cambrian	Generally shallow marine	Various siltstones, sandstones, and carbonates within several individual minibasins; limited description of influence of halokinesis on sedimentology	Dyson and Marshall 2007
<b>La Popa Basin, Mexico</b>	Upper Cretaceous/lower Paleogene; Delgado Sandstone Member	Shelf-Shoreface-Foreshore	Delgado SS consists of a series of 5-20 m-thick coarsening-upward parasequences, generally with shelf mudstones at the bases and shoreface sands at the tops. Several other units, including carbonates and mudstones, are present in the minibasin and remain undescribed.	Aschoff and Giles 2005; also see Rowan et al 2003; Laudon 1984
<b>Persian Gulf, Iran</b>	Cretaceous-Tertiary	Shallow marine	Rudist shoals on diapir flanks, diapiric material in surrounding sediment; diapirs were likely emergent; substantial subsidence related to underlying withdrawal not described	Ala, 1974
<b>Willouran Ranges, South Australia</b>	Cryogenian- Ediacaran; Primarily Burra Group	Shallow water, peritidal shelf, with rare deeper, continental, and glacial episodes	Sandstones, siltstones, and carbonates. Diapir-derived conglomerate beds and laterally variable, rotated beds adjacent to diapir.	Hearon et al 2014
<b>Flinders Ranges, South Australia</b>	Ediacaran; Sandison Subgroup	Shelf to Shallow Marine	Sandstones and Shales- Tempestites lower in section, coarsening upward to tidally influenced quartzites. Unit thickness changes and conglomerates on Beltana diapir flanks	Dyson 1999, 2004
<b>Atlas Mountains, Morocco</b>	Jurassic: Multiple formations;	Slope-Shelf-Mixed Platform	Platform carbonates interfingering with hemipelagic and slope sediments, eventually shallowing upward to shallow marine and continental sediments; asymmetric minibasins flanking salt weld hundreds to thousands of meters in thickness; limited description of sedimentology	Saura et al 2014
<b>Pyrenees Mountains, Spain</b>	Cretaceous (Albian)	Shelf-slope-deepwater	Shelf/slope marls, limestones, carbonate debris at base, with upper siliciclastic unit containing turbidites separated by numerous unconformities	Ferrer et al., 2014 Arbues et al 2012
<b>Flinders Ranges, South Australia</b>	Cambrian; Hawker Group, Donkey Bore Syncline	Deepwater and slope	Carbonates, shales and sands deposited in several cycles; Abundant turbidites and gravity flow deposits within shales	Reilly, 2001
<b>Flinders Ranges, South Australia</b>	Ediacaran; Billy Springs Formation	Slope- Deepwater	Thick mudstone succession with abundant intrabasinal slumps and rare diamictites, with sandy turbidites more common up section	Counts and Amos 2014 (this study)
<b>Magellanes Foreland Basin, southern Chile, South America</b>	Late Cretaceous; Cerro Toro and Tres Pasos Formations	Continental Slope	Stacked, bioturbated, tabular turbidite sands within silty mudstones, deposited in an intraslope minibasin. Growth faults, mud-rich chaotic deposits, coarsening-upward packages common.	Shultz and Hubbard 2005

Previous Investigations of the Billy Springs Formation

Author	Year	Type of Study	Notes	Correlation
Campana et al.	1961	1:63,360 Map Sheet	First detailed geologic map of the area	Not specified
Forbes	1966	Mines Department Report	Initial, brief description of 5,200 metre-thick Wilpena Group sediments near Mt. Freeling; siltstones, sandstones, marbles, dolomite	Brachina and Wonoka Fmts.
Coats and Blissett	1971	SA Geologic Survey Bulletin	Divided Mt Freeling sediments into upper shaly member and lower silty member; termed sediments "Billy Springs Beds". Noted slump structures and lenticular boulder breccia	"below the Pound Quartzite"
Von der Borch and Grady	1982	Peer-reviewed Publication	Reconnaissance study; measured a similar section to OSCS; noted slumps, a thick laminated unit; and a breccia with a variety of exotic lithologies, attributed to mass movement	Bonney Sandstone
Jenkins et al.	1988	Abstract	First interpretation of breccia/boulder beds as glacial in origin	Upper Wonoka/Lower Pound
Dibona	1989	PhD Thesis	Measured section in Umberatana Syncline, noted 1200 metres of silts and sands, one diamictite bed	Uncertain
Dibona	1991	SA Geologic Survey Notes	Mapped Billy Springs in general near base of formation, noted synsedimentary slumped beds and diamictite; interpreted as glacial in origin	Uncertain
Reid	1992	Honours Thesis	Detailed mapping and measurement of sections in the Mt. Freeling area, noted Ediacaran-type fossils and sandy sediments equivalent to Bonney Sandstone and Rawnsley Quartzite; shallowing-up succession.	Pound Subgroup
Pell et al.	1993	Peer-reviewed Publication	Isotope stratigraphy study, incorporating Billy Springs carbonates from Mt. Freeling.	Mid-Billy Springs to Upper Wonoka
Jenkins	2011	Peer-reviewed Publication	Focuses on potential glacial origin of diamictite bed, emphasizing exotic nature of large clasts and deformed laminae, suggesting that they originate as dropstones	Wilpena Group/Pound Subgroup
Sheard	2012	Map Sheet Explanatory Notes	Divided Billy Springs into four members in the Mt. Freeling area; partially based on mapping of Reid (1992)	Lower two members correlate to Bonney Sandstone, upper members to Rawnsley Quartzite

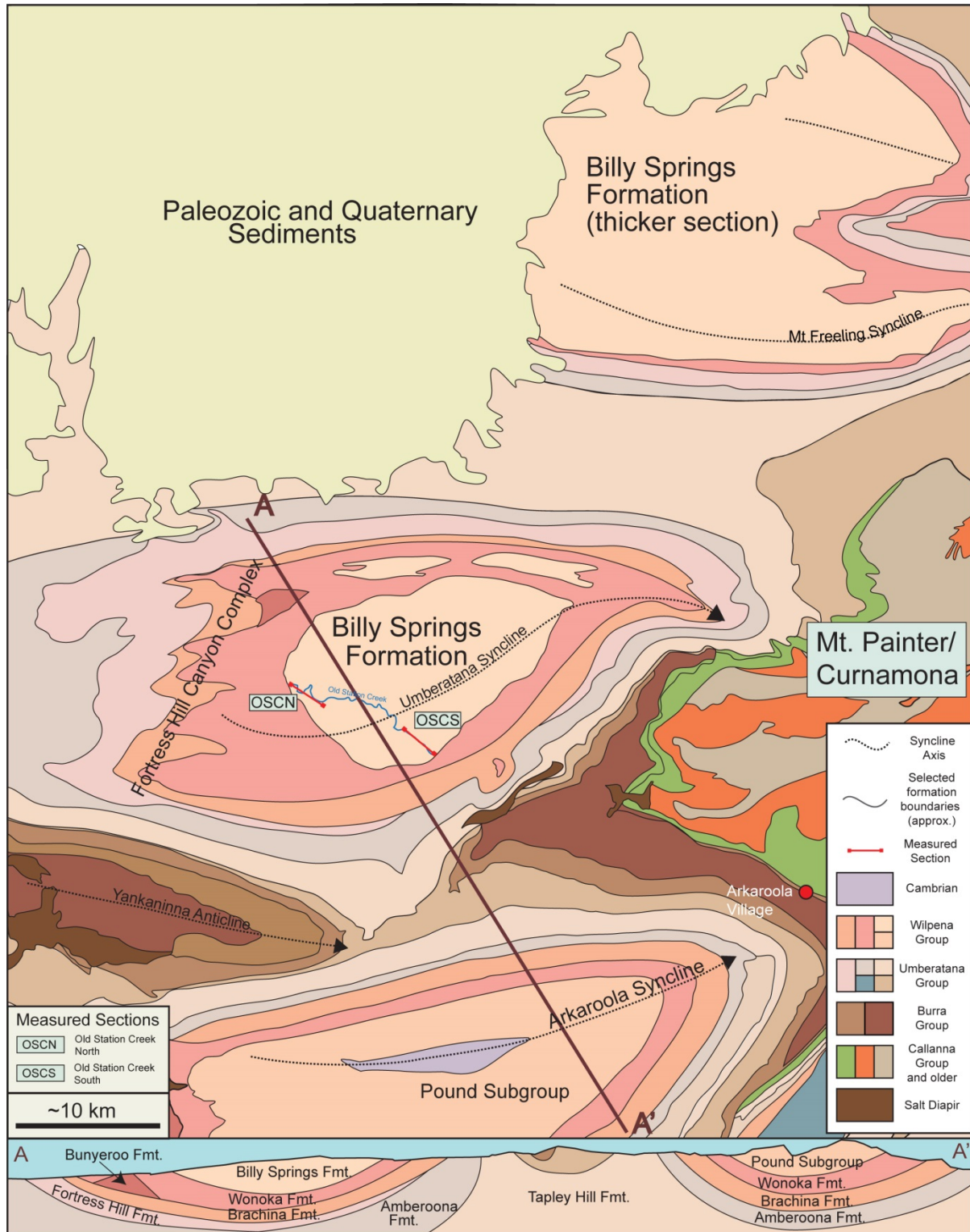


Figure 4: Geologic map of the field area, from the GSSA Copley and Maree 1:250,000 map sheets published in 1973 and 2012, respectively. Modified from Coats (1973).

*Preceding pages:*

*Table 1: Summary of salt-withdrawal minibasin studies in published literature, including only those where some component of sedimentology has been described. Studies are arranged by the dominant depositional environment in which the minibasin formed, though several examples encompass many different depositional settings.*

*Table 2: Comprehensive list and summary of previous investigations of the Billy Springs Formation that discuss sedimentology or stratigraphy.*

## **6.5: Field And Laboratory Methodology**

This study focuses on the lower unit of the Billy Springs Formation exposed in the Umberatana Syncline, on the Umberatana Station property in the northern Flinders Ranges. Two relatively continuous sections were measured for this study, named Old Station Creek North (OSCN) and Old Station Creek South (OSCS; locations shown in Fig. 4). These sections comprise over 1370 m and 316 m of vertical thickness, respectively. Both sections were measured from the base of the Billy Springs Formation, as determined from field observations and the 1 : 63,360 Umberatana geological map sheet (Campana et al., 1961). Exposures were relatively continuous, with beds dipping approximately 10 to 25° (magnitude) to the east in the section OSCN, and 50 to 65° to the north-west at the base of section OSCS, becoming shallower up section to 10 to 20° dip magnitude. In each section, lithologies were examined closely with regard to bed thickness, bed continuity, grain size and sedimentary structures, and samples were taken at selected representative intervals for further analysis.

Polished thin sections of selected samples were analysed for mineralogy using both traditional petrography and QEMSCAN (Quantitative Evaluation of Minerals by Scanning Electron Microscopy) methodology, performed by staff at the University of South Australia. The QEMSCAN method uses both backscattered electron (BSE) intensity and low-count energy dispersive X-ray spectra (EDX) to automatically identify the composition of a selected point against an internal mineral



database.

<b>Wonoka Fmt.</b>	Shale with sparse decimeter scale tabular beds of vfg sand and silt that increase in frequency upward.
<b>OSCS-A</b>	At base, first appearance of slumping/ folding/ soft-sediment deformation. Matrix similar to shales below, but with coarser discontinuous beds of highly deformed muddy silts/sands (slump "pods"). Slumps have both sharp boundaries with exterior matrix, and also grade laterally into shalier sediments. Larger clasts throughout, but locally concentrated, especially in upper beds. Clasts range from granule to boulder size, and do not occur outside of slumped sediment. Clasts are composed of a wide range of lithologies, including chert, dolomite, and limestone.
<b>OSCS-B</b>	Very few slumps; planar-bedded grey-green silts/silty mudstone. Not fissile as in unit A.
<b>OSCS-C</b>	Planar silts with discontinuous slump beds, similar to those seen below, but slumps are much rarer. Slump beds contain very few or no exotic clasts.
<b>OSCS-D</b>	Slump beds of similar lithology to those below, but more continuous. Uppermost appearance of slumping in section. Few or no clasts present.
<b>OSCS-E</b>	Thick, monotonous section of planar- laminated silty mudstone, laminated on a millimeter scale. Laminae vary in clay/silt content, causing them to weather differentially. In places, laminae are rhythmic and somewhat regularly spaced. No larger clasts or significantly coarser material seen.
<b>OSCS-F</b>	Top of unit not well-defined; base marked by first appearance of decimeter-scale tabular beds of very fine-grained sandstone with tepee/loading structures at bases and wavy and rippled tops. Sand beds rare upward through unit.
<b>OSCS-G</b>	Monotonous planar-laminated silts, similar to OSCS-E, but with more restricted exposure.
<b>OSCS-H</b>	Uppermost unit very fine- to lower fine-grained, clean, white, quartz arenite. Faint cross-stratification present in tabular, planar beds. Exposed as rubble.

*Table 3: Brief description of stratigraphic units, measured section OSCS. Corresponds to Units in Fig. 5A.*

*Table 4 (following page): Brief description of stratigraphic units, measured section OSCN. Corresponds to listed units on stratigraphic column in Fig. 5B*

<b>Wonoka Fmt.</b>	Greenish-grey fissile silty muds, interbedded with sparse lighter-coloured layers of carbonate-rich or coarser material
<b>OSCN-A</b>	Green and grey silty muds. All bedding in the form of slumping, complex folds and chaotic bedding. Slumps range from large, open, meter-scale folds to small, isoclinal complex structures. Laminae comprising folds are cm- to mm-scale apart, and weather differentially, indicating slight differences in composition. Large decimeter-scale clasts rare, compositionally similar to matrix.
<b>OSCN-B</b>	Lithology indistinguishable from below, but without any slump structures. Planar-laminated at cm-scale (0.5-10 cm).
<b>OSCN-C</b>	Similar to Unit A, but with slump folds generally on much smaller scale.
<b>OSCN-D</b>	Interbedded silty muds (matrix) and thin silt laminae. Upper 1.7m exposes asymmetric ripples and cm-scale sandy lenses. 10-cm thick "slump" bed near base of unit. Larger clasts rare.
<b>OSCN-E</b>	Blocky base with slumped top.
<b>OSCN-F1</b>	Similar lithology to lower Unit D. Grey silty matrix with vfg sand interlaminae, some thicker beds with internal convolute laminae. Ball and pillow structures present in thicker, sandier layers. Base sharp but slightly undulating.
<b>OSCN-F2</b>	Discontinuous slump unit- pinches out and grades laterally into planar beds
<b>OSCN-F3</b>	Planar-laminated/bedded unit similar to F1 below. Top contact deeply scoured by overlying Unit G. Bed thickness between laminae varies from mm to decimeter scale. Minor slump beds present within unit.
<b>OSCN-G</b>	Slumped beds, ranging from massive/ structureless to chaotic, to large, open folds. Contains numerous large intraformational clasts of similar or identical lithology as surrounding matrix. Series of folds with near-vertical axes near top.
<b>OSCN-H</b>	Planar laminated with prominent cm-scale sandy interbeds. Cm-scale ripples in thicker beds. Sandier beds contain ball and pillow structures and contorted internal bedding.
<b>OSCN-I</b>	Similar to Unit G- Slumped and folded beds in a range of styles. More-vertical beds near top weather "chalky" and may have increased carbonate content. Numerous large, discrete clasts within folds, of similar or identical lithology except for color.
<b>OSCN-J</b>	Planar bedding, more fissile and disturbed-looking than other planar beds.
<b>OSCN-K</b>	Chaotic/massive slump unit; no large-scale open folds or planar laminae visible. Larger clasts also present.
<b>OSCN-L</b>	Planar-bedded grey/green siltstone/mudstone. Laminae more regularly spaced and rhythmic than below. Near top, gently undulating beds & laminae resemble HCS, with truncation surfaces cutting underlying beds. Possible cross-strata near top could be incipient slumps. Definite small-scale slump structures at top, grading into the larger-scale folds of unit M.
<b>OSCN-M</b>	Very thick unit comprised of a range of slump morphologies and folds. Large clasts rare but present. Cleavage planes increasingly dominant, obscuring bedding. Unable to determine true vertical thickness- this unit is discontinuous, as evidenced by the presence of planar bedding in correlative outcrops exposed in downstream creek meander loops. See equivalent section adjacent.
<b>OSCN-N</b>	Generally planar laminae, grading into "shalier" type weathering/ bedding near top. Sandy lenses in lower part. No large clasts seen on outcrop. Thicker, coarser, tabular beds visible near top, resembling turbidites. Near centre of unit, a channel-shaped bed containing slumped and folded strata cuts across planar beds/laminae. Truncation of planar laminae clearly visible.
<b>OSCN-N</b>	Slumped and folded strata visible in main outcrop near base of unit. Thicker, coarser, tabular beds near top, resembling turbidites. Beds often have a clear fining-up structure at a decimeter-scale. Bedding is planar, tops of beds may be gently undulating but ripples are not usually present. Adjacent to the main outcrop of this unit, granule-cobble-boulder-sized clasts are abundant in the lower portion of the unit, where exposed. Laminae often warped/draped around clasts.

## 6.6: Observed Lithofacies: Description, Distribution and Interpretation

Stratigraphic sections are presented in Fig. 5, and brief descriptions of stratigraphic units are presented in Table 3 (OSCS) and Table 4 (OSCN). The Billy Springs Formation contains four distinct lithofacies that occur throughout the succession, in varying degrees of abundance: (i) planar-laminated silty mudstone; (ii) convolute-laminated silty mudstone; (iii) matrix-supported diamictite; and (iv) tabular-bedded sandstone. Two facies associations are described. Individual lithofacies are often contained in discrete units, separated by sharp contacts, but more gradational transitions also exist. The formation is dominated by silty mudstones, often containing millimetre-scale planar interlaminae of very fine sands and silts ('laminated' defined here as being stratification <1 cm in thickness). In both sections, sand-dominated beds are more abundant in stratigraphically higher intervals, with decimetre-scale, fine-grained sandstones interbedded with planar mudstones similar to those seen below (Fig. 5). Although measured sections are partially correlative, significant differences in lithofacies distribution exist between the two (Fig. 5). These are described in more detail below.

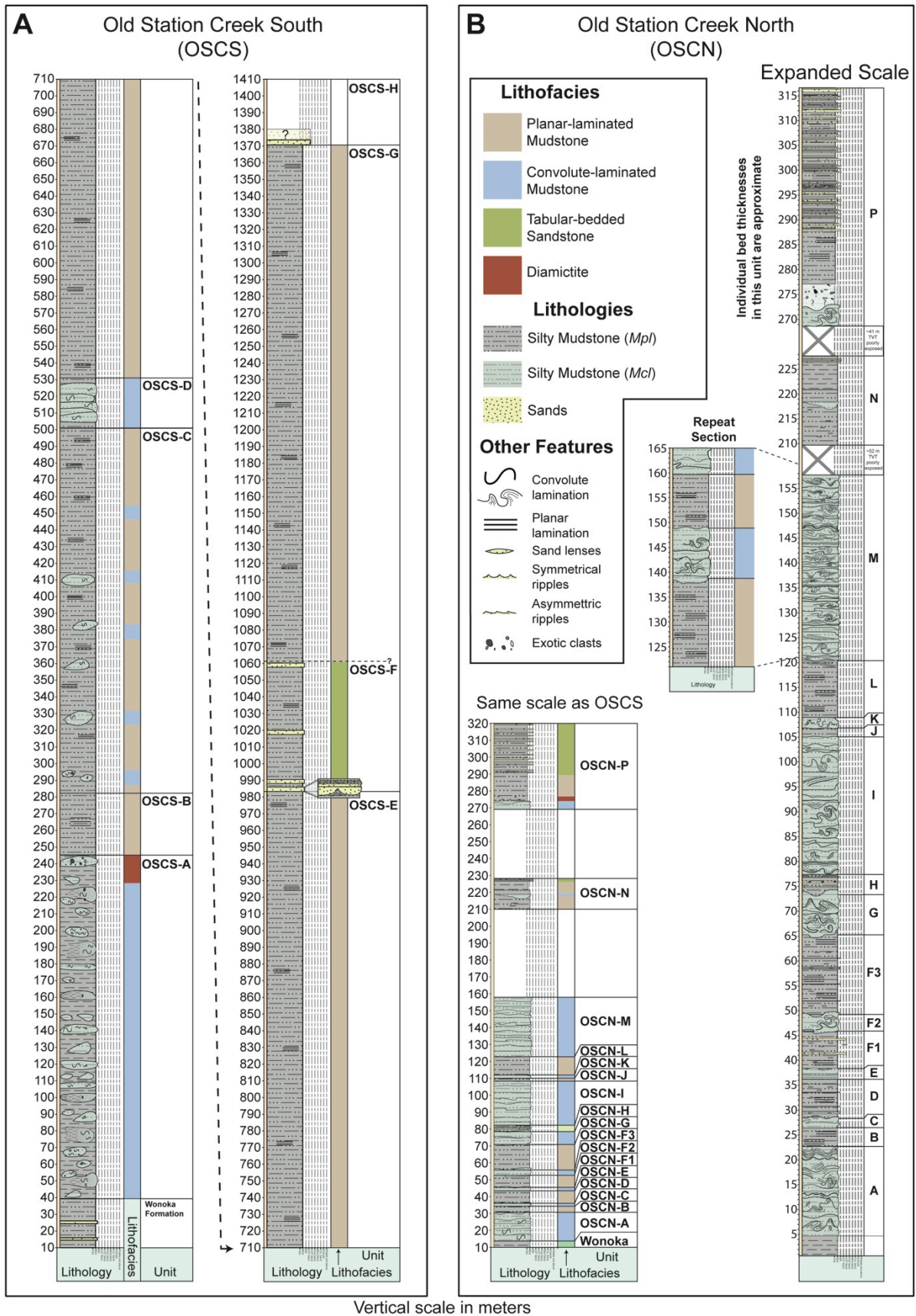


Figure 5: Stratigraphic sections measured in this study. A) OSCS, and B) OSCN. Both sections were measured in Old Station Creek (see locations in Fig. 4). Sections were measured from the base of the Billy Springs Formation, and are thus potentially equivalent. Section OSCN is also shown at an expanded scale, and includes the shorter, repeat section (approximately 250 distant) seen in creek meanders that illustrates the discontinuous nature of convolute- and planar-laminated units in this area.

## 6.6.1: Planar-laminated silty mudstone (Lithofacies Mpl)

### 6.6.1.1: Description

This lithofacies is dominated by silt-sized and clay-sized particles. Individual laminae are a product of textural and compositional differences (Figs 6A and 7A),

although millimetre-scale laminae are not always present and are commonly not visible in thin

section (Fig. 6B). Based on thin-

section observations, overall silt

content varies considerably. The

QEMSCAN mineralogical

analysis of a single finely

laminated interval (Fig. 7) reveals

that these sediments are

composed primarily of quartz,

clay minerals and micas. Layers

that are lighter coloured in hand

sample have a higher percentage

of coarse silt-sized, quartz grains,

while finer-grained, darker laminae are dominated by clays and micas. Neither type

of laminae is consistently thinner or thicker than the other. Detrital carbonate and

feldspar grains are interspersed throughout the sample, and are slightly more

common in coarser laminae, because most of them are closer in size to the silt-sized

grains that make up coarser intervals. Pyrite and euhedral Titanium-bearing

minerals, probably rutile, are also present throughout, and macroporosity is virtually

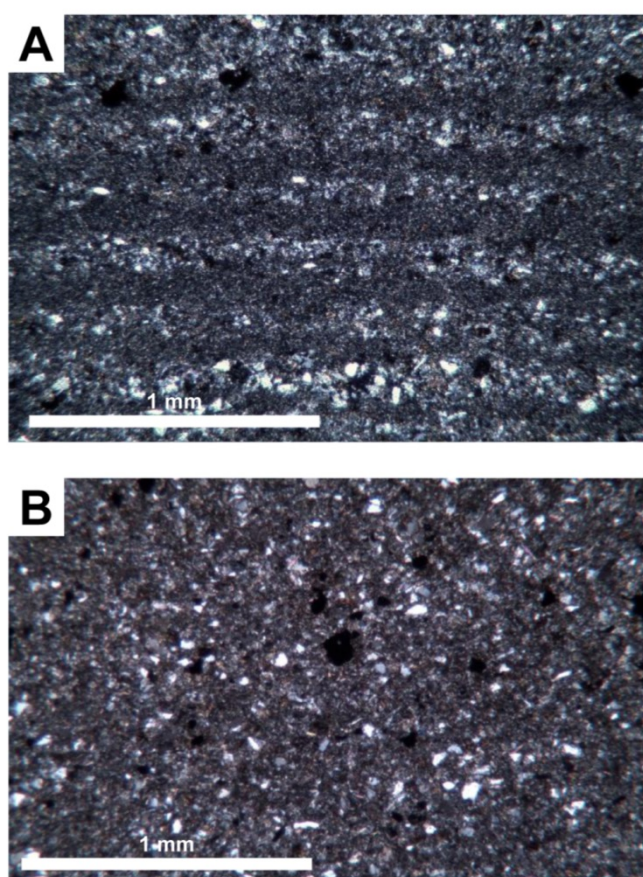
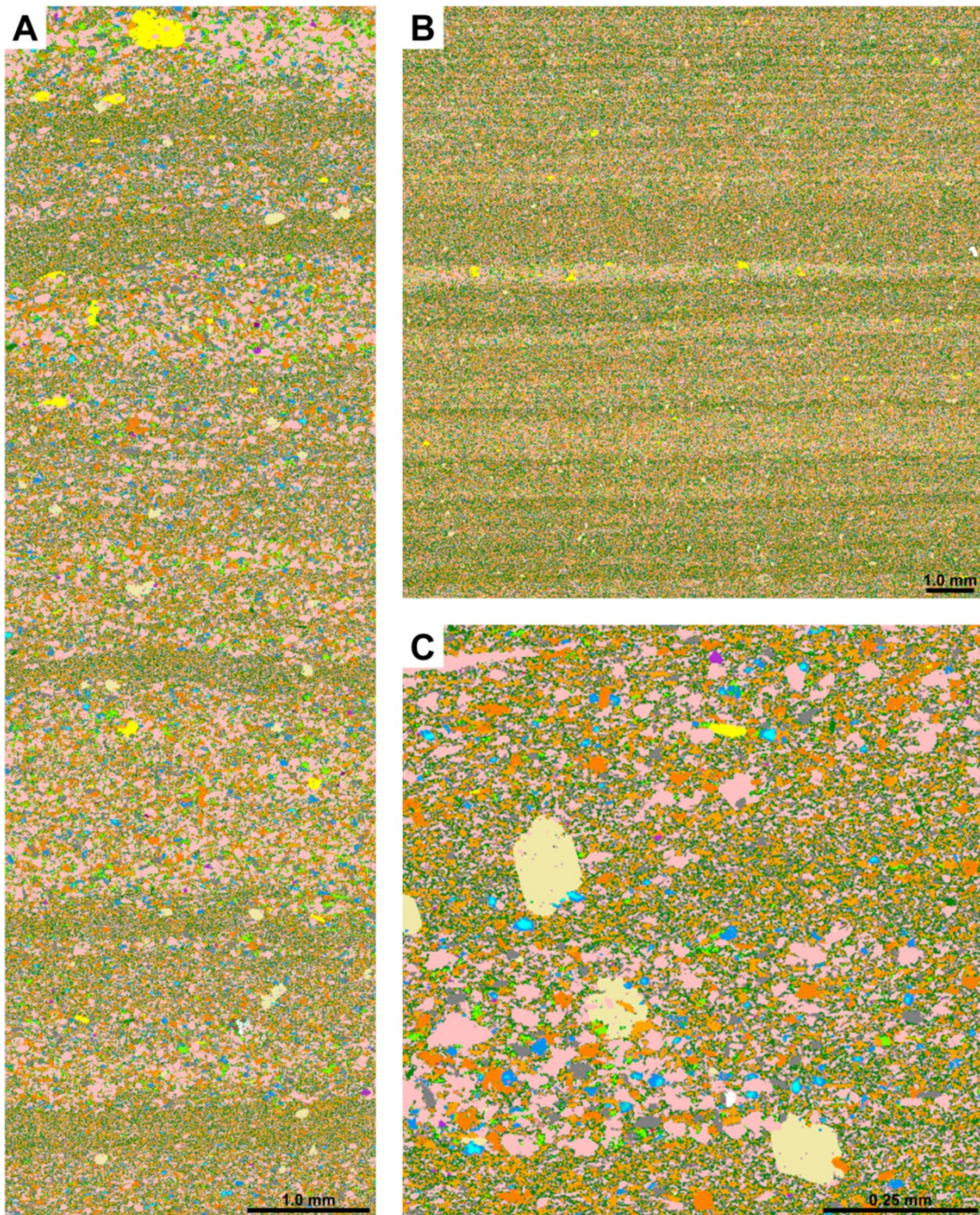


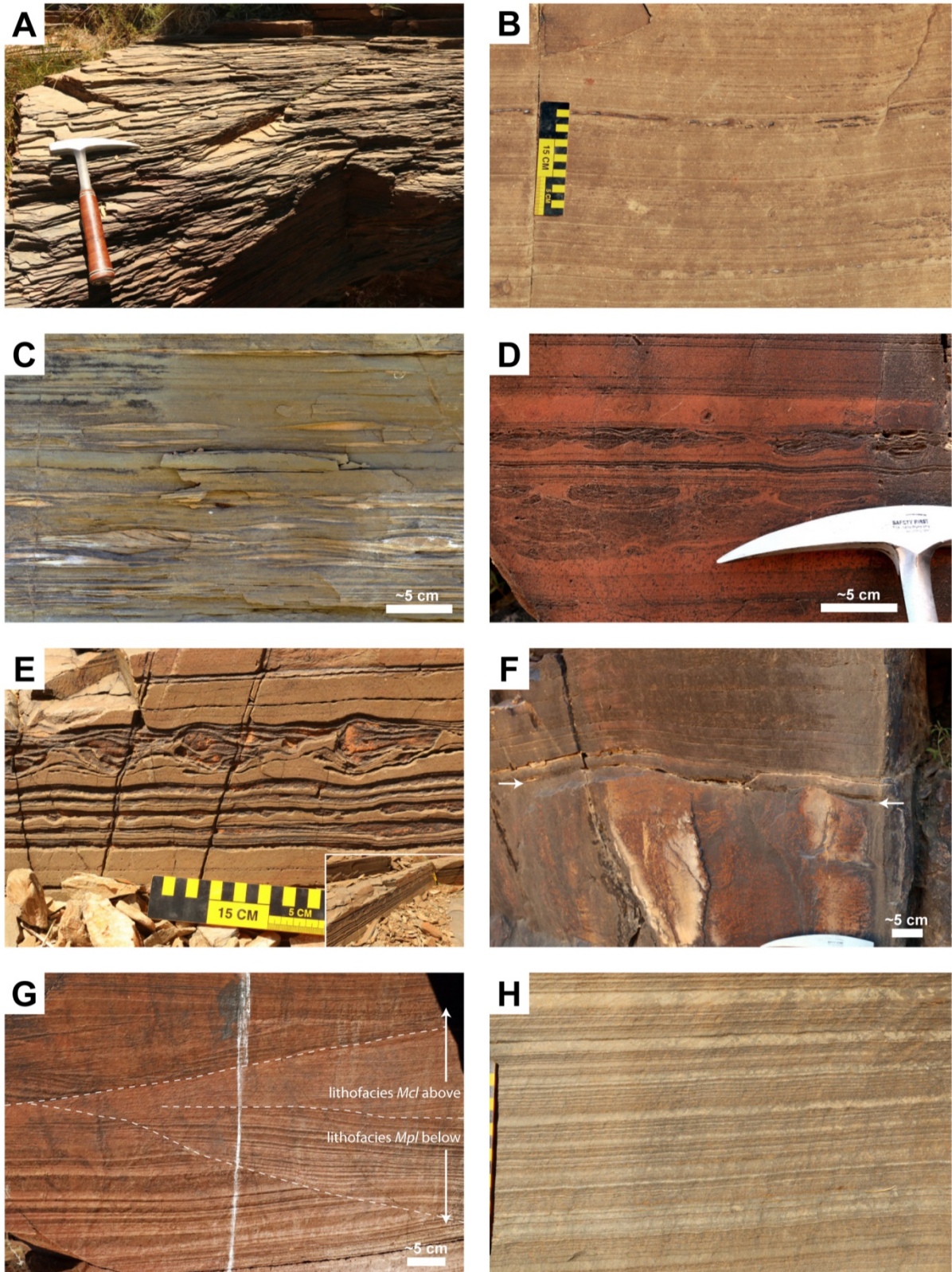
Figure 6: Planar-laminated mudstone in thin-section. A) In more rhythmic intervals, individual laminae have a stronger compositional difference in the amount of quartz silts, which can be seen in thin section. B) Typical matrix of planar-laminated silty mudstones, wherein individual laminae are very faint with respect to sediment composition.

non-existent.



Laminae are generally horizontal, and range from less than 1 mm apart (Fig. 8A and B) to several centimetres between visible laminae (Fig. 8C). Spacing of laminae is generally irregular, although apparent rhythmicity on a centimetre-scale is present in places throughout unit OSCS-E. Within these silty mudstones are some less-common sandy laminae that display a variety of sedimentary structures. These thin sands are often in the form of very fine-grained lenses or asymmetrical starved ripples (Fig. 8C). Flame structures (Fig. 8D) and 'ball and pillow' structures (Fig. 8E) are also present, some having current indicators (for example, oriented, asymmetrical flames, clay drapes, etc.) indicating a west or north-westerly flow direction. These sandier layers never attain thicknesses greater than 2 cm in this lithofacies and are uncommon throughout the Billy Springs Formation. Transitions to other lithofacies are either sharp (Fig. 8F), or more gradual, with internal erosive surfaces and microfaulting occurring at some transitions to the convolute-laminated lithofacies (Fig. 8G). In some locations, planar laminae appear to have a rhythmic or cyclical character of thickness variation (Fig. 8H). In these areas, laminae thickness appears to be regular or rhythmic, so a small section was analysed for the presence of cyclicity. The thicknesses of 524 laminae in a sample were measured and categorized as to whether they were light or dark in colour. Fourier analysis of this set of apparently rhythmic laminae reveals the presence of at least two periods of cyclicity in laminae thickness distribution (Fig. 9). Cycles occur every 64 and 32 laminae primarily, with a smaller, less apparent, cycle occurring approximately every 21 laminae. Although the analysis shows the presence and periodicity of a cycle, it does not specify other information about cycle properties or constituent laminae.

*Figure 7 (Previous page): QEMSCAN images of planar-laminated lithofacies, Unit OSCS-G. A) Wide-field view of typical planar-laminated interval, showing mineralogical differences in laminae related to alternation between quartz and clay percentage. B) Same sample as A), showing preservation of micron-scale laminae. C) Quartz-dominated layer, showing sediment composition including euhedral Rutile (?) crystals.*



**Figure 8: Planar-laminated mudstone lithofacies: macroscopic character and sedimentary structures.** A) Representative nature of planar laminae in OSCS-E, showing planar laminae. B) Typical nature of planar-laminated lithofacies in most outcrops, lacking significant sand laminae or readily identifiable rhythmicity, unit OSCN-L. C) Very fine-grained sand laminae, lenses, and starved ripples in silty mudstone matrix, OSCN-D. D) Ball-and-pillow and flame structures, unit OSCN-B. Darker laminae forming reentrants are composed of slightly higher silt content than surrounding well-indurated mudstones. E) Sandy laminae and clay-draped ball-and-pillow structures, OSCN-H, showing generally northwestern flow direction. Inset: continuous nature of same cm-scale beds/laminae. F) Sharp boundary between OSCN units A and B. Planar laminae can be seen to drape over undulatory contact (contact noted by arrows). G) Synsedimentary microfaulting and scour, at the transition between units OSCN-L and OSCN-M. Beds gradually become increasingly contorted upward. Minor scours/faulting in white dashed line. H) Mid-unit OSCS-E, showing rhythmic nature of planar laminae in certain intervals.



### 6.6.1.2: *Distribution*

Silty mudstones with planar laminae form a significant lithofacies in both the southern and northern sections (Fig. 5). Above the uppermost slumped unit in section OSCS (at ca 530 m), Unit OSCS-E is characterized by a thick, continuous section of planar-laminated silty mudstones. In this unit, no slumping, large clasts, or sedimentary structures are present for approximately 450 m of vertical section (ca 530 to 980 m). Although exposures are relatively continuous, neither sand-dominated laminae nor thicker sand beds were seen within this interval. In the north, units dominated by planar-laminated mudstones were common, interbedded with convolute-laminated mudstones.

### 6.6.1.3: *Interpretation and controls on planar laminae*

Small grain size, the consistent fine-grained nature of planar-laminated mudstones, and the lack of high-energy sedimentary structures suggests deposition in a low-energy environment with few significant perturbations. Many of the planar-laminated silty mudstones described here most closely resemble muddy contourites or pelagites (e.g. Pickering et al., 1989; Shanmugam, 2008; Rebesco et al., 2014); sediments deposited below storm wave base in deeper marine environments. Such deposits can occur on the continental shelf, slope and abyssal plain. However, the proximity, both spatial and stratigraphic, to known shallow-water deposits (for example, shoreface sands in the Bonney Sandstone tens of kilometres to the south) makes it unlikely that sea-levels in the Adelaide Rift Complex reached abyssal depths; previous reconstructions suggest that sediments were deposited on a platform between two landmasses (Preiss, 1990). It is unlikely that water depths reached more than several hundred metres at maximum. Planar-laminated

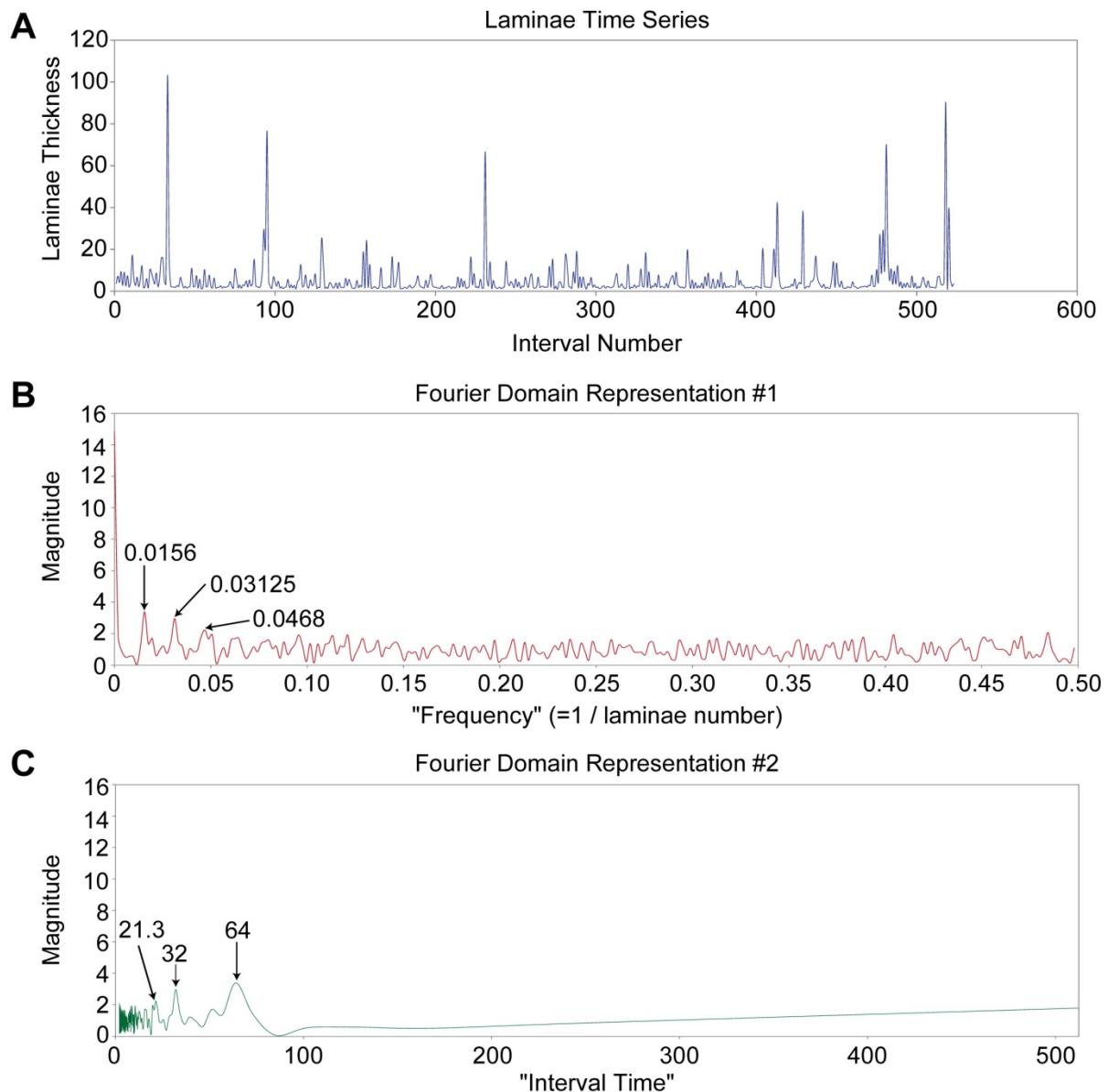


Figure 9: Rhythmite histogram and analysis. A) Thickness of each laminae within a preselected interval similar to that seen in Fig. 8H. B) Fourier Analysis plot, showing magnitude of Fourier transform vs. frequency, assuming one time unit per laminae. C) Same data as in B, with frequency converted to laminae number.

mudstones are thus interpreted to be the product of background sedimentation below storm wave base but close enough to source areas to receive substantial amounts of silt and occasional sands. Intermittent, centimetre-thick beds of very fine-grained sand or silt with current indicators (for example, Fig. 8C to E), as well as the overall abundance of silty laminae, suggest that bottom currents were weak, but were fairly common occurrences, possibly related to storm activity. The lack of infaunal organisms in the Ediacaran accounts for the preservation of micron-scale laminae; analogous deposits from the Phanerozoic commonly include some degree

of bioturbation.

The periodicities of 32 and 64 laminae from the analysed example represent a count of both light (coarser-grained) and dark (finer-grained) layers. In similar analyses on other rhythmically laminated sediments, laminae have been interpreted as comprising a light/dark pair (e.g. Williams, 1988). Thus, a cycle period of 32 laminae in the Billy Springs Formation corresponds to 16 pairs of light and dark layers. In the Elatina Formation elsewhere in the Adelaide Rift Complex, rhythmic sediments are composed of bundles with 11 to 14 laminae each (Williams, 1988). The Reynella Siltstone has cyclic laminae bundles composed of 14 to 15 laminae, each with a lighter sand and darker clay component (Williams, 1990), and the Chambers Bluff Tillite contains bundles with 15 to 25 light–dark pairs (Williams, 1988). The individual light–dark laminae pairs in these sediments are interpreted as being the product of diurnal or semi-diurnal tidal deposition, with bundles ('lamina-cycles') representing lunar fortnightly cycles. The Billy Springs laminae may be interpreted similarly – a cycle of 16 light–dark pairs is the maximum number reported from the Elatina and is not dissimilar to cyclicity reported in these other Neoproterozoic sediments. Laminae in the Billy Springs could therefore be interpreted as diurnal and the cyclicity resulting from neap–spring tidal processes. The larger, stronger cycle of 64 laminae (32 light–dark pairs) may then represent a monthly cycle, as are sometimes seen in both modern environments and in ancient may be semi-diurnal, with four laminae deposited per day, leading to 32 light–dark pairs per fortnight, with the secondary cycle representing only the strongest of asymmetrical semidiurnal tides. The smallest cycle of 21 laminae (ca 10 light–dark pairs) is not as strong, and does not tie readily to known processes. Given that the data analysed contain a fair amount of noise, and some error exists in measuring

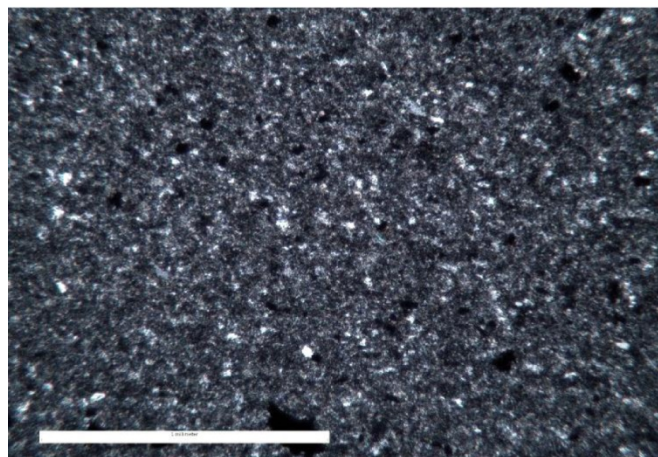
sub-millimetre-scale laminae, such conclusions should be taken as speculative, underscoring the need for further research. Other time periods for cycles are possible, but would lead to unreasonably long deposition times for the entire succession.

Similar laminated clastic deposits have been interpreted in the past as the product of seasonal meltwater cycles (Cowan et al., 1999; Eyles and Januszczak, 2004, and references therein), tidal deposits (Cowan et al., 1998; Mazumder and Arima, 2013) or climate-related storm activity (Shanmugam, 1980). Millimetre-scale, fine alternations in grain size similar to those seen here have also been interpreted as the distal ends of muddy turbidite deposits (Stow and Piper, 1984). Some laminae and thin sands have probably been reworked subsequently by weak bottom currents, resulting in the range of unidirectional current features seen on occasion.

#### *6.6.2: Convolute-laminated silty mudstone (Lithofacies Mcl)*

##### *6.6.2.1: Description*

Lithologically, convolute-laminated silty mudstones are almost identical to planar-laminated silty mudstones. In thin section, both lithofacies show a clay-dominated matrix with abundant silt-sized quartz grains (Fig. 10); very fine to fine-grained sands are also present but uncommon. Like the planar-laminated mudstones, laminae are visible due to differences in silt or



*Figure 10: Convolute-laminated lithofacies in thin-section. This lithofacies is often indistinguishable from planar-laminated mudstone lithofacies petrographically.*

quartz content between individual layers, although sub-centimetre-scale laminae do not exist in all beds. Larger isolated clasts (cobble to boulder-sized) are rare, but present, within some convolute-laminated mudstones, especially in the northern section. These are distinguished from more concentrated intervals of larger clasts, which form a different lithofacies and are discussed below.

To compare lithofacies *Mcl* with lithofacies *Pcl*, X-ray diffraction analysis was conducted on two samples from each lithofacies (Fig. 11). Results show that both share a very similar assemblage of detrital grains. Relative abundances can be deduced very generally from peak heights. The primary constituent of both lithofacies is quartz, followed by plagioclase feldspar, carbonates (dolomite and calcite) Chlorite (Chamosite) and Muscovite (including Phengite). Although the exact mineralogical composition and abundance varied between samples, overall lithologies were consistent across the four units analysed.

Despite these similarities, the nature of bedding and laminae varies substantially between the two lithofacies. Convolute-laminated mudstones display soft-sediment deformation at a range of scales, from centimetre-scale, tight isoclinal folds (Fig. 12A and B), to broad, gently curving arcs several metres across (Fig. 12C and D). This lithofacies is generally contained within discrete, metre-scale beds, especially in the northern section, but may pinch out or, in the southern section, grade laterally into planar-laminated mudstone lithofacies (Fig. 12E and F). Within convolute-laminated units, internal scour or truncation surfaces are sometimes present, indicating that individual units may be composed of a series of multiple erosive, slump-generating events (Fig. 12G). Individual beds cannot be readily distinguished within this lithofacies, and laminae within folds are relatively continuous. Minor sedimentary structures include radial fluid-escape structures (Fig.

12H), which are likely to be related to the highly fluid sediment associated with soft-sediment deformation.

Convoluted-laminated beds in the lower part of section OSCS take the form of discontinuous, metre-scale 'pods' of silty sediment that weather in relief in comparison to surrounding shales (similar to Fig. 12F). Internally, beds can be seen to contain laminae with a range of deformation styles and scales. In areas with good exposure, convoluted beds can be seen to grade laterally into finer-grained, planar-bedded shale units. Elsewhere in OSCS, slumps are more continuous.

#### 6.6.2.2: *Distribution*

The first appearance of convoluted-laminated sediments is taken here to be the base of the Billy Springs Formation, because lithologies below this point agree with published descriptions of the Wonoka Formation, and the first appearance of significant slumping marks a distinct lithofacies change from units below. Convoluted-laminated facies (*Mcl*) are interbedded with planar-laminated lithofacies (*Mpl*) for the lower ca 530 m of section OSCS, becoming more continuous towards the top of this interval. For several hundred metres above this distinct marker unit (at ca 240 m), discrete convoluted beds are sparser, until about 500 m above the base of the formation where the succession of slumped beds terminates with a relatively continuous unit.

The northern measured section also shows a distinct lithofacies change with the underlying Wonoka Formation, at a point which coincides with the formation boundary as previously mapped on the 1 : 63 360 map sheet. The uppermost Wonoka Formation in this area is also grey, clay-rich, silty shale, similar to that seen in the southern section. Here, (30°11030.24"S, 139°101.30"E), the formation

boundary is marked by a sharp-based contact with a thick (18 m) unit composed entirely of convolute bedded-silty mudstones. Lithofacies *Mcl* occurs throughout most of the rest of the northern section, alternating with lithofacies *Mpl*.

#### *6.6.2.3: Interpretation*

The convolute-laminated beds in this lithofacies are interpreted to be the depositional products of submarine slumping, a process distinct from both turbidity currents and debris flows (Stow and Mayall, 2000; Strachan, 2008). Unlike these other mass flow processes, slumping results in a cohesive deposit that maintains internal structure while deforming it, in contrast to other mass flow deposits in which traces of original stratification are destroyed by shearing, mixing and dilution (Strachan, 2008). Thus, slumps and their products typically represent an earlier or less mature stage in mass movements (Stow, 1985). The variety of soft-sediment fold morphologies seen in these beds may be related to the transport distance of each slump bed; laminae would become progressively deformed with further transport. The presence of larger, isolated clasts within this lithofacies is discussed below.

#### *6.6.3: Lithofacies association 1: Planar-laminated and convolute-laminated mudstones*

##### *6.6.3.1: Occurrence*

close proximity throughout both sections. In OSCN, this lithofacies association occurs in the northern section as alternating, discrete beds that are composed entirely of one lithofacies or the other (OSCN, 0 to 158 m from the base of the section), each several metres thick. Boundaries are generally sharp, but in at least one instance the degree of slumping decreases upward, eventually

transitioning into planar laminae (parts of this transition can be seen in Fig. 8G). In the southern section, convolute-laminated beds form both continuous and discontinuous beds within larger packages of planar-laminated mudstone, with discontinuous beds laterally adjacent to lithofacies *Mpl*. In section OSCN, unit F2, a convolute-laminated unit, gradually becomes thinner and appears to pinch out to the south-east over the course of several tens of metres of lateral exposure. Elsewhere along the same section, creek meander bends allow the same stratigraphic interval to be viewed several hundred metres apart; in these sections, the same sequence of slump and planar units does not repeat (for example, Fig. 5). This suggests that these units are not laterally continuous throughout the area, and that the specific arrangement and thicknesses of units would vary in other exposures.

Planar-laminated and convolute-laminated lithofacies commonly occur in close proximity throughout both sections. In OSCN, this lithofacies association occurs in the northern section as alternating, discrete beds that are composed entirely of one lithofacies or the other (OSCN 0-158 metres from the base of the section), each several metres thick. Boundaries are generally sharp, but in at least one instance the degree of slumping decreases upward, eventually transitioning into planar laminae (parts of this transition can be seen in Fig. 8G). In the southern section, convolute-laminated beds form both continuous and discontinuous beds within larger packages of planar-laminated mudstone, with discontinuous beds laterally adjacent to lithofacies *Mpl*. In section OSCN, unit F2, a convolute-laminated unit, gradually becomes thinner and appears to pinch out to the southeast over the course of several tens of metres of lateral exposure. Elsewhere along the same section, creek meander bends allow the same stratigraphic interval to be viewed several hundred metres apart; in these sections, the same sequence of



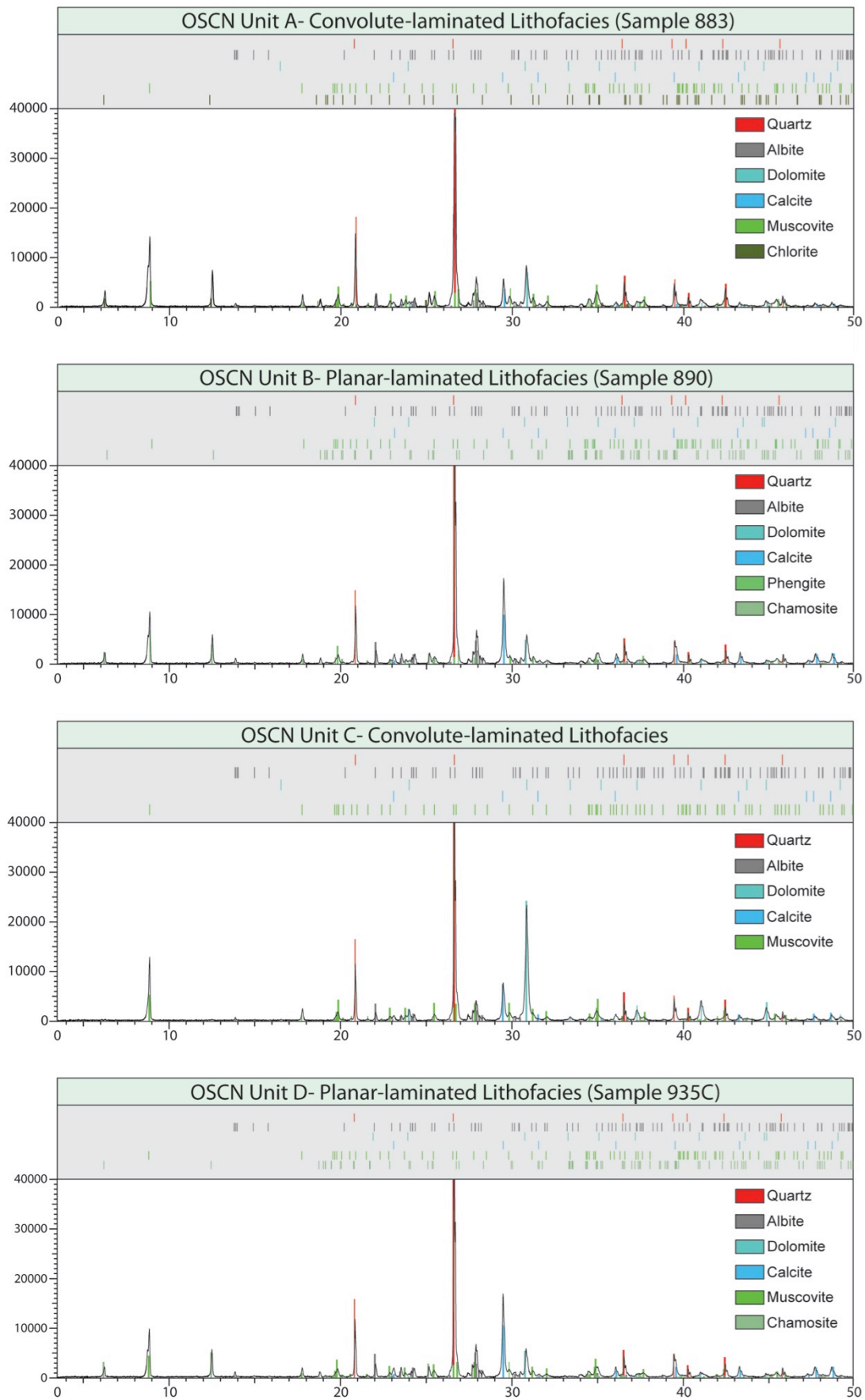
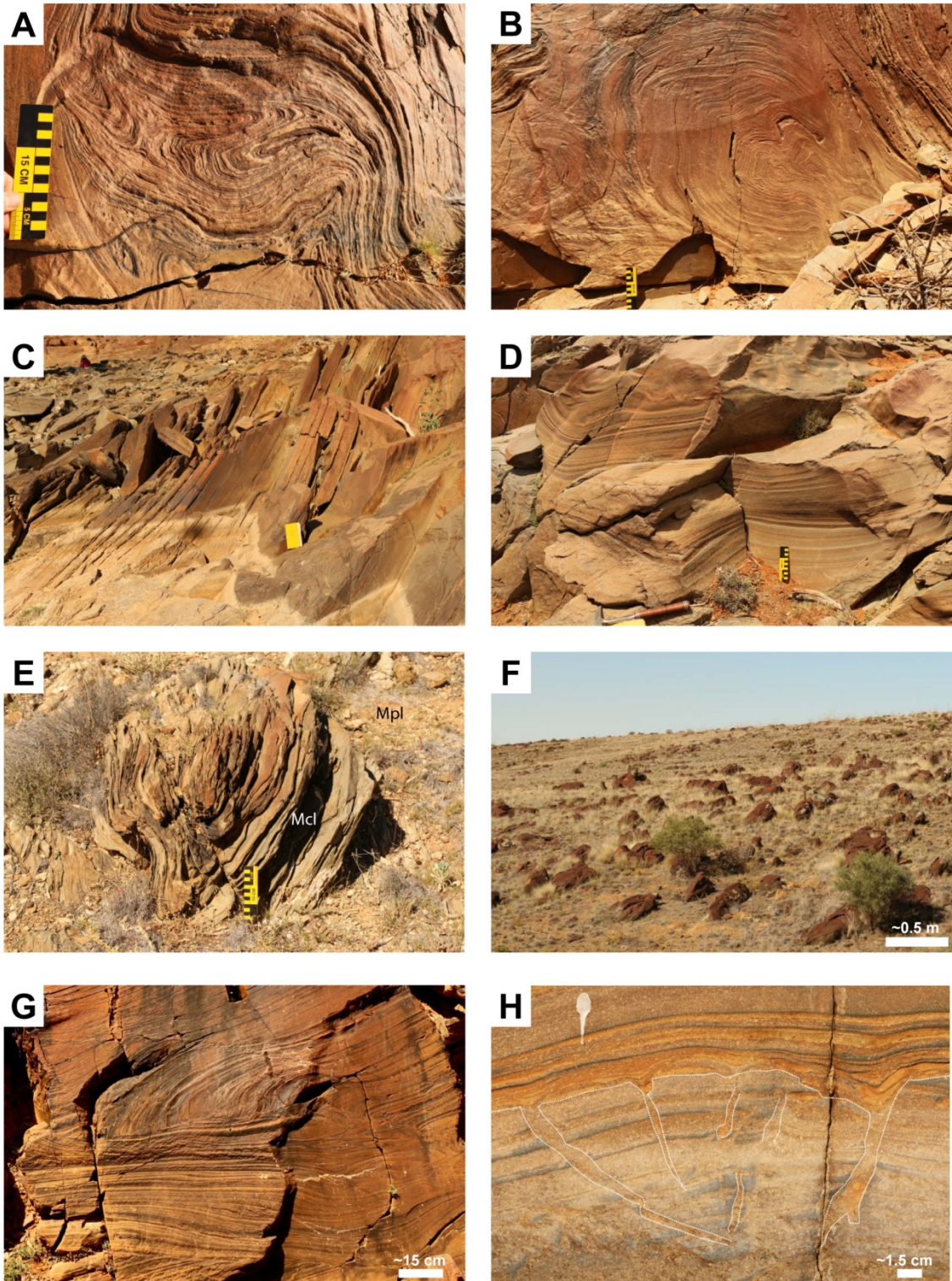


Figure 11: X-Ray diffraction analysis of silty mudstones from planar- and convolute-laminated lithofacies. Colored bars in grey-shaded stick chart denote known peaks for each mineral, and correspond to highlighted peaks in sample. Listed order of mineralogy does not imply differences in quantitative abundance.

slump and planar units does not repeat (e.g. Fig. 5). This suggests that these units are not laterally continuous throughout the area, and that the specific arrangement and thicknesses of units would vary in other exposures.



*Figure 12 (preceding page): Convolute laminated silty mudstone lithofacies: outcrop photos. A, B) Decimetre- to metre-scale beds containing highly convolute laminae, unit OSCN-I. C, D) Broad, irregular folds in units OSCN-G and OSCN-I, respectively. Such folds occur in conjunction with smaller scale folds as seen in (A) and (B). In Fig. 7C, field notebook is 15 cm high. E, F) Discontinuous nature of convolute-laminated lithofacies in OSCS. E), showing individual slump body within overall planar-laminated mudstone, and F), showing slump bodies weathering in relief along strike to OSCN-A. G) Distinct reactivation or scour surface with downlapping laminae, near base of unit OSCN-M. H) Radial fluid escape structure in OSCN-C. Note sharp boundaries, distinct surface, and infilling of overlying laminae into subvertical pipes.*

### 6.6.3.2: Interpretation

The compositional similarity between planar-laminated and convolute-laminated lithofacies suggests that the convolute-laminated deposits were initially deposited as planar-laminated muds, and then deformed and re-transported by slumping. Although the distance over which slumps can travel before flow transformation into turbidity currents is dependent on a number of factors (gradient, sediment composition, etc.), the lack of other, more mature types of mass flow deposits within this facies association also suggests that this lithofacies is relatively close to its origin.

In section OSCS, discontinuous slump beds several metres across can be seen laterally adjacent to planar-laminated mudstones (Fig. 12E and F). This is also indicative of an intrabasinal, proximal origin for these features; slumping in these areas was taking place on a relatively small scale. This exact arrangement of slump bodies at this scale has not been reported previously, although mass-transport deposits, including slumps and debris flows, are commonly part of minibasin fill (e.g. Winker, 1996; Beaubouef et al., 2003; Beaubouef and Friedmann, 2000; Olson and Damuth 2010). Jackson (2012), for instance, records a large number of discontinuous slide blocks (which may be slump bodies similar to those described here) within a single minibasin, most at a scale of tens of metres to ca 300 m across. The abundance of planar-laminated lithofacies (with no slump deposits for hundreds

of metres) in the upper two-thirds of the measured section also indicates a relatively stable environment for parts of the Billy Springs interval studied here. The active movement of nearby diapirs and associated subsidence may provide a trigger for slump movement and generation of the convolute-laminated lithofacies. Slope failure and mass transport of sediments are often associated with minibasins, and have been attributed to slope instability resulting from the movement of nearby salt bodies (Giles and Lawton, 2002; Jackson, 2012). Given the common occurrence of slumping and internal lithological consistency of sediments in the sections described here, this intrabasinal triggering is the preferred interpretation for the Billy Springs slump deposits. However, Olson and Damuth (2010) relate mass-transport complexes to external climate cycles, and Aschoff and Giles (2005) interpret some minibasin conglomerates as tsunami deposits; thus, external factors are also known to influence intrabasinal sediment transport.

#### *6.6.4: Matrix-supported diamictite (Lithofacies Dms)*

##### *6.6.4.1: Description*

Intervals where large clasts are more concentrated (Fig. 13A) are considered diamictites, because the term does not carry a genetic implication, and form lithofacies *Dms*. Even in these intervals (which lack sharp boundaries), clast abundance is generally sparse. Unlike larger clasts found isolated within convolute-laminated mudstones (Fig. 13B and C), lithofacies *Dms* is characterized by an abundance of clasts within a small stratigraphic interval. Large isolated clasts elsewhere in the measured sections are not considered a part of this lithofacies, because they do not occur in dense concentrations.

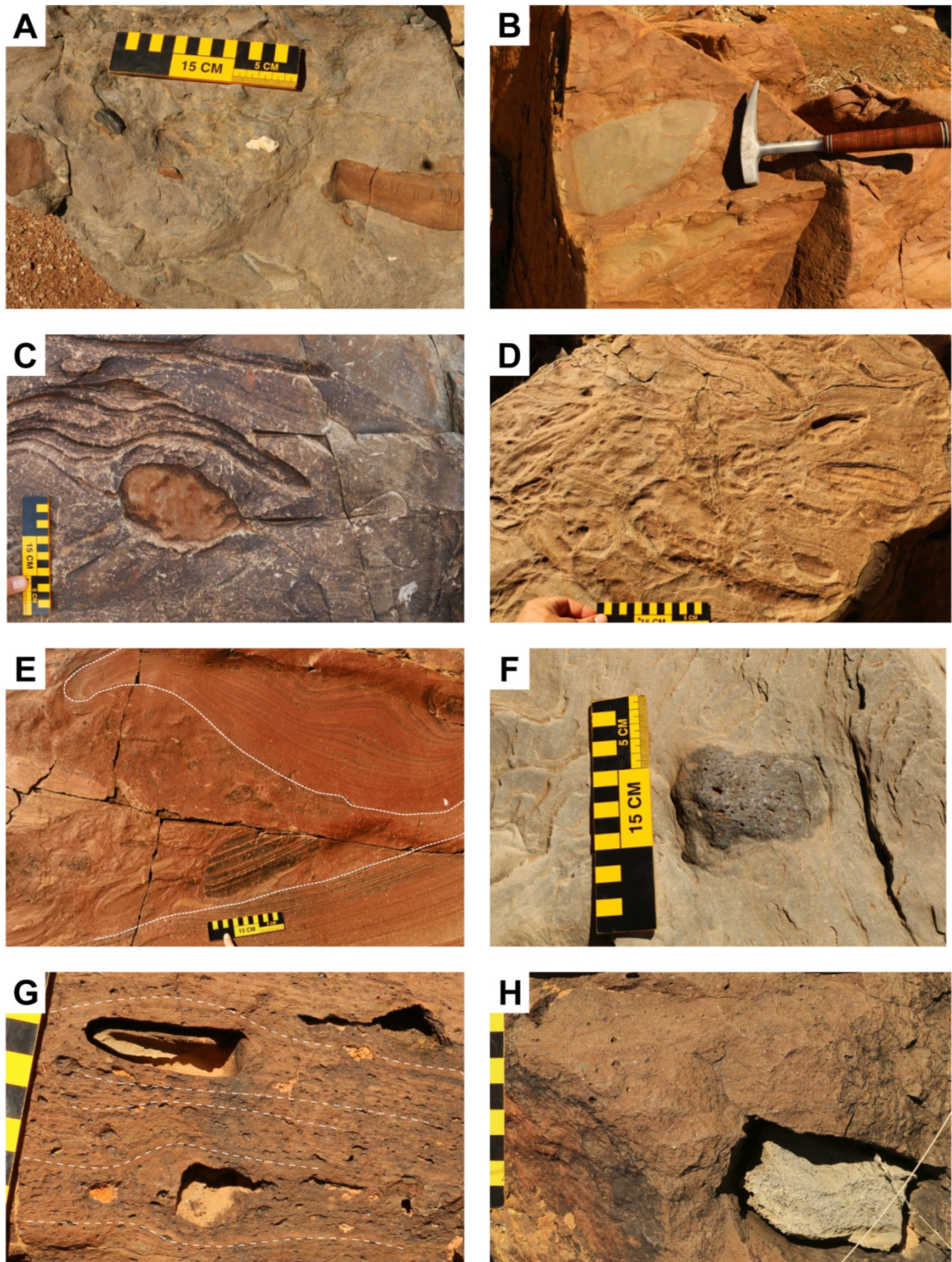


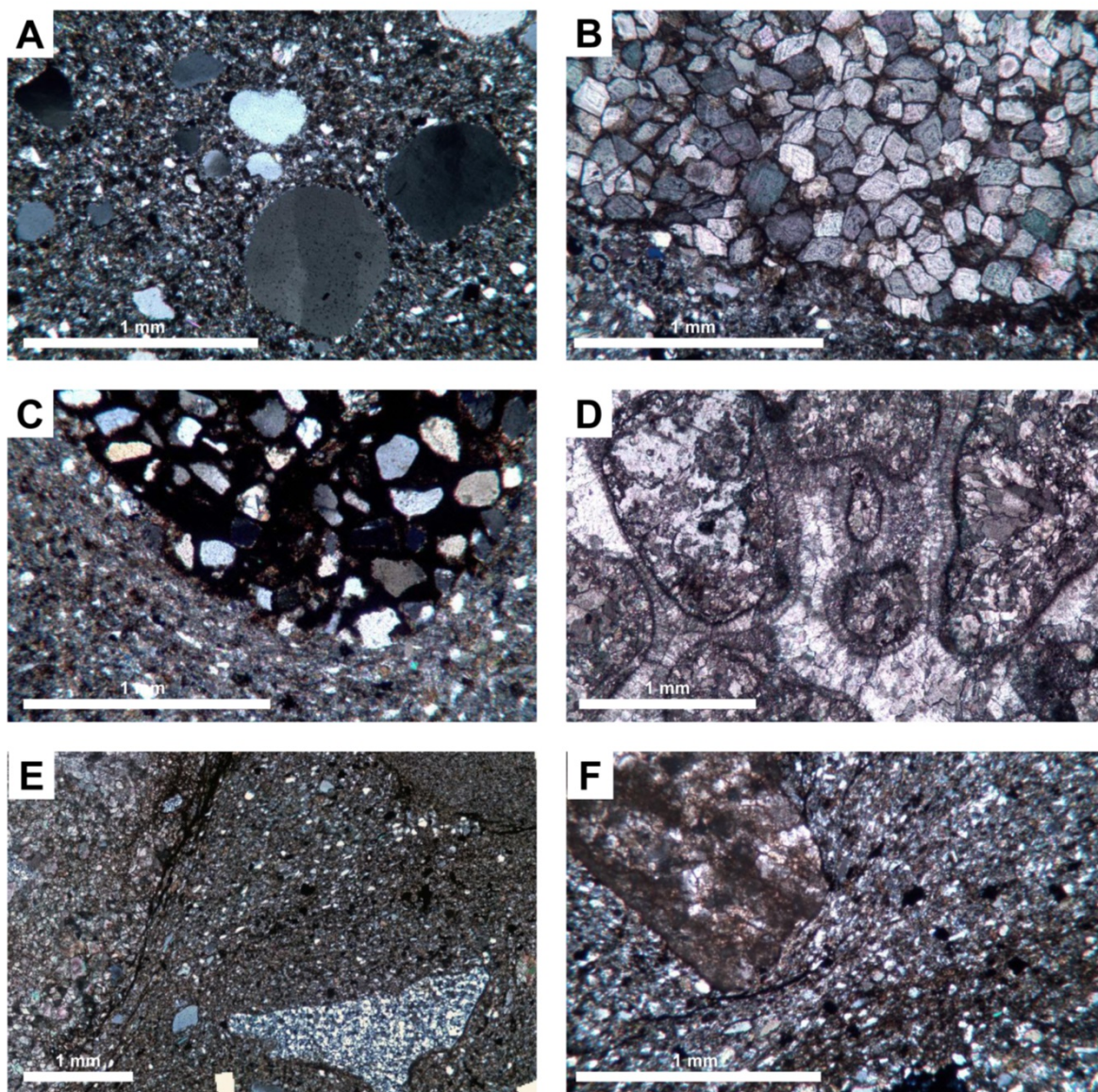
Figure 13: Diamicrites, boulders, and exotic clasts found in the Billy Springs Formation. A) Upper OSCS-A, one of the few intervals with sufficient clast density to be classified as a diamicnite. Visible are black and white cherts and reddish-brown-weathering limestone/dolomite clasts. B) Well-rounded mudstone boulder in OSCN-C. C) Well-rounded carbonate cobble in OSCN-M. D) Autobrecciated slump bed, with contorted clasts of the same or similar lithology to surrounding matrix. E) Discrete clast-bearing unit between convolute-laminated beds, OSCN-M. F) Cobble of vesicular basalt found in lower OSCN-P. G) Clast within convolute-laminae, showing distortion of laminae around clasts. H) Large, partially dissolved carbonate clasts, as well as smaller sand and granule sized particles in mudstone matrix.

The composition of large clast assemblages (i.e. all grains larger than sand) falls into two categories: monomictic–intraformational and polymictic. Monomictic clast assemblages are generally composed of silty mudstone that has a very similar lithological composition to the surrounding planar or convolute-laminated sediment. These types of clasts may be found in isolation as part of lithofacies Mcl, or in discontinuous beds where they form dense, non-oriented concentrations as part of lithofacies Dms (Fig. 13D and E).

The composition of polymictic clast assemblages is entirely different. In these intervals, especially in section OSCS, clasts with 6 to 10 cm diameters were most common. The primary ‘boulder bed’ (as originally described by Coats and Blissett, 1971) is found in the southern section (Unit OSCS-A) and contains clasts composed of carbonates, white and black chert, quartz and mudstone. The lower section of Unit OSCN-P contains a similar clast assemblage, in addition to at least one large clast of vesicular basalt (Fig. 13F). Within these intervals, silt and mud laminae can sometimes be seen to warp and deform around the clasts on both the top and bottom (Fig. 13D and G). In other instances, such deformed laminae are not immediately obvious (Fig. 13H).

Thin sections and QEMSCAN images reveal a range of smaller clasts in addition to the cobbles and boulders visible in outcrop. Observed clasts include well-rounded coarse quartz sand (Fig. 14A), dolomite composed of euhedral rhombic crystals (Fig. 14B), sandy mudstone (Fig. 14C), coated carbonate grains (Fig. 14D), angular chert fragments (Fig. 14E) and micritic carbonate (Fig. 14F). Clay-sized particles, which could not be definitively identified using traditional petrography, were identified through QEMSCAN and tied to thin sections. Background matrix is composed primarily of quartz, clays and micas, not dissimilar to that seen in planar-

laminated mudstones (Fig. 7). Thin laminae can be seen within the matrix, and laminae are deformed around larger clasts, with clays and micas more common near



*Figure 14: Wide range of exotic clasts seen in two 2"x3" thin sections from upper unit OSCS-A. All samples oriented correctly except (C), found as a float block. A) Well-rounded fine- to upper coarse-grained monocrystalline quartz sand within a matrix of silty/sandy mudstone. B) Large clast of well-packed crystals of rhombohedral carbonate (mineralogy from Qemscan; presented in Fig. 15). Euhedral zoning visible in crystal interiors. Between crystals is an isotropic groundmass of undetermined composition. C) Mm-scale clast in silty mudstone matrix, composed of very-fine to fine-grained sand within a dark, clay-rich matrix. D) Interior of large clast containing coated grains of crystalline carbonate. Rounding and micritic rims of grains predate cementation and indicate extended weathering of grain cores prior to coating. E) Composite image showing range of clast lithologies on sub-cm scale: microcrystalline quartz (chert), micrite, cryptocrystalline carbonate, and sand. Note variable silt content of matrix. F) Micrite-dominated carbonate clast deforming grain alignments in silty mudstone matrix.*

clast margins (Fig. 15A). The largest clasts in the QEMSCAN sample were well-rounded, equant carbonates. Carbonate clast interiors ranged from micritic dolomite

(Fig. 15B), to dolomite rhombs with calcite rims and sparse matrix with silica-filled pores (Fig. 15C), to sutured, euhedral dolomite rhombs (Fig. 15D; same clast as in Fig. 14B) and microcrystalline calcite (Fig. 15E). A detailed view of the clastic matrix (Fig. 15F) shows iron oxides (goethite), calcite-filled fractures and bimodal distribution of quartz grains.

#### *6.6.4.2: Distribution*

Concentrated intervals of larger clasts, sized from <1 cm to tens of centimetres, were observed within the mudstone matrix in some areas. In section OSCS, anomalous clasts are most abundant within an interval several metres thick – the ‘boulder bed’ or breccia described by previous workers (e.g. Campana et al., 1961; Coats and Blissett, 1971). Outsized clasts are present but rare outside of this unit, and are not seen in OSCS above 530 m (Fig. 2). In the northern section, the only interval of more abundant clasts seen in that section was a relatively thin portion of Unit OSCN-P.

#### *6.6.5: Lithofacies association 2: Diamictites, outsized clasts and onvolute-laminated mudstones*

##### *6.6.5.1: Occurrence*

Although diamictites are considered to be a separate lithofacies from isolated outsized clasts, they are both associated with Lithofacies *Pcl* and are discussed here together. In no instances are exotic clasts seen in planar-laminated lithofacies; thus, it is most likely that this unclear instance follows the same pattern. Both diamictic intervals and isolated exotic stones are found exclusively in convolute-laminated (slumped) mudstones, although it should be noted that, in bed OSCN-P, the



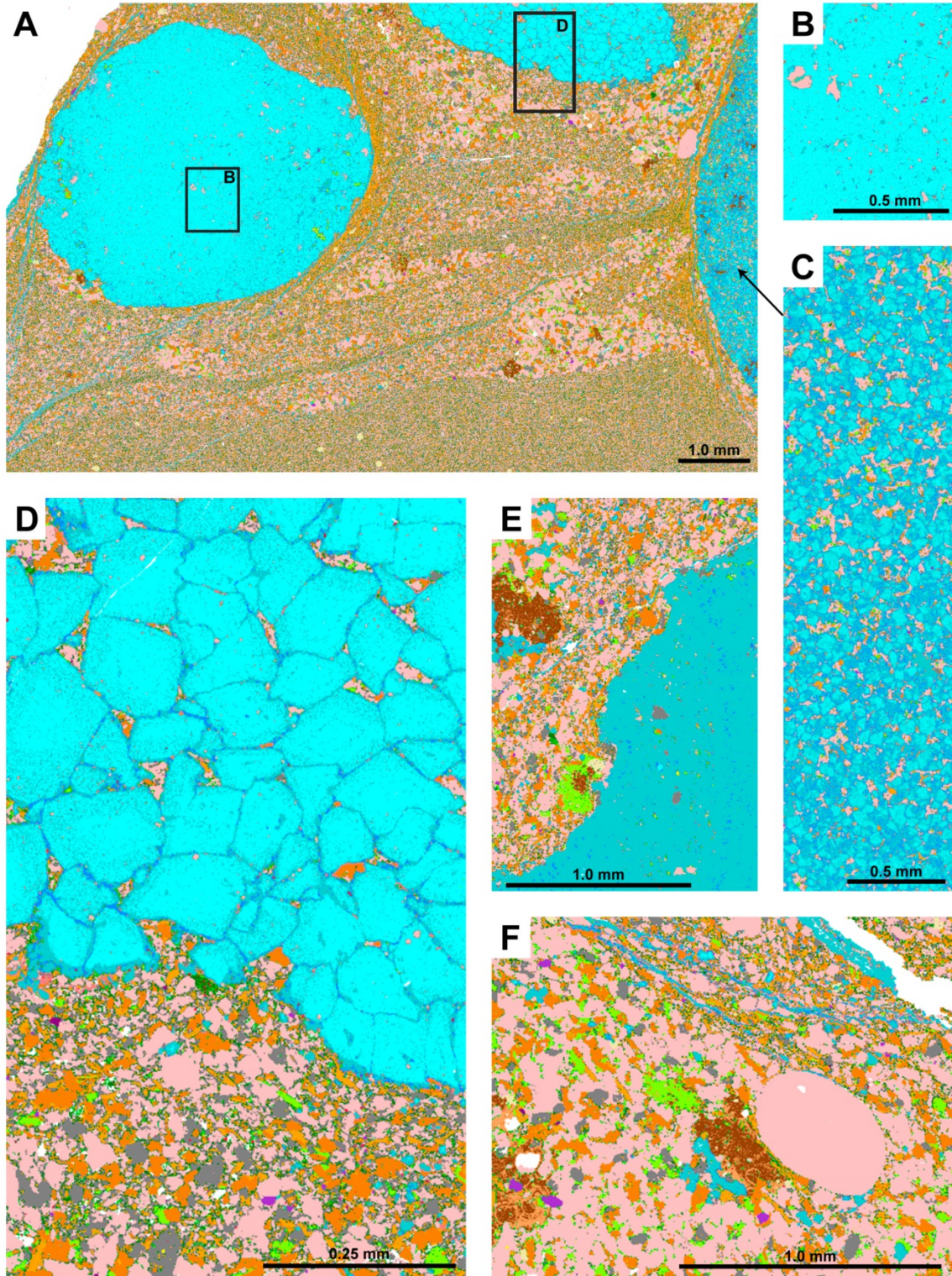


Figure 15 (preceding page): QEMSCAN images showing detailed mineralogy of sample in unit OSCS-H, diamictite lithofacies. A) Wide-field view showing several mm-scale, well-rounded carbonate clasts in a clastic matrix dominated by quartz, mica, and clays. B, C) detailed views of interior of carbonate clasts seen in A. B) dominated by microcrystalline dolomite, and C) by a mixture of dolomite/calcite crystals with silica in interstices. D) Detailed view of individual clast composed of euhedral, rhombic dolomite crystals with calcite-rich alteration rims and interior zonation. Clastic matrix external to clast is composed predominantly of Quartz, Feldspars, and Micas. E) Micritic Calcite clast boundary, from elsewhere in the same sample. F) Detail of matrix, showing large, well rounded quartz sand grain that differs texturally from background matrix, as well as (possibly authigenic) goethite, chlorite, and fracture-filling calcite.

surrounding context of the clast-bearing interval was unclear due to exposure.

Although Jenkins (2011) notes the presence of exotic clasts ('dropstones') in both planar-laminated and convolute-laminated mudstones in the same section studied here, clasts were not observed in planar-laminated or sandy sediments. A thorough investigation of outcrop in the vicinity of the measured sections showed only the association between exotic clasts and convoluted laminae. Intraformational mudstone clast assemblages are also exclusively associated with convolute-laminated mudstones, although a different process is thought to be responsible for their emplacement.

#### 6.6.5.2: Interpretation: Sedimentation mechanisms and possible glacial influence

Isolated exotic clasts and diamictites in the Billy Springs Formation have previously been interpreted as being the product of ice-rafted debris associated with a nearby glacier (e.g. DiBona, 1991). These interpretations are predicated on the presence of large extrabasinal clasts within silty mudstones. The association between slumped units, outsized clasts and diamictites is important in interpreting the process behind their emplacement; this association suggests that the two are related in their modes of formation.

In cases where larger clasts contained within slump structures are composed of the same lithology as the surrounding matrix (for example, Fig. 13D and E), there is likely to be a genetic link between slumping and clast generation. These types of concentrations are generally uncommon throughout the sections measured, and are

interpreted here as having formed through autobrecciation of semi-consolidated sediment as slumping progresses and becomes increasingly convolute. Reid (1992) draws a similar conclusion in the diamictic intervals in Mount Freeling, although this author attributes clast generation to structural rather than syndimentary folding. In the section described here, it is clear that folding occurred prior to lithification and that sediment deformation is a product of redeposition.

In the interpretation by Jenkins (2011), slumping associated with exotic clasts may be the result of ice blocks overloaded with detritus which sank to the bottom and deformed the existing planar-laminated sediment or, alternatively, from icebergs deforming the sea floor and depositing entrained debris while initiating slumps. However, interaction of ice with the sea floor is known to produce large, straight furrows and gouges with ridges (Weeks, 2010) unlike the slumped beds seen here.

Although glacial processes are able to explain the presence of large, hydrodynamically out of place exotics within much finer-grained sediment, the presence of such clasts can also be explained by other processes which do not require glacial influence to operate. Eyles and Januszczak (2004) note several instances where diamictic lithofacies are probably the result of mass flow deposits rather than glacial sediments. These authors also provide evidence that lonestones are a common occurrence within otherwise fine-grained strata, for example, in Canada, Namibia and Virginia, wherein large clasts are transported downslope by turbidity currents or poorly sorted mass flows. Postma et al. (1988) also describe mechanisms where isolated boulders can be emplaced within turbidites. Several occurrences of previously described 'glacial dropstones' have thus been reinterpreted as having a non-glacial origin. While these examples are not identical to those seen in Billy Springs, in that they are deposited by turbulent flow

rather than slump processes, they demonstrate that there are numerous examples of large clasts having been deposited in a dominantly fine-grained environment by non-glacial, processes.

The lack of definitive glacial indicators such as striated and faceted clasts, the strong association of clasts with slumped beds, the significant lack of these clasts in planar-laminated facies and the limited stratigraphic and spatial extent of diamictite deposits all provide evidence against a glacial interpretation. In addition, because clasts are very sparse overall and do not occur above 300 m from the base of the southern section, such a glaciation would be very limited in both time and space. Glacial diamictites elsewhere in the basin (the Sturtian and Marinoan events) are much thicker (up to 2 km thick in the Sturtian; see Preiss, 1987, fig. 52) and are regarded as 'very reliable' by Hoffman and Schrag (2002), in contrast to the ambiguous features seen in the Billy Springs Formation.

The source of exotic clasts in Billy Springs may then be related to the salt-tectonic environment of the Adelaide Rift Complex. There are numerous examples in the basin of salt diapirs, now exposed in cross-section as dolomitic breccia, having influenced topography or being subaerially exposed during the late Neoproterozoic. Diapir-generated topographic highs are often associated with conglomerates composed of shed diapiric detritus as well as thinning and onlap of formations in the Wilpena Group and elsewhere (e.g. Lemon, 2000; Dyson, 2004a). Diapir-generated conglomerates elsewhere in the succession are composed of extrabasinal clasts brought upward from deeper in the basin, often from the rift sediments of the Callanna Group, and include many of the general lithologies seen here (Preiss, 1987).

### 6.6.6: *Tabular-bedded sandstone (Lithofacies Stb)*

#### 6.6.6.1: *Description*

Sand beds are generally decimetre-scale in thickness and separated by slightly thicker mudstone intervals of lithofacies *Mpl*. Sands are fine-grained, often with rippled or undulatory tops and internal ripple cross-lamination. Sand beds have no obvious lateral bed thickness variation at outcrop scale (Fig. 16), the bases are generally flat or gently undulatory (Fig. 16A) and the tops often contain asymmetrical ripples (Fig. 16B). Internally, sands may be massive, planar-laminated, ripple cross-laminated, hummocky cross-stratified (for example, Fig. 16C), or some combination of these, and also may contain tepee-shaped water escape structures (Fig. 16D; cf. van Loon 2009, fig. 25C). Fining-upward beds (Fig. 16E) and planar to ripple-laminated transitions (Fig. 16F) are suggestive of partial Bouma sequences (B to E divisions). In OSCS, tabular sand beds appear in relatively isolated groups of three or four beds (for example, Fig. 16A and B), or in larger stacked sequences separated by slightly thicker intervals of planar-laminated silty mudstone (OSCN; Fig. 16G). Mudstone intervals between sand beds do not appear to have any vertical trend in distribution or spacing. Thin-section analysis revealed that even in the lowermost, sandiest parts of these beds, clay was still present, and grain size was relatively small (Fig. 17A and B). Basal sand beds were dominated by very fine-grained sand and silt, and included a high proportion of heavy minerals (Fig. 17B and C). At the highest stratigraphic point reached in section OSCS, a thicker bed of quartzose sand was poorly exposed on hilltops (unit OSCS-H) that was either massive or showed faint cross-stratification.

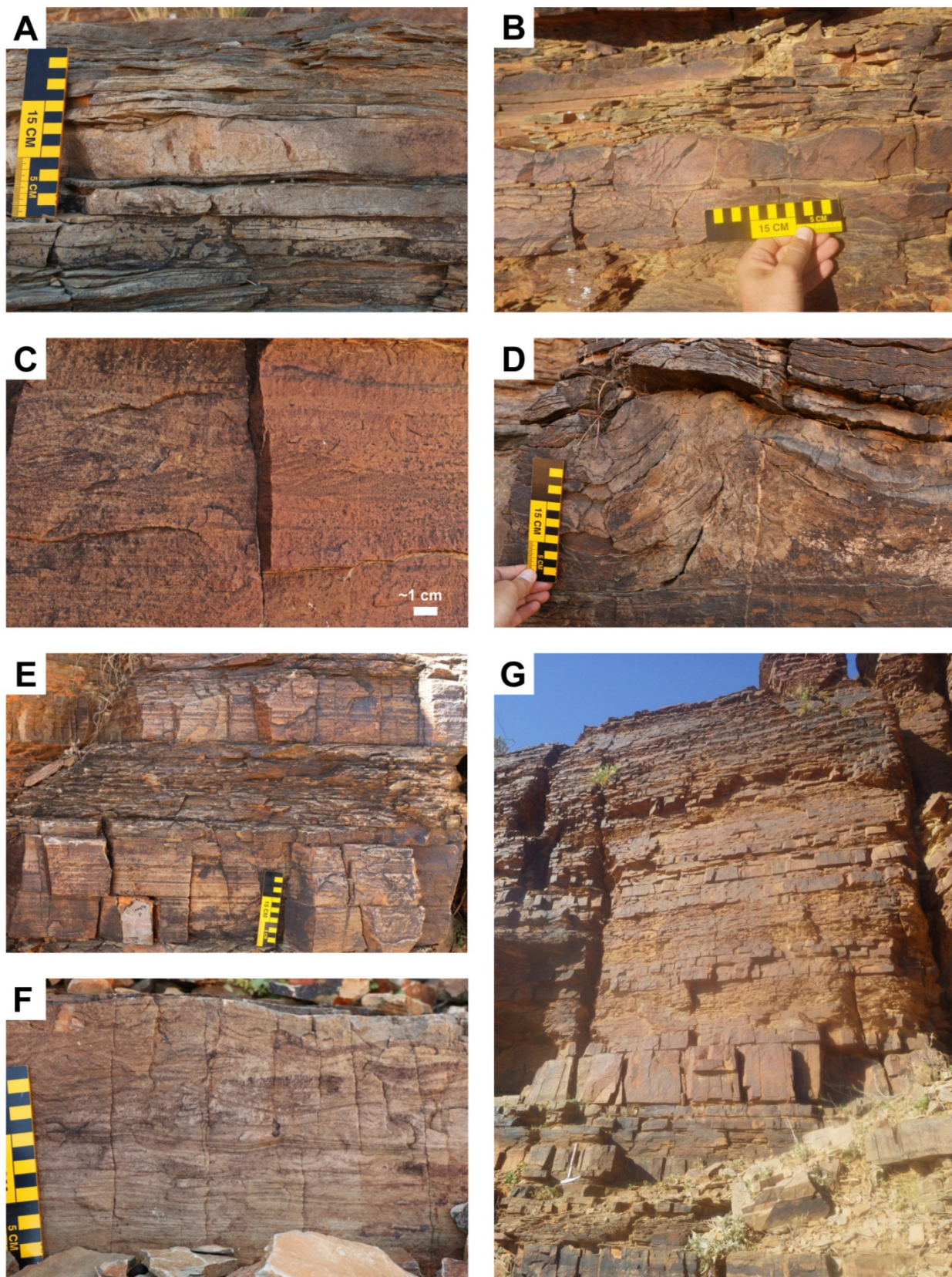


Figure 16: Interbedded sandstone-mudstone lithofacies. A) Centimetre-scale sand beds atop 700 metres of planar-laminated mudstone, OSCS-F. B) Grouped, tabular centimetre-scale beds with asymmetrically rippled tops, OSCN-P. C) Internally-ripple-laminated and hummocky cross-stratified sand bed, OSCN-P. D) Water escape structures in sandstone beds, closely adjacent to beds in Fig. 13D. E) Stacked, tabular centimetre- to decimetre-scale beds, fining-upward from very fine muddy sands in basal beds, to muds and clays in between, unit OSCN-P. F) Tabular sand beds, OSCN-P, showing transition from planar to ripple laminae. G) Irregular stacking pattern of sand beds in unit OSCN-P; rock hammer is 32 cm long.

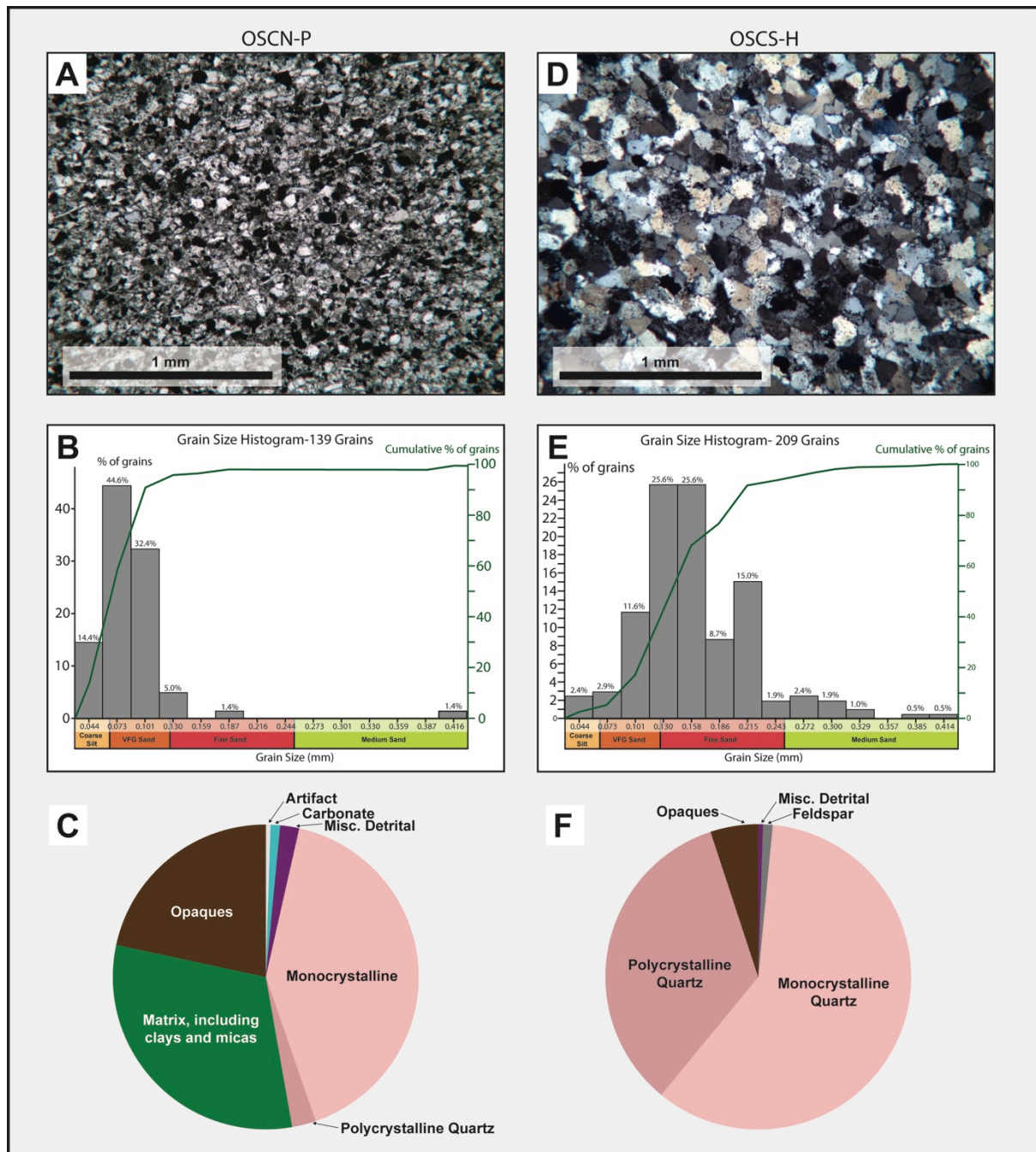


Figure 17: Sand-dominated lithofacies in thin section. A) OSCN-P, showing lowermost bed in cm-scale fining-upward sequence. Sand content decreases in overlying beds. B) Textural histogram of 139 individually measured detrital grains, same sample as above. C) Pie chart showing overall sediment composition. D) Massive sand bed at top of measured section, OSCS-H, showing well-cemented quartzite. E) Textural classification for sample shown in D. F) Pie chart showing composition of sample taken from OSCS-H.

Due to weathering, true thickness of this bed could not be determined, but exposures revealed a bright white, clean sandstone with little or no clay content, confirmed later by petrography to consist almost entirely of upper very fine-grained to lower fine-grained quartz sand (Fig. 17D and E). Quartz grains were dominantly

monocrystalline, and sands included a smaller proportion of heavy minerals than that seen in beds below (Fig. 17F).

#### *6.6.6.2: Distribution*

In section OSCS, this lithofacies is present approximately 980 stratigraphic metres from the base of the formation as very fine to fine-grained sand beds several centimetres thick within the planar-laminated mudstones (Fig. 8C to E). Above these beds, a vertical section exposed for approximately 50 m was reconnoitred for any additional sands, but none were seen, with planar-laminated mudstones again dominant. The thicker quartz arenite bed or beds in section OSCS constitute the stratigraphically highest unit measured. In section OSCN, outcrop exposure becomes less continuous near the top, and thickness measurements are approximate. In the uppermost two units observed (OSCN-N and OSCN-P), tabular, centimetre to decimetre-scale sandy beds are present and weather in relief. These beds have a clear fining-upward grain size and are stacked for several tens of metres to the uppermost point measured in OSCN. It is not possible to directly correlate individual beds in the northern section to specific beds or units in OSCS, although this lithofacies occurs at the tops of both sections.

#### *6.6.6.3: Interpretation of tabular-bedded sandstones*

Interbedded sandstone–mudstone lithofacies are interpreted as turbidites based on the observed sedimentological features within beds, including fining-upward grain sizes, sharp-based sands and partial Bouma sequences. Compared with the other lithofacies, the presence of these coarser-grained beds and sediments deposited by turbulent flow implies a change in both the depositional process and the likely proximity to source areas. Because slumped sediments are still mud



dominated and do not show a marked increase in sand content, it is more likely that they are formed by deformation of local, intrabasinal sediment. Although slump and turbidite processes can generally be seen as part of the same sediment gravity flow continuum, the lithological, geometric and thickness differences between these two lithofacies implies that these lithofacies are not necessarily genetically related.

Turbidites, being dominated by sands, probably have a different source and may be brought in by gravity flows from outside the immediate area of deposition.

The distribution of these turbidites has implications for the sequence stratigraphic interpretation of the Billy Springs Formation. As sandy turbidite lithofacies are limited only to intervals stratigraphically higher in the section, the Billy Springs Formation is interpreted to be progressively shallowing upward as sand-rich sediments prograde out over the deeper water muds. The formation may represent the distal portion of a highstand systems tract, with the turbidite sands seen near the top being the earliest prodelta deposits in the sequence to be deposited far into the basin (Fig. 18) although, without clear correlations to other formations, such an interpretation is not conclusive. The time-equivalent Bonney Sandstone has been interpreted elsewhere as having been deposited in an interval of relatively falling sea-level during a highstand systems tract (sequence M4.3 of Preiss, 1999; and 4.4 of Preiss, 2000) that terminates with an erosional surface at the base of either the Chace or Ediacara members within the Rawnsley Quartzite (Preiss, 1987, 1999; Gehling, 2000). The Billy Springs Formation sediments consist of thick fine-grained lithologies that are likely to be deposited in deeper water than much of the rest of the Wilpena Group, and show an overall, large-scale coarsening-up profile. Such profiles are characteristic of late highstand, where sedimentation rate surpasses the rate of sea-level rise, and accommodation space begins to fill during normal

regression (Posamentier and Allen, 1999). Reid (1992) also interprets uppermost sandier beds to represent the incursion of the Pound Subgroup; an interpretation which generally agrees with the observations and interpretations herein, although this study cannot definitively assess exactly where in the upper Wilpena Group these sandy turbidites originate from.

## 6.7: Discussion and Significance

### 6.7.1: A glacial source for extrabasinal clasts?

The hypothesis of a ‘Billy Springs glaciation’ in the late Ediacaran requires the support of several lines of evidence to be widely accepted. Thus far, the only evidence lies in the presence of extrabasinal clasts within relatively narrow intervals. Potentially glacial sediments would be expected to be related to known glacial intervals in the surrounding area and beyond. Given the established low latitude for South Australia during this time (Li et al., 2008), a Billy Springs glaciation would

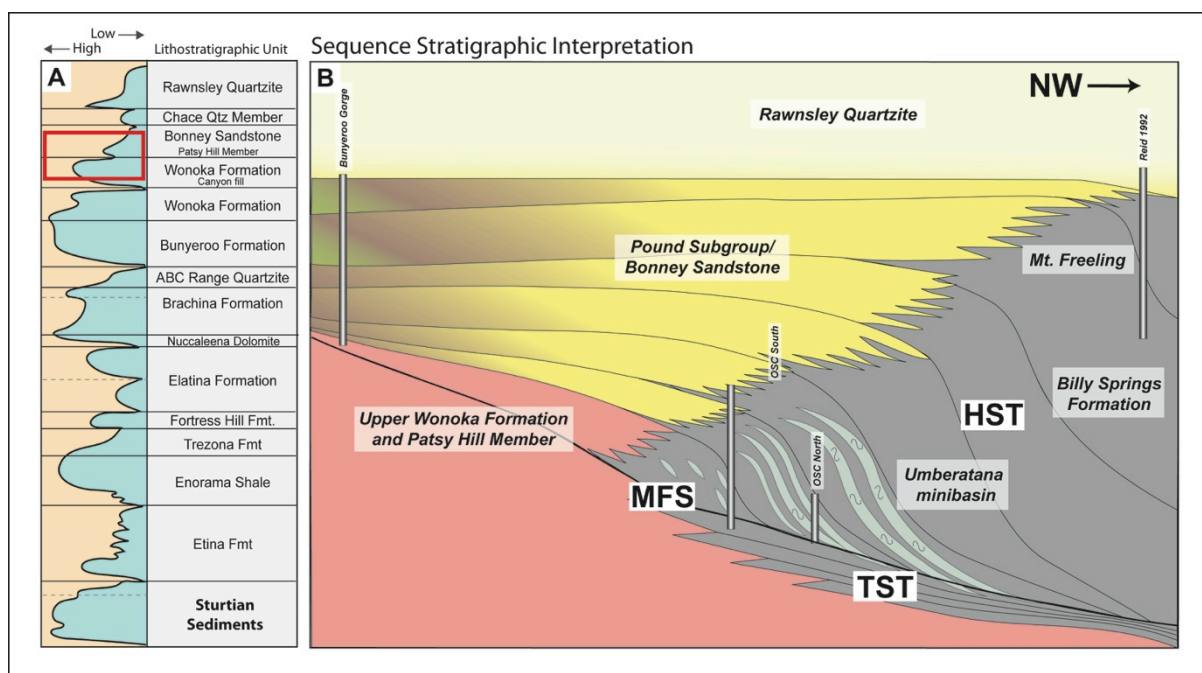


Figure 18: A) Marinoan bathymetric curve for the Adelaide Rift Complex, from Preiss (2000). Red square highlights approximate stratigraphic location of B), Sequence stratigraphic interpretation of the relationship between the Wonoka Formation, Billy Springs Formation, and Wilpena Group. HST= Highstand Systems Tract, MFS=Maximum Flooding Surface, TST=Transgressive Systems Tract. Influenced by Dyson (2003).

need to either be global in scale, or be due to extensive high-altitude glaciers reaching sea-level. The well-known Sturtian and Marinoan glacial episodes are present stratigraphically below the Billy Springs Formation by hundreds or thousands of metres. Therefore, any potential glacial debris in the Billy Springs Formation probably postdates these events by millions of years. The best candidate for a correlative interval in Australia that may show glacial evidence is the Egan Formation in the Kimberley Region of Western Australia, which contains diamictites and has been interpreted to post-date the Elatina/Marinoan glaciation (Corkeron and George, 2001; Bao et al., 2012). Grey and Corkeron (1998) tie the Egan interval to the Wonoka Formation on the basis of stromatolite biostratigraphy; thus, a brief glacial event corresponding to the Egan interval cannot be ruled out for the time of Billy Springs/Wonoka deposition, although it should be noted that there are no glacial deposits elsewhere in either the Wonoka Formation or in the equivalent Julie Formation in the Amadeus Basin. In addition, Coats and Preiss(1980) and several older publications interpret the Egan sediment as Marinoan and equivalent to the Elatina Formation rather than the Wonoka Formation.

The only other widespread Ediacaran glaciation with significant support is the Gaskiers event, known initially from Canadian deposits. Unlike the Sturtian and Marinoan intervals, which are global in scale, the Gaskiers glacial interval is found primarily in areas reconstructed to be in high-latitudes at the time of deposition (Hoffman and Li, 2009). The relatively short duration of the event and the lack of cap carbonates are inconsistent with a global glaciation (Li et al., 2013), making it unlikely that the low-latitude Adelaide Rift Complex would be ice-covered. The glacial interpretations of other low-latitude diamictite-bearing formations associated with the Gaskiers glaciation have also been called into question (e.g. Direen and

Jago, 2008; Hoffman et al., 2009; Carto and Eyles, 2012). Most authors place the Gaskiers event at around 580 Ma (Bowring et al., 2003; Hoffman and Li, 2009; Li et al., 2013). This timing also presents an issue; most time scales place the maximum age of the Bonney Sandstone (and, by extension, the middle Billy Springs Formation; Pell et al., 1993) almost 30 Myr later (Preiss, 2000). Jenkins (2011) acknowledges that the Gaskiers Event may be too early to correlate to the Billy Springs Formation. Thus, it is unlikely that this event resulted in, or was contemporaneous with, deposition of parts of the Billy Springs Formation. Hebert et al. (2010) and a few other authors (e.g. Chumakov, 2009) hypothesize the existence of a post-Gaskiers glaciation, although evidence is not widespread. The glacial-origin scenario is therefore considered less likely than the more parsimonious suggestion of a non-glacial depositional mechanism.

#### *6.7.2: Umberatana Syncline as a salt-withdrawal minibasin*

The structural complexity of the basin fill can make it difficult to recognize syn-sedimentary subsidence and faulting; however, careful examination of thickness variations, relationships to diapir bodies and lateral facies changes show that much deformation occurred during the deposition of the basin fill and prior to the Delamerian event (Dalgarno and Johnson, 1968; Coats, 1973; Lemon, 1985; Rowan and Vendeville, 2006). The majority of this deformation can be attributed to the upward growth of salt diapirs and associated subsidence from mobilization and withdrawal of an underlying bedded salt layer (Hearon et al., 2014). Numerous (>100) diapir bodies are now exposed throughout the Adelaide Rift Complex over an area of approximately 50,000 km<sup>2</sup>, and much of the current structure in the Flinders Ranges is probably due to pre-Delamerian halokinesis instead of structural compression, especially in the northern part of the basin discussed here (Fig. 19)

(Rowan and Vendeville, 2006). Like the Umberatana syncline, many structures originate or terminate at diapirs (Curtis et al., 1991; Dyson, 2001; Rowan and Vendeville, 2006). Previous studies that attribute folding only to tectonic processes (e.g. Paul et al., 1999) ignore the thickness changes in these units, which are unambiguous evidence of a syn-depositional origin. Clear indications of syn-sedimentary diapirism and subsidence are found as far back as the Sturtian glacials in the Umberatana Group, continue into the Cambrian, and are present in all of the formations in between (Coats, 1973; Table 2). Sediments adjacent to diapirs often contain conglomeratic bands within otherwise homogenous, finergrained formations or, in the Enorama Shale, reef development around the emergent diapir margin (Lemon, 2000). Many diapir bodies show relationships with adjacent sediments that indicate that they were exposed or formed topographic relief at the sediment–water interface, with some diapiric highs possibly becoming emergent and forming subaerial islands (Dalgarno and Johnson, 1968; Plummer, 1978; Lemon, 2000).

Sediments that are generally correlative to the Billy Springs Formation also often show indications of minibasin formation near diapirs. Clearly defined onlap or conglomeratic facies are documented in the upper Wilpena Group near the Oratunga, Pinda, Patawarta, Mount Frome, Wirrealpa and Beltana diapirs (Dalgarno and Johnson, 1968; Lemon, 1985; Reilly, 2001; Dyson, 2004a; Kernen et al., 2012; Collie and Giles, 2011; Dyson, 2004b; Hearon et al., 2015), most of which are less than 100 km from the Billy Springs Formation. Such relationships clearly indicate that active salt movement and subsidence was ongoing throughout the basin during the time of Bonney and Wonoka deposition and, by extension, during the time of Billy Springs deposition as well. The Umberatana Syncline has specifically been interpreted previously as a salt-withdrawal minibasin (Rowan and Vendeville, 2006),

with its syncline axis originating from the Lyndhurst diapir *ca* 40 km to the west. Other diapir bodies occur in close proximity as well, with the closest only 4 km from the sections described here. The Burr diapir, the largest in the basin in terms of outcrop area (Fig. 19A; Coats, 1973), is less than 20 km to the west. The size and shape of the Umberatana syncline also conforms to minibasins seen today in the Gulf of Mexico (Bryant et al., 1990; Bouma and Bryant, 1994) and the Santos basin (Jackson, 2012), where minibasins form sub-circular depressions with diameters of 10 to 20 km separated at depth by irregular salt piercements (Fig. 19C). Later erosion, however, prevents precise reconstruction of halokinetic sequences in the Umberatana area, because the contact between the upper Ediacaran sediments and the diapir body is not preserved.

Sedimentation in the Umberatana syncline shows similarities with other documented intraslope or lower shelf minibasins. Alternating intervals of pelagic deposition and mass-transport complexes are also seen in the Gulf of Mexico (e.g. Madof et al., 2009), although at a scale much larger than that seen here and visible on seismic data. In core from the subsurface of the Gulf of Mexico, minibasins in modern and Pleistocene sediments have also been described as being partially filled by homogenous and finely laminated muds (Mallarino et al., 2006). Section OSCS bears some degree of similarity to that observed by Shultz and Hubbard (2005), who describe ponded turbidites increasing in frequency upward in an intraslope minibasin from Chile, as well as slumps, slides and debris flows. Likewise, the fine-grained nature of the Umberatana minibasin resembles conceptual models by Banham and Mountney (2013a; see Fig. 13F) occurring in high subsidence, low sediment supply continental environments, where lacustrine settings would dominate. Thus, these sediments add further evidence to a growing compilation of recurring features in

these environments across space and time. However, the Umberatana Syncline is also unique among outcropping minibasins in that it is finer-grained, less variable in lithology and was formed in a deeper water environment than many others described in the literature (see Table 1). The minibasin described in this study, therefore, represents an end-member in the spectrum of depositional settings in which minibasins form. As such, it more closely matches the environment of deposition of many of the actively producing hydrocarbon plays, which are common in deepwater, offshore settings.

The sections described here are dominated by hundreds of metres of silty mudstone (Fig. 5), interpreted as having been deposited in a shelf or slope environment. The lower Billy Springs Formation thus provides an example of a minibasin wherein much of the basin fill is lacking in sediments which would have the potential to be hydrocarbon reservoirs. The rarity of sand-dominant sediments in the Umberatana minibasin interior implies that either: (i) no coarser sediments were available from the source; (ii) subsidence was relatively slow, forming only a low gradient which did not favour the trapping of sands; or (iii) coarser sediment depocentres are elsewhere in the basin and sands have laterally bypassed the Umberatana area (sediment bypass of minibasins is described by Mallarino et al., 2006). Turbidites and slumping are often characteristic features of minibasins (Table 1). Minibasin sedimentation patterns are often related to halokinetic control (e.g. Giles and Lawton, 2002); in the Umberatana syncline, slumping is probably intrabasinal, and the frequency of slumped intervals suggests that it may be halokinetically triggered. However, the overall sequence stratigraphic setting and depositional environment may be more dominant in controlling lithologies, because the coarsening-upward succession of sediments described here fits better with a

larger change in sediment supply.

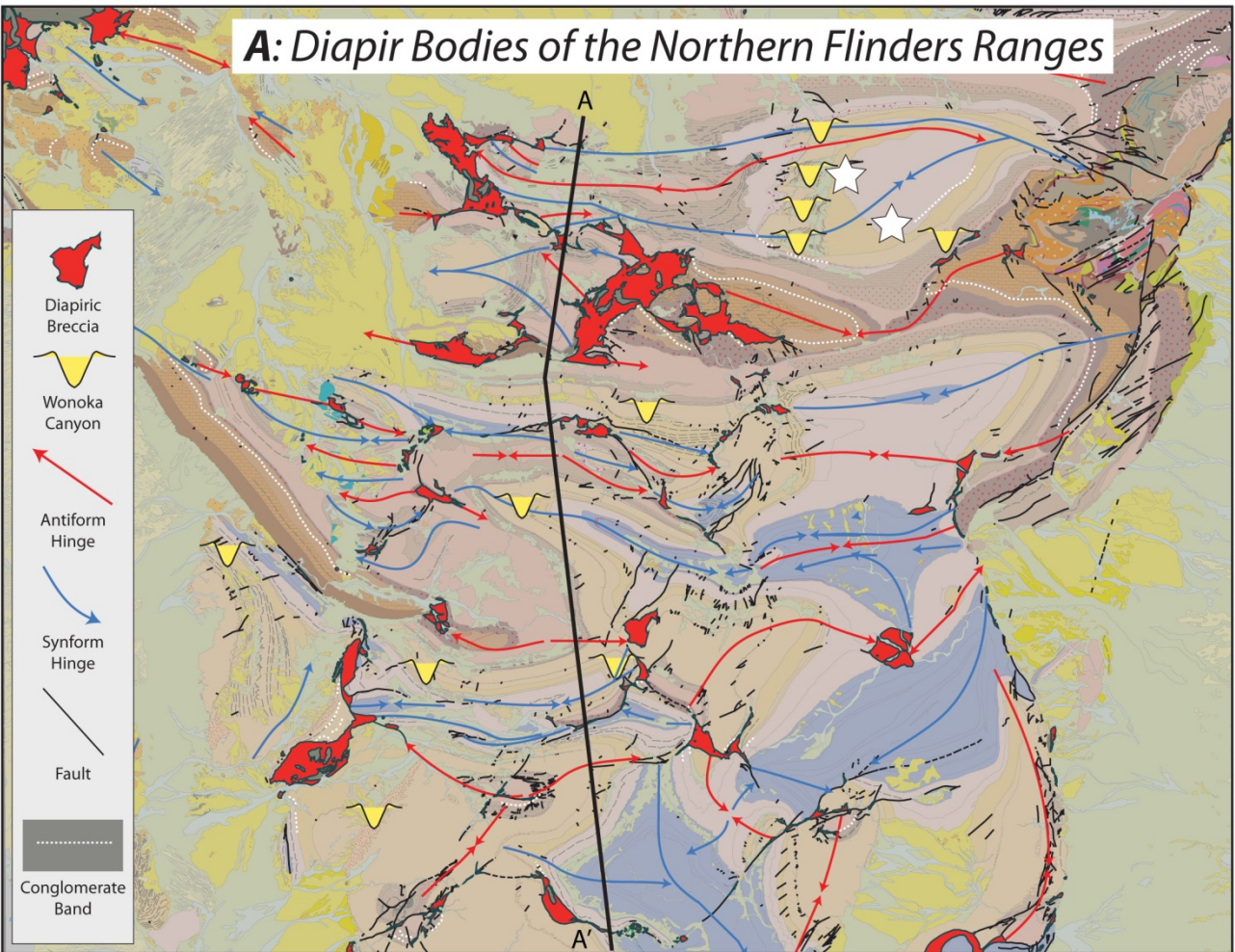
### *6.7.3: Relevance to the Ediacaran metazoan assemblage*

This study provides further environmental and stratigraphic context for the Ediacaran fossil fauna preserved in the Ediacara Member of the Rawnsley Quartzite (for background, see Gehling, 2000; Narbonne, 2005). It is likely that the primary fossil-bearing strata directly overlie the Billy Springs Formation sediments discussed here, as reported by Reid (1992), with fossils occurring north of the study area. Pound Subgroup sands atop the Billy Springs Formation are likely to be part of the continued progradation of coarser sediments over those seen in the Umberatana area, and suggest a widespread shallowing-upward sequence across the basin in upper Wilpena Group time. The presence of a definitively marine, shelf/slope facies in the immediately subjacent sediments should also influence palaeogeographic reconstructions of the area. Such a depocentre implies an overall deepening of the basin, and possibly an oceanic connection to the north-west of the central basin axis, which would probably have persisted to some degree during the time of Rawnsley deposition. Future studies reconstructing regional palaeoenvironments during the time of metazoan colonization may benefit from this study. Given the widespread indications of syn-sedimentary diapirism during Pound Subgroup time, more work should also be done to better understand the effects of diapir-induced topography on the distribution of fossils and the lithofacies in which they are found.

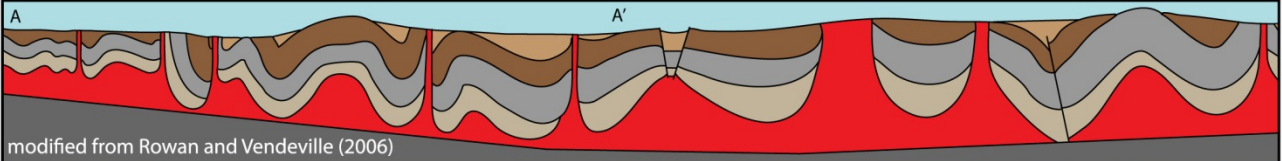
*Figure 19 (following page): A) Diapirs of the northern Flinders Ranges. Modified from Coats (1973). B) North to south cross section through the Flinders Ranges, showing synforms and antiforms as the product of salt mobilization. Modified from Rowan and Vendeville (2006). Left hand portion of cross section corresponds to line in Fig. 19 (A). C) Current Gulf of Mexico topography, showing surface expression of active salt-withdrawal minibasins. Modified from NOAA (2015). ([http://www.ncddc.noaa.gov/website/google\\_maps/OE/mapsOE.htm](http://www.ncddc.noaa.gov/website/google_maps/OE/mapsOE.htm))*



**A: Diapir Bodies of the Northern Flinders Ranges**

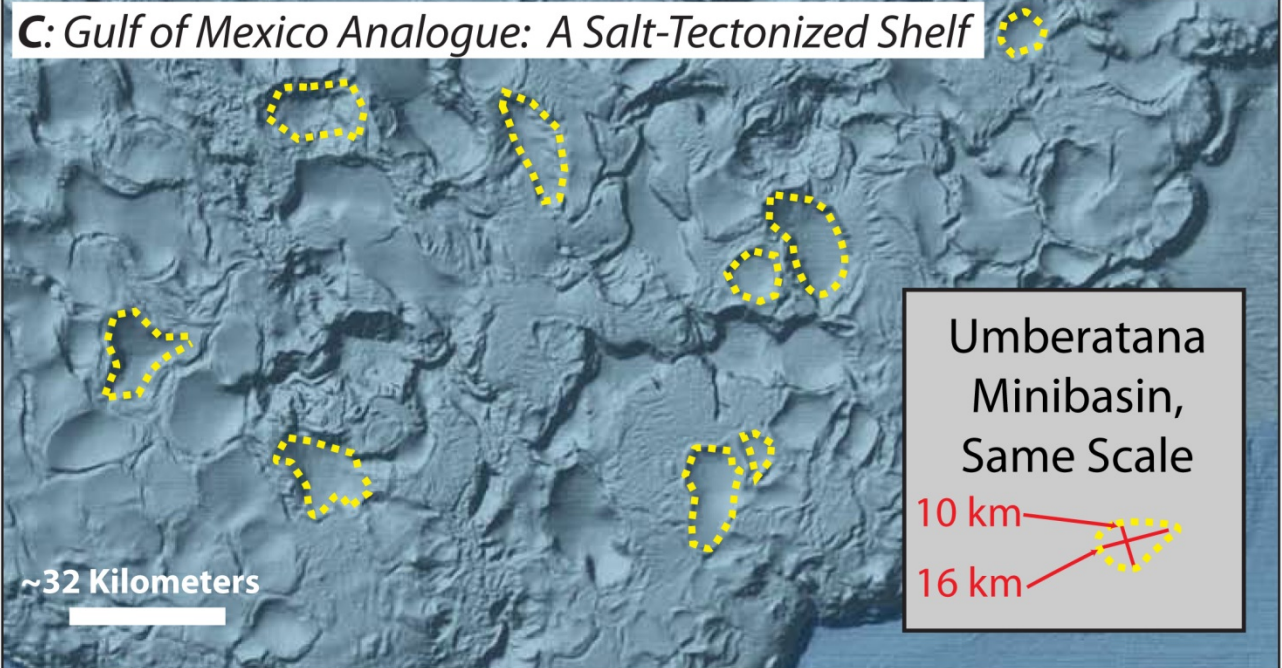


**B: Adelaide Rift Complex Cross-Section**



modified from Rowan and Vendeville (2006)

**C: Gulf of Mexico Analogue: A Salt-Tectonized Shelf**



Umberatana  
Minibasin,  
Same Scale

10 km

16 km

## 6.8: Conclusions

Sediments of the Billy Springs Formation, described in detail for the first time here, show a range of features (fine-grained laminated sediments, slump structures and turbidite deposits) consistent with deposition within a deepwater intra-shelf or intra-slope minibasin. Although minibasins are known from several outcrops elsewhere in Australia and around the world, few have been studied from a sedimentological perspective, and the Umberatana minibasin is a unique exposure in terms of its sedimentary character and palaeogeographic setting. Lithofacies within the basin reflect background pelagic deposition, intrabasinal slumping and progradation of turbidite sands into the basin. Rhythmically laminated facies may be the product of changing depositional energy related to short-term cycles, possibly tidal. Association between diamictites and slump structures suggests that these lithofacies were emplaced by the same depositional processes. Large extrabasinal clasts are probably sourced from nearby salt diapirs, which are present throughout the basin and are known elsewhere to shed conglomerates. Clasts are likely to have originated from deeper in the basin, and were subsequently brought to the surface by nearby salt diapirs and re-deposited. Previous interpretations that clasts are glacial in origin are inconsistent with the timing and extent of known glacial intervals, except potentially for the Egan Glacials of northwestern Australia, for which timing is poorly constrained; sediments are probably too young to correlate to the Gaskiers event. Because deepwater sediments are uncommon in the Adelaide Rift Complex, the presence of a shelf or slope environment within the northern Flinders Ranges also has important implications for the palaeogeography of the larger basin. The northern Adelaide Rift Complex, therefore, may have been a more complex depositional system than previously believed, and is an excellent outcrop analogue

for similar depositional settings in the geological record.

## **6.9: Acknowledgements**

This research is supported in part by the Nancy Setzer Murray Memorial Grant from AAPG Foundation, a part of AAPG Grants In Aid program, and the University of Adelaide, who supported this research through an International Postgraduate Research Scholarship. The authors would like to thank Bob Dalgarno, Jim Gehling and Wolfgang Preiss for helpful discussions throughout this process, as well as the Reservoir Analogues Research Group (RARG) at the Australian School of Petroleum, University of Adelaide. We thank James Manual at the Ian Wark Research Institute at the University of South Australia who performed QEMSCAN analysis, and Melissa Craig, who assisted with Fourier analysis. Thanks are also due to Umberatana Station owners Chris and Jenny Mahoney, who graciously provided land access, and Claudia Valenti, who proved to be an invaluable assistant during field work. We acknowledge the traditional owners of the lands on which this research was conducted. This paper forms record number 333 of the Centre for Tectonics, Resources, and Exploration at the University of Adelaide. We wish to thank Jim Gehling, Steven Banham and the editors of *Sedimentology* for helpful comments on this manuscript.

## 6.10: References

- ALA, M.A., 1974, Salt diapirism in southern Iran. *AAPG Bulletin*, v. **58**, p. 1758–1770.
- ARBUES, P., FERRER, O., ROCA, E., GILES, K., ROWAN, M., DE MATTEIS, M. AND MUÑOZ, J.A., 2012, The Bakio salt wall and its effects on synkinematic deepwater sedimentation (Basque Pyrenees, Northern Spain). *EGU General Assembly Conference Abstracts*, v. **14**, p. 9659.
- ARCHER, A.W., 1991, Modeling of tidal rhythmites using modern tidal periodicities and implications for short-term sedimentation rates. In: *Sedimentary Modeling: Computer Simulations and Methods for Improved Parameter Definition* (Ed. E. Franseen), *Bulletin of the Kansas State Geological Survey*, v. **233**, p. 185–194.
- ASCHOFF, J.L. AND GILES, K.A., 2005, Salt diapir-influenced, shallow-marine sediment dispersal patterns: insights from outcrop analogs. *AAPG Bulletin*, v. **89**, p. 447–469.
- BANHAM, S.G. AND MOUNTNEY, N.P., 2013a, Evolution of fluvial systems in salt-walled mini-basins: a review and new insights. *Sedimentary Geology*, v. **296**, p. 142–166.
- BANHAM, S.G. AND MOUNTNEY, N.P., 2013b, Controls on fluvial sedimentary architecture and sediment-fill state in saltwalled mini-basins: Triassic Moenkopi Formation, Salt Anticline Region, SE Utah, USA. *Basin Research*, v. **25**, p. 709–737.
- BANHAM, S.G. AND MOUNTNEY, N.P., 2014, Climatic versus halokinetic control on sedimentation in a dryland fluvial succession. *Sedimentology*, v. **61**, p. 570–608.
- BAO, H., CHEN, Z.Q. AND ZHOU, C., 2012, An 170 record of late Neoproterozoic glaciation in the Kimberley region, Western Australia. *Precambrian Research*, v. **216**, p. 152–161.
- BARDE, J.P., CHAMBERLAIN, P., GALAVAZI, M., GRALLA, P., HARWIJANTO, J., MARSKY, J. AND VAN DEN BELT, F., 2002, Sedimentation during halokinesis: Permo-Triassic

- reservoirs of the Saigak field, Precaspian basin, Kazakhstan. *Petroleum Geoscience*, v. **8**, p. 177–187.
- BEAUBOUEF, R.T. AND FRIEDMANN, S.J., 2000, High resolution seismic/sequence stratigraphic framework for the evolution of Pleistocene intra slope basins, western Gulf of Mexico: depositional models and reservoir analogs. In: Deep-Water Reservoirs of the World (Ed. P. Weimer), p. 40–60. 20<sup>th</sup> GCSSEPM Bob F. Perkins Research Conference
- BEAUBOUEF, R.T., ABREU, V. AND VAN WAGONER, J.C., 2003, Basin 4 of the Brazos-Trinity slope system, western Gulf of Mexico: the terminal portion of a late Pleistocene lowstand systems tract. In: Shelf Margin Deltas and Linked Down Slope Petroleum Systems: Global Significance and Future Exploration Potential (Eds H.R. Roberts, N.C. Rosen, R.F. Fillon and J.B. Anderson), p. 45–66. 23rd GCSSEPM Bob F. Perkins Research Conference.
- BOGDANOVA, S.V., PISAREVSKY, S.A. AND LI, Z.X., 2009, Assembly and breakup of Rodinia (some results of IGCP Project 440). *Stratigraphy and Geologic Correlation*, v. **17**, p. 259–274.
- BOUMA, A.H. AND BRYANT, W.R., 1994, Physiographic features on the northern Gulf of Mexico continental slope. *Geo-Marine Letters*, v. **14**, p. 252–263.
- BOWRING, S., MYROW, P., LANDING, E., RAMEZANI, J. AND GROTZINGER, J., 2003, Geochronological constraints on terminal Neoproterozoic events and the rise of metazoans. *Geophysical Research Abstracts*, v. **5**, 13219.
- BROWN, L.F., JR, LOUCKS, R.G., TREVIO, R.H. AND HAMMES, U., 2004, Understanding growth-faulted, intraslope subbasins by applying sequence-stratigraphic principles: examples from the south Texas Oligocene Frio Formation. *AAPG Bulletin*, v. **88**, p. 1501–1522.
- BRYANT, W.R., BRYANT, J.R., FEELEY, M.H. AND SIMMONS, G.R., 1990, Physiographic and bathymetric characteristics of the continental slope, northwest Gulf of Mexico. *Geo-Marine Letters*, v. **10**, p. 182–199.
- CALLOT, J.P., RIBES, C., KERGARAVAT, C., BONNEL, C., TEMIZ, H., POISSON, A., VRIELYNCK, B., SALEL, J.F. AND RINGENBACH, J.C., 2014, Salt tectonics in the

- Sivas basin (Turkey): crossing salt walls and minibasins. *Bulletin of the Geologic Society of France*, v. **185**, p. 33–42.
- CAMPANA, B., COATS, R.P., HORWITZ, R.C. AND WEBB, B.P., 1961, UMBERATANA Map Sheet, 1:63,360 Series. South Australia Geological Survey, Adelaide.
- CARTO, S.L. AND EYLES, N., 2012, Sedimentology of the Neoproterozoic (c. 580 Ma) Squantum 'Tillite', Boston Basin, USA: mass flow deposition in a deep-water arc basin lacking direct glacial influence. *Sedimentary Geology*, v. **269**, p. 1–14.
- CHUMAKOV, N.M., 2009, The Baykonurian glaciohorizon of the late Vendian. *Stratigraphy and Geological Correlations*, v. **17**, p. 373–381.
- COATS, R.P., 1973, COPLEY Map Sheet, 1:250,000 Series. South Australia Geological Survey, Adelaide.
- COATS, R.P. AND BLISSETT, A.H., 1971, Regional and economic geology of the Mt. Painter Province. *Bulletin of the Geologic Survey of South Australia*, v. **43**, p. 426 p.
- COATS, R.P. AND PREISS, W.V., 1980, Stratigraphic and geochronological reinterpretation of Late Proterozoic glaciogenic sequences in the Kimberley region, Western Australia. *Precambrian Research*, v. **13**, p. 181–208.
- COLLIE, A.J. AND GILES, K., 2011, Comparison of Lower Cambrian carbonate facies and halokinetic sequences in minibasins developed on opposite sides of the Wirrealpa Diapir, Central Flinders Ranges, South Australia. *AAPG Search and Discovery Article #50442*.
- CORKERON, M.L. AND GEORGE, A.D., 2001, Glacial incursion on a Neoproterozoic carbonate platform in the Kimberley region, Australia. *Geologic Society of America Bulletin*, v. **113**, p. p. 1121–1132.
- COWAN, E.A., CAI, J., POWELL, R.D., SERAMUR, K.C. AND SPURGEON, V.L., 1998, Modern tidal rhythmites deposited in a deep-water estuary. *Geo-Marine Letters*, v. **18**, p. 40–48.
- COWAN, E.A., SERAMUR, K.C., CAI, J. AND POWELL, R.D., 1999, Cyclic sedimentation

- produced by fluctuations in meltwater discharge, tides and marine productivity in an Alaskan fjord. *Sedimentology*, v. **46**, p. 1109–1126.
- CURTIS, J.W., JENKINS, G.W. AND GRAVESTOCK, D.I., 1991, Mississippi valley type Lead-Zinc mineralization northern Flinders Ranges, South Australia. *Geological Survey of South Australia Report Book*, 91/102, p. 280.
- DALGARNO, C.R. AND JOHNSON, J.E., 1968, Diapiric structures and late Precambrian-early Cambrian sedimentation in Flinders Ranges, South Australia. In: Diapirism and Diapirs (Eds J. Braunstein and G.D. O'Brien) *AAPG Memoir*, v. **8**, p. 301–314.
- DAVISON, I., BOSENCE, D., ALSOP, G.I. AND AL-AWAH, M.H., 1996, Deformation and sedimentation around active Miocene salt diapirs on the Tihama Plain, northwest Yemen. *Geological Society of London Special Publication*, v. **100**, p. 23–39.
- DIBONA, P., 1989, Geological History and Sequence Stratigraphy of the Late Proterozoic Wonoka Formation, Northern Flinders Ranges, South Australia. PhD thesis. Flinders University, Adelaide, Australia.
- DIBONA, P.A., 1991, A previously unrecognised Late Proterozoic succession: Upper Wilpena Group, northern Flinders Ranges, South Australia. *Quarterly Geological Notes Geological Survey of South Australia*, v. **117**, p. 2–9.
- DIBONA, P.A., VON DER BORCH, C.V.D. AND CHRISTIE-BLICK, N., 1990, Sequence stratigraphy and evolution of a basin-slope succession: the Late Proterozoic Wonoka Formation, Flinders Ranges, South Australia. *Australian Journal of Earth Science*, v. **37**, p. 135–145.
- DIREEN, N.G. AND JAGO, J.B., 2008, The Cottons Breccia (Ediacaran) and its tectonostratigraphic context within the Grassy Group, King Island, Australia: a rift-related gravity slump deposit. *Precambrian Research*, v. **165**, p. 1–14.
- DREXEL, J.F., PREISS, W.V. AND PARKER, A.J., eds., 1993, The Geology of South Australia, vol. 1, Precambrian. *Bulletin of the Geologic Survey of South Australia*, v. **54**, 242 p.

- DYSON, I.A., 1996, A new model for diapirism in the Adelaide Geosyncline. *MESA Journal*, v. **3**, p. 41–48.
- DYSON, I.A., 1999, The Beltana Diapir – a salt withdrawal minibasin in the northern Flinders Ranges. *MESA Journal*, v. **15**, p. 40–46.
- DYSON, I.A., 2001, The diapir-base metal association in the northern Flinders Ranges. *MESA J.*, 22, 37–43. Dyson, I.A. (2003) A new model for the Wonoka canyons in the Adelaide Geosyncline. *MESA Journal*, v. **31**, p. 49–58.
- DYSON, I.A., 2004a, Interpreted shallow and deep water depositional systems of the Beltana mini-basin in the northern Flinders Ranges, South Australia. In: Salt-Sediment Interactions and Hydrocarbon Prospectivity: Concepts, Applications, and Case Studies for the 21<sup>st</sup> Century (Eds P.J. Post, D.L. Olson, K.T. Lyons, S.L. Palmes, P.F. Harrison and N.C. Rosen), p. 997–1030. GCSSEPM Bob F. Perkins Research Conference.
- DYSON, I.A., 2004b, Christmas Tree Diapirs and Development of Hydrocarbon Reservoirs: a model from the Adelaide Geosyncline, South Australia. In: Salt-Sediment Interactions and Hydrocarbon Prospectivity: Concepts, Applications, and Case Studies for the 21<sup>st</sup> Century (Eds P.J. Post, D.L. Olson, K.T. Lyons, S.L. Palmes, P.F. Harrison and N.C. Rosen), p. 133–165. 24<sup>th</sup> GCSSEPM Bob F. Perkins Research Conference.
- DYSON, I.A., 2005, Formation of submarine unconformities in halotectonic mini-basins during passive margin development of the Adelaide Geosyncline, South Australia. In: Petroleum Systems of Divergent Continental Margin Basins (Eds P.J. Post, N.C. Rosen, D.L. Olson, S.L. Palmes, K.T. Lyons and G.B. Newton), p. 679–721. 25<sup>th</sup> GCSSEPM Bob F. Perkins Research Conference.
- DYSON, I.A. AND MARSHALL, T.R., 2007, Neoproterozoic salt nappe complexes and salt-withdrawal mini-basins in the Amadeus Basin. In: Proceedings of the Central Australian Basins Symposium (CABS), Alice Springs, Northern Territory, 16–18 August, 2005 (Eds T.J. Munson and G.J. Ambrose), p. 16–18.
- DYSON, I.A. AND ROWAN, M.G., 2004, Geology of a Welded Diapir and Flanking Mini-Basins in the Flinders Ranges of South Australia. In: Salt-Sediment



Interactions and Hydrocarbon Prospectivity: Concepts, Applications, and Case Studies for the 21st Century (Eds P.J. Post, D.L. Olson, K.T. Lyons, S.L. Palmes, P.F. Harrison and N.C. Rosen), p. 69–89. GCSSEPM Bob F. Perkins Research Conference.

EYLES, N. AND JANUSZCZAK, N., 2004, 'Zipper-rift': a tectonic model for Neoproterozoic glaciations during the breakup of Rodinia after 750 Ma. *Earth-Science Reviews*, v. **65**, p. 1–73.

FERRER, O., ARBUÉS, P., ROCA, E., GILES, K., ROWAN, M.G., DE MATTEIS, M. AND MUNOZ, J.A., 2014, Effect of Diapir Growth on Synkinematic Deepwater Sedimentation: the Bakio Diapir (Basque-Cantabrian Basin, Northern Spain). AAPG Search and Discovery Article #90189.

FORBES, B.G., 1966, The geology of the Marree 1: 250,000 map area. *Department of Mines Report of Investigations*, v. **28**, p. 47.

FORBES, B.G., 1971, Stratigraphic subdivision of the Pound Quartzite (late Precambrian, South Australia). *Transactions of the Royal Society of South Australia*, v. **95**, p. 219–225.

GEHLING, J.G., 1982, Sedimentology and Stratigraphy of the Late Precambrian Pound Subgroup, Central Flinders Ranges, S.A. MSc thesis. University of Adelaide, Adelaide, Australia.

GEHLING, J.G., 2000, Environmental interpretation and a sequence stratigraphic framework for the terminal Proterozoic Ediacara Member within the Rawnsley Quartzite, South Australia. *Precambrian Research*, v. **100**, p. 65–95.

GILES, K.A. AND LAWTON, T.F., 2002, Halokinetic sequence stratigraphy adjacent to the El Papalote diapir, northeastern Mexico. *AAPG Bulletin*, v. **86**, p. 823–840.

GREY, K. AND CORKERON, M., 1998, Late Neoproterozoic stromatolites in glacial successions of the Kimberley region, Western Australia: evidence for a younger Marinoan glaciation. *Precambrian Research*, v. **92**, p. 65–87.

HEARON, T.E., ROWAN, M.G., LAWTON, T.F., HANNAH, P.T. AND GILES, K.A., 2014, Geology and tectonics of Neoproterozoic salt diapirs and salt sheets in the

- eastern Willouran Ranges, South Australia. *Basin Research*, doi:10.1111/bre.12067.
- HEARON, T.E., ROWAN, M.G., LAWTON, T.F., HANNAH, P.T. AND GILES, K.A., 2015, Geology and tectonics of Neoproterozoic salt diapirs and salt sheets in the eastern Willouran Ranges, South Australia. *Basin Research*, v. **27**, p. 183–207.
- HEBERT, C.L., KAUFMAN, A.J., PENNISTON-DORLAND, S.C. AND MARTIN, A.J., 2010, Radiometric and stratigraphic constraints on terminal Ediacaran (post-Gaskiers) glaciation and metazoan evolution. *Precambrian Research*, v. **182**, p. 402–412.
- HOFFMAN, P.F. AND LI, Z.X., 2009, A palaeogeographic context for Neoproterozoic glaciation. *Palaeogeography, Palaeoclimatology, Palaeoecology*, v. **277**, p. 158–172.
- HOFFMAN, P.F. AND SCHRAG, D.P., 2002, The snowball Earth hypothesis: testing the limits of global change. *Terra Nova*, v. **14**, p. 129–155.
- HOFFMAN, P.F., CALVER, C.R. AND HALVERSON, G.P., 2009, Cottons Breccia of King Island, Tasmania: glacial or nonglacial, Cryogenian or Ediacaran? *Precambrian Research*, v. **172**, p. 311–322.
- JACKSON, C.A.L., 2012, The initiation of submarine slope failure and the emplacement of mass transport complexes in salt-related minibasins: A three-dimensional seismic reflection case study from the Santos Basin, offshore Brazil. *Geologic Society of America Bulletin*, v. **124**, p. 746–761.
- JACKSON, M.P.A. AND HARRISON, J.C., 2006, An allochthonous salt canopy on Axel Heiberg Island, Sverdrup Basin, Arctic Canada. *Geology*, v. **34**, p. 1045–1048.
- JENKINS, R.J., 2011, Billy Springs Glaciation, South Australia. In: The Geological Record of Neoproterozoic Glaciations (Eds E. Arnaud, G.P. Halverson and G. Shields-Zhou), *Geologic Society of London Memoir*, v. **36**, p. 693–699.
- JENKINS, R., HAINES, P.W. AND GOSTIN, V.A., 1988, The Ediacaran revisited. *Geological Society of Australia Abstracts*, v. **21**, p. 203–204.
- JOHNSON, S.P., 2013, The Birth of Supercontinents and the Proterozoic Assembly

- of Western Australia. Geological Survey of Western Australia, Perth, 78 p.
- KERNEN, R.A., GILES, K.A., ROWAN, M.G., LAWTON, T.F. AND HEARON, T.E., 2012, Depositional and halokinetic-sequence stratigraphy of the Neoproterozoic Wonoka Formation adjacent to Patawarta allochthonous salt sheet, Central Flinders Ranges, South Australia. *Geologic Society of London Special Publication*, v. **363**, p. 81–105.
- LAMB, M.P., TONIOLO, H. AND PARKER, G., 2006, Trapping of sustained turbidity currents by intraslope minibasins. *Sedimentology*, v. **53**, p. 147–160.
- LAUDON, R.C., 1984, Evaporite diapirs in the La Popa basin, Nuevo Leon, Mexico. *Geologic Society of America Bulletin*, v. **95**, p. 1219–1225.
- LEMON, N.M., 1985, Physical modeling of sedimentation adjacent to diapirs and comparison with late Precambrian Oratunga breccia body in central Flinders Ranges, South Australia. *AAPG Bulletin*, v. **69**, p. 1327–1338.
- LEMON, N.M., 2000, A Neoproterozoic fringing stromatolite reef complex, Flinders Ranges, South Australia. *Precambrian Research*, v. **100**, p. 109–120.
- Li, Z.X., Bogdanova, S.V., Collins, A.S., Davidson, A., De Waele, B., Ernst, R.E., Fitzsimons, I.C.W., Fuck, R.A., Gladkochub, D.P., Jacobs, J., Karlstrom, K.E., Lu, S., Natapov, L.M., Pease, V., Pisarevsky, S.A., Thrane, K. and Vernikovsky, V., 2008, Assembly, configuration, and break-up history of Rodinia: a synthesis. *Precambrian Research*, v. **160**, p. 179–210.
- LI, Z.X., EVANS, D.A. AND HALVERSON, G.P., 2013, Neoproterozoic glaciations in a revised global palaeogeography from the breakup of Rodinia to the assembly of Gondwanaland. *Sedimentary Geology*, v. **294**, p. 219–232.
- MADOF, A.S., CHRISTIE-BLICK, N. AND ANDERS, M.H., 2009, Stratigraphic controls on a salt-withdrawal intraslope minibasin, north-central Green Canyon, Gulf of Mexico: implications for misinterpreting sea level change. *AAPG Bulletin*, v. **93**, p. 535–561.
- MALLARINO, G., BEAUBOUEF, R.T., DROXLER, A.W., ABREU, V. AND LABEYRIE, L., 2006, Sea level influence on the nature and timing of a minibasin sedimentary fill

- (northwestern slope of the Gulf of Mexico). *AAPG Bulletin*, v. **90**, p. 1089–1119.
- MANNIE, A.S., JACKSON, C.A.L. AND HAMPSON, G.J., 2014, Shallow-marine reservoir development in extensional diapir-collapse minibasins: an integrated subsurface case study from the Upper Jurassic of the Cod terrace, Norwegian North Sea. *AAPG Bulletin*, v. **98**, p. 2019–2055.
- MATTHEWS, W.J., HAMPSON, G.J., TRUDGILL, B.D. AND UNDERHILL, J.R., 2007, Controls on fluviolacustrine reservoir distribution and architecture in passive salt diapir provinces: insights from outcrop analogs. *AAPG Bulletin*, v. **91**, p. 1367–1403.
- MAZUMDER, R. AND ARIMA, M., 2013, Tidal rhythmites in a deep sea environment: an example from Mio-Pliocene Misaki Formation, Miura Peninsula, Japan. *Marine and Petroleum Geology*, v. **43**, p. 320–325.
- NARBONNE, G.M., 2005, The Ediacara biota: Neoproterozoic origin of animals and their ecosystems. *Annual Review of Earth and Planetary Sciences*, v. **33**, p. 421–442.
- NEWELL, A.J., BENTON, M.J., KEARSEY, T., TAYLOR, G., TWITCHETT, R.J. AND TVERDOKHLEBOV, V.P., 2012, Calcretes, fluviolacustrine sediments and subsidence patterns in Permo-Triassic salt-walled minibasins of the south Urals, Russia. *Sedimentology*, v. **59**, p. 1659–1676.
- OLSON, H.C. AND DAMUTH, J.E., 2010, Character, Distribution and Timing of Latest Quaternary Mass-Transport Deposits in Texas—Louisiana Intraslope Basins Based on High- Resolution (3.5 kHz) Seismic Facies and Piston Cores. In: Submarine Mass Movements and Their Consequences (Eds D.C. Mosher, L. Moscardelli, R.C. Shipp, J.D. Chaytor, C.D.P. Baxter, H.J. Lee and R. Urgeles), p. 607–617. Springer, Dordrecht, The Netherlands.
- PAUL, E., FLOTTMANN, T. AND SANDIFORD, M., 1999, Structural geometry and controls on basement-involved deformation in the northern Flinders Ranges, Adelaide Fold Belt, South Australia. *Australian Journal of Earth Science*, v. **46**, p. 343–354.
- PELL, S.D., MCKIRDY, D.M., JANSYN, J. AND JENKINS, R.J.F., 1993, Ediacaran carbon

- isotope stratigraphy of South Australia—an initial study. *Transactions of the Royal Society of South Australia*, v. **117**, p. 153–161.
- PICKERING, K.T., HISCOTT, R.N. AND HEIN, F.J., 1989, Deep-Marine Environments: Clastic Sedimentation and Tectonics. Unwin Hyman, London, 416 p.
- PILCHER, R.S., KILSDONK, B. AND TRUDE, J., 2011, Primary basins and their boundaries in the deep-water northern Gulf of Mexico: origin, trap types, and petroleum system implications. *AAPG Bulletin*, v. **95**, p. 219–240.
- PLUMMER, P.S., 1978, Note on the palaeoenvironmental significance of the Nuccaleena Formation (upper Precambrian), central Flinders Ranges, South Australia. *Journal of the Geological Society of Australia*, v. **25**, p. 395–402.
- POPRAWSKI, Y., BASILE, C., AGIRREZABALA, L.M., JAILLARD, E., GAUDIN, M. AND JACQUIN, T., 2014, Sedimentary and structural record of the Albian growth of the Bakio salt diapir (the Basque Country, northern Spain). *Basin Research*, v. **26**, p. 746–766.
- POSAMENTIER, H.W. AND ALLEN, G.P., 1999, Siliciclastic Sequence Stratigraphy: Concepts and Applications (Vol. 7). SEPM (Society for Sedimentary Geology), Tulsa, 204 p.
- POSTMA, G., NEMEC, W. AND KLEINSPEHN, K.L., 1988, Large floating clasts in turbidites: a mechanism for their emplacement. *Sedimentary Geology*, v. **58**, p. 47–61.
- PRATHER, B.E., 2000, Calibration and visualization of depositional process models for above-grade slopes: a case study from the Gulf of Mexico. *Marine and Petroleum Geology*, v. **17**, p. 619–638.
- PREISS, W.V., 1987, The Adelaide Geosyncline—Late Proterozoic stratigraphy, sedimentation, paleontology and tectonics. *Bulletin of the Geological Survey of South Australia*, v. **53**, p. 438.
- PREISS, W.V., 1990, A stratigraphic and tectonic overview of the Adelaide Geosyncline, South Australia. In: The Evolution of a Late Precambrian–Early Palaeozoic Rift Complex: The Adelaide Geosyncline (Eds J.B. Jago and P.S.

- Moore), *Geological Society of Australia Special Publication*, v. **16**, p. 1–33.
- PREISS, W.V., 1999, Parachilna, South Australia, Sheet SH54-13. 1: 250 000 Geological Series Explanatory Notes, 2<sup>nd</sup> edn. PIRSA, Adelaide, 52 p.
- PREISS, W.V., 2000, The Adelaide Geosyncline of South Australia and it's significance in Neoproterozoic continental reconstruction. *Precambrian Research*, v. **100**, p. 21–63.
- REBESCO, M., HERNANDEZ-MOLINA, F.J., VAN ROOIJ, D. AND WAHLIN, A., 2014, Contourites and associated sediments controlled by deep-water circulation processes: state-of-the art and future considerations. *Marine Geology*, v. **352**, p. 111–154.
- REID, P.W., 1992, Stratigraphy, Structure, and Stable Isotope Analysis of the Billy Springs Formation, Mt. Freeling Syncline, S.A. Honors Thesis. University of Adelaide, Adelaide, Australia.
- REILLY, M., 2001, Deepwater Reservoir Analogue – Bunkers Sandstone, Donkey Bore Syncline, Flinders Ranges Australia. Honours Thesis. University of Adelaide, Adelaide, Australia.
- RIBES, C., KERGARAVAT, C., BONNEL, C., CRUMEYROLLE, P., CALLOT, J.P., POISSON, A., TEMIZ, H. AND RINGENBACH, J.C., 2015, Fluvial sedimentation in a salt-controlled mini-basin: stratal patterns and facies assemblages, Sivas Basin, Turkey. *Sedimentology*, v. **62**, p. 1513–1545.
- RINGENBACH, J.C., SALEL, J.F., KERGARAVAT, C., RIBES, C., BONNEL, C. AND CALLOT, J.P., 2013, Salt tectonics in the Sivas Basin, Turkey: outstanding seismic analogues from outcrops. *First Break*, v. **31**, p. 93–101.
- ROWAN, M.G. AND VENDEVILLE, B.C., 2006, Foldbelts with early salt withdrawal and diapirism: physical model and examples from the northern Gulf of Mexico and the Flinders Ranges, *Australia. Marine and Petroleum Geology*, v. **23**, p. 871–891.
- ROWAN, M.G., LAWTON, T.F., GILES, K.A. AND RATLIFF, R.A., 2003, Near-salt deformation in La Popa basin, Mexico, and the northern Gulf of Mexico: a

- general model for passive diapirism. *AAPG Bulletin*, v. **87**, p. 733–756.
- Saura, E., Verges, J., Martín-Martín, J.D., Messenger, G., Moragas, M., Razin, P., Grelaud, C., Jousiaume, R., Malaval, M., Homke, S. and Hunt, D.W., 2014, Syn-to post-rift diapirism and minibasins of the Central High Atlas (Morocco): the changing face of a mountain belt. *Journal of the Geological Society of London*, v. **171**, p. 97–105.
- SHANMUGAM, G., 1980, Rhythms in deep sea, fine-grained turbidite and debris-flow sequences, Middle Ordovician, eastern Tennessee. *Sedimentology*, v. **27**, p. 419–432.
- SHANMUGAM, G., 2008, Deep-water bottom currents and their deposits. In: *Contourites* (Eds M. Rebesco and A. Camerlenghi), *Developments in Sedimentology*, v. **60**, p. 59–81.
- SHEARD, M.J., 2012, Explanatory Notes for MARREE 1:250,000 Geological Map, Sheet SH 54–5. Report Book 2012/00004. Department for Manufacturing, Innovation, Trade, Resources and Energy, Adelaide, 231 p.
- SHULTZ, M.R. AND HUBBARD, S.M., 2005, Sedimentology, stratigraphic architecture, and ichnology of gravity-flow deposits partially ponded in a growth-fault-controlled slope minibasin, Tres Pasos Formation (Cretaceous), southern Chile. *Journal of Sedimentary Research*, v. **75**, p. 440–453.
- STOW, D.A.V., 1985, Deep sea clastics: where are we and where are we going? In: *Sedimentology: Recent Developments and Applied Aspects* (Eds P.J. Brenchley and B.P.J. Williams), p. 67–93. Blackwell Scientific Publications, Oxford.
- STOW, D.A. AND MAYALL, M., 2000, Deep-water sedimentary systems: new models for the 21st century. *Marine and Petroleum Geology*, v. **17**, p. 125–135.
- STOW, D.A.V. AND PIPER, D.J.W., 1984, Deep-water fine-grained sediments: facies models. *Geological Society of London Special Publication*, v. **15**, p. 611–646.
- STRACHAN, L.J., 2008, Flow transformations in slumps: a case study from the Waitemata Basin, New Zealand. *Sedimentology*, v. **55**, p. 1311–1332.

- TRUDGILL, B.D., 2011, Evolution of salt structures in the northern Paradox Basin: controls on evaporite deposition, salt wall growth and supra-salt stratigraphic architecture. *Basin Research*, v. **23**, p. 208–238.
- TRUDGILL, B.D. AND PAZ, M., 2009, Restoration of mountain front and salt structures in the northern Paradox Basin, SE Utah. In: *The Paradox Basin Revisited – New Developments in Petroleum Systems and Basin Analysis* (Eds W.S. Houston, L.L. Wray and P.G. Moreland), p. 132–177. RMAG Special Publication, Denver, CO.
- TRUDGILL, B., BANBURY, N. AND UNDERHILL, J., 2004, Salt evolution as a control on structural and stratigraphic systems: northern Paradox foreland basin, southeast Utah, USA. In: *Salt–Sediment Interactions and Hydrocarbon Prospectivity: Concepts, Applications, and Case Studies for the 21st century* (Eds P. Post, D. Olson, K. Lyons, S. Palmes, P. Harrison and N. Rosen), pp. 669–700. 24<sup>th</sup> Annual GCSSEPM Bob F. Perkins Research Conference.
- VAN LOON, A.J., 2009, Soft-sediment deformation structures in siliciclastic sediments: an overview. *Geologos*, v. **15**, p. 3–55.
- VENUS, J.H., MOUNTNEY, N.P. AND MCCAFFREY, W.D., 2015, Syn-sedimentary salt diapirism as a control on fluvial system evolution: an example from the proximal Permian Cutler Group, SE Utah, USA. *Basin Research*, v. **27**, p. 152–182.
- VON DER BORCH, C.C. AND GRADY, A.E., 1982, Wonoka Formation and Billy Springs Beds: reconnaissance interpretation. *Transactions of the Royal Society of South Australia*, v. **106**, p. 217–219.
- VON DER BORCH, C.C., SMIT, R. AND GRADY, A.E., 1982, Late Proterozoic submarine canyons of Adelaide Geosyncline, South Australia. *AAPG Bulletin*, v. **66**, p. 332–347.
- WEEKS, W., 2010, *On Sea Ice*. University of Alaska Press, Fairbanks, 664 p.
- WILLIAMS, G.E., 1988, Cyclicity in the late Precambrian Elatina Formation, South Australia: solar or tidal signature? *Climate Change*, v. **13**, p. 117–128.
- WILLIAMS, G.E., 1990, Precambrian cyclic rhythmites: solar, climatic or tidal



signatures? *Philosophical Transactions of the Royal Society of London Series A, Mathematical and Physical Sciences*, v. **330**, p. 445–458.

WINKER, C.D., 1996, High-resolution seismic stratigraphy of a late Pleistocene submarine fan ponded by salt-withdrawal mini-basins on the Gulf of Mexico continental slope. *Offshore Technology Conference Paper 8024*, p. 619–628.

*Manuscript received 27 March 2015; revision accepted 27 October 2015*

## **Chapter 7: Conclusions**

## 7.1: Summary and Implications

Together, the papers presented in this thesis document the sedimentological and stratigraphic properties of the Bonney Sandstone and related strata. By integrating numerous field and laboratory methodologies, the work presented here reconstructs key aspects of the paleogeography, depositional environments, and sediment sources for the Adelaide Rift Complex. In addition to the specific relevance for Australia, this thesis can also be considered a case study in the analysis and interpretation of an ancient sedimentary system. The results presented here serve as a useful analogue for similar sediments in other localities and time periods, especially those where available data is limited in quantity or quality.

The Bonney Sandstone and Billy Springs Formation are the product of deposition on the passive margin of the Australian subcontinent during the late Ediacaran Period. Due to the lack of detailed work on these formations prior to this thesis, few definitive interpretations have previously been put forward. Thus, the basic sedimentological analysis presented here is the first in-depth study on this interval, filling a knowledge gap in the larger understanding of the history of the Adelaide Rift Complex. The findings discussed in Chapters 3 and 4 show that the interval is dominated by marine deltaic and fluvial sediments contained in a series of stacked, internally shallowing-upward parasequences. These parasequences also show a shallowing-upward trend across the formation as deltaic sands prograde outward into the basin and decrease available accommodation space. Spatial changes in depositional process reflect geographical proximity to the delta mouth, with Sections CR and MW in the northern part of the basin (discussed in Chapter 3) containing a higher proportion of fluvially influenced sediments compared to the type

section further south (Section BG). Sections CR and MW also preserve additional parasequences atop those seen in the central Flinders Ranges where the type section is located, with thickness increasing threefold over the course of ca 100 kilometres. This is consistent with a significant depocentre in the northern part of the basin.

U/Pb ages determined from over 2000 individual detrital zircon grains in the Bonney Sandstone, Rawnsley Quartzite, and Billy Springs Formation all show a highly consistent spectrum of source ages. Each sample analysed is dominated by a single population of zircons formed between 1100-1200 million years ago. This time period is consistent with zircon-forming events in several cratonic provinces in both Australia and Antarctica, which were connected at the time. However, the most parsimonious reconstruction of sediment transport pathways suggests that the late Ediacaran sediments in the Adelaide Rift Complex originate from the central Australian Musgrave province. Sediment was likely transported to the southeast via the Willouran Trough, an aulacogen extending northwest/southeast that may have held an axial river system at the time of deposition. Although no Ediacaran sediments are preserved in this area, this hypothetical transport system is consistent with both zircon provenance and sedimentological evidence, which indicates increased fluvial input in the area where this system would enter the basin. Zircons in the Rawnsley Quartzite and Billy Springs Formation show this same pattern of age distribution, suggesting a widespread, consistent sediment source across millions of years.

The sediments discussed here are also relatively unique in that they display numerous features that indicate the presence of active salt tectonics during deposition. In Chapters 5 and 6, these salt-influenced sediments are discussed in

the context of two separate salt-withdrawal minibasins. These two minibasins may have formed at roughly the same time, but display very different internal character. The Mt. Frome minibasin (Chapter 5) is filled by a succession of Pound Subgroup and Cambrian sediments that show numerous indications of interaction between sediments and exposed salt. The Wonoka Formation and Bonney Sandstone in particular contain abundant clastic pebble-cobble conglomerates within otherwise sand, shale, or carbonate-dominated formations; a lithofacies not seen outside of the immediate area surrounding the diapir body. Conglomerates are interpreted to have been reworked from exposed diapir caprock and redeposited into the formation, and are most abundant nearest the diapir-minibasin contact and in the areas near significant fault scarps. Syndepositional growth faulting, diapir uplift, and the subaerial/subaqueous exposure of diapir caprock also influence the depositional processes occurring in the formation, with gravity-driven mass flow processes being more common than elsewhere in the formation. Sedimentation in the minibasin is therefore a complex interplay between background environmental conditions, diapir proximity, and the degree and rate of erosion of diapir body.

Internal sedimentological variability in minibasin settings is exemplified by comparing the features seen in Mt. Frome with those exposed in the Umberatana syncline, discussed in Chapter 6. This minibasin lies in the northern part of the basin and is filled with the dominantly fine-grained Billy Springs Formation. Unlike the sediments seen at Mt. Frome, minibasin fill in this instance is dominated by mudstones, with very few sandstone interbeds. Mudstones are either planar- or convolute-laminated, reflecting immature gravity-flow processes (slumping) in a deepwater setting. The presence of shelf-slope sediments in the northern Adelaide Rift Complex indicates the presence of a northern depocentre and possible oceanic

connection in this area. This study is one of few worldwide to document an outcropping deepwater minibasin, providing an excellent analogue for the many of the currently producing offshore provinces, e.g., those in the Gulf of Mexico, west Africa, and eastern Brazil.

The geological descriptions and interpretations in this thesis provide a new window into the landscape of Ediacaran Australia, and are a rare example of a Precambrian fluvial-deltaic system strongly influenced by salt tectonics. By examining the sedimentology, paleogeography, provenance, or halokinetic influence in these deposits, each chapter contributes significantly to the larger reconstruction of the basin as a whole. An in-depth understanding of each of these aspects, as presented here, is essential in assessing the utility of these sediments as an analogue for those elsewhere in the geologic record where less information may be available. By using multiple field and laboratory methodologies to investigate a sparsely studied depositional setting, this thesis is also a model for how similar research can be conducted in the future. When combined with additional research on other aspects of deposition, the types of studies conducted here have the potential to significantly impact interpretations of ancient strata beyond the immediate region. An analogue-based approach to interpretation has proved highly successful in the past; studies of sediments in the Mesozoic Book Cliffs (USA), for instance, have revolutionized our understanding of clastic depositional sequences, with research continuing over several decades. With more studies like the one presented here, the Adelaide Rift Complex also has the potential to become hugely important in the development of sedimentary and stratigraphic models that have global implications.

## 7.2 Future work

Although no significant issues were encountered during this research, much work remains to be done on the depositional environments of the basin fill, including the Bonney Sandstone. The measured sections that form the basis of this study are primarily located in the central and north-western areas of the Flinders Ranges; the sedimentary units that comprise them are also exposed in many other localities in the basin, some of which are hundreds of kilometres from the locations discussed here. Additional work on the lower Pound Subgroup should focus on expanding the spatial expanse of detailed measurements. Additional stratigraphic sections to the south, northwest, and east would greatly add to the paleogeographic reconstruction put forward here. Although the southernmost limit of Pound Subgroup sediments lies relatively far north (near Quorn), the change in environmental conditions toward the south is especially important, since most previous basin reconstructions interpret a connection to the open ocean in this direction. A change to deeper water conditions toward the southeast would support this hypothesis, as would the presence of clear indicators of tidal processes. Thus, a comparative study examining the change in sedimentary character along a north-south axis would improve understanding of the large-scale basin palaeogeography. Such a study would also be applicable to other units as well, and a future PhD project centred around determination of the paleogeography in the southern Flinders Ranges through time would have a significant impact on future basin reconstructions.

The provenance data reported here also provides a starting point from which to conduct future studies. Detrital zircon grains from the Bonney Sandstone and Billy Springs Formation are interpreted to originate from the central Australian Musgrave

Province; however, the Grenville-aged zircons seen in the Pound Subgroup also match zircon-forming events in Antarctica and in western Australia. Additional geochemical and isotopic fingerprinting techniques can provide a more certain determination of the origin of Adelaide Rift Complex sediments—Hafnium isotopes in zircons can be used to determine the origin of the cratonic provinces in which they are formed. Compositional isotopic differences exist between mantle-derived and recycled, melt-derived sources, which are imparted into the zircon grain and can be matched to known signatures of age-matching cratons. While zircon age populations were relatively consistent across the samples analysed in this study, more work could also be done on the changing source of zircons through time, as initially reported in previous literature. Sediments from lower in the basin fill contain more diverse populations sourced from other areas, and more detailed work could be done to better characterize the stratigraphic and geographical changes in these populations and the significance of changing sediment sources through time.

Research on the interaction between sediments and diapirs is currently an active research topic in the Adelaide Rift Complex, but generally from a structural or salt-tectonic viewpoint. Only recently have studies begun to study the detailed effects of diapirism on sedimentary character. There are over 100 individual diapirs exposed in the Flinders Ranges; the majority of these have not been studied in detail. Diapirs interact with the hundreds of formations that form the basin fill, and were active before, during, and after deposition. Each of these likely has unique properties, and much future work remains to be done characterizing diapir-influenced sediments in the basin.



## **Chapter 8: Appendices**

## 8.1: Files on CD

**PDF file of Chapter 3, as published in the *Australian Journal of Earth Sciences***

**PDF file of Chapter 6, as published in the journal *Sedimentology***

**Supplementary Data Set, Chapter 4:** Age determinations and error bars for each of the 2,424 zircon grains described in this study.

**Supplementary Data Set, Chapter 5:** KMZ file showing locations of measured sections. Waypoints correspond to bases of sections in Fig. 5.

**Supplementary Data Set, Chapter 6:** Fourier analysis spreadsheet related to Chapter 6, Figure 9, produced with assistance from Melissa Craig.

## 8.2: Supplementary Figures, Chapter 4

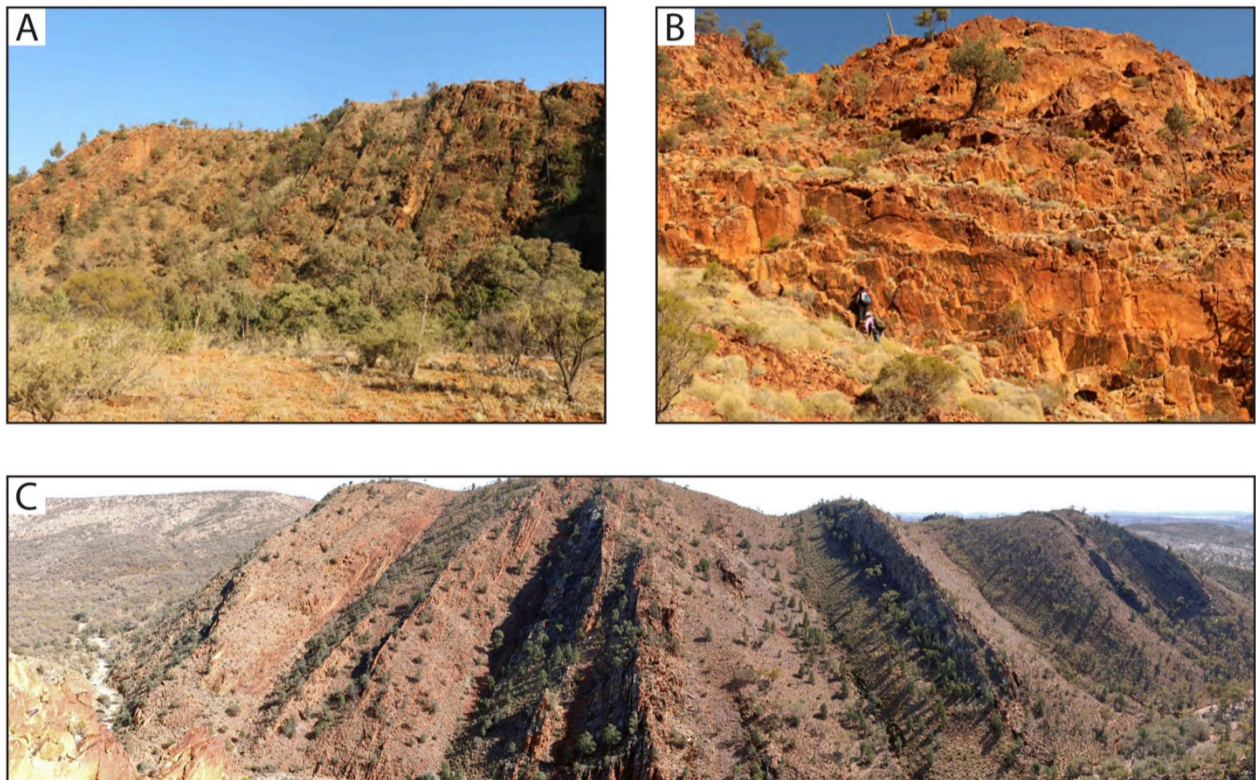


Figure 1: Representative outcrops of the Pound Subgroup in the northern Flinders Ranges, showing quality of exposures. A) Bonney Sandstone, section MW, Vulkathunha-Gammon Ranges National Park. B) Bedding-plane view of amalgamated sandstones in the upper Bonney Sandstone, section CR, Maynard's Well Station. Geologists measuring ripple marks for scale; view is of the underside of beds looking up section. C) Panorama view of section CR, including both the Bonney Sandstone and Rawnsley Quartzite. Exposure of rocks is continuous in creek bed. This photograph can be viewed in high resolution at <http://www.gigapan.com/gigapans/160548>.

### Convolute Lamination and Load Structures, Section MW

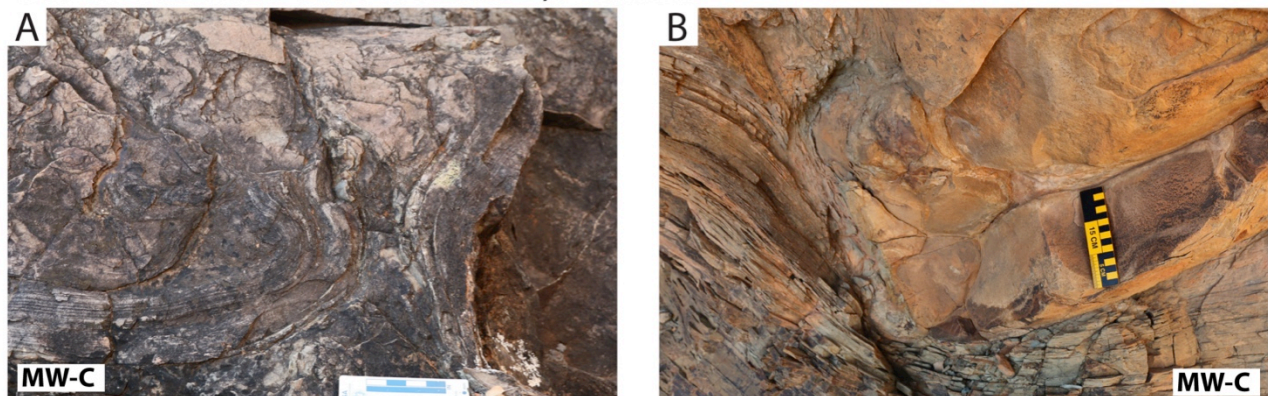


Figure 2: Photos of loading structures and and convolute lamination seen in unit MW-C and

**Lithofacies A1**

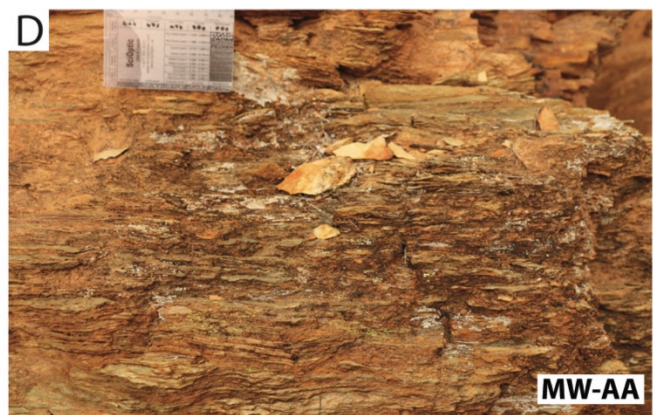


Figure 3: Additional photographs of Lithofacies A1. Section (MW or CR) and unit correspond to Figures 3 and 4.

**Lithofacies A2**

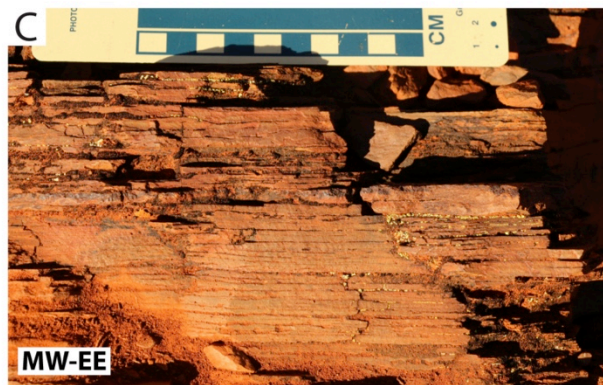
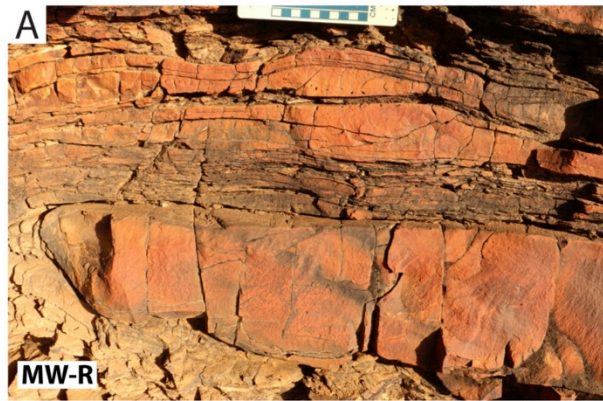
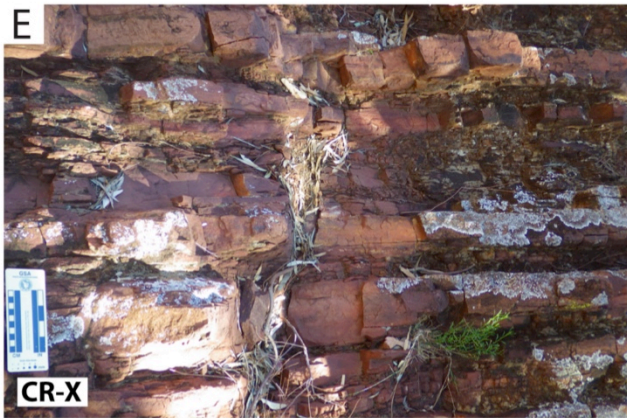


Figure 4: Additional photographs of Lithofacies A2. Section (MW or CR) and unit correspond to Figures 3 and 4.

**Lithofacies A3**



*Figure 5: Additional photographs of Lithofacies A3. Section (MW or CR) and unit correspond to Figures 3 and 4.*

**Lithofacies B1**

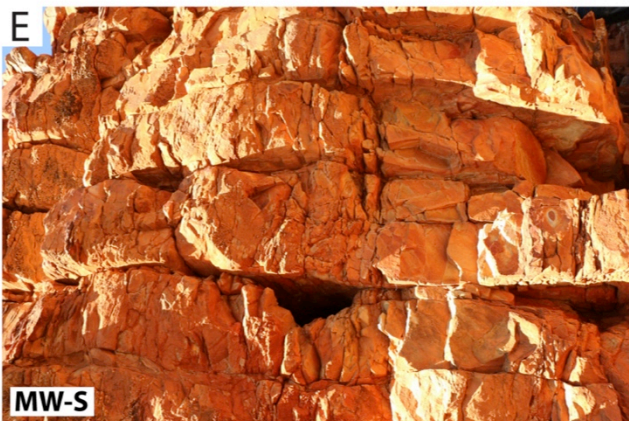
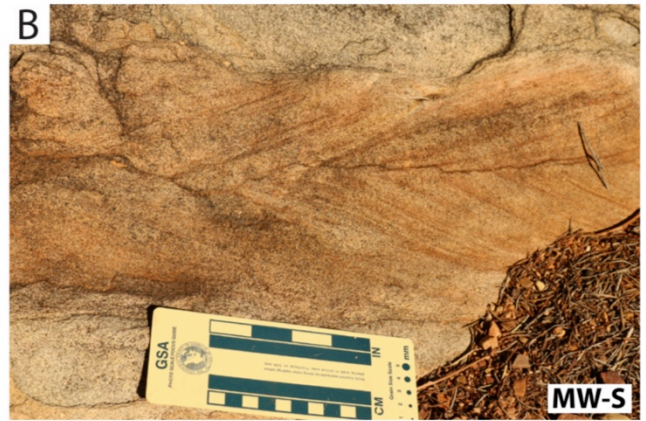


Figure 6: Additional photographs of Lithofacies B1. Section (MW or CR) and unit correspond to Figures 3 and 4.

**Lithofacies B2**



*Figure 7: Additional photographs of Lithofacies B2. Section (MW or CR) and unit correspond to Figures 3 and 4.*

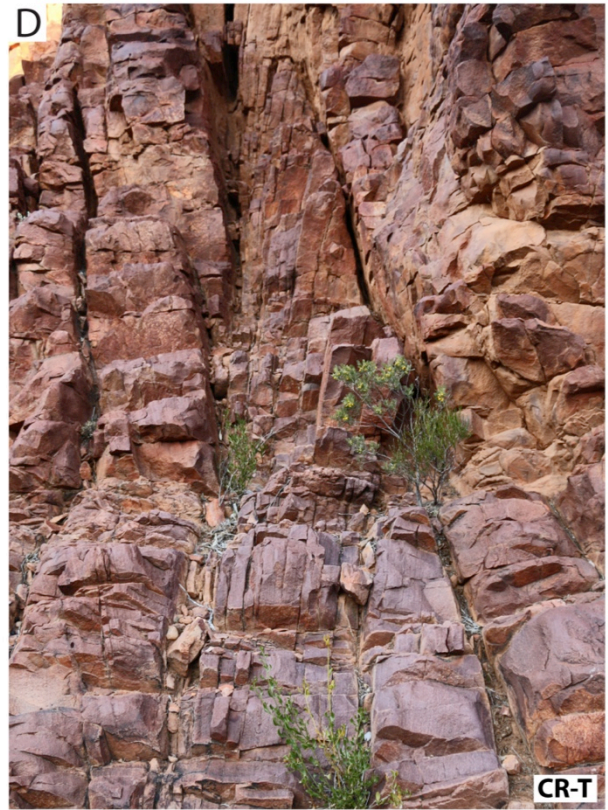


**Lithofacies C**



*Figure 8: Additional photographs of Lithofacies C. Section (MW or CR) and unit correspond to Figures 3 and 4.*

**Lithofacies D**



*Figure 9: Additional photographs of Lithofacies D. Section (MW or CR) and unit correspond to Figures 3 and 4.*

**Lithofacies F**

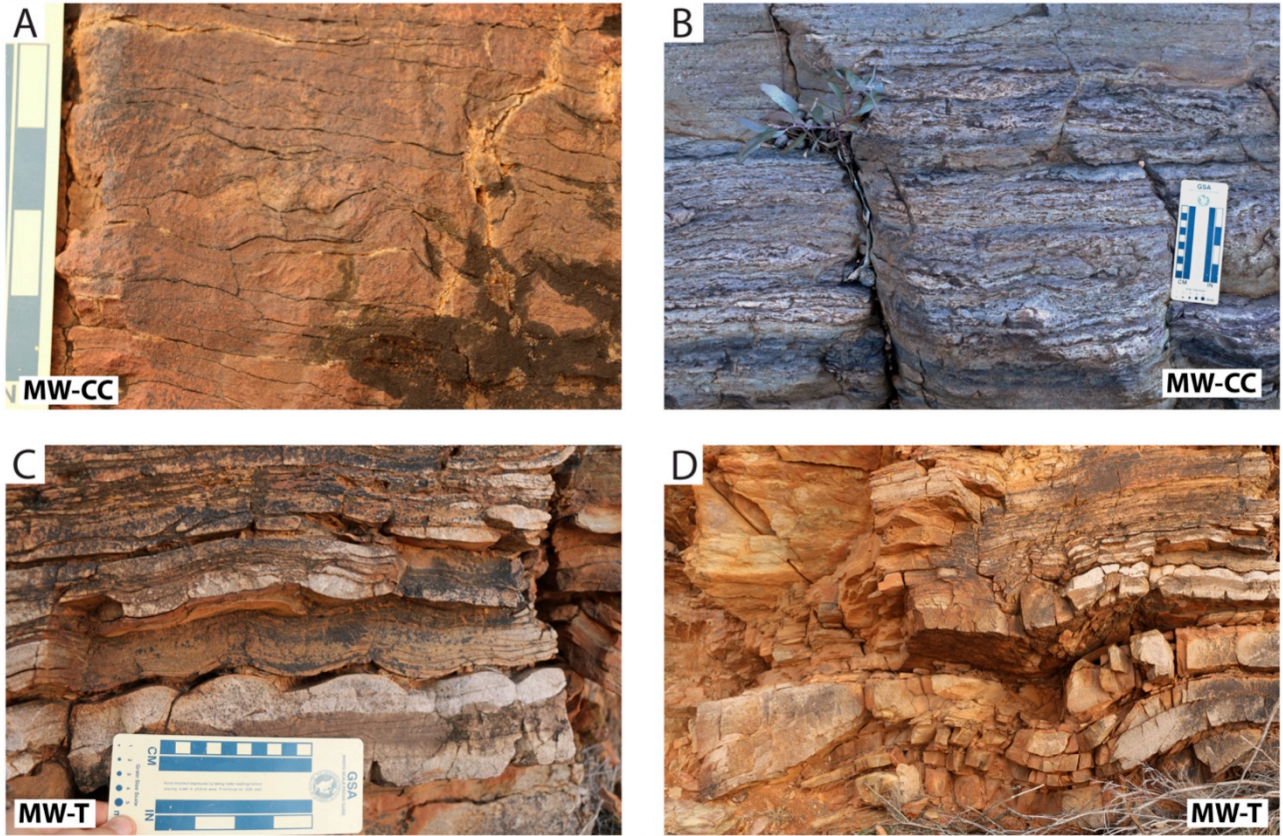


Figure 10: Additional photographs of Lithofacies F. Section (MW or CR) and unit correspond to Figures 3 and 4.

Age / Error	Unit or Sample
607.9 +/- 10.07	BG 378
610.1 +/-11.08	BG 375
568.3 +/- 9.1	CR-I
603.4 +/- 8.93	CR-R
561.9 +/-7.53	Rawnsley
595.5 +/-7.8	MW-TT
647.1 +/- 13.5	MW-H

Table 1: Summary of youngest individual concordant zircon ages in each sample.

## Section CR

Parasequence 7	
Interval	Interpretation
1049-1081	Chace; fluvial
1039-1049	Immature sands; floodplain
978-1039	Fluvial channels and overbank sands

Parasequence 6	
Interval	Interpretation
967-978	Channel sands
953-967	Channel sands / overbank/floodplain shales
910-953	Channel sands
875-910	Proximal or storm-dom. prodelta / interdistributary bay

Parasequence 5	
Interval	Interpretation
856-875	Immature sand; Mouth bar or channel
841-856	Lower USF
833-841	Storm sand?
808-833	Abundant thin sands; increasingly proximal
783-808	Storm-dominated shelf or prodelta

Parasequence 4	
Interval	Interpretation
752-783	Delta front / upper shoreface
722-752	Delta front
692-722	Proximal prodelta
682-692	Distal prodelta

Parasequence 3	
Interval	Interpretation
636-682	Fluvial; channel bar / proximal D.M.B.
620-636	Foreshore
609-620	Upper shoreface
596-609	Distal prodelta

Parasequence 2	
Interval	Interpretation
576-596	Proximal prodelta

Parasequence 1	
Interval	Interpretation
560-576	Distributary mouth bar
530-560	Delta front
515-530	Distal prodelta, increasingly proximal
500-515	Shelf/LSF

## Section MW

Parasequence 10	
Interval	Interpretation
1204-1224	Tidal or storm-inf. lagoon, washover flat?
1198-1204	Storm inf. lagoon
1190-1198	Fluvial-inf. Shoreface
1173-1190	Channelized TF?
1075-1173	Foreshore/USF w channels

Parasequence 9	
Interval	Interpretation
1054-1075	Distributary mouth bars
1018-1054	Fluvial/channel sands
1006-1018	Tidal flat or interdistributary bay

Parasequence 8	
Interval	Interpretation
991-1006	Upper shoreface / distributary mouth bar
986-991	Tidal/washover flat
945-986	Possible foreshore
937-945	Upper shoreface

Parasequence 7	
Interval	Interpretation
887-937	Tidal/washover flat
865-887	Channelized deltaic or fluvial sands
840-865	Shoreface/TF
835-840	Lagoon/back barrier
817-835	Dunes? USF bar/crest
775-817	Storm-dominated LSF or lagoon/back barrier

Parasequence 6	
Interval	Interpretation
704-775	Fluvial channel and washover sands
687-704	Algal tidal/washover flat
658-687	Channelized USF
650-658	Algal-dominated sandy tidal/washover flat
607-650	Storm-dominated prodelta

Parasequence 5	
Interval	Interpretation
589-607	Tidal channel? Similar to unit MW-H
585-589	Tidal flat / tidal-influenced lagoon
537-585	Distributary mouth bars
475-537	Channelized tidal flat?
454-475	Delta front sands
447-454	Storm dominated prodelta
425-447	Shoreface/foreshore
415-425	Lower shore face

Parasequence 4	
Interval	Interpretation
360-415	Thick delta front sands; more channel influence; / Distributary mouth bars
335-360	Proximal prodelta

Parasequence 3	
Interval	Interpretation
310-335	Thick delta front amalgamated sands
285-310	Increasingly proximal deltaic deposits
270-285	Storm-dominated proximal prodelta

Parasequence 2	
Interval	Interpretation
250-271	Upper shoreface
218-250	Upper shoreface

Parasequence 1	
Interval	Interpretation
132-218	Distributary mouth bars
125-132	Submarine tidal channel?
110-125	bay/inter-lobe/ upper LSF
70-110	Storm-deposited sands
0-70	Shelf/distal prodelta

Table 2: Detailed interpretations of sedimentary environments for sediments found in sections CR and MW. Interpretations represent only one possibility and are not regarded as definitive. Colors in tables represent lithofacies associations described in Table 1; parasequences can be found in Figure 11.

### 8.3: Supplementary Figures, Chapter 5

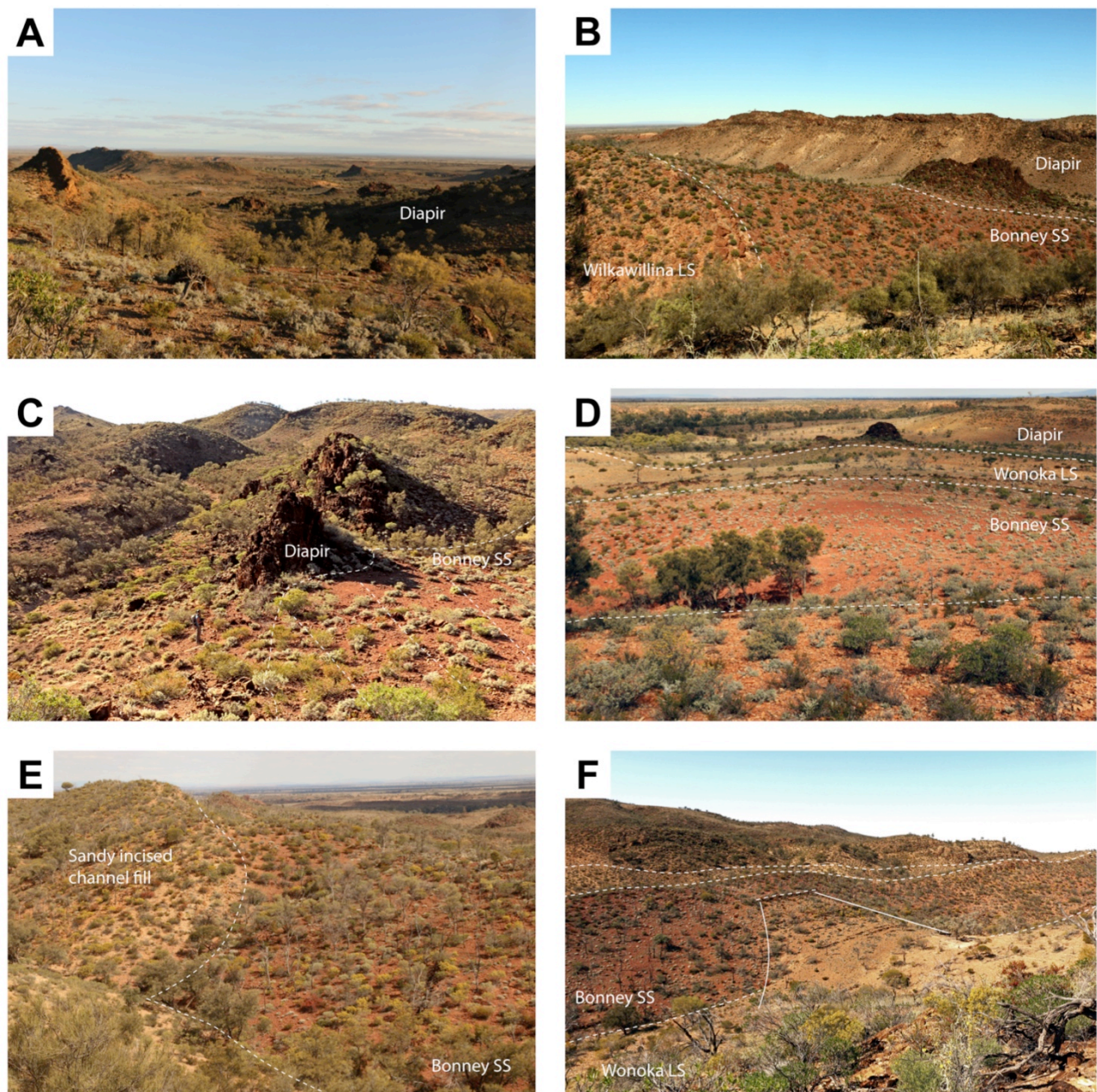
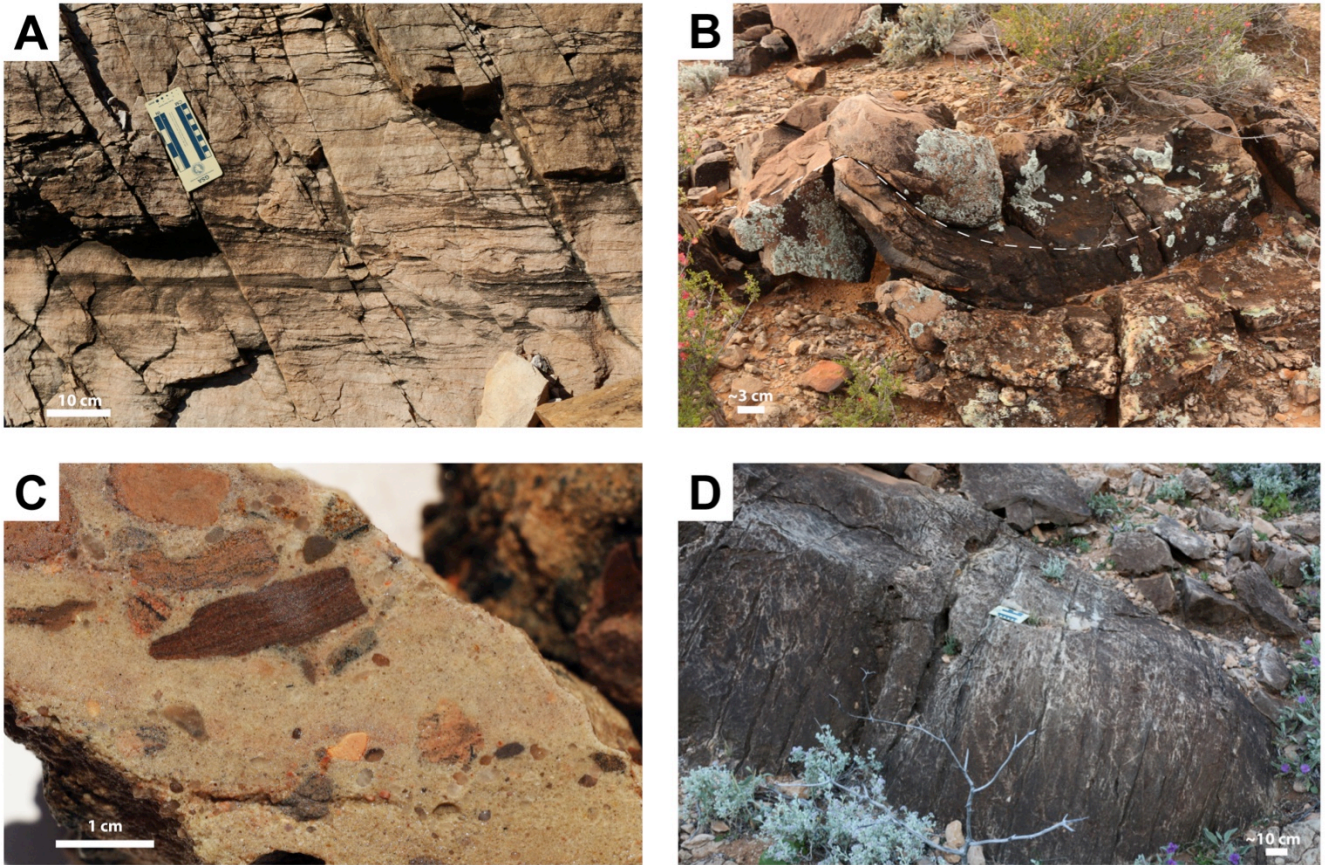


Figure 1: Landscapes and outcrop expression in study area. A) Typical landscape atop diapir body, with numerous irregular, resistant blocks of dolomitic breccia outcropping in high relief. B) Minibasin margin near section E, where Precambrian sedimentary units are relatively thinner than elsewhere in the transect. Here, no Wonoka Formation is present. C) Diapir- Bonney contact at section D, where Bonney Sandstone is rotated and in angular contact with diapir matrix. D) Minibasin margin just south of section B, looking west from Wilkawillina Formation. E) Incised channel fill in the Bonney Sandstone, between sections A and B. The base of this sand is shown by the orange line in Figure 3. F) Upthrown block or remnant ridge of Wonoka Formation protruding stratigraphically upward into Bonney Sandstone, just south of section A. This would have likely been an area of high topographic relief during Bonney deposition, as it is not caused by postdepositional faulting.



*Figure 2: Representative lithologies in the Rawnsley Quartzite and Wilkawillina Formations. A) Typical Rawnsley Quartzite sandstones, showing microfaulting, irregular horizontal laminae, and indistinct bedding. B) Large tepee structure in sandstone, origin and formation mechanism unknown. C) Slabbed face of the only observed conglomerate in the Rawnsley Quartzite. Pebble composition similar to that seen in other units below. D) Massive grey, thickly bedded micritic limestones typical of the Wilkawillina limestone. No clastics or conglomerates were seen in this formation.*

<i>Diapir</i>	<i>Known Movement</i>	<i>Notes</i>
Worumba	Torrensian-Sturtian	Unconformities and conglomerates in Sturtian sediments*
Arkaba	Sturtian	Thinning on eastern flank; no conglomerates*
Upalinna	Sturtian	Unconformities and conglomerates in Sturtian sediments*
Moralana	Sturtian	Unconformities and conglomerates in Sturtian sediments*
Oraparinna	Sturtian-Marinoan	Unconformities and conglomerates, associated E graben
Enorama	Sturtian-Marinoan	Onlap, reef growth, and boulder conglomerates*
Blinman	Sturtian	Boulders in surrounding units*
Oratunga	Marinoan	Conglomerates and onlap in surrounding units*
Wirrealpa	Cambrian	Erosion of diapir and Hawker Group near diapir, clastic cong. in CO <sub>3</sub>
Mt Frome	Ediacaran-Cambrian(?)	Conglomerates in Ediacaran, thinning in Cambrian, minibasin
Chambers	Cambrian	Allochthonous minibasin within diapir*
Nantawarrina	Ediacaran (?)	Intrusive into Ediacaran; uncertain whether syndepositional*
Pinda	Ediacaran	Conglom.in Bunyeroo & Bonney SS; Unconformity at base of Pound*
Patawarta	Ediacaran	Depositional thinning; conglomerates in Bonney Sandstone
Beltana	Ediacaran- E. Cambrian	Unconformities, conglom., and encased minibasin in Wilpena Gp.
Loch Ness	Sturtian-Cambrian	Reef associated w syndep. syncline; weld progresses to Cambrian
Burr	Sturtian	Little information available; angular uncon. on flanks*
Lyndhurst	Sturtian	Little information available; angular uncon. on flanks*
Willouran Ranges	Sturtian-Marinoan	~Five diapirs with unconformities, minibasins, and conglomerates

Data from Dalgarno and Johnson, 1968; Lemon, 1985; Cooper, 1991; Lemon, 2000; Dyson, 2004, 2004a; Dyson and Rowan, 2004; Hearon et al., 2015

\* Movement ages constrained by limited surrounding outcrops; no units of other ages in contact with diapir

Torrensian- Pre-glacial sediments >680 Ma

Sturtian- 720-680 Ma; older glacial sediments

Marinoan- 680-542 Ma; younger glacials; includes Ediacaran (635-542 Ma)

Table 1: Timing of movement of selected diapirs throughout the Adelaide Rift Complex. See Chapter 5 for references.

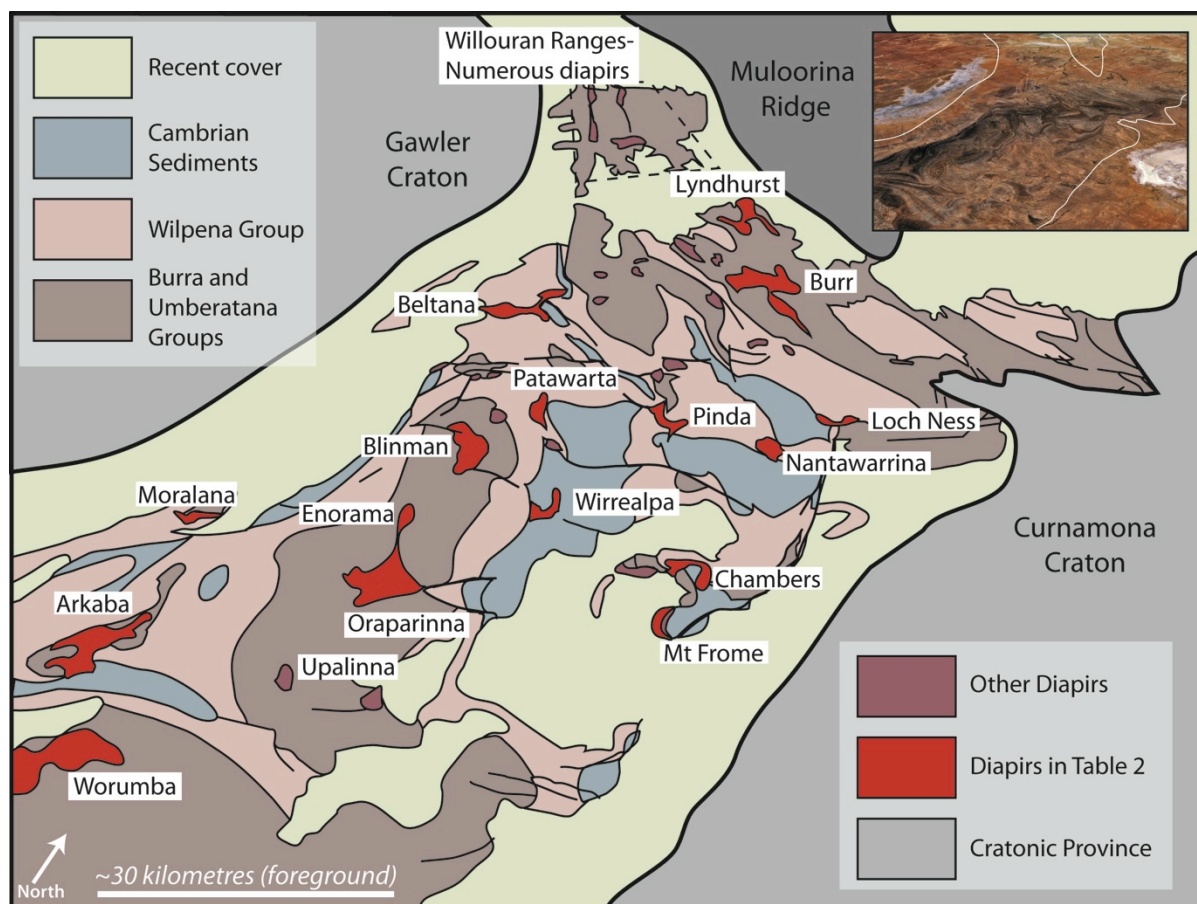


Figure 3: Other diapirs found throughout the Adelaide Rift Complex. Based on Preiss (1987), Reid and Preiss (1999), and Coats (1973)

### Hypothesized Diapir Movement

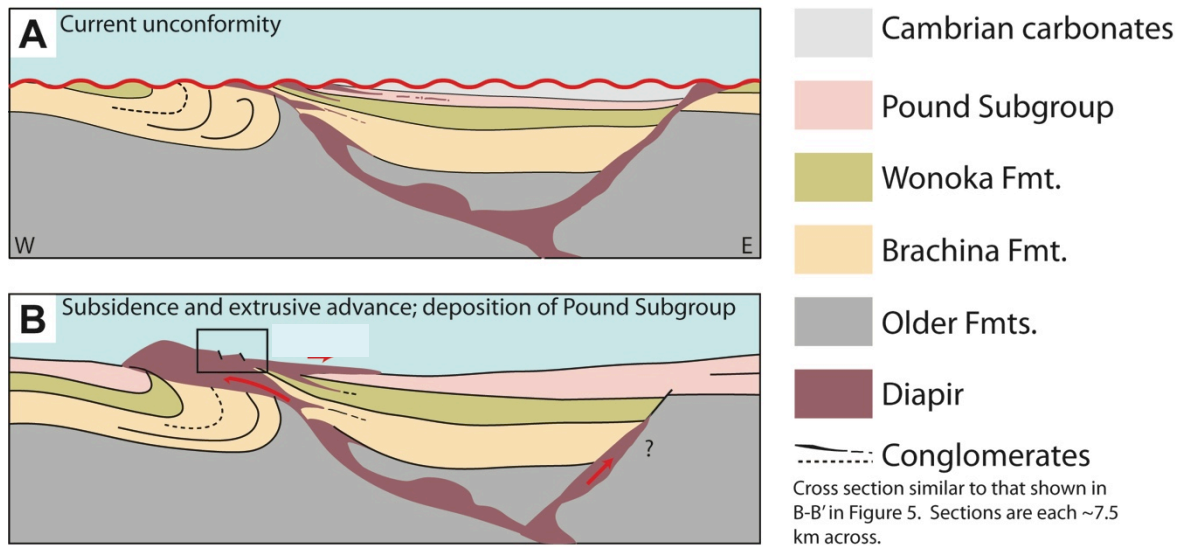


Figure 4: Hypothetical cross-section and model for movement of Mt. Frome diapir. Modified from unpublished work by Bob Dalgarno.

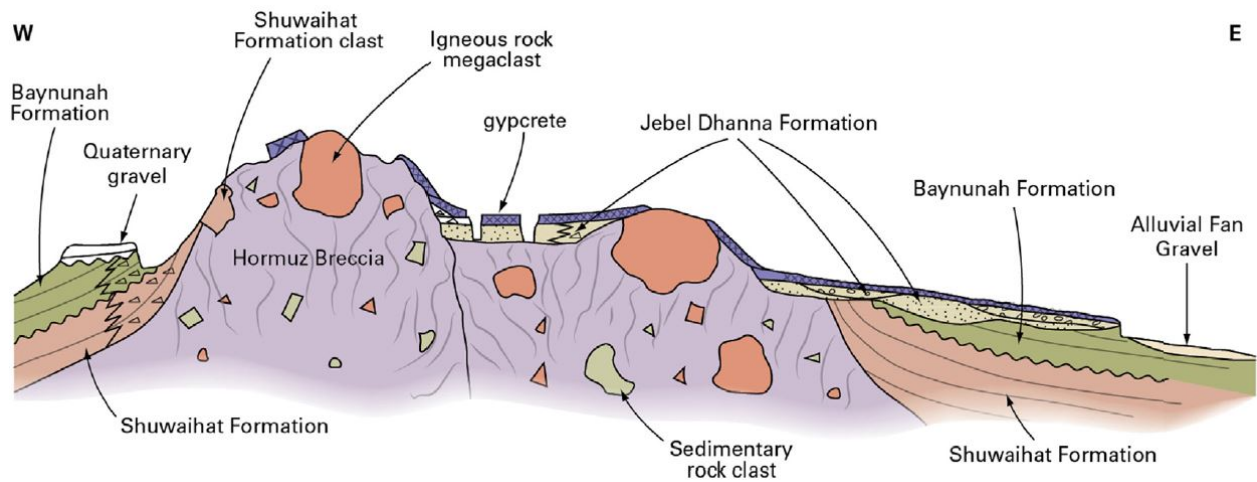


Figure 5: Typical extrusive salt dome in the Arabian Gulf. Note similarities to Mt. Frome sediments in Figure 17. Reprinted from Thomas et al. (2015).